QC
225
.B3

ACOUSTIC EXPERIMENTS WITH THE PIN-HOLE PROBE AND THE INTERFEROMETER U-GAGE

BY

CARL BARUS, PH.D., LL.D.
Professor of Physics, Emeritus, in Brown University

PUBLISHED BY THE CARNEGIE INSTITUTION OF WASHINGTON
WASHINGTON, NOVEMBER 1927

FEB 27 1928

UNIVERSITY OF MAINE

RAYMOND H. FOGLER LIBRARY

Digitized by the Internet Archive
in 2026

https://archive.org/details/acousticexperime0000carl

CARNEGIE INSTITUTION OF WASHINGTON
PUBLICATION NO. 383

1927

J. B. LIPPINCOTT COMPANY
EAST WASHINGTON SQUARE
PHILADELPHIA, PENNA.

ACOUSTIC EXPERIMENTS WITH THE PIN-HOLE PROBE AND THE INTERFEROMETER U-GAGE

BY

CARL BARUS

Professor of Physics, Emeritus, in Brown University

PUBLISHED BY THE CARNEGIE INSTITUTION OF WASHINGTON
WASHINGTON, 1927

FEB 20 1928

130250

PREFACE

The pin-hole probe (a finely perforated plate or cone mounted on a quill-tube as described in the preceding Reports*) measures the residual nodal intensity or potential energy per cubic centimeter, at any point along the axis of a stationary sound wave, by the aid of an interferometer **U**-gage of mercury. The pressure indicated by the displacement (s) of white-light fringes is therefore a maximum at any node and falls off harmonically to zero at the succeeding antinodes. Progressive waves are without effect on the probe. It is advisable to use small fringes (0.01 cm. in the ocular of the telescope), so that one scale-part may be roughly 10^{-6} atm., or s nearly standardized in dynes/cm^2.

In view of the large number of tests made in the lapse of the present experimental investigation, the only practical method of communicating the results is by the way of graphs. To facilitate the reading of these, inserts showing the character of the apparatus or the method employed accompany the graphs in all essential cases, in order that anyone interested may get much of the information under consideration from this inspection. To summarize the contents of the present experimental report otherwise seems hardly feasible.

It is to be understood that the purpose of the experiments is an orientation of the acoustic phenomena, the tryout of a method under conditions as varied as possible. The excitation of organ-pipes by telephone is an efficient and sometimes the only method available in the furtherance of this aim, as anything of the nature of air-currents would be fatal. Large inductances were therefore needed, and I used iron-cored coils because of their convenience and as presumably adequate for the purposes specified. Though certain inductance measurements are attempted acoustically, these are used as illustrations only; for, ultimately, the pin-hole probe can not of course compete with the galvanometer or the ear. Later, I had frequent occasion to regret the use of iron-cored coils, for the pin-hole probe work came out better than I had anticipated and would have sufficed for more satisfactory electric work than the coils permitted.

Inductions treated acoustically by differential telephones in Chapter I, therefore, gave crude results only. On the other hand, the experiments showing continuous change of reflection without, into reflection with change of phase, of the continuous change of the phase relations of the two coöperating telephone-plates (Para. 11, et seq.) make an interesting exhibit, I think. In the final sections of the chapter much work was done with the object of specifying the induction phenomena from the location of crests and troughs of the acoustic graphs, from their intersections, from zero and exchange devices, etc. I did not, however, in spite of the sharply delineated graphs, reach satisfactory solutions for the problems involved.

* Carnegie Inst. Wash. Pub. No. 310, Washington, D. C.; Part I, 1921; Part II, 1923; Part III, 1924

The preceding experiments had already indicated the incidental occurrence of electric oscillation. Direct telephonic coupling of acoustic and electric oscillations were thus suggested. In Chapter II a condenser is inserted into the circuit which energizes the telephones, to facilitate the interpretation of results. The graphs, in fact, become more precise and are more satisfactorily construed. At first a motor-break was used as an interrupter in the primary. Later an ordinary platinum-spring break released the vibrations and gave surprisingly steady service. The purpose of using electric oscillations to interpret the anomalous presence of apparently low notes in short and slender pipes has in a measure succeeded.

Pin-hole probes may be used singly, if they open out from a closed air region vibrating acoustically. As a rule, it is advantageous to use them in pairs, in which case they may be set either to coöperate with or to oppose each other. Chapter III gives a summary of remarkably varied results obtained with paired pin-hole probes, and it was hoped that these experiments would throw definite light on the phenomena as a whole. What they do exhibit is the important function of the quill-tube prolongation or connection on either side of the pin-hole. So much is this the case that paired quill-tubes, without pin-hole constriction but of suitable lengths, may be made to function, though the pressure produced is relatively feeble. The presence of a constriction, however, even if perfectly cylindric like a very short end of capillary tube, enhances the result. One suspects that the production of vortices on the inside of the probe at the shoulder and node is the ultimate cause of pin-hole or constriction phenomena. Such vortices decrease the outflow by locking up a part of its translatory energy in eddies. In other words, the excess of the flow alternating across and through the pin-hole walls is into the region of excess vorticity. At the end of Chapter IV (Para. 90, et seq.) this view is in a measure confirmed by pin-holes pricked in the thinnest sliver of mica. Even if cemented between identical quill-tubes, this ideally thin pin-hole has exceptionally efficient but opposed properties on its two sides. Although acoustic pressure may be built up in a region of almost any volume and in a surprisingly short time, provided its boundaries are closed and rigid, the pin-hole probe can not be used to produce a persistent flow of air into an expansible region of constant pressure, even though below that producible by the probe. This may be neatly shown with regions closed with liquid films.

The short and slender air-columns used in the above experiments are without influence on the telephone-plates and at their mercy, as it were. The case of relatively massive air-columns should be different. The behavior of a closed organ-pipe of variable depth, blown without the presence of air-currents within, is first treated, with the necessary reference to the quill-tube connection with the U-gage. The exploration of nodal intensity at different depths below the mouth in case of horns, cylindrical tubes, follows. These are blown by the telephone. Two methods of varying the pitch of the telephone are contrasted: the motor-break giving the pitch directly and the spring-break with an oscillating circuit giving pitch indirectly.

The results of the two procedures differ more widely than one would anticipate. In the latter case it is observed that the graphs obtained frequently consist of linear elements, particularly in the case where circuits are rhythmically charged and discharged. As the cylindrical pipe offers good opportunities for the comparison of salient and reëntrant pin-hole probes, both of the conical and plate types, such tests (as already instanced) are carried out. The use of mica plates makes it possible to increase the sensitivity of the latter even above the conical type, though this is always more expeditious.

In the last chapter a number of incidental investigations are grouped together. The first of these treats the pressure of the electric wind driven from a highly charged point upon an opposed electrode connecting with the U-tube interferometer. The results point out the efficiency of the mucronate electrode, as it may be called, in which a sharp point projects about half a millimeter from the electrode. The axial pressure of the ionized convection current, when checked by the opposed electrode, may be increased 10 or even 20 times by this device, which seems to dip into an anode or cathode minimum. Pressure ceases instantly on the occurrence of sparks or any sputtering.

A tentative method for the measurement of the energy of X-rays was tried out, but it failed because of contemporaneous temperature discrepancies. Finally a promising modification of the U-gage was also a disappointment, because it could not be freed from the capillary adhesion of parts.

Carl Barus.

CONTENTS

CHAPTER I—SHORT AND SLENDER AIR-COLUMNS. CIRCUITS WITHOUT EXPLICIT CAPACITY

PAGE

1. Circuits. Figs. 1 to 5 1
2. Table of inductances 1
3. Survey in pitch. Figs. 6 to 10 2
4. Continuous change of phase difference. Fig. 11 3
5. Phase difference apparently passing through zero. Figs. 12 to 14 4
6. Phase reversal owing to inductance. Figs. 15 to 17 5
7. Data. Fig. 18 6
8. The equations completed. Single circuit 8
9. Circuits in phase and in sequence 8
10. Improvement of telephones. Figs. 19 and 20 9
11. Comparison of primary and secondary. Figs. 21 to 30 9
12. Layers of transformer in parallel. Figs. 31 to 36 11
13. Single half layer. Fig. 37 14
14. Incidental origin of initial phase differences. Figs. 38 to 41 14
15. Circuits without transformer. Figs. 42 to 44 16
16. Telephone-plate subject to an external magnetic field. Fig. 45 17
17. Remarks. Figs. 46 to 48 17
18. Zero methods. Primary and secondary. Fig. 49 18
19. Primaries only. Figs. 50 to 54 19
20. Zero method with the secondary. Figs. 55 and 56 21
21. Exchange of loads. Circuits in parallel. Figs. 57 to 62 21
22. Further experiments. Figs. 63 to 71 23
23. Summary. Quantitative considerations. Fig. 72 26
24. High-resistance telephones. Zero methods. Figs. 73 to 75 29
25. The same with small inductor. Figs. 76 to 79 31
26. Compensating inductances. Fig. 80 33
27. Same without commutator. Figs. 81 and 82 34
28. Electrolytic resistances. Figs. 83 to 85 36
29. Single circuits isolated. Figs. 86 and 87 37
30. Data 39
31. Troughs of the paired graphs 40
32. The intersection of paired graphs 41
33. Parallel circuits actuated by single inductor open circuits. Figs. 88 to 95 43
34. Minima and intersections 45
35. Resistances in the air-gap 2, 3. Double symmetrical inductor. Fig. 96 46

CHAPTER II—SHORT AND SLENDER AIR-COLUMNS. CIRCUITS WITH LOCALIZED CAPACITY

36. Capacities in the air-gap. Figs. 97 and 98 47
37. Single inductor, unsymmetrical. Figs. 99 to 101 49
38. Effect of the lower harmonics. Figs. 102 to 105 51
39. Detailed survey near the crest. Figs. 106 to 112 53
40. Non-coupled inductances inserted. Reductions. Fig. 113 55
41. Low-resistance telephones. Fig. 114 57
42. Spring mercury contact-breaker of inaudibly low pitch. Figs. 115 and 116 59
43. Inductor with variable core. Figs. 117 to 120 60
44. Increased currents. Figs. 121 to 123 62
45. Longer and wider organ-pipe. Figs. 124 and 125 63
46. Long thin pipe. Figs. 126 and 127 64
47. Short thin pipe. Figs. 128 to 130 66
48. Long and short pipes compared. Combined primaries. Figs. 131 and 132 67
49. Opposed mutual inductions and similar comparisons. Figs. 133 to 135 69
50. Primaries in parallel. Fig. 136 71

CHAPTER III—MUTUAL RELATIONS OF PIN-HOLE PROBES. QUILL-TUBES

51. Outer pin-hole of the pipe enlarged. Figs. 137 and 138 73
52. Reversal of outer pin-hole probe. Figs. 139 to 142 74
53. The same. Cases of smaller length increments. Figs. 143 to 153 76

CHAPTER III—MUTUAL RELATIONS OF PIN-HOLE PROBES. QUILL-TUBES—*Continued*

PAGE

54. The same. Summary. Fig. 154 80
55. Pin-holes in series. Change of length and electric capacity. Figs. 155 to 160 82
56. Effect of the number of pin-holes. Figs. 163 to 167 84
57. Outer quill-tubes of varying lengths, all open. Figs. 161 and 162 87
58. Data for identical reëntrant plate pin-hole probes of different lengths. Figs. 168 to 171 88
59. Inner quill and outer conical glass pin-hole. Fig. 172 92
60. Coöperating quill-tubes without pin-holes. Figs. 173 to 178 93
61. Reversal of the preceding adjustment. Figs. 179 to 181 95
62. Quill-tubes of constant external diameter, reduced in length and bore conjointly. Figs. 182 to 185 97
63. Acoustic pressures in case of a soap-bubble. Figs. 186 and 187 100

CHAPTER IV—PIPES WITH RELATIVELY MASSIVE AIR-COLUMNS. ORGAN-PIPES. HORNS

64. Pin-hole record for variable organ-pipe. Apparatus. Fig. 188 102
65. Results. Fig. 189 102
66. Further experiments. Figs. 190 and 191 103
67. Reduced diameter of pin-hole probe connector. Fig. 192 105
68. Steady blast. Figs. 193 and 194 107
69. Miscellaneous tests 109
70. Mean total pressure in organ-pipe. Soap-film. Fig. 195 110
71. Same. Direct **U**-gage measurement. Fig. 196 111
72. Acoustics of the conical horn. Apparatus. Broad horn. Figs. 197 and 198 111
73. Results for horn. Figs. 199 to 204 113
74. Slender horn (70). Figs. 205 to 210 115
75. Cylindrical pipe. Figs. 211 to 218 117
76. Extensible pipe. Figs. 219 to 223 119
77. Closed organ-pipe. Figs. 224 and 225 121
78. Alternating current. Figs. 226 and 227 122
79. Remarks 124
80. Charging circuit. Figs. 228 to 230 125
81. Reëntrant pin-hole probe. Figs. 231 to 236 127
82. The same; s and x graphs. Figs. 237 to 239 129
83. The same; direct tests. Figs. 241 to 243 130
84. Plate pin-hole with anterior and posterior quill-tubes. Fig. 240 131
85. The same; plate pin-hole reversed. Figs. 244 and 245 133
86. The same; further experiments. Figs. 246 to 250 133
87. Salient glass pin-hole with anterior quills. Figs. 251 to 256 135
88. Rear quill-tubes variable. Figs. 257 to 262 137
89. Further experiments. $\delta = 10$ cm. δ' variable 140
90. Pin-holes varied. Figs. 263 to 268 141

CHAPTER V—MISCELLANEOUS EXPERIMENTS WITH THE INTERFEROMETER **U**-GAGE

91. Pressure phenomena of the electric wind. Apparatus 146
92. Needle electrode. Figs. 269 and 270 146
93. Mucronate electrode. Figs. 271 to 275 148
94. The same with micrometer. Figs. 276 to 279 150
95. Contributory results. Figs. 280 to 282 151
96. Velocity of the winds 153
97. A method of measuring the energy of X-rays. Introductory apparatus. Fig. 283 .. 154
98. Computation 156
99. Data. Figs. 284 and 285 157
100. Modified **U**-gage. Apparatus and results. Figs. 286 to 288 157

CHAPTER I

SHORT AND SLENDER AIR-COLUMNS. CIRCUITS WITHOUT EXPLICIT CAPACITY

1. Circuits—In my earlier papers I have frequently taken up this investigation, more or less incidentally. The present work is intended to be more systematic. All measurements of nodal pressure indicated by the pin-hole probe are made with the U-tube interferometer. Antinodes do not respond.

The trend of the work may most easily be shown by describing the successive circuits used and the acoustic effects observed with each. In figure 1*a*, E is the primary electromotive force (one or two storage-cells) sending a current in series through the two telephones T and T' and the resistance R. This current is periodically broken by the plate commutator B, rotated at controllable speed by a small motor (not shown). In this way, both telephones give out the same note, the pitch being determined by the angular velocity of B. One of the telephones, T', is provided with a switch, S, so that its current may be reversed.

The two telephones are connected at the mouthpieces by the tube tt', originally 15 cm. long (effectively) and 1.5 cm. in diameter. At right angles to it and at its center, the two pin-hole probes (salient s and reëntrant r) are inserted and s is joined to the one shank of the interferometer U-gage by a short end of rubber tubing. All joints are sealed with wax. This circuit (fig. 1*b*), in series, admits of the more useful modification (1*c*) with the telephone circuits in parallel. Additional resistances, inductances, capacities, may here be inserted at L.

In figure 2, a small inductor I (about 0.5 henry in the secondary) has been introduced, cell E feeding the primary. The telephones T and T' are now operated by the induced current with a switch at S for one of them. A resistance at R is convenient. In the arrangement, figure 3, two identical secondaries, I and I', are wound side by side on the same primary, the other adjustments remaining as before.

In figure 4, the primary circuit from E actuates the telephone T directly, whereas the secondary circuit at I with a switch, S, passes through the telephone T'. This (series) arrangement has been improved in figure 5, where a branch circuit from the primary passes through the telephone T. The advantage of this is the easy equalization of telephone-currents by a resistance, R, placed in either circuit, additional inductance being added at L.

2. Table of inductances—As determined by conventional methods, the approximate values of the resistances and inductances to be used in the following tests are summarized in table 1. The two layers of the inductor are unfortunately not equally efficient. Though they were usually joined in

series or in parallel, there are a number of cases in which it was desirable to use them independently and in opposition. At high values of L the method became insensitive and the data are probably low. The coil L_2 was probably defective. The table refers to wire or laminated cores. In the experiments solid cores were often used when they were convenient, as it was the object here to bring out the character of the acoustic behavior as a whole, over a wide range. Steps of increasing inductance, therefore, are frequently useful. Large continuous changes of L are most efficiently made by inserting a core

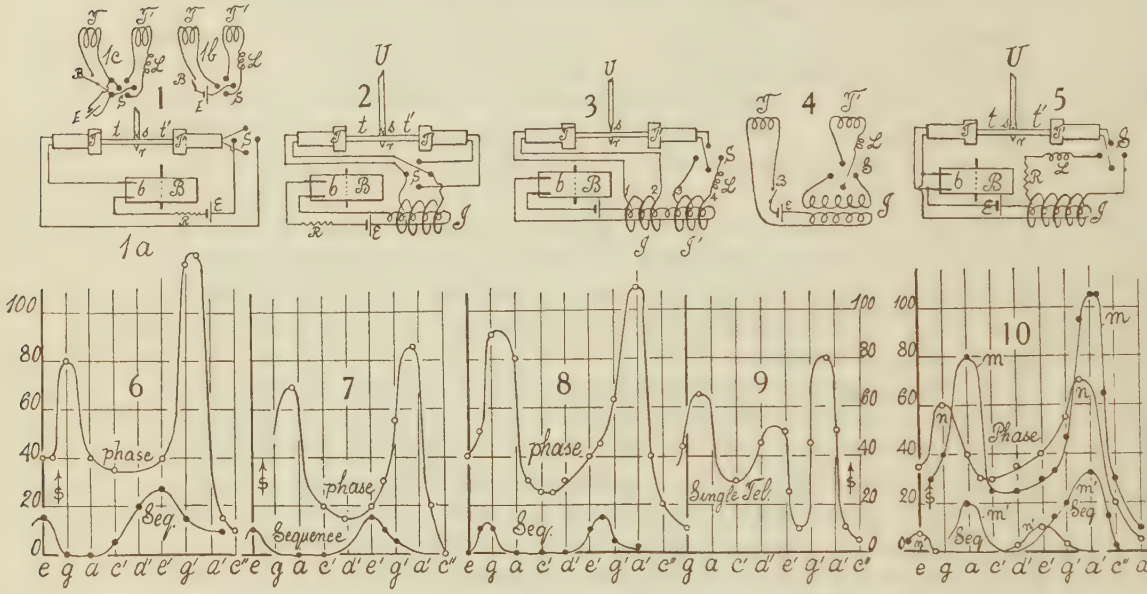

into the coil, and this plan, in spite of its deficiencies, will have to be used below. The use of cored coils, otherwise objectionable, is permissible here, where the object is to exhibit the acoustic phenomena, and these demand large inductances.

TABLE 1—Resistances and inductances of the coils used. Conventional, single impulse methods. All coils wire cored

Coil No.	R ohms	L henry	Coil No.	R ohms	L henry
L_1	9.9	0.32	Common telephones T'	84.3	0.060
L_2	301	.13+	Common telephones T	85.3	.060
L_3	550	1.35+	Radio telephones T'	1110	1.2
L_4	1.1	.042	Radio telephones T	1090	1.2
Inductor secondaries I'	30.5	.39	L_w	1.1	.011
Inductor secondaries I	31.8	.29	M. H. standard	9.7	.010 to .034

3. Survey in pitch—The graphs (figs. 6, 7, 8, 9, 10) obtained with each of the circuit designs, showing the fringe displacement s (nodal intensity) as the pitch gradually rises from c (4-foot octave) to a' (2-foot octave) are

given below the corresponding diagrams of circuits. With the telephone-plates in phase (*i. e.*, the plates moving outward or inward together) there is marked response (node) between a' and g' and again between a and g; above a' the tube is silent indefinitely. Between a' and a there is here apt to be multiresonance, so that the air-column vibrates at all pitch intervals. The saliency at a', a, though usually very pronounced (figs. 6, 7, 8), is sometimes reduced as in figure 10, n, n', possibly owing to inherent differences of phase in the two circuits, but probably incidental, as the curves m, m', obtained with somewhat modified telephones, imply.

When the current in the telephone T' is reversed by the switch S, the plates vibrate inward and outward, respectively; *i. e.*, in sequence; the nodes thus vanish from the middle of the tube and appear at the ends. There is therefore no middle pin-hole pressure (s) at pitches a, a'. Curiously enough, there was response (middle node) in this case at e, e', sometimes quite marked, as in figure 6, but usually weak. This e may be due to multiresonance, as the pipe tt' in these experiments was attached to the telephones by short quill-tubes. One would therefore expect a response for the pipe tt' alone and another corresponding to the added space around the telephone-plates, a sort of Rayleigh neck effect. It was subsequently traced to an inequality in the mouthpiece of the telephones.

If but one of the telephones is actuated, the other being silent, the resonance at a and at e' were sometimes clearly in evidence, as in figure 9. When both vibrate in phase, however, the salient e' is wiped out or obscured. Later the e' was eliminated.

4. Continuous change of phase difference—This is most easily brought about by inserting increasing resistances in one of the duplicate telephone circuits, leaving the other unchanged. The first test was made with the design of figure 3 and the results are shown in figure 11. Between 0 and 1,000 ohms, the fringe displacements, s, are given in steps of 100 ohms; between 1,000 and 10,000 ohms, in steps of 1,000 ohms. The *phase* displacement graph falls, while the *sequence* graph rises at a rapid rate continually. From the initial difference of $\Delta s = (87 - 3) = 84$ at $R = 0$ to the final difference of $\Delta s = 60 - 60 = 0$ at $R = 10{,}000$ ohms, the curves have become asymptotically coincident. The fall of (middle) nodal intensity from $s = 87$ to $s = 60$ is due to the fact that in the latter case but a single telephone-plate vibrates, whereas the other reflects like a rigid wall. In the former case both plates vibrate, reinforcing each other. The Δs curves (fig. 11) show that the decrease also begins gradually, as though some inherent phase-difference were first to be compensated. As a whole, we have in the sequence graph an interesting exhibit of a *continuous change of the type of reflection;* initially without change of phase, without middle node ($s = 3$) it passes eventually into reflection with change of phase and a strong middle node ($s = 60$). The lower graph offers a means of converting any Δs observed into the corresponding excess resistance R.

5. Phase difference apparently passing through zero—In figure 11, one telephone is silenced before appreciable phase reversal occurs, possibly because the initial resistances, etc., in the T and T' circuits (fig. 3) are large. The trial was therefore repeated with the adjustment figure 1*c*, and an example of the results obtained is given in figures 12, 13, and 14. The curves now intersect at 1,000 ohms when one of the telephone-plates is effectively at rest. Thereafter this telephone, as it were, tends to vibrate more and more in phase again; but the relatively high resistances soon cut the modified circuit out. One notes that the sequence curve still rises with increasing resistance after the phase graph has ceased to fall.

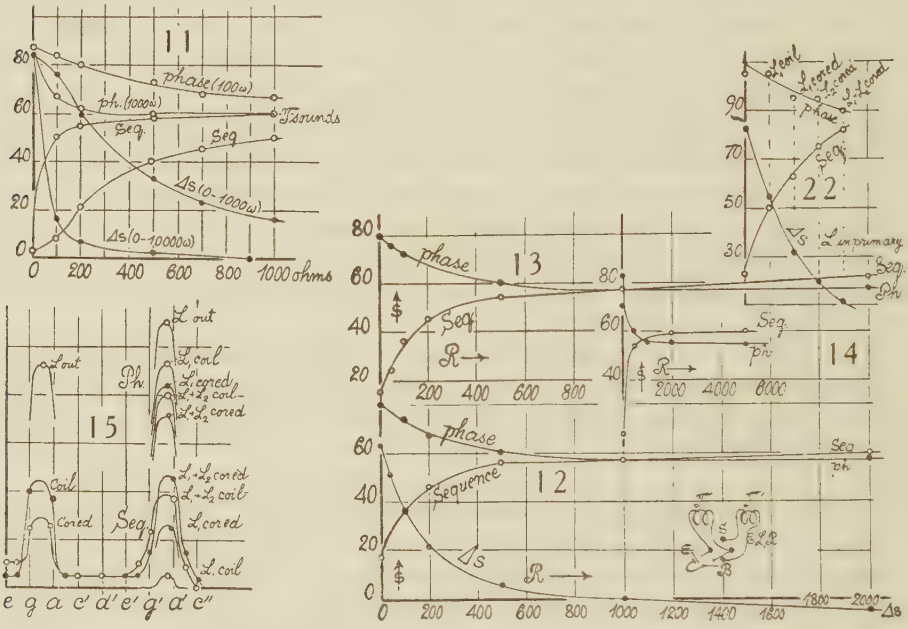

Anticipating the results below (cf. § 23), if we suppose a telephone to be more efficient when vibrating under phase conditions (or the reverse) than under sequence conditions, and introduce to constants c and c' to allow for this difference, we may picture the case of intersecting or nonintersecting phase-sequence graphs perhaps as follows: Since the circuits T, T' in the adjustment in figure 1*c* are in parallel, and if Δs is the fringe displacement in the sequence case and Σs in the phase case,

$$(1) \qquad \Delta s = \varepsilon \left\{ 1/c \sqrt{R_v^2 + L^2\omega^2} - 1/c' \sqrt{R_c^2 + L^2\omega^2} \right\}$$

$$(2) \qquad \Sigma s = \varepsilon \left\{ 1/c \sqrt{R_v^2 + L^2\omega^2} + 1/c \sqrt{R_c^2 + L^2\omega^2} \right\}$$

where R_v is the varied and R_c the constant resistance of the telephone-circuits, L their (identical) inductance, ε the e. m. f. in proper units. Now, if $R_v = \infty$, apart from signs

$$(3) \qquad -\Delta s/\Sigma s = c/c'$$

i. e., they are unequal. If, however,

$$\Delta s = \varepsilon \left\{ 1/c \sqrt{R_c^2 + L^2\omega^2} - 1/c' \sqrt{R_v^2 + L^2\omega^2} \right\} \tag{4}$$

i. e., if the varying resistance is in the other circuit, then, if,

$$R_v = \infty \qquad \Delta s / \Sigma s = c/c = 1 \tag{5}$$

In the case (3), if $c' > c$, the phase-sequence graphs would eventually intersect; whereas in the case (5) they would meet at $R_v = \infty$. The results would be the same if in equation (2) the constant were c', the argument being that if both telephones vibrate in phase, *i. e.*, alike, they are equally efficient, but not so in the opposite case. Both cases occur in the present experiments.

Equation (3) and figure 14, then, give us the ratio of telephone efficiency, $c/c' = 40/34 = 1.18$, a value which reappears below, § 23.

6. Phase reversal owing to inductance—After this a large number of experiments were made with capacities (C) and inductances (L) with the hope of observing more striking phase reversals, but at first without much success.

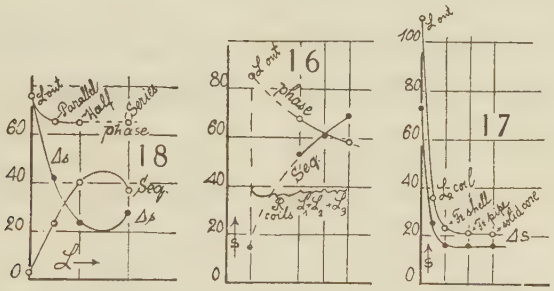

I give a few examples in figure 15, the empty coils being first inserted into one telephone-circuit (T', fig. 3) and the iron core thereafter. The steps of inductance L may be estimated as within one henry (cf. § 12), though they were not nearly so large at the frequency a' (440), since the cores of iron were not laminated. The survey in pitch carried out in the graph at each L is in conformity with the unloaded graph.

Figure 16 is a summarized example of the fringe displacements s found (adjustment, fig. 1*c*) after the inserting of the coils (resistance R) and after the subsequent insertion of the iron cores (L_1, L_2, L_3). In these cases the phase curve tends to become horizontal, while (after the intersection) the sequence curve still rises in marked degree. Hence the explanation of the apparent L-effect is probably the same as that in the preceding section.

An interesting result was obtained in comparing hollow and solid iron cores. The L-effect in the two cases was about the same. Thus, in inserting an inch solid rod into the coil L_2, the Δs observed with and without iron was not appreciably larger than when the same length of inch gas-pipe was inserted. Thus the iron at frequencies above 400 per second here exhibits an astonishing magnetic skin or shielding effect.

To give two examples (fig. 17) among many for coil II, when a tin-plate tube, inch gas-pipe, and solid inch rod were used as cores successively:

Full displacement.....	$\Delta s = 110, 72$	Coil with gas-pipe core.....	$\Delta s = 21, 16$
Coil in (without iron).....	$\Delta s = 35, 25$	Coil with solid core.....	$\Delta s = 21, 16$
Coil with shell core.....	$\Delta s = 23, 16$		

7. Data—Treating the fringe displacements Δs as equivalent to the effective or virtual current in the telephone, a few tentative tests were begun, using the graphs, figure 12, for converting s into the excess resistance R in circuit, E, R, L, C, ω having their usual meaning. Hence if we temporarily disregard, as both figures 11 and 12 seem to permit, the inherent phase differences, the telephone amplitude may be written $E/\sqrt{R^2 + (1/C\omega - L\omega)^2}$, E being the voltage applied and R (allowing for the telephone resistance) following from Δs in figure 12.

If, therefore, the same reduction of Δs is produced in one case by additional resistance (coils only) and in the other by additional inductance (iron core in) from the same initial Δs, we may write

$$E/\sqrt{R'^2 + (1/C\omega - L\omega)^2} - E/\sqrt{R''^2 + (1/C\omega - L\omega)^2} =$$
$$E/\sqrt{R'^2 + (1/C\omega - L\omega)^2} - E/\sqrt{R'^2 + (1/C\omega - L'\omega)^2}$$

whence on inverting the squared quantity,

$$(L\omega - 1/C\omega)^2 - (L'\omega - 1/C\omega)^2 = R''^2 - R'^2 = \Delta R^2$$

or,

$$\omega(L + L') - 2/C\omega = \Delta R^2/\omega\Delta L$$

where $\Delta L = L - L'$ is negative. For another coil, L_1, R_1, of the same C and ω,

$$\omega(L_1 + L'_1) - 2C\omega = \Delta R_1^2/\omega\Delta L_1$$

whence

$$\omega^2\{(L_1 + L'_1) - (L + L')\} = \Delta R_1^2/\Delta L_1 - \Delta R^2/\Delta L.$$

If, therefore, it were permissible to neglect the initial inductance ($L = L' = 0$) of the coils, without iron, observing that ΔL and ΔL_1 are positive if the squares above are not inverted

$$(1) \qquad \pm\omega L'_1 + \Delta R_1^2/\omega L'_1 = \pm\omega L' + \Delta R^2/\omega L' = K = \text{const.}$$

Thus, if K is known, from L' as a standard

$$(2) \qquad L'_1 = \pm (K/2\omega)(1 + \sqrt{1 \mp 4\Delta R^2/K^2})$$

If capacity (C) is excluded, the equations under the same limitations are much simpler and become

$$\sqrt{L^2 - L_0^2} = \sqrt{R^2 - R_0^2}/\omega$$

where L_0 and R_0 refer to the initial circuit and L and R to the circuit after the coil is inserted.

The following data were obtained by the method of figure 1*c*, the full fringe displacement in the absence of coils being $\Delta s = 65$.

The coils I, II, III, IV (cf. § 2) were of the choke-coil type, with removable iron, except the last two, V, VI, where the iron was fixed. These were parts of a little induction coil consisting of two half secondaries. They behaved so peculiarly that the full data are noteworthy (cf. fig. 18).

	Coil out	Layers in parallel	Layers in series	One layer only, V	The other layer, VI
In phase s	75	65	65	65	65
In sequence s	3	23	37	42	40
Δs	72	42	28	23	25

So far as the phase graph is concerned it makes little difference how the layers are taken. The sequence graph rises naturally when the two layers are combined in parallel and then in series; but curiously enough, each single layer shows greater impedence alone than when they are taken together in series. These apparently anomalous results remained the same throughout many repetitions. The impedence of the half coil (caet. par.) behaves as if it were greater than the whole. One suspects the occurrence of electric oscillation.

TABLE 2—Initial $\Delta s = 65$, equivalent to $R = 100$ ohms and L_0. $(L^2 - L_0^2) \propto (R^2 - R_0^2)/\omega^2$. Frequency, $n = 440$, $\omega = 2765$.

Coil No.	I	II*	III	IV	Coil No.	I	II	III	IV
Δs (no core)	45	10	8	54	$(R_{cl}^2 - R_0^2) \times 10^{-5}$†	0.156	2.11	2.60	0.169
Δs (iron core)	19	5	3	28	$(R_{co}^2 - R_0^2) \times 10^{-5}$†	.956	3.62	5.08	.525
R (no core)	60	370	420	30					
R (iron core)	225	510	620	150	L_{cl} (henry)‡	.045	...	.185	.030
ΔR (core-coil)	165	140	200	120	L_{core} (henry)‡	.112	...	.258	.083
					Total (henry)	.157	...	.443	...

* Defective coil.
† Corrected for telephone resistance (100 ohms).
‡ Interpolation $L_{obs} = 0.090 + 0.25\,L$.

In table 2 the values of Δs and their reductions to resistance R (fig. 12) are given, together with the tentative values (nearly) computed from them. The difference between the L with and without solid iron cores is astonishingly small, relatively speaking. The data as a whole, compared with table 1, give a crude order of values only. The coil L_2 was subsequently found to be defective. Omitting this, the other values of total L observed here and the data of table 1 (L) conform pretty closely to the equation

$$L_{obs} = 0.090 + 0.25\,L$$

Thus at $L = 1$ henry $L_{obs} = 0.34$. The constant indicates that the postulates are not admissible.

8. The equations completed. Single circuit—Assuming that the current in T remains practically constant in the current designs (figs. 3, 5) adopted, the problem is reduced to the variations of the current I, subject to L, R, ω in the telephone T'. This is to pass to I' when L, R is replaced by L, R', and to I'' when the former is replaced by L', R. These changes involve three phases, $\theta = \tan^{-1} L\omega/R$, $\theta' = \tan^{-1} L\omega/R'$, and $\theta'' = \tan^{-1} L'\omega/R$.

The relations here in question are given in the usual way in the diagram (fig. 24), with the value of all the vectors and angles indicated. C' is the circular locus on the diameter $E/L\omega$, when R only varies (increase counter-clockwise) and C'' the circular locus on the diameter E/R when L (increase clockwise) only varies. As the currents I were identical, the projections of I' and I'' on I must be the same, as they produce the same depression in the Δs graph. Hence

$$I' \cos(\theta - \theta') = I'' \cos(\theta'' - \theta)$$

or

$$(1) \qquad E \cos(\theta - \theta')/\sqrt{R'^2 + L^2\omega^2} = E \cos(\theta'' - \theta)/\sqrt{R^2 + L'^2\omega^2}$$

If we put $\Theta = \cos(\theta'' - \theta)/\cos(\theta - \theta')$ the former equation reduces to

$$(2) \qquad \omega^2 (L'^2 - \Theta^2 L^2) = \Theta^2 R'^2 - R^2$$

thus, if $\Theta = 1$, the old equation would follow.

To find Θ, the equations $\theta = \tan^{-1} L\omega/R$, etc., may be reduced and the result is

$$(3) \qquad \Theta^2 = (1/L^2\omega^2 + 1/R'^2)/(1/L'^2\omega^2 + 1/R^2)$$

If this value is introduced into equation (2), the latter expressed for $L'^2 - L^2$ gives

$$(4) \qquad \omega^2(L'^2 - R^2L^2/R'^2) = (R^2/L^2\omega^2)(R'^2 - L^2R^2/L'^2)$$

If R and L are small, the coefficient of the last L^2 and R^2 may be disregarded; but the approximate result

$$(5) \qquad \omega^2 \Delta L^2 = (R^2/L^2\omega^2)\,\Delta R^2$$

is still essentially dependent on $(R/L\omega)^2$.

9. Circuits in phase and in sequence—The simple premises of the preceding paragraph are inadequate. Each point in the diagram involves two circuits in parallel. If we proceed as in § 23 below, letting the constants c, c' refer to the efficiency of the telephones and suppose the electromotive force ε in proper units, a point in the phase-graph is equivalent to

$$s = \varepsilon\,(1/c\sqrt{R_c^2 + L_o^{12}\omega^2} + 1/c\sqrt{R_v^2 + L_o^2\omega^2})$$

when R_v and R_c are the varied and the constant resistance. A point on the corresponding sequence-graph, however, is equivalent to

$$s = \varepsilon\,(1/c\sqrt{R_o^2 + L_o^2\omega^2} - 1/c'\sqrt{R_v^2 + L_o^2\omega^2})$$

c and c' occurring here, because the telephone-plates vibrate in opposed phases. The constants c and c' may be exchanged. Hence the initial Δs has the form:

$$\Delta s = \varepsilon \left\{ 1/c \sqrt{R_v^2 + L_o^2\omega^2} + 1/c' \sqrt{R_v^2 + L_o^2\omega^2} \right\}$$

If the effect of adding R is identical to the effect of adding L, the new $\Delta s'$ reads

$$\Delta s' = \varepsilon \left\{ 1/c \sqrt{(R_v + R)^2 + L_o^2\omega^2} + 1/c' \sqrt{(R_v + R)^2 + L_o^2\omega^2} \right\} =$$

$$\varepsilon \left\{ 1/c \sqrt{R_v^2 + (L_o + L)^2\omega^2} + 1/c' \sqrt{R_v^2 + (L_o + L)^2\omega^2} \right\}$$

Hence it is the difference of c and c' which complicates this equation. If $c = c'$ the last equation reduces to

$$\Delta R^2 = \omega^2 \Delta L^2$$

giving the approximate values of table 2.

10. Improvement of telephones—Before beginning the next series of observations, the telephones were overhauled as to tightness, etc. Some change seems thus to have been made in the space within the mouthpiece. For after a survey in pitch the graphs like figure 19 appeared. In the resulting phase-curve there is a closer approach to silence between a' and a. In the sequence curve the maxima at e', e, have vanished. They were thus probably due to unequal spaces ahead of the plates, or to some similar effect. The present sequence curve now also has small maxima at a' and a, which being due to inherent differences, now becomes important. The new adjustments were used to try out the inductance of coil II again, with a core of cylindrical iron, shell of gas-pipe, and a solid core respectively. The data (fig. 20), given as heretofore, corroborate the old results. The cylindrical shell is nearly as effective in L as the inch solid-iron core.

11. Comparison of primary and secondary—The design here used is again the circuit shown in figure 5. The effect of resistances in the primary is given in figure 21, both in steps of 100 ohms and of 1,000 ohms. It contains nothing unexpected. The circuit resistances being small and the inherent phases favorable, additional resistances (2,000 ohms) soon practically quench vibration in the loaded circuit. The initial and final nodal intensities s for the phase-curve are as 100 : 75. Here, however, a new feature enters, since the sequence curve begins with an intensity of $s = 27$. The phase-sequence graphs do not cross.

Similar results are summarized in figure 22 (attached to figure 14) for successive loads of self-induction in the primary, L referring, as stated, to the coils either alone or with iron cores. These curves (phase and sequence) could be made to just cross by inserting more inductance. The sequence curve again begins with large s, to be associated with a lag in the primary or a lead in the secondary, since the added L increases s.

The effect of additional resistance, R, in the secondary shown in figure 23,

is also normal in character. The phase and sequence curves gradually approach each other and coincide when $R = 10{,}000$ ohms; but they do not cross. Neither does the initial progress ($R = 0$) suggest any novelty.

In figure 27, however, which indicates the effect of inserting self-induction in steps in the secondary, there is an interesting new departure at the beginning. The phase and sequence graphs no longer finally cross each other, but the sequence graph at first actually descends, showing probably that the opposition in phase is made more perfect; *i. e.*, a lead compensated by an increasing lag, resulting from the initial insertion of inductance. No such effect was heretofore produced with initial resistances (fig. 23) either in the primary or

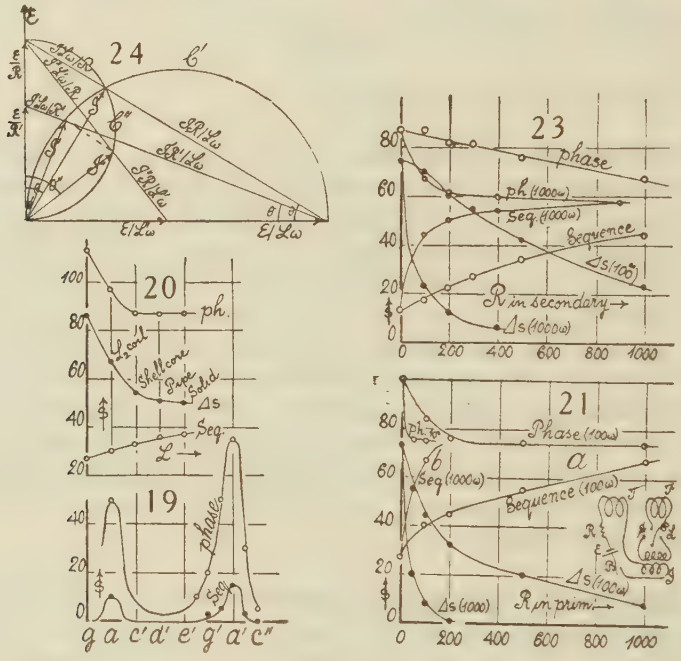

secondary. Thus for the first time we encounter an inherent phase difference equivalent to $\theta = \tan^{-1} L\omega/R$. The L experiments were frequently repeated to test their consistency, and a good example is given in figure 28 for inductance and figure 26 for resistance, for a somewhat larger impressed e. m. f. If we regard the phase difference of primary and secondary as an advance of the secondary, the insertion of inductance at first seems to retard it into complete opposition (sequence) with a maximum, after which, with further inductance, the opposition passes more and more fully, evoking the middle node more and more clearly. The graphs, figures 27 and 28, have therefore been drawn in full through the data as obtained; but a suggestion of the probable course presently to be verified is given by the broken lines in figure 28. If phase reversal is interpreted as a negative, s, the regularity of curves is everywhere enhanced. It appears also that whenever such reversal occurs, the cause

of the production of the middle node passes from one telephone to the other. In the dotted sequence curve, if the telephone T is heard below the abscissa, the telephone T' will be heard above it.

Further detail, obtained with the same adjustment later, is given in figures 29 and 30, where the resistances in the former figure evoke the same march of s-values without minima in the sequence graphs. Figure 30, in which the inductions L_4 are given by a long choke-coil, the iron core of which could gradually be thrust in to the extent indicated in the curves, shows the

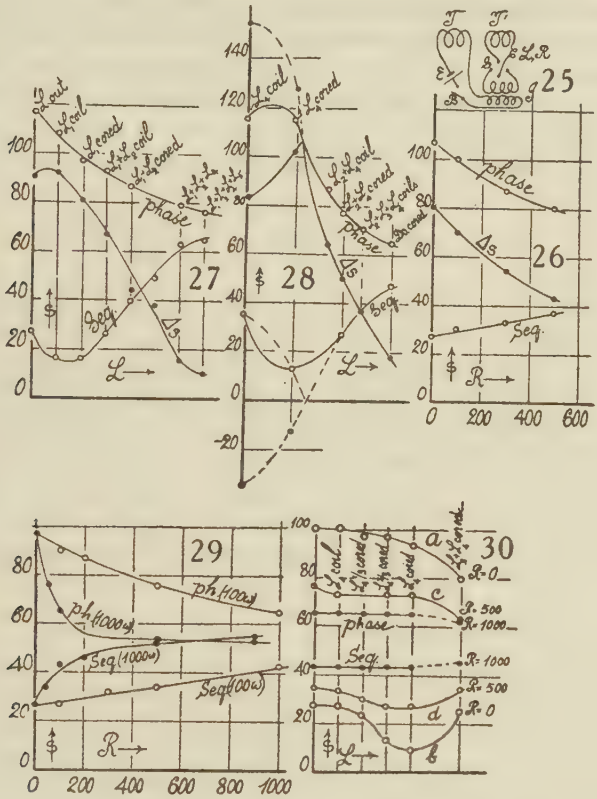

sequence minimum more closely. It may possibly have fallen to $s=0$ in the lower graph, as no inductances between L_4 and L_2+L_4 were available, and the latter carries the observations beyond the minimum. The curves a, b were obtained without excess resistance ($R=0$) in the T' circuit, the curve c d, however, with an excess resistance of $R=500$ ohms. The original minimum has flattened out, since L is now relatively inefficient. At $R=1{,}000$ ohms in the T' circuit, the effect of the inductances used is negligible.

12. Layers of transformer in parallel—After these results it seemed obvious that a greater initial current for the sequence graph would appear on reducing the impedance of the secondary of T' by putting the two identical

layers (fig. 5; compare fig. 3) in parallel. The telephone T is of course left in the primary. This surmise is borne out in figure 31, where the fringe displacements s are given in terms of the inductance L, increasing in steps. The experimental Δs curve here shows a well-marked maximum, while the sequence curve passes sharply through a minimum. By gradually inserting the iron core into the coil L_3, it was possible to trace these curves continuously; but unfortunately the minimum $s=10$ was reached when the core was quite in. It is clear, however, that the sequence graph must actually fall to the abscissa and the curve is drawn to correspond with its resonance location. The graphs in figure 31 are thus an enlargement of figure 28 in sensitiveness and are at the same time pushed to the right, revealing new contours on the left.

If one again considers the descending branch of the sequence curve negative in phase, the ascending branch positive, as suggested by the dotted line, the doubly inflected curve resulting may be regarded as a better picture

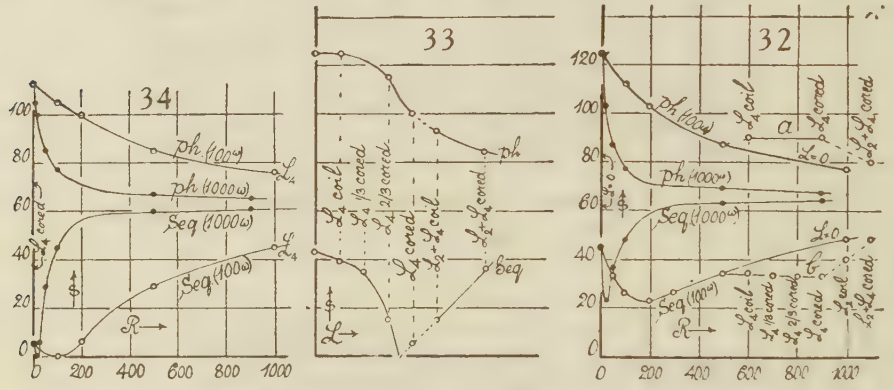

of the phenomenon, as a whole. At $s=0$, the sound passes from one telephone to the other. Apart from the ends, the main run of the graph is now nearly straight. The same is true of the Δs graph if the ascending parts of the sequence graph are regarded negative in phase and therefore to be added to the phase-graph. The Δs line is then surprisingly uniform in character, with the characteristic double inflection.

The interesting results in figure 31 deserve further elucidation, to be obtained by changing the resistance of the T' circuit simultaneously. Figure 32 gives a case of the kind, where R only is increased (in steps of 100 ohms and of 1,000 ohms as stated), without addition of L to the T' circuit. The feature of the diagram is again the minimum at about 200 ohms in the sequence-graph.

Figure 33 (equivalent to figure 31 but obtained under different L conditions) shows the corresponding effect of inductances, increased continuously by inserting the core into the L_4 coil in thirds of its length. The sequence-graph runs through $s=0$, as before.

In figure 32, the additional branches a and b indicated that when the same increments of L are applied when $R=500$ ohms, there is little appreciable

reduction of s and that L becomes effective only when it is relatively large in value $(L_2 + L_4)$.

In figure 34, the R-effect is investigated, beginning with the additional inductance of the cored L_4 coil, in the T' circuit. Naturally the s-values, as a whole, are reduced and the R minimum of the sequence curve now actually falls to zero at $R = 100$ ohms. The sequence-graph has been depressed and the minimum moved nearer the origin, whereas for high resistances the graph asymptotically reaches the preceding graph (fig. 32) for $L = 0$.

In figure 35, R is increased in steps, beginning with an inductance smaller (coil L_4 with core two-thirds inch; curves a, b) and larger (coils L_2 and L_4, not cored, curves c, d, e, f), respectively than observed in figure 34, in which the

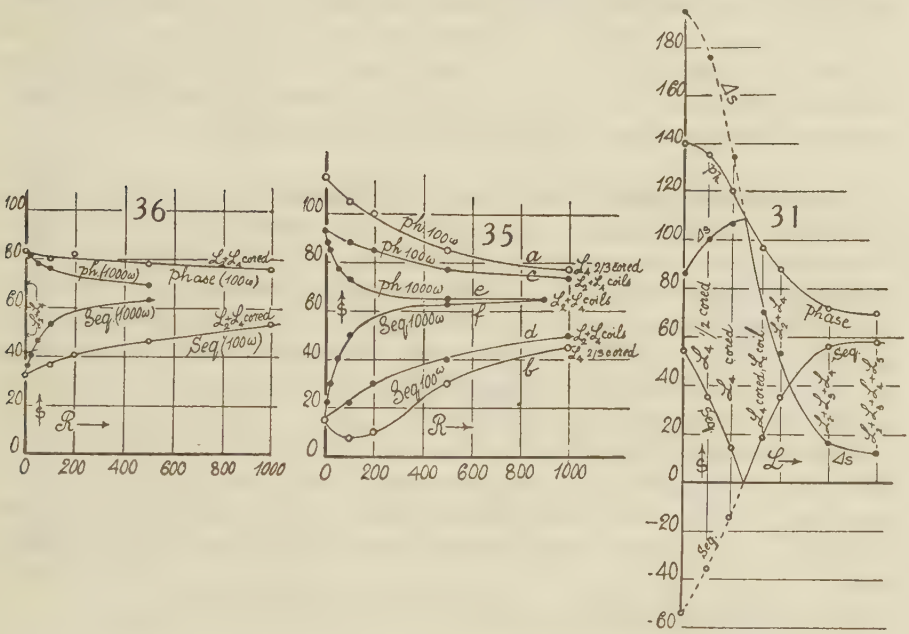

origin is near the sequence minimum. Again the latter has been moved to the right and raised (curves a, b); or moved to the left beyond the coördinates (curves c, d, e, f) consistently with the preceding results.

Finally figure 36 gives the corresponding results when L_2 and L_4 (both cored) are inserted in the T' circuit. The coördinates, as it were, are further displaced to the right in the same sense as in figure 35.

To summarize the cases, therefore: it is found that the s minimum of the sequence-graph moves into smaller R and s toward the origin, when L is successively increased until the minimum vanishes. Thereafter the sequence graphs (without the minimum) rise again as L increases further; but this may in part be due to the R-values of the new coils added in the later stages. The increased difficulty not only of obtaining an s minimum in the sequence graph (compared with the preceding case of L variation), but of bringing this mini-

mum down to $s=0$ when R is the variable, deserves notice. The next paragraph is a correlative illustration.

13. Single half layer—Using but one of the identical layers of the inductor I, figure 5, fringe displacements indicating the intensity of the middle node were obtained as summarized in figure 37. This is virtually a return to figure 28 for the series experiment, except that the nodal intensities are larger throughout. The decreased impedence is an advantage; but the high initial intensity of the sequence curve of figure 31 has been lost because of the double resistance at the beginning. By continuously inserting the iron coıes, it was here possible to bring the sequence curve actually to and through $s=0$, from which it follows that this must also have been the case in the preceding figures 27, 28, 31, where the relevant data are incomplete. The dotted curves indicate the passage through zero, where the phase opposition would be complete, when descending sequence branches are treated as negative in phase. They closely resemble figure 31, so that the remarks already made apply.

14. Incidental origin of initial phase differences—If the telephone-plates are exactly in opposed phases, the sequence-graphs should begin at the origin. This is very rarely the case. In the circuit-figure 5, the initial phase differences might be referred to the comparison made of primary and secondary; but in circuit figure 3, both telephone circuits are secondaries excited under apparently like conditions. Nevertheless, the sequence-graph begins much above $s=0$. Thus the inherent phase differences in large part are referable to differences in the induction coils.

To test this preliminarily, the secondary circuits (fig. 3) were combined differentially, by joining the telephone leads to the points and 3, 2, and 4 respectively, so that the induced currents traverse the telephones in opposite directions. The residual fringe displacements obtained were quite marked; viz,

First switch position, $s=35$ (Increased primary current) $s=55$
Second switch position, $s'=23$ $s'=40$

Thus it follows that the two secondaries I and I' in figure 2 are not equal, for neither s nor s' are zero, and that the telephones are not equally efficient in case of a reversal of current, since $s'>s$.

Moreover, in total strength, circuits figure 2 and figure 5 do not differ much; viz,

No. 3 { ph. 140 / seq. 33 } $\Delta s=107$ | No. 5 (in series) { ph. 140 / seq. 30 } $\Delta s=110$ | No. 5 (in parallel) { ph. 140 / seq. 60 } $\Delta s=80$

To throw further light on the question, experiments were made with the arrangement of figure 3, by putting resistance R first in the secondary I and telephone T and thereafter into the secondary I' and telephone T'. The results are given in figures 38 and 39 with the resistances in steps of 100 and of 1,000 ohms, as indicated, the fringe displacements s being mapped for each

case. The results are very different. As a whole the s-values of figure 39 lie much above those of figure 38, showing greater impedance (probably largely resistance) in the latter case, viz,

	Telephone T		Telephone T'	
	Initially	Finally	Initially	Finally
Phase.....	140	95	140	116
Sequence..	28	93	37	120
Δs.....	112	2	103	−4

so that the latter curves cross as in the above figures 12, 13, 14. Again, while the phase-graph for T falls more rapidly than for T', the sequence

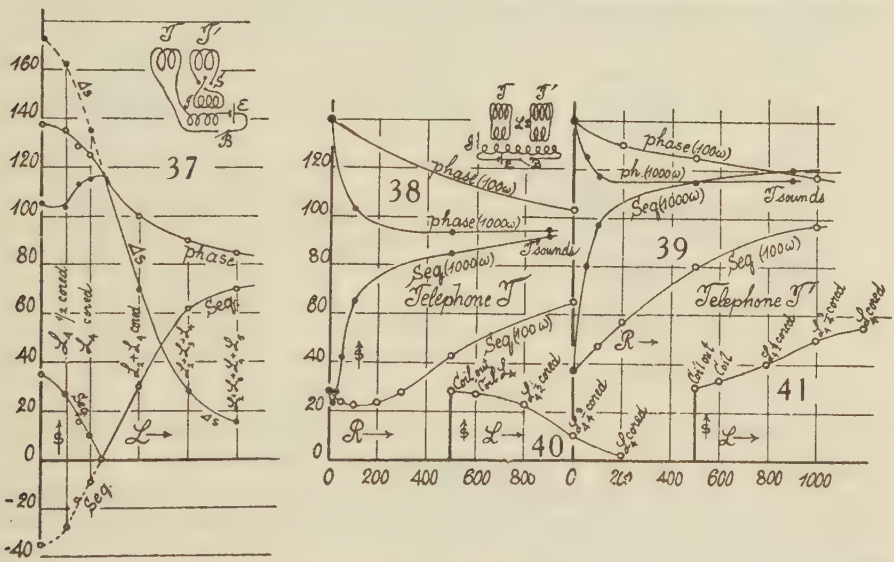

graph of T rises more slowly than for T', both of which culminate in the different s-levels, at the end, when one telephone is apparently silent. Finally, the insertion of resistances into T actually reduces the initial s-values, which pass through a minimum s but never approach $s=0$ (seq. graph, fig. 38). As a whole, therefore, the behavior (figs. 38 and 39) is very much as if IT were an outer coil of smaller inductance and larger resistance, $I'T'$ an inner coil of larger inductance and smaller resistance, wound about the same primary. The minimum sequence s of figure 38 will have to be referred to changes of phase due to R, since the current and phase difference ($\tan^{-1} L\omega/R$) both decrease with R.

To bring the minimum of figure 38 quite to zero is accomplished by inserting additional inductances L, continuously. I again used the choke-coil L_4, as above, and figures 40 and 41 show the results when the iron core is gradually pushed in. The abscissa is just reached in figure 38 (so that this

graph is ahead of the minimum) and with larger inductances, the curve would rise again as heretofore (figs. 31, 37). Figure 39 is beyond the minimum and s increases continually in the sequence graph while the telephone T' is being hushed.

It follows, therefore, that the method, figure 3, unless the coils have been specially wound, complicates the interpretation of results. These difficulties vanish in case of such methods as in figure 25, particularly when the two half-coils, if used, are joined in parallel. It is thus clear that in the latter cases the assumption of a phase difference between primary and secondary due to R, L, C is trustworthy.

The insertion of induction, after the sequence-graph (cf. fig. 40) has been raised by resistance, merely diminished the L-effect for $R=0$. Thus at $R=400$ ohms in figure 40, the graph drops from $s=35$ to $s=26$ for the full-cored L_4 coil

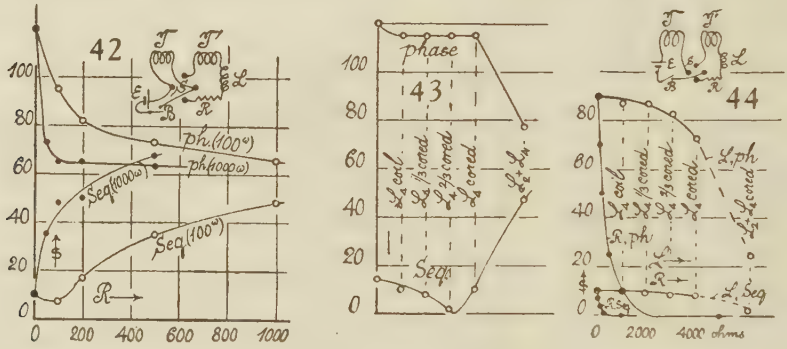

pretty uniformly. At $R=600$ ohms the fall of s is but two or three scale-parts, so that the L-effect is nearly negligible.

One may notice that whereas in figure 39 the phase-sequence graphs intersect, this is not the case in figure 38. Thus these observations agree with the explanation given in § 6.

15. Circuits without transformer—The design of figures 3 and 5 have the advantage for the present purposes of admitting large initial or inherent phase differences, equivalent to a lead in the telephone T' to be loaded. This is not at once the case with circuits of the type figure 1*c*; but these circuits, being simpler, are in a measure better adapted for computation. There is, however, liable to be some small inductive difference or its equivalent in the telephones, as shown in figures 42, 43, with the adjustment in parallel given in the inset, figure 42, B being the break. The effect of resistance is the usual fall of phase-graph and rise of sequence-graph, with some hesitation of the latter at the beginning. Figure 43, however, shows a small initial lead of the T' circuit, which could be wholly wiped out by gradually inserting the iron core of the L_4 coil as the sequence graph indicates. The lag of T' does not appear until after the whole of the L_4 core is thrust within the coil. The further inductance

L_2 acts in part through its coil resistance, which can not here be excluded, so that a broken curve results. The phase-graph is almost stationary with L_4, but drops rapidly with L_2+L_4. If the design (insert, fig. 42) is adjusted in series (insert, fig. 44), the current in the single circuit merely drops off, both with increasing R and L, as shown in figure 44. Both telephones cease to respond on loading, together. R is particularly effective.

16. Telephone-plate subject to an external magnetic field—The question occurred whether in case of the adjustment (fig. 42, insert), it would be possible to produce a lead in T' by external magnetic attraction. In figure 45, T shows the mouthpiece of the telephone, the bent magnet M being placed as near as possible to it, straddling the acoustic pipe t. The results given by the graphs in figure 45 are very definite. The vibration in phase is much diminished in strength, but is not otherwise abnormal. The sequence graph, below, is peculiar. The former lead at the beginning (field off)

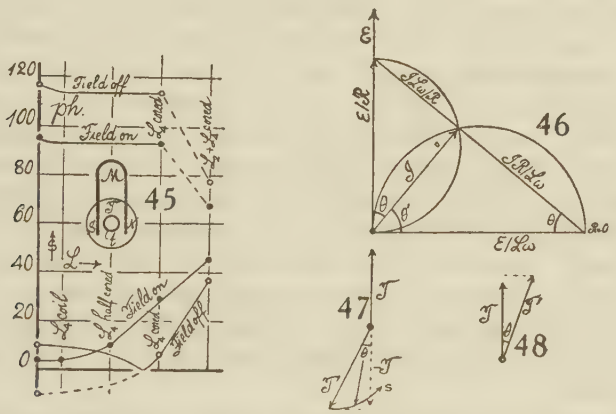

passing through zero with increased inductance, has practically vanished. Instead, the curve now rises continually and the divergence of curves is most marked when the sequence-graph, in the absence of field, is at zero. This implies that the sequence vibration is also less intense, so that the graph as a whole rises higher throughout when the field is on. If the lead in the sequence-graph (field off) is plotted negatively, as shown by the dotted line, the initial similarity of the two sequence curves is evident.

If the magnet M, figure 45, is reversed into the position NS from SN, its effect on s is similar but only about half as large. At the opposed telephone T the use of a second magnet gave only small differences. The effect observed is therefore incidental, depending on the mounting of the plate of the telephone.

17. Remarks—When a single telephone is active, the opposed plate functioning like a rigid wall, the nodal intensity s was found to be about two-thirds of the intensity observed when both are vibrating in phase. Hence, in so far as the fringe displacement s measures the nodal intensity, the vibrat-

ing plate in phase action contributes about as much intensity as the fixed plate reflecting.

In case of the adjustments, figures 3 and 5, we may to a first degree of approximation consider the vibration vector of the unloaded telephone T constant. In this case the vibration vector of the loaded telephone T' differs from it in magnitude and is set at a phase angle with regard to it, both of which vary with R and L in the above experiments. The magnitude eventually vanishes.

If we consult the usual diagram of relations between the quantities R, L, $\theta = \tan^{-1} L\omega/R$, figure 46, it appears that θ, in comparison with the corresponding change of the current I, increases most rapidly with L at constant R, when L is small; similarly $\theta' = 90° - \theta$ in relation to I increases most rapidly with R at constant L when R is small; for I under these circumstances is nearly normal (diametral) to the arcs of the corresponding circular loci of variation. We may therefore expect to find characteristic variations in the relations of θ and I at the beginning of the s-curves in the above graphs, as observed.

If in figure 47, T denotes the vibration vector of the unloaded telephone and T' the corresponding vibration vector of the loaded telephone at any instant, T' will be set at an angle to T. In the above work θ has appeared to be a lead, while T' was apparently larger than T. Hence the fringe displacement will depend on the difference of T and the projection of T' on T in the sequence curves and on their sum (fig. 48) in the phase curves. The s-effect will not be simply additive, however, for the reasons given at the beginning of this paragraph. Moreover, the s-curves do not distinguish between sign changes of phase, unless the curve branch is reversed as in figures 31, 37.

Hence, if $T' > T$, we may have the s-curves passing through zero (minimum) in the sequence graphs by the simple shrinkage of T' with L or R, where T remains constant.

Or, if T' and T are appreciably equal, we may have the sequence curves passing with increasing R through a minimum usually greater than zero, by the shrinkage of the angle θ taken as a lead, if $\cos\theta$ increases relatively more rapidly than T' decreases.

Or finally, if the lead θ passes through zero into a lag with increasing L, while T' remains relatively stationary in value, the s minimum should be much more strikingly reached, and for $T' > T$ easily pass through zero, as has been observed throughout the above experiments. Illustrative cases are seen in figures 31, 33, 37, etc., recalling that both an excess and a deficiency in T' may produce the condition for a central node, the activity passing from one telephone to the other. If the T' vector shrinks through zero and becomes positive (for reasons of the kind exhibited in figure 45), figure 47 would pass to figure 48 and the s-curves would cross for large R or L.

The complete explanation along these lines would of course require a further specification of data than is now available.

18. Zero methods. Primary and secondary—The difficulty with the above comparisons (equation (4), § 8) lies in the complicated equations which

would have to be used in any case to detach the L from the other quantities.* Greater convenience is to be expected if differential methods corresponding to the two circuits of two telephones T, T' in operation are substituted. Thus, for instance, the adjustment (insert, fig. 49), when tested out by a millihenry standard at LT' and the coil L_4 successively in $L'T'$ (secondary), gave results in the sequence graph

$L=10$ mh.	$s=24$ L_4 coil only	$L=10$ mh.	$s=10$ L_4 cored
35	14 L_4 coil only		14 L_4 ⅔ cored
			20 L_4 ⅓ cored

In figure 49 the graphs have been plotted linearly and from this (deducting the coil effect) 35, 25, 10 mh. would be estimated for the wholly or partially cored coil. The total $L_4=45$ mh. is nearly correct. But the conditions are clearly not so simple. The phase-graph changes but little in these cases (10 mh., $s = 83$; 35 mh., $s = 80$).

Putting the millihenry standard in the primary LT, the results are even more striking. Here 10 mh. passed the primary lead of 24 s into a lag of 10 s and 35 mh. increased this lag to 57 s.

19. Primaries only—Tests were begun with the adjustment without secondary adjustment I' shown in figure 50, the coils inserted at L and L' being compared. The sequence-graph only was observed, as the phase-graph varies but slightly. The upper three curves show the results obtained when the millihenry was put in LT and the coils only (not cored) in $L'T'$. The resistance of L_1 exceeds that of L_4.

The two lower curves give the corresponding results with one layer of the L_1 and the L_4 coils, cored. In both cases the phase difference passes through zero (dotted lines), particularly in the case L_4. Thus we obtain the following s-differences cored-uncored:

At 35 mh.	L_4 (cored), $\Delta s=37$	L_1 (cored), $\Delta s=-$
30	36	21
20	36	19
10	27	15

allowing for the positive and negative values in the lower graphs. These Δs values are equivalent in the millihenry region to which they apply on the same horizontal, in the mean to $L_4=35$ mh. and $\frac{1}{2}L_1=20$ mh. In so far as the interpretation is admissible, Δs falls off at the lower stages (10 mh.) in the table.

In figure 51 the results of experiments with the millihenry standardal one inserted in the T' circuit and also with the same standard and one layer of the L_2 cored coil, inserted in the same circuit. The graphs here would be practically straight if the L_1 semi-coil could be taken at 20 mh., which, however, is too small, unless the solid core is ineffective.

In figure 52 the measurements for the L_4 coil and the one and two layered L_1 coil are carried out with greater fullness. Within the errors of reading

*The values of R and L of all parts of the apparatus will be found in table 1 (above), with which the present estimates may be compared.

the results agree with the preceding set (fig. 50), though the L_4 curves (fig. 53) are straighter. The graphs of the coil L_1, in whole or halves, preserve their characteristic curvature. Three different cores (*a*, solid; *b*, wire; *c*, two bundles of wire) are used. In the cored half-coil there is very little difference for an addition 0 or 10 mh.

As a rule, the Δs values (cored-uncored) increase with L; viz,

	$L_1/2$	L_1	L_4
$L=$ 0 mh.	$\Delta s=12$	$\Delta s=38$	$\Delta s=27$
10	17	31	29
20	24	28	39
30	22	32	39

The mean values are of the same order as before.

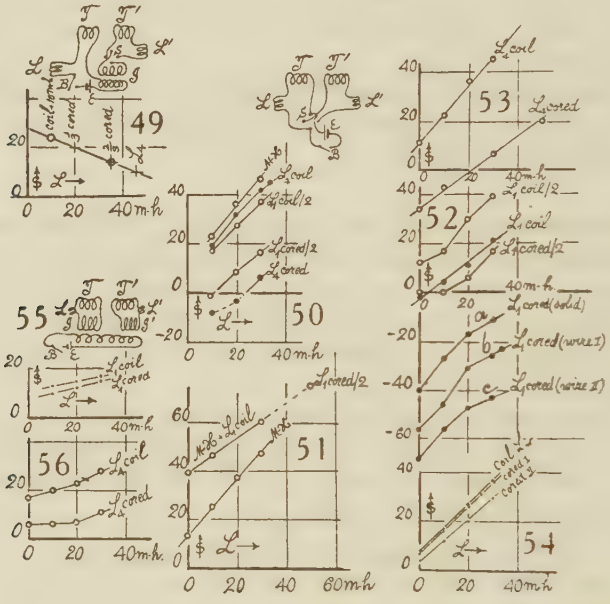

If the initial conditions (R, L) in the two branches T and T' are restored, we might assume that the horizontal distance apart of the graphs will be the L required. Using this as an approximation we get

	L_4	$L=36-0=36$ mh. at $s=11$
(Solid core)	$L_1/2$	$L=26-0=26$ $s=12$
(Solid core)	L_1	$L=50-0=50$ $s=-2$ (prolonged)

an order of values, like the preceding, evidencing the ineffectiveness of the solid core in L_1. The mean slope of the curves naturally decreases rapidly as the inductance contained increases. Thus in case of L_4, figure 53, $s=1.2$ per millihenry falls to $s=0.9$ per millihenry after the L_4 iron core is inserted.

The contrast of the solid and wire cores of L_1 (curves *a*, *b*, *c*) is noteworthy. The solid core was 2 cm. in diameter; the wire core (case *b*) consisted of about 60 threads of iron wire, each 0.05 cm. in diameter; the wire cores (case *c*)

of 120 threads of the same wire. If we imagine the curves a, b, c prolonged till they intersect the axis for $s=0$, it will be seen that the L equivalent has been increased enormously, as must obviously be the case compatibly with the lamination.

The tendency to linear graphs for small inductances and small increments of L is again apparent in figure 54, where the weak coil L_w, wire-cored as stated or not, is compared with the millihenry standard. Shifting horizontally, L_w comes out somewhat less than 10 mh.

20. Zero method with the secondary—With the adjustment, figure 3 (or insert fig. 55), the method is necessarily less sensitive, because of the excess inductance I, I' already in the opposed circuits. The graphs obtained on comparison of the L_4 and L_1 coils, cored or not, as stated, rise with the millihenries opposed but slowly. They are farther apart in case of L_4 (fig. 56) than of L_1 (fig. 55), because of the solid core and the inherently greater resistance in the latter case. This method therefore contemplates the comparison of large inductances and would in such a case show acceptable results, as already indicated in the preceding work.

21. Exchange of loads. Circuits in parallel—The above relations are throughout complicated. It was therefore thought desirable to devise means for exchanging inductances only. The adjustments are indicated in the insert of figure 57, where T and T' are the opposed telephones, E the cell with periodic break, B and S, S' switches for reversing the current in T or T'. The inductances L and L' can be inserted either into the circuits T and T' respectively, as in the figure, or reversed so that L is inserted into the T' and L' into the T circuit. This is done by the four-fold commutator K, in which the brass strips a, when pointing toward the left, join the corresponding four contacts (1 to 4) below, or when pointing to the right (swivel) join the contacts 3 to 6 below. Contacts 1 and 5, 2 and 6 are metallically joined, and 1 and 2 or 5 and 6 contain the inductance L, 3 and 4 the inductance L'. The position of the strips a, as in figure, will be denoted by I, the other portion by II; so that for I, L is in the T and L' in the T' circuit.

In the experiments following L is the continuously variable millihenry standard, L' the coil L_1 with or without iron cores, solid or fasciculated wire as stated (see scheme in figure 57). The fringe displacements s obtained are given in figure 57 for loads L of 10, 20, 30 millihenries as abscissas, when the counter-load is the coil L_1 only. In figure 58 the solid iron core is thrust into L_1 and in figure 59 the core is of wire. The three cases represent a succession of increasing inductance with the resistances constant.

The phase-graphs usually present no marked peculiarity. Their mean s-values (I and II) decrease with the load L_1, while at the same time the graphs nearly coincident in figure 57 (uncored) separate widely in figure 59. The II graph in 59 is in part even above the II graph in figure 58 for a lower value of L_1.

Very characteristic differences appear in the sequence-graphs. In figure 57 the observed graphs cross. This indicates deficient singing in the position *I* of the millihenry circuit, since the graph rises with the increasing millihenry inductance, while the L_1 (coil) circuit carries the sound. The graph *II* has therefore been reversed into the dotted line *II'*, figure 57, for now the opposite conditions rule. The two graphs are parallel and the rate is about 1.1 *s*/millihenry for each.

In figure 58 the sound is carried by the millihenry standard circuit in both positions *I* and *II*. The impedance L_1 is now excessive. The graphs have therefore been reversed, as shown in *I'* and *II'*. The two graphs are here

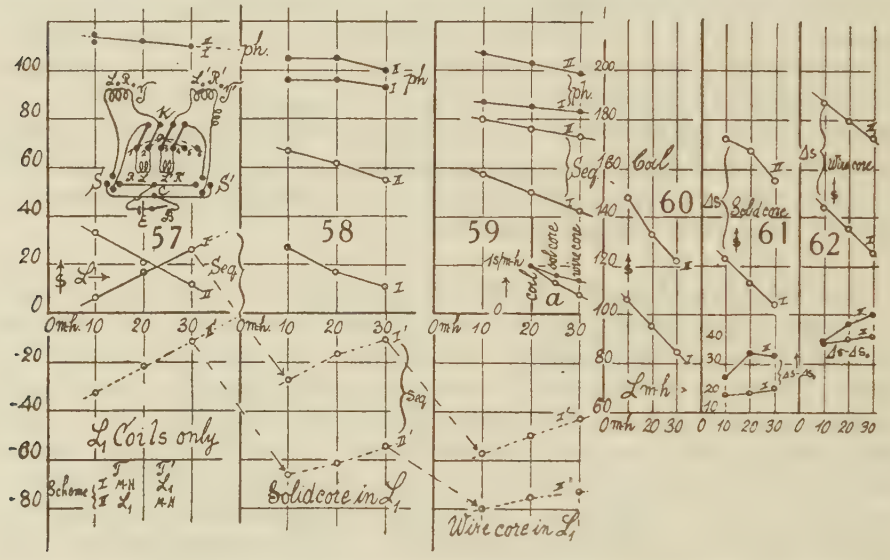

farthest apart. The mean rates are respectively 0.8 *s*/millihenry for case *I'* and 0.6 *s*/millihenry for case *II'*.

In figure 59 the relations are of the same nature, but reach a higher degree of displacement. The reversed curves *I'* and *II'* are lower than before, but (unexpectedly) nearer together. The rates have decreased further to 0.7 *s*/millihenry for case *I* and 0.4 *s*/millihenry for case *II*. This gradual fall of rate is summarized in the insert *a* in figure 59.

The drop below the corresponding graphs of figure 57 has been:

Fig. 58	*I*	*II*
10 mh.	*s* = 34	34
20	34	40
30	37	43
Mean	*s* = 35	39
(1) Mean rates *s*/mh.	.80	.60
(1) *L* estimated	44	65 (solid core)
(2) Mean rates *s*/mh.	.90	.83
(2) *L* estimated	39	47 (solid core)

Fig. 59	*I*	*II*
10	*s* = 64	47
20	66	54
30	67	61
	s = 66	54
	.70	.40
	94	135 mh. (wire core)

Since in each of the positions *I* and *II* there is a mere exchange of the excess inductance, the first results (1) are rather disappointing. The reason of this, however, is the rapid change of the rates of fringe displacement per

millihenry s/mh. as the load L increases. Thus it is better to take the mean rate of the initial graphs (fig. 57 s/mh. = 1 for position I and 1.05 for II) and the final graph in question. In this way it was thought the results (2) would be improved as a whole and rendered more trustworthy. In figure 58 the trouble is to be associated with the curved graphs. The effect of lamination has thus increased the inductance more than twice, but the estimates are all too low.

Finally, a comparison of the Δs-values (phase minus sequence) may be given:

Inductance	10		20		30		10		20		30		10		20		30 mh.	
Position..	*I*	*II*	*I*	*II*	*I*	*II*	*I*	*II*	*I*	*II*	*I*	*II*	*I*	*II*	*I*	*II*	*I*	*II*
Δs....	−106	−148	−95	−133	−84	−132	123	172	113	167	104	155	144	187	135	179	125	172
$\Delta s-\Delta s_0$.	.....		.....		.....		17	24	18	34	20	33	38	39	40	46	41	50

The data for $\Delta s - \Delta s_0$, which indicate the difference between the cases of cored and uncored coils, are here far from constant, particularly in the position II. They are also not much more than half as large as the corresponding s-values of the preceding table.

Apart from irregularities, the data for Δs make a coherent graph of rising inductances as shown in figures 60, 61, 62. For the position I the rates are nearly the same; for the position II, for some reason, there is irregularity, the mean results being:

Position		Coil	Solid core	Wire core
Rates	*I*	1.10	0.95	0.95 s/mh.
	II	1.3	.9	.75
Mean $\Delta s-\Delta s_0$	*I*	....	18	40
	II	....	30	45

The smoothed data for L so to be found would be far too small. They are only about half as large as obtained from the sequence-graph alone. Since the phase and sequence graphs trend toward each other, such a discrepancy would be expected; but it was not estimated to be so large.

22. Further experiments—It appears from the preceding methods that the sequence-graph taken alone is better adapted for practical purposes than the combined graphs (Δs). A number of further experiments were, therefore, tried out with the coils of small resistance L_4 and L_w. The data were given for the latter in figures 63, 64, 65 with the coil, L_w, respectively empty, cored with solid iron, and wire cored. From these one obtains:

Coil empty			Solid core in		Wire core in	
Position.....	*I*	*II*	*I*	*II*	*I*	*II*
Mean s =	36	0	32	−2	27	−5
Mean $s-s_0$	....	..	4	2	9	5
Rate r	1.05	.5	1.10	.55	1.0	.75s/mh.
Mean $(r+r_0)/2$	...	..	1.07	.52	1.03	.63s/mh.
Estimated L_w	...	..	3.7	3.9	8.8	8.0 mh.

so that for positions *I* and *II* the agreement is within 1 millihenry and not much below the true values 11 mh.

For the coil L_4 similarly (figs. 66, 67):

	Coil empty		Coil wire cored	
	I	*II*	*I*	*II*
Position				
Mean s	33	−1	+1	−33
Mean $s-s_0$	....	..	32	32
Rate r	1.05	.4	.4	1.05
Mean rate $(r+r_0)/2$	....	..	.72	.73
L_4 estimated	....	..	44	44 mh.

data which happen to coincide. Results computed from the individual observation at 10, 20, 30 millihenries of the standard give practically the

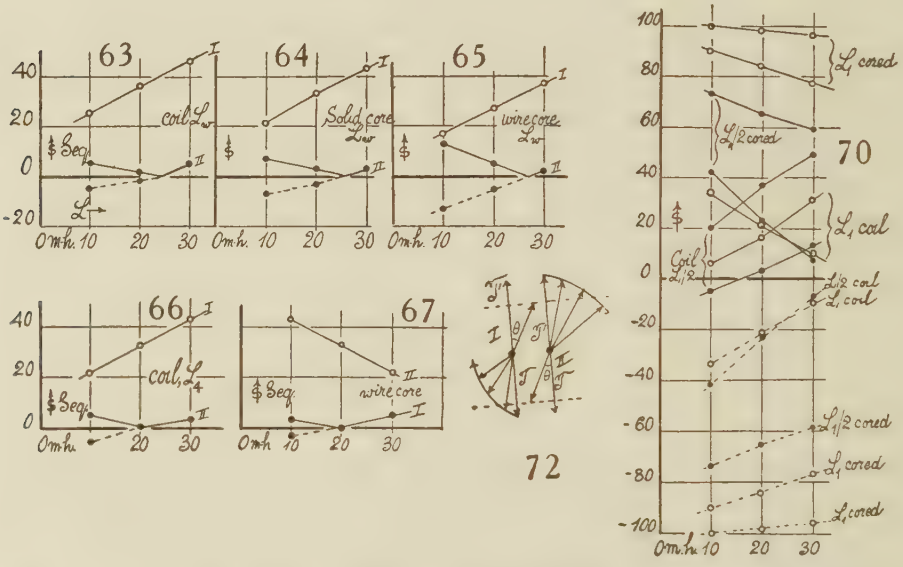

same values and are nearly correct. Readings near zero are usually trying, because the small displacements and slow accommodation of fringes make it difficult to pick out the resonance pitch. As the rate for mean $s=0$ is large, this difficulty makes such measurements rather crude. A sharp adjustment in pitch is essential, and at $s=0$ a tendency to multiresonance is often in evidence.

A number of similar experiments were completed, without, however, reaching any marked improvement, and a uniform schedule of rates (s/mh.) at definite mean s-values could not be constructed. For example, on comparing a given coil of two parallel layers with a single one of its layers, results (figs. 68, 69) were obtained in which the means only were in proper ratio. Thus $2L=83$ *I;* 107, *II;* mean 95 mh., and $L=34$ *I;* 66, *II;* mean 50 mh. etc., point out an inductive difference, or else a difference in sensitiveness in

the telephones. Figure 69, moreover, indicates a serious case of the difficulty of obtaining the rates s/mh. when mean $s=0$. It was necessary to interpolate them. In the half-coil, the discrepancy of the halved resistance must first be allowed for.

In the further measurements of the relative inductance of coil, and half-coil with large fringe displacements (3 storage-cells in circuit), the proportionality of the displacement s to the effective currents seems to have broken down. Thus

Position....	$L=10$	20	30 mh.	Mean rate		
$\frac{1}{2}L_1$	I.....$\Delta s=62$	60	62	1.6	38	mean $L_1/2=$ 61 mh.
	II.... 68	68	68	.8	84	
L_1	I.....$\Delta s=96$	100	108	.95	107	mean $L_1=104$ mh.
	II.... 66	67	86	.75	101	

The individual results are given in the usual way in figure 70, the circuits being adjusted as in figure 57. The plan of assuming proportionality between the displacements Δs and rates (s/mh.) together with the effective currents, is of course a shortcoming of the method pursued, as a whole, and was merely adopted tentatively. With an increase of range, the discrepancy becomes rapidly more noticeable.

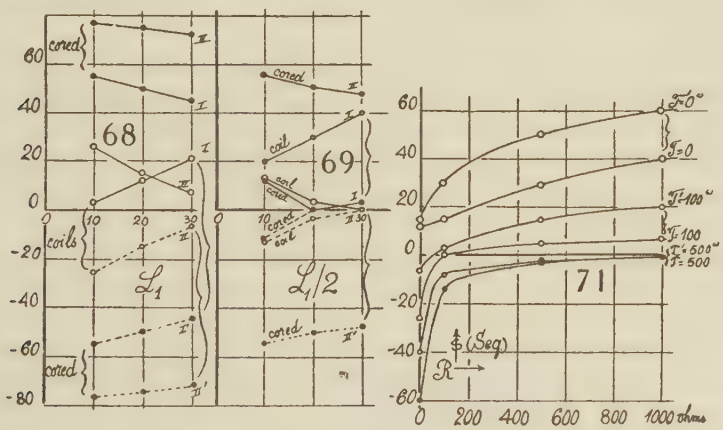

To throw additional light on these phenomena (cf. § 14) resistances R in two identical rheostats were directly compared as detailed in figure 71. Keeping the resistance of one circuit constant ($R=0$, 100, 500 ohms) the other was increased in steps. The graphs show at once that one telephone is more efficient than the other. There seems to be no crossing of curves here, indicating that the change of phase due to R is not of much importance, R being usually large. The response, moreover, is feeble for excess resistances above a few hundred ohms in one of the circuits, unless more cells are put in use. This implies correlative limitations in the L_w work, although the phase-change is here continuous.

It is also probable that this difference of response will vary with temperatures, owing to expansions of the case holding the telephone-plate.

If we consider the distribution of current in the parallel circuits T and T' and write $Ri = e = \text{const.}$, etc., the equations reduce to

$$i_0 (1 - R_0/R) = \Delta i$$

where R_0 is the resistance kept constant in one of the circuits. Hence if the sequence condition is perfect, $\Delta i = 0$, and $R = R_0$, where R, R_0 include the initial resistances as well as the added resistance. This presupposes that the telephones, etc., are identical and makes no allowance for their inductance. If the plate-mounting of one contributes to greater sensitiveness than the other, $\Delta i = 0$ is a spurious balance, as in the case of figure 71. The subject will be treated in the next section.

23. Summary. Quantitative considerations—The results contained in the graphs submitted imply that the two telephones are unequally sensitive. This is a little puzzling, since their resistances and inductances are the same ($R = 84$ ohms, $L = 0.06$ hen.) and the resistances of the standard ($R = 9.7$ ohms) and of the standard coil ($R = 9.9$ ohms) are about the same. Everything should therefore depend on the external resistance or inductances, and if these are the same there should be no change of fringe displacement, s, on commutation.

The difference in the paired and similar telephones may be due to the set of the plates; but as it occurs very uniformly, so far as I have observed, it probably results from an induction impulse chiefly in one direction. In case of the sequence-graph, the plates of the telephone would therefore be attracted and released, respectively, at any given time. These forces are liable to be unequally strong, the attraction probably being in excess.

Hence if we call the amplitudes or displacement vectors of the plate T' and T, where $T' > T$, the postulates $T' \cos\theta < T$ slightly, and $T' > T \cos\theta$ in marked degree would account for most of the observations, if θ is the lag due to the inductance L, initially. Subsequently T or else T' are reduced by the successively increasing inductance L of the standard, as indicated by the diagram (fig. 72). In case I the graph rises; in case II the observed graph falls and $s = 0$ is reached much later.

Since $\tan\theta = L\omega/R$ and $L = 0.38$ hen. (cored coil 0.32, telephone 0.06) while $R = 94$ ohms (coil 10, telephone 84) and $\omega = 2{,}765$, we find $\tan\theta = 11.2$, or $\theta = 84.9^0$, and $\sqrt{R^2 + L^2\omega^2} = 1{,}054$ ohms, $L\omega = 1{,}050$.

On the side of the standard $R = 94$ ohms also, while the L changes from 0.010 to 0.035 hen., thus

$L =$	0.010	0.020	0.030	hen.
$\theta =$	16.4^0	30.5^0	41.4^0	
$\sqrt{R^2 + L^2\omega^2} =$	98	111	125	ohms
$L\omega =$	27.6	55.3	82.9	ohms

when L and the standard are exchanged, the specifications (except L) remain about the same.

If we take the case of the sequence-graph, since the currents i and i' in the branches T, T' (fig. 57, inset) are in parallel,

$$\varepsilon = i\sqrt{R^2+L^2\omega^2} = i'\sqrt{R'^2+L'^2\omega^2} = \Delta i/\Delta\sqrt{R^2+L^2\omega^2}$$

follows as usual. But as the equality of fringe displacements s, s', is primarily in question, we may then postulate for small currents, $i=s/c$ and $i'=s'/c'$, in view of the difference of telephones in question. Hence the last equation reduces to

$$\varepsilon = \Delta s/\left(c/\sqrt{R^2+L^2\omega^2} - c'/\sqrt{R'^2+L'^2\omega^2}\right)$$

If $\Delta s = 0$ in the sequence graph, the denominator must also be zero. Thus

$$R^2+L^2\omega^2 = (c/c')^2\,(R'^2+L'^2\omega^2).$$

Here the values of R, L, etc., are the total resistances and inductances. If we replace R by $R+R_0$, L by $L+L_0$, etc., where R, L are the external and R_0, L_0 the internal data, the modified equation is

$$(R+R_0)^2+(L+L_0)^2\omega^2 = (c/c')^2\,((R'+R'_0)^2+(L'+L_0)^2\omega^2)$$

This equation on commutation becomes

$$(R_1+R_0)^2+(L_1+L_0)^2\omega^2 = (c/c')^2\,((R'_1+R'_0)^2+(L'_1+L'_0)^2\omega^2)$$

where L_1 and L' are read off on the standard.

Now, in the above circuit the resistances R are the same; *i. e.*, $R=R'=R_1=R'_1$; $R_0=R'_0$, also $L_0=L'_0$, and $L=L'_1$ is the constant exchanged inductance. Hence if we subtract the two equations

$$(L+L_0)^2-(L_1+L_0)^2 = (c/c')^2\left\{(L'+L_0)^2-(L+L_0)^2\right\}$$

This equation determines L if c/c' is known for a previous determination with known L and L_0, since

$$\left(\frac{c}{c'}\right)^2 = \frac{(L+L_0)^2-(L_1+L_0)^2}{(L'+L_0)^2-(L+L_0)^2}$$

where L_1 and L' are given.

The difficulty of applying this equation to graphs figure 57 et seq. is that $\Delta s = 0$, or the intersection of the graphs with the abscissa would have to be extrapolated, and this is only feasible in figure 57, where unfortunately the L_0 of this coil without core was not directly determined; but equation states, nevertheless, if the data given be inserted,

$$(c/c')^2 = \frac{(L+60)^2-(65)^2}{(100)^2-(L+60)^2}$$

so that L must lie between 40 and 5 mh.; or, since $c/c'>1$, between 25 and 5 mh. In general, however, $i=s/c$ is not adequate, the more approximate equation being of the form $s_0=se^{i_0/i}$, which is here inconvenient.

When the sequence-graphs cross, as in figure 57, the unknown inductance is determinable at once. If we rewrite the first of the above equations and

remember that here $R=R'$, etc., that L (constant) is exchanged, $\Delta s/\epsilon$ remaining constant on commutation,

$$c+c'=c\frac{\sqrt{R^2+L^2\omega^2}}{\sqrt{R^2+L'_1{}^2\omega^2}}+c'\frac{\sqrt{R^2+L^2\omega^2}}{\sqrt{R^2+L'^2\omega^2}}$$

but at the point of intersection $L_1=L'_1$ whence $L=L_1$. In figure 57, therefore, the inductance of the coil is 23 mh.

From this and the numerical equation for $(c/c')^2$ the result is

$$c/c'=\frac{\sqrt{4421}}{\sqrt{3111}}=1.19$$

indicating the degree of inequality of the two telephones in relation to the sequence graphs and resulting from the asymmetry of vibration of plates.

Such cases as figures 58, 59, etc., would have needed a much larger standard of comparison, L.

Graph 71, obtained with the mere exchange of resistances, merits some further attention. If R is the fixed resistance commutated, R' and R'' the counter-values corresponding to positions I and II, since internally $L'_0=L'_0$ and $R_0=R'_0$, the equations reduce to

$$\frac{c+c'}{\sqrt{(R+R_0)^2+L_0^2\omega^2}}=\frac{c}{\sqrt{(R''+R_0)^2+L_0^2\omega^2}}+\frac{c'}{\sqrt{(R'+R_0)^2+L_0^2\omega^2}}$$

A solution of this equation is $R'=R''=R$, so that the paired curves of figure 71 intersect near $R=0$, $R=100$, $R=500$ ohms.

The case of $\Delta s'=0$ and $\Delta s''=0$, for the two positions I and II, is available for $R=100$ ohms. The other cases ($R=0$ and $R=500$) do not reach the abscissa. We thus have again

$$\frac{c'}{c}=\frac{\sqrt{(R+R_0)^2+L_0^2\omega^2}}{\sqrt{(R'+R_0)^2+L_0^2\omega^2}}=\frac{\sqrt{(R''+R_0)^2+L^2\omega^2}}{\sqrt{(R+R_0)^2+L^2\omega^2}}$$

If we insert the values $R=100$, $R'=50$, $R''=150$ ohms, as given by the graphs and the constants $L_0=0.06$ and $R_0=84$, we obtain $c/c'=1.16$, in both cases, which agrees very well with $c/c'=1.19$ deduced from inductances, in the preceding section.

In the semi-coil graphs in figure 69, another case of intersection occurs at about $L=0.007$ henry. The equations for $\Delta s'=\Delta s''$ (positions I and II with identical Δs), $R/2$ and $L/2$ for the coil would now be:

$$\frac{c+c'}{\sqrt{(R/2+R_0)^2+(L_0+L/2)^2\omega^2}}=$$

$$\frac{c}{\sqrt{(R+R_0)^2+(L_0+L')^2\omega^2}}+\frac{c'}{\sqrt{(R+R_0)^2+(L_0+L'')^2\omega^2}}$$

Since $L'=L''$ at the intersection, the equation reduces to

$$\left(L_0+\frac{L}{2}\right)^2=\frac{R^2}{\omega^2}(R_0+3R/4)+(L_0+L')^2$$

Inserting $L_0=0.06$, $R=10$, $\omega=2{,}765$, $L'=0.07$, the value of $L=0.016$ henry is obtained.

We can here also use the datum L_1 for $\Delta s=0$ by prolonging the graph *I* till it meets the abscissa. Thus $L_1=10$ mh. and the corresponding $L_2=30$ is found directly from the graph *II*. Here the equation reads

$$\left(\frac{c}{c'}\right)^2=\frac{(R/2+R_0)^2+(L_0+L/2)^2\omega^2}{(R+R_0)^2+(L_0+L_1)^2\omega^2}=\frac{(R+R_0)^2+(L_0+L_2)^2\omega^2}{(R/2+R_0)^2+(L_0+L/2)^2\omega^2}$$

Equating these values, reducing and inserting the data given, the result is $L=0.019$ henry. The inductances 16 and 19 mh. are both low as compared with $L=23$ mh. inferred from the double-coil measurement; but the trouble lies in the crude graph used and not in the method and could be easily rectified.

24. High-resistance telephones. Zero methods—It was anticipated that in dealing with larger inductances, the radio telephones would be more useful. Furthermore, an enlargement of the end connections of the pipe joining the paired telephones suggested itself. The junction above was made with the aid of perforated rubber stoppers and quill-tube connectors. In the present case the tube ends were attached to the telephone mouthpieces with cement, directly, in order to introduce the least obstruction possible. The result, however, was but a slight rise in pitch, from the a' above to $\flat b'$ in the present adjustment.

At the outset great confusion was experienced, afterwards traced to a slightly loose cap in one telephone. With the parallel adjustment of figure 73, the telephones together, and for positions *I* and *II* of the switch, gave at the maximum but

$$I:\ s=65,\ c'' \qquad II:\ s=50,\ d''$$

with a decided difference in pitch. The telephone *T* alone gave *I:* $s=0$ and *II:* $s=50$, a' to $s=20$, e'', data which indicate the seriousness of even a slight leak.

After remedying the defect, the individual telephones showed

$$T\begin{cases} I: & s=120,\ \flat b \\ II: & \quad 70,\ \flat b \end{cases} \qquad T'\begin{cases} I: & s=100,\ \flat b \\ II: & s=\ 60,\ \flat b \end{cases}$$

The pitch has thus become fixed; but the telephone circuits are nevertheless unequally responsive; while both are more sensitive in the *I* position than in the *II* position of the switch (switches being here provided for both telephones). This is probably the inevitable exchange of attraction and release already discussed.

To use the telephones together it was necessary to reduce the storage-cells, *E*, from 3 to 2. Even then the fringes at $\flat b'$ and $\flat b''$ pitch went just out of the

field. Figure 73 gives evidence of the extreme sharpness of the resonance crests for the *I* position of the switch (phase). Below *e'*, however, there is multiresonance which is difficult to construe, as a definite ♭*b* crest could not be found, unless the *c'* crest here replaces it. The occurrence of the sharp, strong ♭*b''* crest must have had an analogue in the above work, though for some reason it was not detected. It may have been deadened by the quill-tube connectors.

The sequence curve, figure 74, is very weak throughout and practically without elevation at ♭*b''* and ♭*b'*. It has, however, picked up its own small harmonies at *f'* and *f''* with a little one at *b*. It follows that the balance in the absence of auxiliary inductances and resistances is apparently rather better here than above, but this is probably due to the fact that the currents are now excessive, *i. e.*, the limit displacement of both telephone-plates has nearly

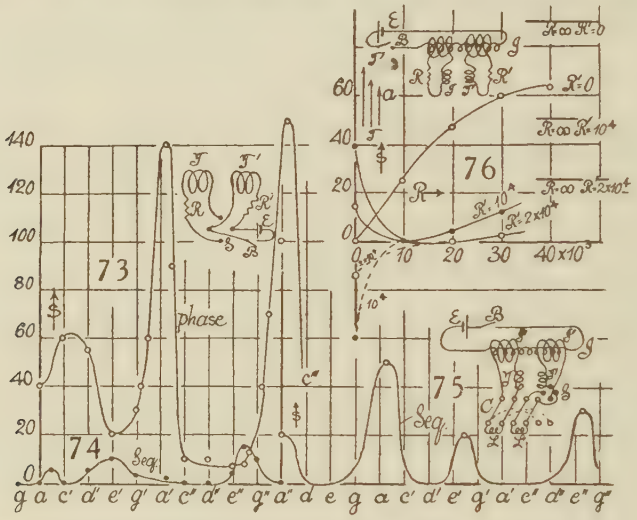

been reached in each telephone, so that small differences of current are no longer registered. Similarly, the inductions may reach limits.

It is interesting to inquire into the cause of the *f* crests in the sequence-graph (fig. 75) and the suggestion is at hand, since the *f* is the fifth of ♭*b* and the telephone note is rich in overtones. In the sequence-graph, therefore, while the ♭*b* is eliminated, the *f* overtone would not be. In fact, if we take the usual equations $y=a \sin(\varphi-\varphi_0)$ and $y'=a' \sin(\varphi-\varphi')$, the compound harmonic is $y+y'=A \sin(\Phi-\psi_0)$ where $\tan\Phi_0=\Sigma a \sin\varphi_0/\Sigma a \cos\varphi_0$ and $A^2=(\Sigma a \sin\varphi_0)^2+(\Sigma a \cos\varphi_0)^2$. Hence, if we put $a=a'$, $\varphi_0=0$ and $\varphi'_0=\pi/2$ for the *f* harmonic, it follows that $\Phi_0=45^0$ and $A=a\sqrt{2}$; so that the *f* is not eliminated but appears $\sqrt{2}$ times more strongly in the compound note than in either harmonic separately.

For the ♭*b* phase-graph in the same way $A=a+a'$ and for the sequence-graph $A=a-a'=0$, as hitherto assumed. A divergence enters, however, as *s* is only proportional to the effective current within a small range near the origin.

In the balanced sequence-graph there is probably no audible fundamental $\flat b$, inasmuch as a single wave runs from end to end of the tube without interference.

25. The same with small inductor—As it is the chief purpose of the present adjustment to meet the case of large resistances and inductances, the small inductor I, figure 75, was inserted as there shown, using the device C for the exchange of auxiliary inductances L, L', etc., as already explained. Each telephone, T, T', has its own secondary and T' is provided with a switch S. B is the periodic break. Under these circumstances a single cell at ε will throw the crests of the phase-graph far out of the field of view, the curve in the absence of external inductances rising nearly twice as high as in figure 73. The sequence-graph (fig. 75) is correspondingly developed with the f crests sharper than in figure 74. The strong b crest here obtained is a new feature and there was a further marked development even as low as c. These crests, however, are to be avoided and the measurements made corresponding to the sharp $\flat b''$ or $\flat b'$ resonance in the phase-graph. Taken singly, the telephones produce fringe displacements of $s=120$ to 130, one of the telephones being kept free from current. Taken together in sequence, there is no displacement at $\flat b'$, as figure 75 shows.

There are two difficulties encountered in making these experiments: The first is the sharpness of the resonance crests; the other, the rather slow growth of the maximum displacement. There seems also to be a loss of sensitiveness in the lapse of time, for which many reasons might be assigned. Hence, in the examples given in figure 76 of the effect of auxiliary resistances ($R=0$ to 40,000 ohms) in the T and T' circuits, there is often a lack of precision in the graphs. The data s refer to a resistance R (in thousands of ohms) in the T circuit and R' in the T' circuit. The limiting fringe displacements for $R'=\infty$ is also indicated. The dotted lines are reversals, showing change of phase between telephones. The results here are practically the same on commutation. In case of $R'=0$, the curve given is probably nearly right. When $R'=10{,}000$ or 20,000, the sensitiveness soon drops off. In the latter case neither $R=10{,}000$ nor $R=20{,}000$ give perceptible fringe deflections and for $R=\infty$, $s=25$ only. As the displacement vector of the T' plate decreases with R', the excess of the T plate vector is first registered in the sequence graphs and ultimately ($R=\infty$) the excess of the diminished T' vector. This is indicated figuratively at a, figure 76.

The endeavor to compensate a resistance by an inductance is marked by more complicated behavior. To begin with, a relatively small inductance of the wire-cored coils L_1, and L_4, it was desirable to enlarge the sequence graphs by using the storage-cell with 20 ohms resistance in the primary instead of the former 30 ohms. The graphs a of figure 77 are for this reason higher than in figure 76 and the phase-graph would be quite beyond the field charted. Considering the difficulties mentioned, the graphs of figure 77 are satisfactorily smooth. They show that in the II positions of the double commutator

(C, fig. 75) no balance, but only a flat minimum, is possible, whereas in the I position the balance occurs (appreciably at least) at $R=0$. The lines a, I and II, intersect at about $R=4{,}000$ ohms.

To further exhibit this behavior a larger inductance L_3 given by the secondary of a small lecture model of an induction coil (6 cm. long, 4 cm. diam.), from which the core could be withdrawn, was tested. The results are given, figure 77b, and are a further development of the a set, inasmuch as the minima now appear for both positions I and II of the C commutator. These curves would intersect at about 40,000 ohms, probably, as the fringe displacements when $R=\infty$ are greater for position I than for II of the commutator C. Initially curve I is always below curve II, as in curve a.

Finally (fig. 78, $R'=0$), the graphs for the combined inductances $L_1+L_3+L_4$ were tried out. They correspond very closely to the b curves of figure 77. The s displacements are naturally throughout smaller. The minima are a more pronounced feature of the graphs and farther to the right.

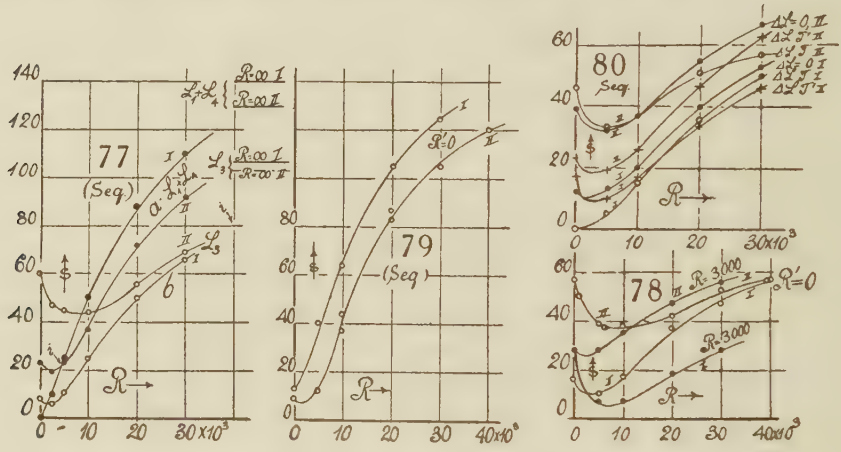

The endeavor to bring these graphs ($R'=0$) to approximate coincidence at the beginning ($R'=0$), by inserting additional resistance ($\Delta R=3{,}000$) in one of the T circuits gives rise to the curious increased departure from each other of the two graphs, also exhibited in figure 78. The coincidence has, as it were, been displaced from $R=40{,}000$ to $R=0$.

Thus the evidence indicated, in the first place, that the paired secondary coils, I', I'', of the inductor I of figure 75, are unequal. To test this directly, excess resistances R and R' are again compared as in figure 76, but with the present enhanced sensitiveness seen in figure 79. The curve $R'=0$, for position I, is here throughout above the curve of II, even though the latter begins as usual with the suggestion of a minimum.

Available inductances larger than L_3 were not at hand and the usual laboratory induction coils if inserted must act much like a break circuit.

26. Compensating inductances—The endeavor to equalize the coils I', I'' of the same inductor would have been extremely laborious. Since the telephones are not equally sensitive, figure 80 gives an example of results obtained on inserting a small inductance ΔL in the T or T' circuit, respectively, and then removing it ($\Delta L = 0$). The curves are worked out for both positions of the commutator, which does not of course commutate ΔL. As in case of the ballast in figure 78, it is so hard to follow what is taking place that the graphs are not suggestive. Thus for resistances below $R = 10^4$ ohms, the graphs $\Delta L = 0$, II and ΔL, T, II, as well as the graphs $\Delta L = 0$, I, and ΔL, T', I, could be made to nearly coincide by a slight lateral displacement of one of the curves of a pair. ΔL, T', II, and ΔL, T, I, lie apart. If we tabulate these adjustments, viz,

	I		II		
	T	T'	T	T'	
(1)	L_4	$R + \Delta L$	R	$L_4 + \Delta L$	(3)
	L_4	R	R	L_4	
(3)	$L_4 + \Delta L$	R	$R + \Delta L$	L_4	(2)

it will be seen that the cases (1) and (2) are mere shifts, as specified, whereas the parts of the diagonal case (3) are effectively distinct curves. This means that the fringe displacement s is not much changed when ΔL is added on the R side; but that the graphs are notably different when the increment ΔL is added on the L_4 side.

Results quite similar to these are obtained when an excess resistance ΔR is used in place of ΔL and are therefore equally difficult to construe.

If the currents i, i' of the two telephones be expressed by the usual equations, the effective current would be (φ, φ', phase lags behind e. m. f.):

$$\Delta i = i - i' = E(\cos\varphi \sin(\omega t - \varphi)/R - \cos\varphi \sin(\omega t - \varphi')/R')$$

where $\cos\varphi = R/\sqrt{R^2 + L^2\omega^2}$, etc., and the potential amplitude E of both is taken as equal. This expression is transferred to

$$\Delta i = E' \sin(\omega t - \tan\Phi')/R$$

which may be regarded as the simple harmonic responsible for the observed acoustic pressure. Here the new phase $\tan\varphi'$ and new amplitude E' are

$$\tan\varphi' = \Delta(\cos\varphi \sin\varphi/R)/(\Delta \cos^2\varphi/R)$$

$$E'^2 = E^2R^2((\Delta \cos^2\varphi/R)^2 + (\Delta \cos\varphi \sin\varphi/R)^2)$$

where the Δ refers to differences of values in φ and φ', respectively.

When the two electromotive amplitudes E are unequal, *i. e.*, E and Er respectively, in circuit T and T', the adjustment may be made by replacing R' by R'/r.

If the compound amplitude $E'=0$, $\Delta s=0$ results, and the two squared binomials in the last equation must each be zero. Hence

$$\cos\varphi \sin\varphi/R=r\cos\varphi' \sin\varphi'/R'$$

and

$$\cos^2\varphi/R=r\cos^2\varphi/R'$$

Hence $\tan\varphi=\tan\varphi'$, the phases are the same, and $r=R'/R$. If $r=1$, $R'=R$.

Owing to the asymmetric vibration of plates in the sequence graph, these conditions are further modified. For small currents we may write, as heretofore, $i=s/c$ and $i'=s'/c'$, so that $\Delta i=0$ is equivalent to $s/c-s'/c'=0$ or $s-s'$ would not be zero.

Without recalling § 23, a simple method of procedure would regard the minima as cases in which the sequence vibrations are quite in phase but of different amplitudes, hence at the minima $L/R=L'/R'$ (1). If the amplitudes are also equal the balance is complete. In this case the equation

$$R^2+L^2\omega^2=R'^2+L'^2\omega^2$$

again holds, so that $L=L'$ and $R=R'$. In the above work, the inequality of the voltages in T and T' would have to be allowed for. Moreover, s is not generally proportioned to the current.

The L and R here treated are the sum of internal and external values. Calling the former L_0 and R_0, the latter L and R, the first equation is actually $(L+L_0)/(R+R_0)=(L'+L'_0)/(R'+R'_0)$. If L_0, R_0, are the same in the circuits and L, R (external) are initially negligible, $L_0/R_0=L'/R'$, or a fixed ratio holds at the minima. Unfortunately, these conditions are not here present and the reduction of the complicated equations does not seem promising.

27. Same without commutator—To guard against complications from a commutator of insufficiently high resistance, the commutator C was excluded and the connections made directly (insert, fig. 81). The results are given in figures 81, 82, the group a referring to a comparison of external resistances $R'=0$ and $R=0-4\times10^4$ ohms, only: The group b is a comparison of inductances L_1+L_4 and $R=0$ to 4×10^4 ohms; the group c of L_3 and $R=0$ to 4×10^4 ohms. These measurements were repeated many times and are definite. Since at $R'=0$ and $R=10^4$, mean $s=64$, while $R'=0$ and L_1+L_4 gives mean $s=10$ and $R'=0$ and L_3 gives mean $s=44$, the inductances would be of the order of 56 and 230 mh. if computed linearly. The order of values is thus the same as above and much too small.

The graphs a (excess $L=0$) differ essentially from the group of figure 79 for about the same conditions. The two circuits T (weaker) and T' (stronger) are still quite unequally efficient (meaning probably that the coils of I' and I'' are not equivalent); nevertheless, they now balance appreciably when $R=R'=0$ under the given sensitivity. If R is added in the T circuit, T' sings, and vice versa. The tendency to conform to an initial minimum is more marked in the lower curve, where R is added to the stronger circuit T'; but it is difficult to see why the minimum is not more developed.

In the graphs *b*, figure 81, when $R=0$ is replaced by L_1+L_4, the character of the curves, figure 79, is preserved, but the quantitative divergence is otherwise again very marked. The lower graph (fig. 81*b*) is now distinctly hooked at the beginning when L_1+L_4 is inserted in T, the weaker circuit; thus when the strong T' is reduced by R', the minimum naturally appears. On the other hand, when L_1+L_4 is inserted in T', T is still less intense than the reduced T' and no minimum appears in the upper curve, figure 81*b*. In the hooked graph we may surmise that on the near side of the minimum T' sings, whereas on the far side T sings, louder as R increases.

In figure 82, graphs *c*, where the larger inductance L_3 is placed in one circuit or the other, both graphs exhibit a minimum. In the upper curve *c*, T' though reduced by L_3, nevertheless, is in excess at the beginning and remains so as T is decreased by R. In the lower curve *c*, the minimum is very

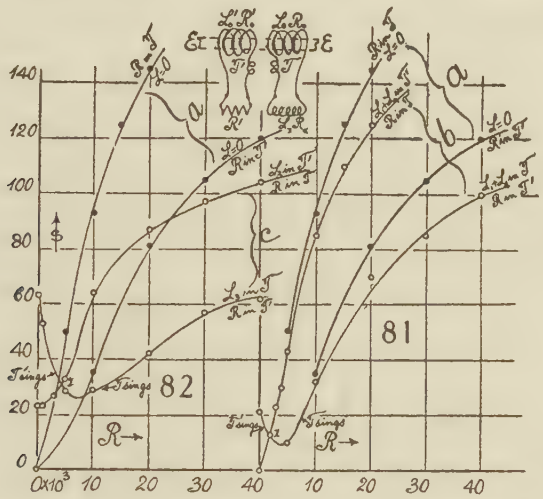

developed, since T' at the outset is much in excess of T reduced by L_3, and higher values of R' in T' are needed to reduce it below the diminished T value. The previous minimum at R below 5,000 ohms (curve *b*) now appears at R above 5,000 ohms. Before this T' sings, and after T is responsible for the fringe displacements s.

A comparison of figure 82*c* with figure 77*b*, each of which determines L_3, again shows curves of the same character but differing in detail. Thus the intersection in 77*b* is about at 4×10^4 ohms, whereas in 82*c* it is below 5,000 ohms. The deep minimum of the latter contrasts with the flat minimum of the former.

The minima are not at $s=0$ and seem to rise with the magnitude of L. In other words, if the phases of the two telephones are opposed the amplitudes are unequal, whereas for equal amplitudes the phases would not be opposed. The curves indicate that the two conditions do not occur together, remembering, however, that the two coils I' and I'' are unequally efficient.

28. Electrolytic resistances—The discrepancies of § 25 et seq. suggested a direct compensation by electrolytic resistances and capacities in one of the circuits. For in view of the high resistances (40,000 ohms) to be used and the advent of the damp summer months, it seemed not unlikely that the commutator C (fig. 75) would become appreciably leaky. It might thus be supposed to introduce not only conductances but electrolytic capacities, sufficiently grave to mar the graphs. The resistances were made to favor polarization and consisted simply of two platinum wires, each about 8 cm. long, held about 7 cm. apart in a beaker of distilled water. The adjustment is given in figure 83, where c is the water-cell.

The graphs a of figure 84 and figure 83, identical with the above, were obtained with the short-circuited cell ($R_0 = 0$). The T' circuit is, as before, much the stronger.

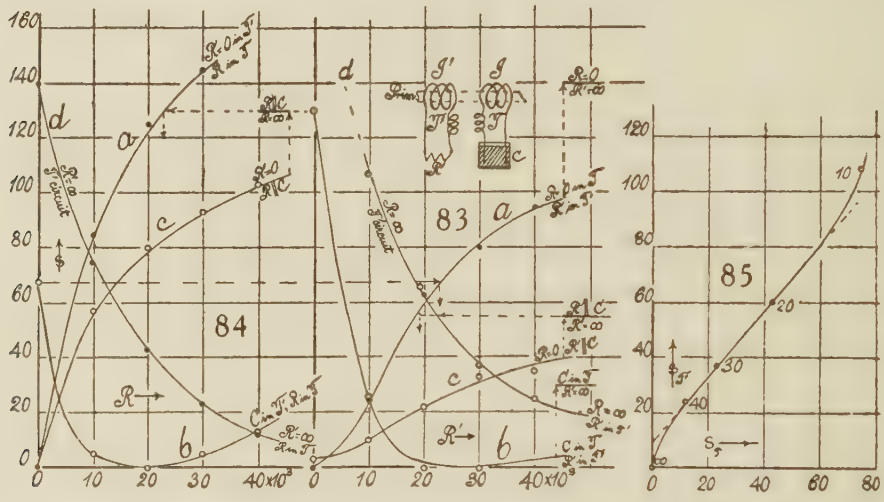

The graphs b of figures 83, 84, show the fringe displacements s when the cell is balanced by a resistance R. These graphs immediately recall the group in figure 76, where a similar balance is made by metallic resistances. The cell thus seems to act merely as a resistance, and as the curves where s vanishes indicate, of somewhat in excess of 20,000 ohms.

The high initial ordinate in figure 83 as compared with the low initial ordinate in figure 84 of the b curves are explained by projecting their values horizontally across to the opposed a curves. Thus, in figure 84, if $R = 0$, the T telephone sings and therefore $s = 68$, in accordance with figure 83 is about 22,000 ohms. In the same way $s = 130$ in figure 83, for $R = 0$, if interpreted by the a curve in figure 84, is equivalent to 23,000 ohms.

The curves c finally give the data when the excess resistance in one of the circuits is $R' = 0$, and the variable R in the other circuit is inserted *in parallel* with the cell c. Here also c acts as a parallel resistance, reducing the ordinates of the a curves of figures 84 and 83 about one-third. When $R = \infty$, the resistance

of c is alone effective. If we measure each of the limiting ordinates on its own a curve, the cell resistance again comes out a little larger or smaller than 20,000 ohms. The projections in question are indicated on the diagrams.

Thus there is nothing here to account for the difference of figures 76 and 82, etc. To obtain final evidence, I tested the paired connectors of the commutator for c, figure 75, directly, by removing either L or L'. This is equivalent to a break and should coincide with $R=\infty$ in one circuit. The graphs so obtained are given under d, in figures 84 and 83. They were quite identical, no matter whether the terminals of the circuits T or T' ended in the (open) commutator or in hard-rubber standards. The commutator had therefore remained trustworthy and the cause of discrepancy must be sought elsewhere (§ 29).

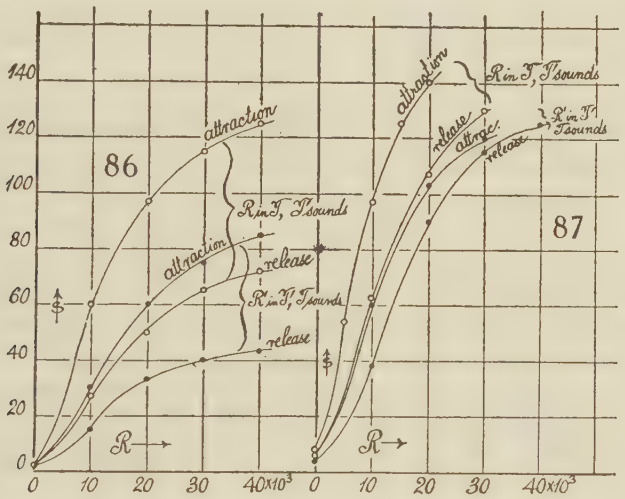

29. Single circuits isolated—The two curves d for $R'=\infty$ and R and for R' and $R=\infty$, respectively, are themselves interesting. In figure 85 I have constructed the fringe displacements s_T and $s_{T'}$ obtained at the identical resistances marked in ohms $\times 10^3$ on the graphs. T' being more efficient circuit shows greater displacement, and the main part of the graph (20,000 to 40,000 ohms) is so nearly linear that the equation $s_{T'}=10+1.16s_T$ reproduces the results very well. Below $R=20{,}000$ there is increasing curvature, attributable to the large excursions of the telephone-plates.

From this we get a definite suggestion as to the cause of the discrepancies in question and of the inequality of circuits. For if we regard the induction (ε, ε') as occurring mainly during the break circuit, and therefore being unidirectional, the two telephones act under opposed conditions in the sequence adjustment. For while the plate of one is additionally attracted, that of the other will be released, and it is quite probable that these two impulses will not be of equal intensity. At least, we would expect the attraction impulse to be stronger, probably at the ratio 1.16 just recorded. To test this, it is

necessary to reverse both telephones simultaneously, virtually by supplying two switches of the type S (fig. 75), one for each telephone.

The results of these experiments are recorded in the graphs (figs. 86 and 87), which corroborate the surmise, but provide additional conditions showing that the divergence is much increased when the currents in the circuits are relatively weak (fig. 86) as compared with stronger currents (fig. 87).

In figure 86, when R is in the T circuit, $R'=0$, the T' telephone sounds strongly in the upper graph (attraction of plate) and weakly in the lower graph (release of plate). The relations are the same when R' is in the T' circuit ($R=0$) and T sounds. The case of attraction of plate for T (upper curve) is also much in excess of the case of release (lower curve). It is interesting to note that T for an attracted plate is stronger than T' for a released plate. If for figure 86 we construct the mean ratio, ds_{attr} / ds_{rel}, of fringe displacements for attraction and release, respectively, the results lie between 2.3 and 2.0.

The same interpretations follow from figure 87 for stronger currents, except that the two graphs for T' sounding both lie above the graphs for T sounding, though the intermediate graphs are practically coincident. The graphs for s_{attr} compared with s_{rel} are here quite curved, so that a mean initial rate $ds_{attr} / ds_{rel} = 1.5$, falling off to 1 near the middle of the curves and finally to 0.7 near to end. Hence for weak currents these rates are about twice as large as for the strong currents.

The group of figure 86 can not adequately be made to pass into the graph of figure 87 by a mere change of the scale of the abscissa. For a constant electromotive force, $E=ir=i_0r_0$ and a simple circuit, the equation $s_0=se^{r/r_0}=se^{i_0/i}$ reproduced the observed data approximately. Hence for two different circuits and different constant electromotive forces and at the same external resistance R ($r=r_0+R$; $r'=r'_0+R$),

$$\log s_0/s'_0=\log s/s'+R(1/r_0-1/r'_0)$$

whence $\log s/s'=A-BR$, A and B being constants.

On passing from figure 86 to figure 87 for the same pair of graphs, if A, B, R remain the same

$$\frac{s}{s'}=\frac{s_1}{s'_1}$$

where s_1 and s'_1 are the new values of s and s'.

If $A=\log s_0/s'_0$ and $B=1/r_0-1/r'_0$ have assumed new relations in the second group,

$$\log s/s'-\log s_1/s'_1=A-A_1 \text{ (since } B \text{ is constant)};$$

or

$$\frac{s/s'}{s_1/s'_1}=\frac{s_0/s'_0}{s_{01}/s'_{01}}.$$

Thus the ratios s/s' vary as the initial ratio s_0/s'_0, which supplies no reason, however, why the latter should vary, other than that these should approach unity.

30. Data—Owing to the inequality of electromotive forces, ε, ε' operating in the circuits T, T' and the asymmetric character of the paired telephone vibrations in the sequence adjustment, full computations on the basis of the graphs investigated would be very tedious and not worth while. It will suffice to make a numerical survey and then supply a brief interpretation of the occurrence of minima in single graphs and of the intersection of paired graphs.

In most cases the telephones T, T' and the secondaries I, I' coöperated with the internal resistances R_0, R'_0, and inductances L_0, L'_0 as follows:

Circuit T', I'	Circuit T, I
Secondary: $R_0=$ 31, $L_0=$ .39 Telephone: 1,110, 1.2 Total: $R_0=1{,}141$ ohms, $L_0=1.6$ henries	$R_0=$ 32, $L_0=$ .29 1,090, 1.2 $R_0=1{,}122$ ohms, $L_0=1.5$ henries

To these the external, R, L were added. If we take the example of figure 82, curves c, with R in T and L_3 ($R=500$ ohms, $L_3=1.4$ hen.) in T', the full impedances, I, I' would be:

Circuit T', I'	Circuit T, I
$R_1=1{,}691$ ohms, $L_1=3.0$ hen. Impedance $I'=8{,}964$	$R_1=1{,}122+R$ ohms, $L_1=1.5$ hen. $I=4{,}542$, if $R=0$

if we estimate L_1 by its equivalent resistance ($L_1\omega=8{,}800$ and 4,400 ohms, respectively, where $\omega=2{,}934$). The same data applied to the case where R' is in T' and L_3 in T, give us

Circuit T'	Circuit T
$R'_1=1{,}141+R$; $L'=1.6$ $I'=4{,}817$ if $R'=0$	$R_1=1{,}670$; $L=2.9$ $I=8{,}672$

after adding the equivalents of $L\omega$ (4,680 and 8,510).

The case of figure 81, curves b, is similarly construed. Here L_1+L_4 adds resistances of $R=9.9+1.1=11$ ohms and $L=0.32+0.04=0.36$ henry. Thus for R in T and L_1+L_4 in T'

Circuit T', I'	Circuit T, I
$R'_1=1{,}152$ ohms; $L_1=2.0$ henry	$R_1=1{,}122+R$ ohms; $L_1=1.5$ henry

or reducing to ohms roughly as before

$$I'=5{,}982 \qquad I=4{,}541 \text{ if } R=0$$

If R' is in T' and L_1+L_4 in T, the case stands

$$R'_1=1{,}141+R;\ L'_1=1.6 \qquad R_1=1{,}133;\ L_1=1.9$$

or briefly

$$I'=4{,}817 \text{ if } R=0 \qquad I=5{,}821$$

31. Troughs of the paired graphs—To interpret these results as to the positions of the troughs, one may recall that each of the paired graphs, figures 82 and 81, is the superposition of two individual graphs, one belonging to the circuit with variable R and the other to the parallel circuit with L, of resistance R. The former (2) decreases regularly with R, while the latter (s) increases. Hence the equations for parallel coupling will read

$$s'\sqrt{(R'+R'_0)^2+L'_0{}^2\omega^2}/c' = s\sqrt{(R_c+R_0)^2+(L+L_0)^2\omega^2}/c$$

if we postulate roughly $i=s/c$, $i'=s'/c'$, where c and c' are the constants determining the efficiency of telephones, possibly associated with unequal coils.

If we further define the minimum as the $R'=R$ value, for which $s=s'$, the latter cancels out, whence

$$(1) \qquad (R'+R'_0)^2=\left(\frac{c'}{c}\right)^2((R_c+R_0)^2+(L+L_0)^2\omega^2)-L'_0{}^2\omega^2$$

where R' is the position of the minimum for the load L, L_0, R_0, L'_0, R'_0, are the constants (telephones and secondary coils) of the circuits and R_c the resistance of the load coil L. On commutation, this equation becomes

$$(2) \qquad (R+R_0)^2=\frac{c}{c'}((R_c+R'_0)^2+(L'+L'_0)^2\omega^2)-L_0{}^2\omega^2$$

where R is the position of the minimum for the load $L'=L$ in the parallel circuit.

If the inherent constants L_0, L'_0, R_0, R'_0, are nearly the same and if $c=c'$, nearly, since $L=L'$, equations (1) and (2) are identical and $R=R'$. This means that the paired graphs of figures 82, 81, must coincide and there is but one minimum. If, however, $c/c'>1$ then $c'/c<1$, from which the occurrence of separated paired graphs, each with its own minimum, results. The equations show, moreover, that R will be larger as L' is larger, conformably with the graphs investigated.

Equations (1) and (2), however, suffice for the elimination of c/c', if they are multiplied together, so that the geometric mean is really in question in relation to R, and R', the positions of the troughs.

If we now use the data of paragraph 30, given for the circuit $L_1+L_4=L=L'$, we obtain

$$(R'+1{,}141)^2=(c'/c)^2(\overline{1{,}133}^2+(2.0\omega)^2)-(1.6\omega)^2$$

and

$$(R+1{,}122)^2=(c/c')^2(\overline{1{,}152}^2+(2.0\omega)^2)-(1.6\omega)^2$$

whence if $c/c'=1$, $R'=2{,}560$ ohms and $R=2{,}550$ ohms, a mean value.

If the former datum $c/c' = 1.2$ or $(c/c')^2 = 1.4$ be taken, $R' = 720$ ohms and $R = 4{,}170$ ohms results. These data agree reasonably well with the graphs figure 81, although the c/c' found for the old telephones is here merely tentative.

The constants for the circuit L_3 give us

$$(R' + 1{,}141)^2 = (c'/c)^2(\overline{1{,}622}^2 + (3.0\omega)^2) - (1.6\omega)^2$$

and

$$(R + 1{,}122)^2 = (c/c')^2(\overline{1{,}641}^2 + (3.0\omega)^2) - (1.6\omega)^2$$

whence if $c/c' = 1$, $R' = 6{,}480$ ohms and $R = 6{,}500$ ohms, a good mean value for the position of the minimum, if the graphs coincide. If $(c/c')^2 = 1.4$ as above, $R' = 4{,}790$ ohms and $R = 8{,}375$ ohms, which are both somewhat high, showing that for large inductances like L_3, the insufficiency of the approximations imposed is perceptible.

Moreover, in all cases, if the minimum R were sharply determined, L would follow by an inverse computation.

In equation (1) or (2) if L denotes the inductance of the coil only (uncored) and if this is small compared with $L_0 = L'_0$, the equations become, since $R'_0 = R_0$

$$(R' + R'_0)^2 = (c'/c)^2(R_0 + R_c)^2 + L_0^2\omega^2((c'/c)^2 - 1)$$

If $c' = c$, then $R' = R_c$. Thus the resistance position of the minimum R' for the uncored coil, gives its resistance. Equation (1) for the cored coil takes the form $(c = c')$, since R_c is now given

$$(R' + R_c + 2R_0)(R' - R_c) = (L + 2L_0)L\omega^2$$

where R' is now the position of the minimum for cored coil, L. These two operations suffice to determine L; hence it is obvious that the desideratum $c = c'$ must be secured as nearly as possible in any efficient apparatus.

We may, however, eliminate c and c' by rewriting equations (1) and (2) with these coefficients and multiplying the equations together. Since $L_0 = L'_0$ and $R_0 = R'_0$ this gives

$$(R_c + R_0)^2 + (L + L_0)^2\omega^2 = \sqrt{((R' + R_0)^2 + L_0^2\omega^2)((R + R_0)^2 + L_0^2\omega^2)}$$

where R and R' are the observed minima and R_c the coil resistance of L. If L (uncored) is small compared with L_0, R_c is determined from R' and R in a first operation. With R_c given, L (cored) is then determined from R and R' for the complete coil.

32. The intersection of paired graphs—If we treat the present experiments in which the currents in the T, T' circuits are coupled by mutual induction as if they were ordinary currents in parallel, the results are a close approach to the actual case. The later data of figures 82 and 81 are available for testing the case by computing R for the points at I, at which the graphs

b and c intersect. The equation for the purpose has been given ($\Delta s = \Delta s'$) in § 36 and may here be put in the form, if $i = s/c$, etc.,

$$\frac{c'}{\sqrt{(R'+R'_0)^2+L'^2_0\omega^2}}+\frac{c}{\sqrt{(R+R_0)^2+L_0^2\omega^2}}=$$

$$\frac{c'}{\sqrt{(R'_0+R_x)^2+(L_x+L'_0)^2\omega^2}}+\frac{c}{\sqrt{(R_0+R_x)^2+(L_x+L_0)^2\omega^2}}$$

Here R_x and L_x are the resistance and inductance of the coil commutated and $R' = R$ are the observed resistance at the point of intersection. R_0, L_0, R'_0, L'_0 are the constants of the secondaries and telephones as indicated in figure 82. The data are ($\omega = 2{,}934$)

Telephones: T', $R'_0 = 1{,}110$; $L_0 = 1.2$	T, $R_0 = 1{,}090$; $L_0 = 1.2$
Secondaries: I', 30 .4	I, 32 .3
Total: $R'_0 = 1{,}140$ ohms; $L_0 = 1.6$ henries	Total $R_0 = 1{,}122$ ohms; $L_0 = 1.5$ henries

These values are nearly enough alike for the T and T' circuits that a mean may be taken with the object of simplifying the cumbersome equation just stated. This reduces, if $L_0 = L'_0$, $R_0 = R'_0$, and $R' = R$ at the intersection to

$$(R+R_0)^2 = (R_x+R_0)^2 + \left\{(L_x+L_0)^2 - L_0^2\right\}\omega^2$$

If now R_x, L_x refer to the coils L_1+L_4 of the graph b, figure 81, $R_x = 11$ and $L_x = .36$, so that

$$(R+1{,}131)^2 = (1{,}142)^2 + ((1.96)^2 - (1.6)^2)\omega^2$$

from which $R = 2{,}380$ ohms. The point of intersection in figure 64b is at about 2,000 ohms.

If R_x, L_x refer to the coil L_3 of graph c, figure 82, $R_x = 550$ ohms, $L_3 = 1.4$ henries, whence

$$(R+1{,}131)^2 = (1{,}681)^2 + ((3.0)^2 - (1.6)^2)\omega^2$$

from which $R = 6{,}511$ ohms, while the point of intersection in figure 82c is between 4,000 and 5,000 ohms.

In both cases, therefore, the computed point of intersection lies above the point given by the graphs; but the order of values is very satisfactory, as one can not expect sharp values from the approximate current equations $i = s/c$ and $i' = s'/c'$, postulated. Moreover, the same equations have been made to include the inequalities of induction ε, ε'. The equation for $(R+R_0)^2$, moreover, shows in general that the point of intersection of the paired curves moves to the right both with R_x and L_x of the commutated coils.

If we reverse the process and compute L_x from the intersections, $R = 2{,}000$ and 4,500 of the graphs, the data come out $L_x = 0.28$ and 1.03 henries, respectively. This is $0.28/0.36 = 0.78$ and $1.03/1.40 = 0.74$ of the actual value; or on the average the results obtained from intersections are 24 per cent too small.

33. Parallel circuits actuated by single inductor open circuits—Owing to the effective inequality of the secondaries, certain complications are introduced in the preceding paragraphs, which may be avoided (apparently) by using a single inductor with the circuits in parallel. Figure 88 gives a diagram of the connections. Here P is the primary, with the electromotive force E (3 cells with 20 or more ohms resistance) and B the periodic break. The coaxial secondaries I and I' terminate in the clamps 1, 2, 3, 4, which, when joined at 2, 3, produce a single secondary. Either coil may be used alone, the two joined in parallel, or even differentially, in the usual way. The parallel circuits are branched from the switch S, which admits of the reversal of the current in one of the telephones (T). The two telephones T, T' are joined by the acoustic pipe *tt* with its salient and reëntrant pin-hole probes *s*, *r*, and the interferometer U-gage lies beyond U. The four terminals of these high-resistance telephones end on one side of the commutator K, already described in figure 57. By the aid of it, the external resistances and inductances R, L,

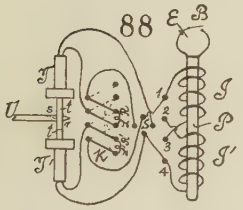

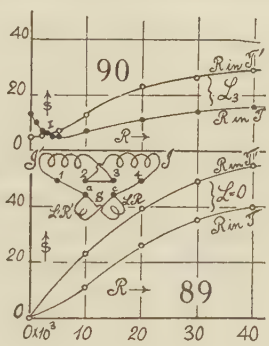

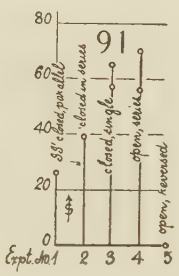

R', L' may be inserted in either one telephone or the other by swiveling the bars of K, as indicated by the dotted lines. Capacities are inserted at pleasure between clamps 2, 3.

On trying out this arrangement with I and I' joined, it was astonishing to find an extremely low sensitiveness compared with the preceding results, other things being the same. Figures 89 and 90 (sequence-graphs) give the results (2 cells, 10 ohms in the primary). The inset shows that the clamps 2 and 3 are joined and the secondaries I, I' in series. In figure 89 the branch circuits from S contain the telephone inductances only. The external resistance of one circuit is left at zero, while that of the other is increased from $R=0$ to 4×10^4 ohms. In figure 90, the external inductance $L=1.4$ henry and $R=550$ ohms is added to the constant circuit. The feeble fringe displacements s obtained in both cases are clearly evidenced when their figures are compared with figure 82, for instance, where the same routine is followed. The character of corresponding figures, however, is otherwise the same, except that the efficiency of telephones happens to be reversed. In figure 90, for instance, while the graph for one telephone (T', R in T) contains a marked trough, the other does not.

To ascertain the reason for this behavior, half-coils I, I' (secondaries) were joined in different ways, with the results summarized in the following schedule. The numbers refer to the terminals in figure 88 and s is the corresponding fringe displacement observed (2 cells, 10 ohms) in the primary and $R=0$, $R'=3\times10^4$ ohms excess resistance in the secondary I, I'.

Terminals used	Terminals joined	Terminals open	s	Remarks
Closed circuits: 1, 2 ; 3, 4	1, 2 ; 3, 4	....	26	Coils I, I', in parallel
1 ; 4	3 ; 2	....	39	Coils I, I', in series
1 ; 3	....	2 ; 4	57	Single coils
2 ; 4	....	1 ; 3	65	Single coils
Open circuits: 1 ; 4	....	3 ; 2	70	Terminals in phase; or opposite potential
2 ; 3	....	1 ; 4	56	Terminals in phase; or opposite potential
1 ; 2	....	3 ; 4	0	Terminals in opposite phases or same potential
3 ; 4	....	1 ; 2	0	Terminals in opposite phases or same potential

These data are further exhibited in figure 91. I, I' in parallel (ohmic resistance 15 ohms) constitute the worst adjustment. I, I' in series (resistance 60 ohms) is better, but much inferior to the single coil I or I' (resistance 30 ohms) used alone. These again are less sensitive than an open arrangement in series), *i. e.*, where the clamps 2, 3 are not joined if 1, 4 are the terminals and vice versa. If the coils I, I' are open and reversed (*i. e.*, 1, 2 terminals and 3, 4 free) the differential effect is practically $s=0$. The reason for this is not at once evident; but the data show that when clamps 2 and 3 are not joined, the highest potential difference will be brought to the clamps a, c of the switch S, figures 92 and 93. There is a partition of the energy of each impulse of the primary, the external circuit receiving a maximum when least is absorbed by the secondary. Thus the electromotive force, E, in an ohmic coil resistance of 30 ohms, is more efficient than E in a resistance 15 ohms, or than $2E$ in a resistance of 60 ohms.

Figure 94 gives a record of the effect of exchanging the clamps 1, 4 into 4, 1 with 2, 3 open; and of 2, 3 into 3, 2 with 1, 4 open, when $R=3\times10^4$ ohms is put in the T circuit and $R=0$ in the T' circuit. These s data may be arranged thus:

(1, 4)	(4, 1)
$s=114$	$s=90$ (2, 3)
72	74 (3, 2)

Since the resistance 3×10^4 ohms in the T circuit virtually removes this telephone, so that in the sequence adjustment T' only sings, the exchange of the terminals 1, 4 into 4, 1 is equivalent to a commutation of the current in the telephone whereby the stronger inductive impulse is replaced by the weaker. The same is true for the change of 2, 3 into 3, 2. On the other hand, the passage of the terminals from 1, 4 to 2, 3 is equivalent to a commutation of the induction coils I and I', which are not equal, as shown above. Hence in 1, 4, 2, 3, the strong phase of the telephone is associated with the stronger coil,

whereas in 4, 1, 3, 2, the weaker phase is associated with the weaker coil, as suggested by the schedule.

Figure 92 was obtained with the favorable arrangement shown in the inset, figure 93, 2,3 open. The graphs are a considerable improvement on the corresponding results in figures 89 and 90, of which they reproduce the general character. One notes that both for $L=0$ and $L=L_3$ the graphs are relatively much nearer together. Two cells and 10 ohms were in the primary.

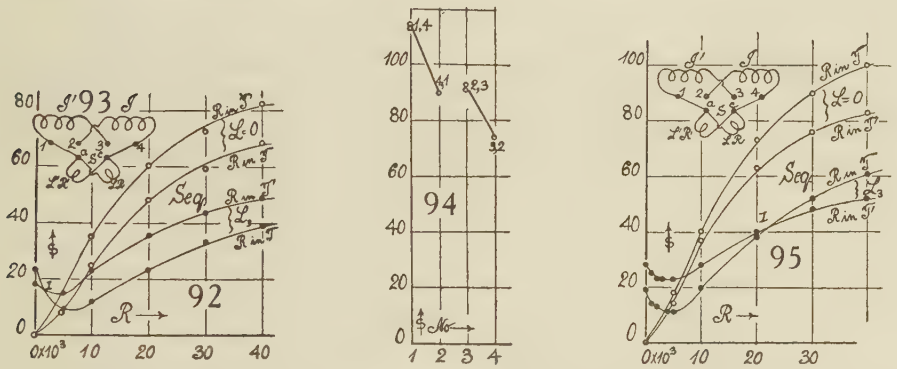

In figure 95, the fringe displacement is further increased by using 3 cells and 20 ohms in the primary, and this enhancement might have been increased indefinitely. In figure 95, however, the graphs for $L=0$ are reversed and those for L_3 intersect at high resistance of about $R=2\times10^4$, as compared with $R=2\times10^3$ of figure 92. Since these departures are due to the telephone only, they are not susprising after the investigations made in the earlier paragraphs. With a perfectly symmetrical telephone, there would be but one curve for each L. The location of minima in figures 92 and 95 is about the same.

34. Minima and intersections—If we make use of the equation in paragraph 31 for the R-location of the troughs and put $c/c'=1$ for the mean value ($\omega=2{,}934$), the result is:

$$(R+1{,}100)^2=\left\{(550+1{,}100)^2+(1.4+1.2)^2\omega^2\right\}-(1.2)^2\omega^2$$

or $R=5{,}870$ ohms.

Here the constants ($R=R'_0=1{,}100$ ohms, $R_c=550$ ohms, $L_0=L'_0=1.2$ henries, $L=L_c=1.4$ henries) have been used, as already defined, and the equation is more fully guaranteed, since the circuits in question are actually in parallel. The R-value found is again somewhat in excess of the mean position of the troughs in figures 92 and 95, owing, no doubt, to the approximations necessarily made and the flatness of the troughs. One notices that in figure 90, as in figure 82, one of the pairs of graphs for the case of L_3 is without a trough, for reasons which are difficult to disentangle.

In figures 90 and 82, moreover, the intersections of the L_3 graphs, like the

troughs, have about the same R-location, these cases corresponding to closed circuits. In figures 92 and 95, however (open circuits), the paired troughs (and particularly the enormously displaced intersection) are virtually new phenomena. The intersections lie at about $R=1{,}000$ and $R=24{,}000$ ohms, respectively. This is beyond the range of approximations (current, $i=s/c$, etc.) tentatively adopted. While in figure 95 the R in T' graph has merely been raised, as compared with figure 92, the R in T graph has been raised and accelerated.

35. Resistances in the air-gap 2, 3. Double symmetrical inductor—In figure 96, curve a (insert) where I and I' are the secondaries and T and T' the telephones, a resistance R was put across the otherwise open clamps 2, 3. The telephone T' was left without external resistance and 30,000 ohms inserted

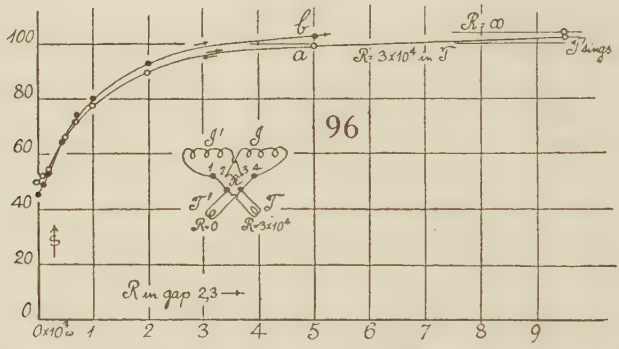

in the branch T, which nearly cuts it out. The fringe displacements s, observed as R increases from 0 to ∞ ohms, are well shown by the graph. It will be seen that s is more than doubled by this procedure; but the R-effect increases very rapidly and a resistance of a few thousand ohms suffices to bring out nearly the whole of the displacement. When $R=0$, the internal resistances are about 31 ohms in each half-coil and 1,100 ohms in the telephone T'. At $R=10^3$ ohms, however, the reciprocation between I and I' is only about half quenched. As the capacity of the open circuit is not known, it is of interest to introduce an external capacity at 2, 3. This will be done in the next paragraph.

Figure 96, curve b, is another survey, made with a somewhat modified circuit, some time after. The graphs are of the same nature, the second having somewhat larger coefficients. It would be an advantage to cut out the telephone T altogether.

CHAPTER II

SHORT AND SLENDER AIR-COLUMNS. CIRCUITS WITH LOCALIZED CAPACITY

36. Capacities in the air-gap—It is thus becoming more and more evident that the conditions of an electric circuit, oscillating in resonance with the acoustic pipe (which measures s), are being approached. Hence a variable capacity was inserted at C between the secondary coils I and I' as shown in the insert, figure 97. T' is the telephone actuating the pipe; the other telephone, T, being cut out from action, its plate serves merely as a wall for the reflection of sound. P is the primary with electromotive force E (3 cells and 20 ohms) and B the periodic break. The results obtained when the capacity added increases in steps of 0.1 microfarad from 0 to ∞, are shown by the graphs a, b, c, for somewhat different adjustments as to sensitiveness and made at different times. The full capacity is now $C+C_0$, where C is the capacity of coils I, I', here (in the apparatus) forming a coaxial structure favorable to capacity. Thus, the fringe displacement s begins in marked degree when $C=0$. If one of the layers is replaced by a similar but remote coil, there is no fringe displacement ($s=0$) at $C=0$.

The curves are seen to be of the same nature, and all insist on a maximum somewhat below 0.05 microfarad, the smallest standard interval here available. The curves, moreover, pass through a definite minimum at about 0.5 microfarad of added capacity. This has been worked out in greater detail in the graph d. At $C=1$ microfarad, the graphs have practically reached the limit, as shown in case of the curve c when the condenser C is short-circuited. At times there seemed to be an actual maximum near $C=1$ microfarad possibly referable to the primary; but this was obscure and not borne out. Thus there is no doubt that the initial sharp maximum is due to electric oscillation. To compute its position in C, the usual equations

$$T=2\pi\sqrt{LC}\sqrt{1+(d/2\pi)^2}$$

where d is the logarithmic decrement

$$d=RT/2L$$

are available. The total resistance of telephone and coils is (as above), $R=1{,}100+62=1{,}162$ ohms and the total $L=1.55$ henries. From this $d=0.65$, the frequency of b' being 467 or $\omega=2{,}934$, $\omega^2=10^6\times 8.61$. Hence $d/2\pi=0.104$ and $(d/2\pi)^2=0.011$. Equation (1) may therefore be written

$$C=1/(L\omega^2(1+(d/2\pi)^2)=0.365.\text{ microfarad}$$

As this is C_c+C_0 the external and inherent capacity, $C_c=0.365-C_0$, which might be regarded as the C-location suggested by the graphs. Since the mutual inductance has been disregarded, L is virtually larger, and hence C_c

should be smaller still. The meager effect of d, in consideration of the large resistances, is noteworthy; but the crests are nevertheless flattened as a consequence.

The minimum at $C=0.5$ microfarad is more difficult to construe, for here the electric oscillation is nearly quenched and the telephone acoustically silent. As C alone varies from its initial value C_r for resonance, $T/T_0=\sqrt{C/C_r}$. Hence $\sqrt{C/0.036}=2$, or $C=0.15$ mf. if the initial period b' were doubled and $\sqrt{C/.036}=3$ or $C=0.33$ mf., if this period were trebled; $C=0.58$, if quadrupled, etc. Nothing seems to occur at $T/T_0=2$, or $=3$, or $=4$ with any bearing on the problem.

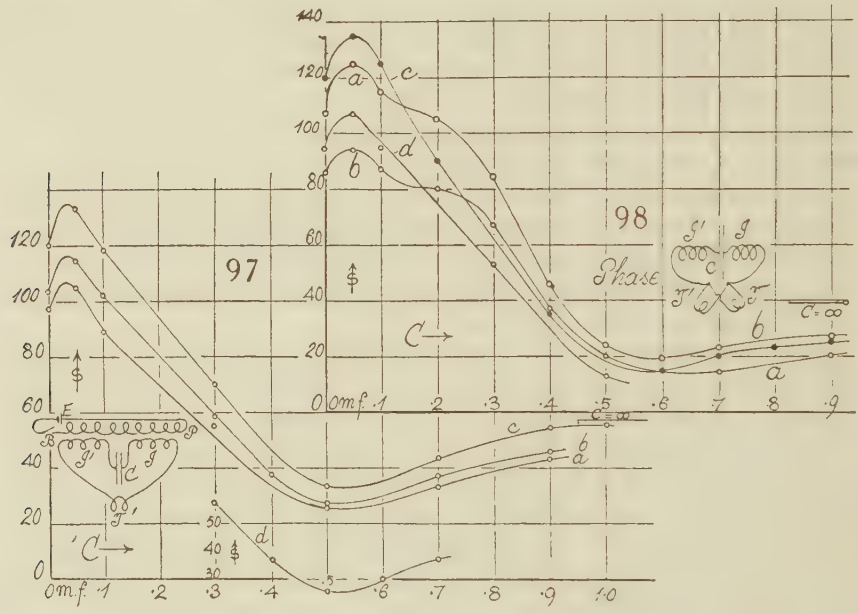

Both telephones T and T' may be used to advantage as in figure 98, provided the telephones vibrate in phase. This nearly doubles the sensitiveness, so that the primary current must be weakened (3 cells, 50 ohms) if the fringes are to remain in the field of view. Considerable difficulty was experienced with the break in the primary, which when freshly polished with slightly oiled paper gave higher s-values than appeared shortly after; but the sinuous character of the curves in figure 98, a and b, is nevertheless warranted. The crests in figure 98, a, b are not sharp. They might suggest a subsidiary crest at about $C=0.25$. The minimum, moreover, has moved to the left and would be expected beyond $C=0.5$. Curves, figure 98, c and d, were also sometimes obtained, rising above the crest of b, nevertheless, falling as low as a and without the retardation at $C=0.2$ of curves a and b; so that an unstable situation is involved. The constants being practically the same as the above, computed data would also be.

37. Single inductor, unsymmetrical—The case of C = ∞ (short circuit) in figure 98*b* has the low value already instanced in paragraph 33, for the symmetrical circuit using *I* and *I'*. In figure 99, *a*, *b*, *c*, the counter cases are shown in which either *I* or *I'* alone are the secondaries of the inductor. In curves *a* and *b* (see insert), but one telephone is used, the silent plate of the other merely reflecting the sound-wave. In curve *c* the two telephones are used in parallel and in phase. The latter is naturally over twice as sensitive, owing to the decreased resistance; so that 3 cells with 20 ohms were used in the former primary and 3 cells with 50 ohms in the latter.

The graphs obtained in figure 99, *a*, *b*, *c*, are quite different from the set in figure 98, for the symmetrical arrangement. Thus at $C = \infty$ the currents *s* are still very high, relatively speaking, and also in conformity with the information in paragraph 33. There is no appreciable current ($s = 0$) when the added capacity is $C = 0$. At $C = 0.05$, the current at once jumps beyond the maximum and falls but slightly thereafter ($C = 0.1$ to 1.0). There is no minimum determinable. Since the resistance of the telephones *T* and *T'* is large as compared with the secondaries *I* and *I'*, the use of the latter singly or together would not make much difference (1,100+62 ohms compared with 1,100+31 ohms; with the telephones in parallel 550+62 and 550+31). The currents change from $s = 40$ in figure 98, to $s = 85$ to 100 in figure 99 when $C = \infty$, and the data are similar relatively to figure 97. The released resistance may therefore be the mutual induction in the coils *I*, *I'*, which is cut down one-half or proportionally and to which no adequate reference has been made. The curves, in fact, are quite similar to the graphs usually obtained in case of closely coupled circuits of primary and secondary and the treatment would be conducted along similar lines to those usually pursued.

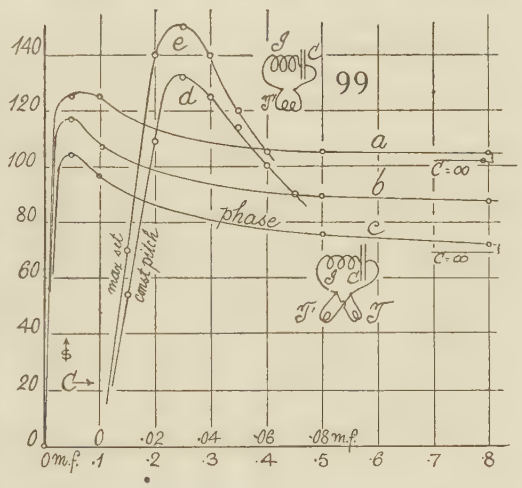

The absence of all fringe displacement ($s = 0$) when $C = 0$ implies that the inherent capacity is virtually $C_0 = 0$ in case of the single coil; whereas the combined coils *I*, *I'* owe their marked inherent capacity to their coaxial arrangement.

At a later date capacities between 0 and 0.1 microfarad in steps of 0.01 microfarad were procured and the graphs *d* and *e* in figure 99 worked out at a somewhat larger current intensity. In the higher curve *e*, the pitch was reset for the maximum at each observation; in curve *d* the motor was kept running at the maximum for the pitch at $C = 0.5$.

The crest now lies definitely nearest $C = 0.03$ microfarad. Since for the primary $\omega = 2{,}934$, it is worth while to compute the effective inductance, including self and mutual inductance in the form $1 = \omega\sqrt{(L + L_{12})C}$. The result is $L + L_{12} = 3.9$ henry; so that if for I and $T + T'$ $L = 0.8$ henry, $L_{12} = 3.1$ henry would be estimated ($C_0 = 0$, as stated). As this is out of the question, it looks as if the harmonic were not b' but b''. The fringe displacements of the graphs d, e, figure 99, were liable to pass out of the field of the ocular. A larger resistance was, therefore, inserted into the primary (3 cells, 60 ohms) to bring the currents within the scale limits. The results are given in figure 100. The enlarged curves b, c are constructed with a $\Delta C = 0.01$ microfarad interval. The general trend of the curves is much the same and for the $C = 0.1$ microfarad interval the graphs now come out sharply with a maximum at about 0.025 microfarad. In the graph b, the primary pitch $\flat b'$ was set and the successive points investigated by changing C in steps of 0.01 microfarad. In

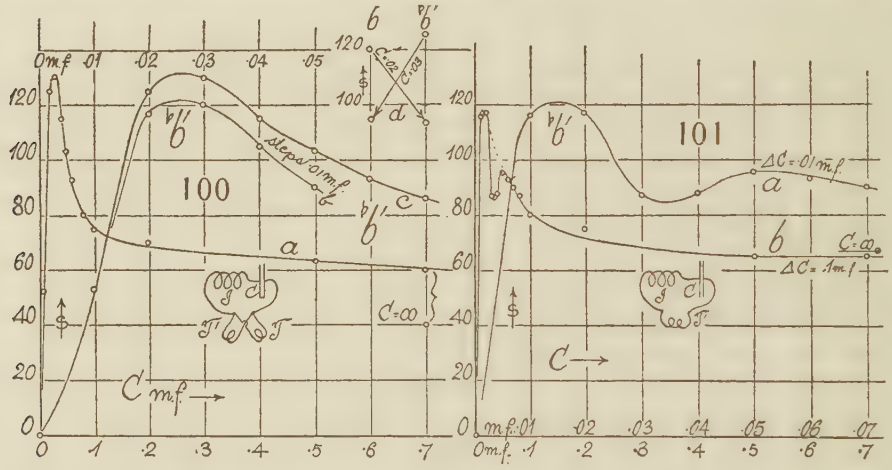

the graph c, however, the maximum s was sought at each C, by changing the frequency. The result was not only a larger s throughout, but the maxima of s were found at slightly higher pitch for a smaller C. This is indicated by the insert d, where at $C = 0.02$ microfarad and a pitch a little below b', the deflection was $s = 120$, falling to 93 at $\flat b'$; while at $C = 0.03$ microfarad the deflection was but $s = 95$ at b', rising to 125 at $\flat b'$, the pitch difference being a diminished semitone. These alternative crests are not uncommon; but it is not easy to assign the cause, except in so far as in $1 = 2\pi n\sqrt{LC}$ a reciprocal change of n and $\sqrt{C}$ does not change the product and is admissible within the resonance limits of the acoustic pipe joining the telephones. As in the insert, however, there is always a maximum among the crests, here at $\flat b'$. Cases as low as a' were observed in other instances.

In figure 101, one telephone (T) is cut out of circuit and is inactive, the sound-wave from T' being merely reflected at the plate of T. Three cells and 30 ohms were therefore used in the primary. The interval 0 to 0.1 microfarad is here mapped out in steps of 0.01 microfarad not available in figure 99.

An interesting new feature is the occurrence of two crests seen in curve *a* (interval $\Delta C = 0.01$ microfarad), but more sharply in curve *b* ($\Delta C = 0.1$ microfarad). This is unexpected, as only one telephone is in action; but the double crest probably presents an adventitiously indented form of a single crest, as indicated by the dotted lines. In fact, in subsequent experiments the double crest did not always appear, so that it is incidental and $C = 0.055$ would mean $L = 0.53$ hen. not identifiable.

38. Effect of the lower harmonics—Figure 102 is an attempt to work out the character of the flat crest of figure 97 in greater detail (curve *a* with steps of 0.01 microfarad); but it presents no essential novelty. The high *s* for $C = 0$ is again attributable to the capacity of the coaxial double coil *I*, *I'*. Details at the minimum were supplied at a later date in curve *c*.

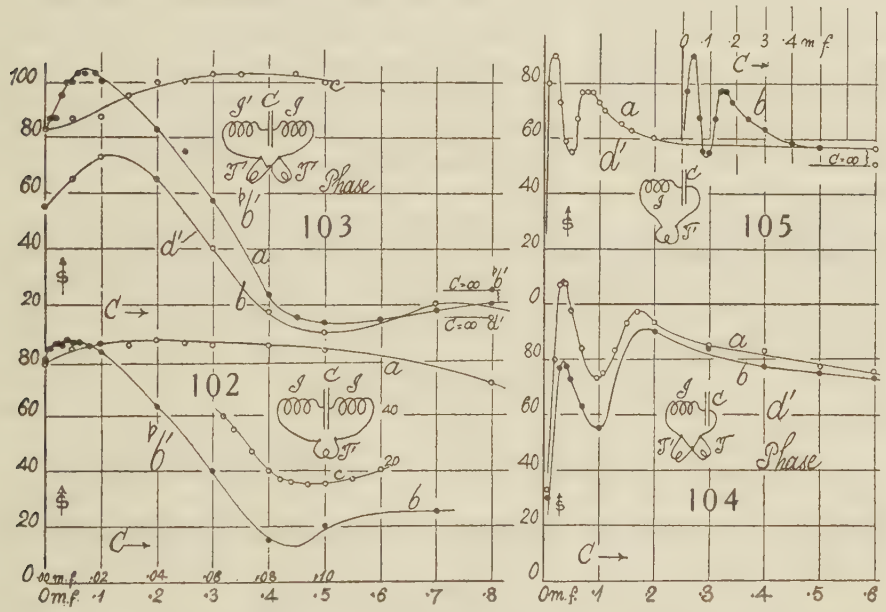

The same is true of the repetition, figure 103, in relation to figure 98, for the primary pitch ♭*b'*. There is initial capacity. The attempt was then made to use the node of a lower (apparent) harmonic of the organ-pipe, as it was possible to isolate a strong one near *d'* for the primary by slowing up the break. The lower graph in figure 103 gives the results, which indicate a shift of the crest to the right (which would be expected) and the occurrence of a probable very flat maximum beyond the minimum. The latter is necessarily uncertain in view of the small *s*-values remaining. The shift in the former case, moreover, is hardly adequate. Since nothing is changed but the primary pitch from ♭*b'* to *d'*, we have

$$\frac{C}{C'} = \frac{T^2}{T'^2} = \left(\frac{n'}{n}\right)^2 = \frac{294}{467} = 0.40$$

In figure 103, if the crest at $\flat b'$ is at $C=0.07$ microfarad, the crest at d' should be at $C'=0.07/(0.4)=0.18$ microfarad, at least, since initial capacity is not easily estimated. Though the figure may so be drawn, it is not convincing.

It is thus preferable to work with the unsymmetric adjustment, figure 104 (compare figure 100), which has no initial capacity. The results are given in the two graphs of the figure, in the upper one, a, of which the resonance was tested at each point. They contain the new feature of two distinct or separate peaks. The first at about $C=0.03$ microfarad, nearly coincides with the peak in figure 100, and would thus be associated with the primary $\flat b'$ pitch. The other at $C=0.17$ microfarad is new and should therefore be referred to the present primary d' pitch.

To account for the presence of both crests it would seem reasonable to refer the latter to the actual period of the spark succession at the break in the primary. The former would then be due to an electrical oscillation sustained between sparks, which happens to be in resonance with the acoustic note $\flat b'$ of the pipe joining the telephones. In other words, although the spark succession corresponds to d', an electric oscillation $\flat b'$ will nevertheless evoke this natural note of the pipe, owing to accentuated overtones of the plate. The electrical oscillation persists from spark to spark.

This explanation, however, encounters difficulties if a computation of the coefficient L is made from the known R and C values at the crests. Since for the coil I, $R=32$ ohms and $L=0.2$ henry, and for the telephones in parallel $R=550$ ohms, $2L=1.2$ henries (inductances in parallel), the logarithmic decrement d computed as

$$d=\pi R/\sqrt{L/C-R^2/4}$$

comes out:

$\flat b'$ crest,	$C=0.17$	$\times 10^{-6}$ farads,	$d=0.80$	$\omega=2{,}934$
d' crest,	$C=0.035$	10^{-6}	$d=0.36$	$\omega=1{,}830$

Hence if L is computed as $L=2/\omega^2C(1+(d/4\pi)^2)$, since the telephones are in parallel,

$n=467$	$\flat b'$ crest	$L=6.6$ hen.
$n=294$	d' crest	3.4 hen.

As nothing has been changed in the secondary but the pitch n, these values ought to be the same, which is far from being the case, while their magnitude is out of the question. It is obvious, therefore, that either something in addition to the mutual induction has been overlooked or that the primary harmonics are irrelevant.* In frequency squared $d'/\flat b'$ is about 2.5, whereas the result is a scant 2. There is nothing else but these two pipe notes (see figs. 73 and 75) to which the two maxima can be referred, unless the sequence adjustment is in some way implicated.

To simplify the circuit still further, the telephone T was cut out and the

*If the secondary harmonics be taken as $\flat b'$ for $C=0.17$ and $\flat b''$ for $C=0.035$, the L values are 0.7 and 0.8 henry, respectively, the actual values being 0.8 henry.

data of figure 105 investigated. The curves *a* and *b* are repetitions made at different times, the break pitch being *d'*. The crests now lie at *C* values about one-half as large as in figure 104. Nothing has been done but a removal of the telephone. The discrepancy just alluded to persists. The logarithmic decrements being $d=0.41$ at $\flat b'$ and smaller are not of immediate consequence. The *L* value for the $\flat b'$ crest follows from *C* below 0.02, $R=1{,}110+32$ ohms, which gives *L* above 6.2 henries. At the *d'* crest, *C* is above 0.075, so that *L* is below 4.0 henries. The results are thus about the same as before and out of all proportion. If, however, the secondary harmonics are $\flat b''$ for $C=0.02$ and $\flat b'$ for $C=0.075$, the *L* values come out 1.45 and 1.55, respectively, the actual value being somewhat above 1.4.

39. Detailed survey near the crest—If we bring together the above data for the *C* position of the flattish crests in so far as these can be specified, the results may be tabulated as follows:

Primary pitch $\flat b'$	$I+I'$	$T+T'$	$C=0.07$ mf.	Fig. 102	$C=0.05$	Fig. 98
		T'	0.04	103		
	I	$T+T'$	0.027	100	0.03	99
		T'	0.015 and 0.055	101		
Primary pitch d'	I	$T+T'$	$C=0.035$ and 0.17	104		
		T	0.02 and 0.08	105		

$T+T'$ denotes that both telephones are used together in parallel circuits, but vibrating in phase; $I+I'$, that the two secondaries are used together in series. In most cases, the T' values of *C* are about one-half the $T+T'$ values, which means that the *L* values for $T+T'$ are half those for T' alone, since *LC* is constant. In other words, the inductances are in parallel in the former case.

It is desirable, however, to test this specifically and to supply the missing brace for the pitch *d'*. This has been done in figures 106 to 112, in which the inserts (figs. 109 to 112) show how $T+T'$, $I+I'$ are to be understood. The agreement of the new crests with the old is satisfactory, seeing that the crests are flat from the large resistances in circuit and considerable lateral shift is therefore inevitable. The new and old graphs may be regarded as coincident observations, the scale of the fringe deflections, *s*, being, of course, arbitrary. If we compare the cases T' and $T+T'$ at the same pitch (caet. par.) as to *C* positions of the crests; viz,

Fig. 107 $C=0.04$	Fig. 108 $C=0.07$
Fig. 106 $C=0.014$	Fig. 106 $C=0.025$
Fig. 111 $C=0.06$	Fig. 112 $C=0.12$
Fig. 109 $C=0.015$; 0.075	Fig. 110 $C=0.035$; 0.170

the *C* of the latter group ($T+T'$) is about twice the former (T'), meaning (since *LC* is constant, nearly) that *L* is halved when $T+T'$ are in parallel, as it should be. This is even more marked for the double-crested graphs (figs. 109, 110) which here are closely tested. Such doublets have occurred incidentally, as in figure 101 (and possibly the uncertain arrangement of points in

figures 107 and 108 might be so interpreted, the two C positions of crests in figure 107 being about doubled in figure 108, nearly); but this was not sustained. The relations of the $\flat b'$ crests and the d' crests is far from obvious, as one would surmise that n^2LC should be nearly constant. It is worth while, therefore, to attempt a systematic computation of the various cases by first finding the rough value, $L = 1/\omega^2 C$; from this L to compute the decrement d and then a corrected L.

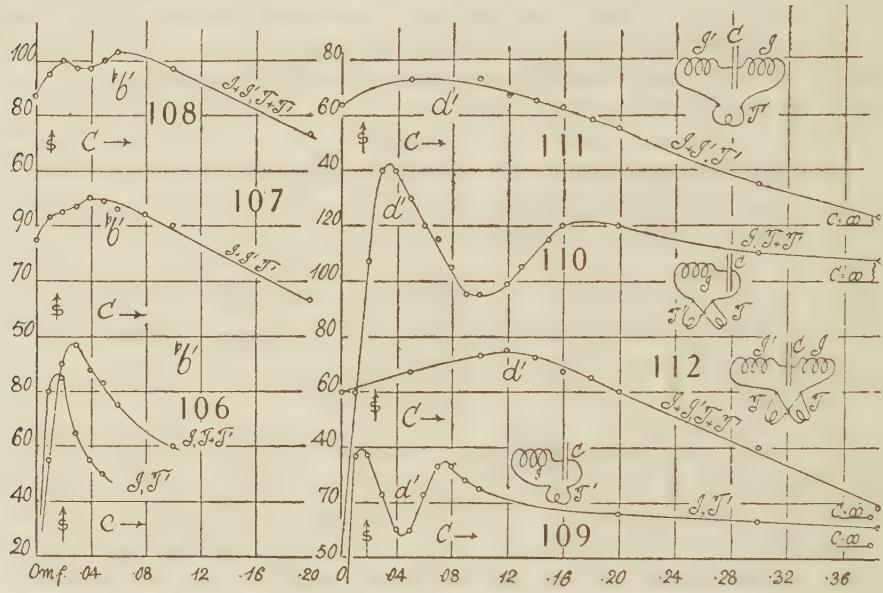

The rough values of L come out as follows:

	$\flat b'$				d'			
	I, T'	$I, T+T'$	$I+I', T'$	$I+I', T+T'$	I, T'	$I, T+T'$	$I+I', T'$	$I+I', T+T'$
$C=$	0.014	0.025	0.04	0.07	0.015, 0.075	0.035, 0.170	0.06	0.12 m.f.
$L=$	8.3	9.3	2.9	3.3	7.8 3.9	6.6 3.4	4.9	4.9 hen.
Fig.	85	85	86	87	88	89	90	91

The results, even granting the difficulty of placing the crests, are highly promiscuous and difficult to construe. It seems certain that when the break corresponds to a given note, $\flat b'$ or d', the telephone-plate vibrates additionally with an overtone that happens to be favored by the pipe.

To indicate the apparent irregularity of data, the ratios of computed L values for an I and $I+I'$ adjustment may be instanced. Calling this ratio L/L', the results are:

$I, T'(\flat b') : I, T'(d') ; L/L' = 8.3/3.9 = 2.1$
$I, T+T'(\flat b') : I, T+T'(d) ; 9.3/3.4 = 2.7$
Mean ratio, 2.4

$I+I', T'(\flat b') : I+I', T'(d') : L/L' = 2.9/4.9 = 0.59$
$I+I', T+T', (\flat b') : I+I', T+T'(d') ; 3.3/4.9 = 0.67$
Mean ratio, 0.63

We should thus have to increase the pitch of $\flat b'$, $\sqrt{2.4} = 1.55$ times in the case of L, I' ($\flat b'$), and increase the pitch of d' $\sqrt{11.63} = 1.26$ times in case of L', $(I + I')$, (d'), to get a rough coincidence of ratios. This would imply an active harmonic somewhat above f'' in the first and a $\#f'$ harmonic in the second instance. But the acoustic tube harbors no such harmonics in the phase adjustment as shown in figure 73. They do occur (nearly) in the sequence adjustment (figs. 73, 75), which, however, is certainly ruled out in all combinations $T + T'$. Again, not only is the passage from $\flat b'$ to d' accompanied by opposite effects (rise and fall) of L in the two comparisons, but changes of L quite of the same character take place in passing from I to $I + I'$ at the same pitch. Thus:

Adjustment $\flat b'$	Adjustment d'
I, T': $I+I', T', L/L' = 8.3/2.9 = 2.9$ $I, T+T'$: $I+I', 1+T', L/L' = 9.3/3.3 = 2.8$ Mean ratio 2.8	$L/L' = 3.9/4.9 = 0.79$ $L/L' = 3.4/4.9 = 0.71$ Mean ratio 0.75

Here the effect at $\flat b'$ is again the opposite of the effect at d' and both are of the same order as in the preceding case involving frequency variation.

Finally, if we assume the L of the coils I or I' to be the same (3.0 henry, for example) and compute the frequency from the capacities, the following notes result:

Break at $\flat b'$				Break at d'			
I, T'	$I, T+T'$	$I+I', T'$	$I+I', T+T'$	I, T'	$I, T+T'$	$I+I', T'$	$I+I', T+T'$
$\#f''$	g''	$\#g'$	a'	f'' $\#d'$	$\#e''$ d'	f'	f'

in which we merely observe a promiscuous group of high notes ($e'' \ldots g''$) with I and of low notes (f' to a') accompanying $(I + I')$. Both occur at the double crests. Nothing has been gained in this way.

40. Non-coupled inductances inserted. Reductions—Owing to the difficulty of recognizing the particular harmonic to be selected, it seemed desirable to introduce known inductances L into the circuit, to facilitate the recognition of the actual frequency. The scheme is shown in the insert, figure 114. The inductances $L = 0$, $L = L_1 = 0.32$ henry, $L = L_3 = 1.4$ henries, described above were used. It was found that the greatest care had to be taken with the tuning to discover the maximum crest among the crests for a small off-tune. If that is not done, the C position of the crest will be too low, as it undoubtedly is in some of the preceding curves.

Figure 113 presents a satisfactory series of graphs with crests at $C = 0.035$ for $L = 0$, $C = 0.025$ for $L = L_1$, and $C = 0.015$ for $L = L_3$. If, now, we compute the total self-induction from the period, without regard to the logarithmic decrement (which would not alter the case appreciably, because of the

flatness of crests) the results are inadmissible if the break-pitch $\flat b'$ is used; but if the pitch is assumed to be $\flat b''$, the first overtone of the break-pitch, the results are reasonably close to the actual values, as, for instance:

	$\omega^2 = 10^6 \times 8.61 \times 4$	$L_T + T' = 0.6$ hen.	$L_I = 0.20$ hen.
Coil	$O + I\ T + T'$	$L_1 + I\ T + T'$	$L_3 + I\ T + T'$
$C =$	0.035	0.025	0.015 mf.
Total $L =$	0.83	1.16	1.94 henries
Do. $- I$	0	0.33	1.11 henries
Actual values	0.60 + 0.20	0.32	1.4 henries

Thus the crest for curve *a* is placed fairly as to the *C;* that in curve *b* is nearly correct; the crest in curve *C* is apparently too high,* but the correspondence of data is clearly such as to point unmistakably to an effective pipe-note $\flat b''$, instead of $\flat b'$, the pitch of the break.

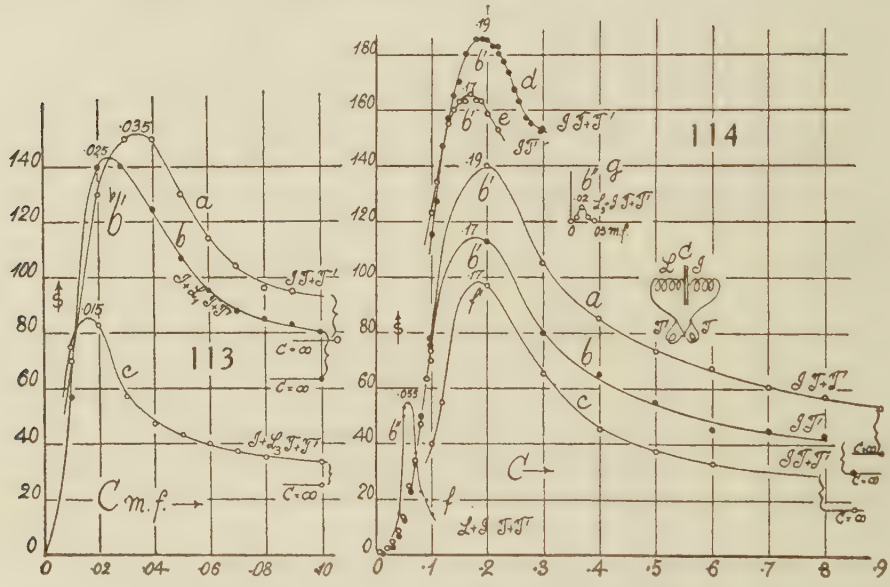

Further tests were made by adding (noninductively) the coils $L_1 = 32$ henries and $L_3 = 1.4$ henries as above. The crests were found at 0.055 microfarad and 0.02 microfarad respectively, the original crest (I') being at 0.18 microfarad. Hence

$$L_1 = (\Delta 1/C)/\omega^2 = (18.2 - 5.6)/9.63 = 1.31 \text{ hen.}$$

and

$$L_3 = (50.0 - 5.6)/9.63 = 4.61 \text{ hen.}$$

if the pitch of the secondary is b'. But as these results are four times too large, the pitch must have been b'' whence $L_1 = 0.33$ henry and $L_3 = 1.15$

*It is more probable that the accepted value 1.4 henries for this coil is too large.

henries, as they should be. This promiscuous octave jump of pitch is very puzzling.

In view of this reasonably good agreement, it is worth while to reëxamine the data of the preceding section, as it is already probable that harmonics other than $\flat b'$ and $\flat b''$ do not occur, even when the break-pitch is d'. The damping coefficient, moreover, may be disregarded, as the crests are too flat for precision. Hence, computing L from the observed values for C and the appropriate $\omega^2(\flat b', \omega^2 = 10^6 \times 8.61; \flat b'', \omega^2 = 10^6 \times 34.4)$, the following adjustment of values results:

Circuit...	I, T'	$I, T+T'$	$I+I', T'$	$I+I', T+T'$	I, T		$I, T+T'$		$I+I'T'$	$I+I', T+T'$
Figure....	106	106	107	108	109		110		111	112
Break-pitch...	$\flat b'$	$\flat b'$	$\flat b'$	$\flat b'$	d'		d'		d'	d'
Crest at C mf....	0.017	0.025	0.04	0.07	0.015	0.075	0.035	0.17	0.06	0.12
L (henry) computed from C...	1.71	1.16	1.43	1.04	1.93	1.55	0.83	0.69	1.94	0.97
L actual..	1.4	.80	1.55	0.95	1.4	1.4	0.80	0.80	1.6	0.95
Pitch taken...	$\flat b''$	$\flat b''$	$\flat b'$	$\flat b'$	$\flat b''$	$\flat b'$	$\flat b''$	$\flat b'$	$\flat b'$	$\flat b'$

In case of figures 107, 108, the initial C_0 within $(I+I')$ was taken as 0.03 microfarad. In case of figures 111 and 112, however, the curves are so flat that such an allowance was disregarded. In general, though the coincidence is very rough, the values of L computed from C agree with the actual values as closely as may be expected; for the C position of the crests admits of considerable shifting.

It is noticeable that the d' harmonic does not occur, except at the break in the primary. This d' merely evokes the upper harmonics $\flat b'$ and $\flat b''$ of the phase adjustment, figure 73. From the table as a whole there can be little doubt, I think, that the $\flat b'$ harmonic does actually occur acoustically in the tube. Moreover, the double crests of figures 109, 110 now appear as octaves of each other, which is a much more plausible interpretation than the suggestion above. This is also true of the phase vibration assumed to occur in all cases, no matter whether the T or $T + T'$ adjustment is in question.

41. Low-resistance telephones — In the preceding experiments the main inductive resistance is in the telephones and it is so high that the required crest capacity must be correspondingly low. Hence, by diminishing the L of the telephones, a larger number of steps in C are at once available without reducing the smallest capacity below 0.01 microfarad. Naturally, the method is restricted to smaller values of the L examined.

Figure 114 gives the results, the graphs (I, $T+T'$, and I, T') corresponding to figure 106. The method is, within its range, much more sensitive (3 cells and 100 ohms in circuit). Owing to the change of telephones (new pipe *tt*,

figure 88, and new pin-hole probes) the fundamental is now $b'(\omega^2 = 10^6 \times 9.63)$, in addition to which $b''(\omega^2 = 4 \times 10^6 \times 9.63)$ often appears. The low crest is now at f'.

In the graphs *a* and *b* the steps are 0.1 microfarad. There is no minimum. At $C = \infty$ (short circuit) the fringe displacement, *s*, reaches a low asymptote. Within the first 0.1 microfarad, observations are made in steps of 0.01 microfarad, with the object of locating an anterior crest; but none could be found. In the graphs *d*, *e*, the interval $C = 0.1$ to 0.2 is explored in steps of 0.01 microfarad, to locate the maxima more nearly.

In the case of graph *c*, the pitch of the primary circuit was f'. Here the region between $C = 0.1$ and 0.2 was also explored in steps of 0.01 (not shown) to locate the maximum, at a somewhat different intensity. But one crest was found and not two, as in the corresponding figure 110. All these crests are at b' pitch in the secondary.

Inserting an additional noncoupled inductance $L_1 = 0.32$ henry in graph *f* and $L_3 = 1.4$ henries in graph *g*, however, the crest in both cases appears at b'' in the secondary, the primary and telephone-pitch remaining at b', sharply. These graphs indicate the rapid dwindling of fringe displacement, *s*, with increasing *L*. Here also but one crest appears, the search for b' being unsuccessful. The great difficulty in this work throughout is the sharpness of the tuning necessary, which must therefore be repeated at each observation. A fraction of a semitone produces a large *s*-effect and hence the graphs *a* . . . . *f* can not be obtained quite smoothly, nor the maximum selected with precision.

The puzzling feature here again encountered is the apparently arbitrary selection of the harmonics b' and b'', under virtually identical pitch of the primary. Sometimes, as in the above graphs, both appear. It is possible that the sufficient nearness of the step in *C* to the particular *C* for a maximum determines the subtle conditions. Chladni plates, moreover, behave not unlike this; but in the present experiments the irregular behavior is consistent.

It is finally necessary to give the data corresponding to the maxima inferred from the curves, remembering that this can not be done with precision, because of flatness and tuning difficulties.

Pitch of primary...	b'	b'	b'	b'	f'	$\omega^2 = 10^6 \times 9.63$
Figure 114, graph..	*ad*	*be*	*f*	*g*	*c*	
Pitch of secondary.	b'	b'	b''	b''	b'	
Circuit.....	I, $T+T'$	I, T	L_1+I, $T+T'$	L_3+I, $T+T'$	I, $T+T'$	
Crest at C.....	0.19	0.17	0.055	0.02	0.17	mf.
Total L.....	0.56(b')	0.61(b')	1.89		0.61	hen.
Individual L.....	0.14(b'')	0.15(b'')	0.33	1.15	0.15	hen.
Actual L.....	0.18	0.21	0.32	1.4	0.18	hen.

In the cases *ad* and *be* the *L* refers to the whole circuit secondary and telephones, the actual *L* to the summarized coefficients of self-induction; so that the b' pitch assumed for curves *a*, *d*, *b*, *e*, *c*, must also be estimated as b'',

though both fit badly. In case of the graphs f and g the coefficients for L_1 and L_3 are found from

$$L = \frac{1}{\omega^2}\,(1/C_{L+I} - 1/C_I) = (\Delta 1/C)/\omega^2$$

The differences are within the possible shift of the eye-location of the crest.

42. Spring mercury contact-breaker of inaudibly low pitch—As in the above experiments with low pitch, the primary d' and f' did not appear in the frequencies of the secondary; and as the acoustic pipe is often multiresonant for low frequencies, the spring contact-breaker of fixed pitch suggests itself for trial. This completely replaces the electric siren or contact-breaker of variable pitch; but naturally calls for more current (3 cells and 5 ohms were

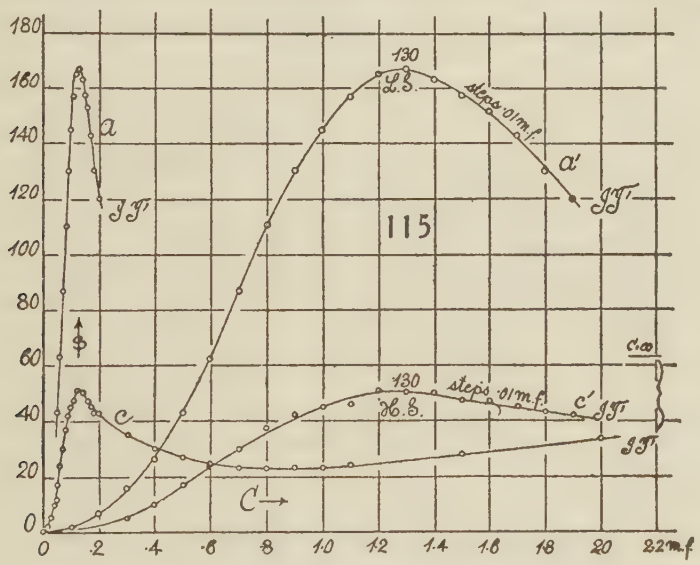

used in the primary). The mercury contact-breaker must be neatly made with provision for washing the surface (heretofore described). Its performance is then surprisingly steady, as shown by the graph, figure 115. The fringes take a definite position almost at once and no tuning difficulties are involved. Eventually, however, the fringe position becomes more and more fluctuating and frequent cleaning is thus necessary. In the lapse of time, moreover, the s-values, as a whole, may increase or fall off, so that the graph should be covered twice in opposite directions.

Two springs, a lighter (*L. S.*) and a heavier one (*H. S.*), the taps of each of which could just be distinguished by the ear, were first used, both with the single (I, T') and double telephone ($I\,T+T'$) adjustment. The data are given in full in figures 115 and 116, both in steps of 0.1 microfarad and 0.01 microfarad as indicated. The tendency to flatness at the crests is often annoyingly present. Even when crests are reached rapidly the descent of curves there-

after is relatively slow. They all pass through minima, the run being observed as far as 2.2 microfarads and the eventual high value of the asymptote for $C = \infty$ (short circuit). The graph at $C = \infty$ is in fact usually above the crest-level in *s*.

The data found are as follows (*L. S.*, light spring; *H. S.*, heavy spring):

Primary break..	*L. S.*	*H. S.*	*L. S.*	*H. S.*	*L. S.*	*H. S.*	
Figure.....	115*a*	115*c*	116*a*	116*d*	116*b*	116*e*	
Pitch of sec.....	*b''*	*b''*	*b''*	*b''*	*b''*	*b''*	
Circuit.....	*I, T'*	*I, T'*	*I'T'*	*I'T'*	*I', T + T'*	*I', T + T'*	
Crest at *C*.....	0.13	0.14	0.14	0.15	0.18	0.18	m.f.
Total *L*.....	0.20	0.19	0.18	0.17	0.16	0.16	hen.
Actual *L*.....	0.26	0.26	0.21	0.21	0.18	0.18	

The results show that when but one telephone is in circuit, the *C* value of the crest which appears may be wavering. The pitch *b''* had to be taken

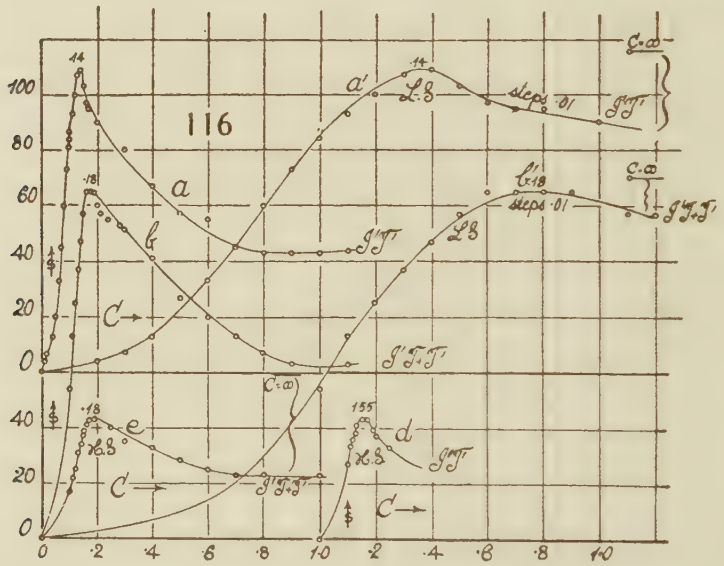

throughout, whereas the pipe-note is *b'*. When both telephones are used in phase, however, the position of the crest is normal, so far as it can be specified. This adjustment, together with the lighter or faster spring (compare curves *a*, *a''*, *b'*, *b*, with *c*, *c'* for the heavier spring in figures 115 and 116), is also far more sensitive and should therefore be preferred.

43. Inductor with variable core—As the spring contact-breaker requires relatively large currents to keep it going, the primary and secondary currents are excessive. To cut the secondary down by a resistance, as in figure 117, curve *c* (3 cells and 2 ohms in primary) where 2,000 ohms are inserted, obliterates the crest altogether. To obviate large resistances in the secondary, the usual device of a weaker or a sliding primary is available. Curves *a*, *a'* show

the results when the coil L_1 was used as a secondary accompanied by a suitably weak primary (3 cells and 5 ohms), here quite within the former. The lighter mercury spring-break functioned faultlessly. The crest is sharply determinable and the rapidly falling curves pass through a flat minimum. Assuming that the effective harmonic is $\flat b''$, and $C = 0.08$

$$L = 1/(4 \times 9.63 \times 0.08) = 0.325 \text{ henry},$$

the estimated value for the circuit being $(0.32 + 0.03)$ or 0.35 henry.

Using 3 cells and 3 ohms in the primary, the graphs were considerably sharpened, as shown in curves b and b', figure 117. The crest may here be placed at 0.075, so that the accuracy should approach 1 per cent. The result is $L = 1/(4 \times 9.63 \times 0.075) = 0.337$ henry.

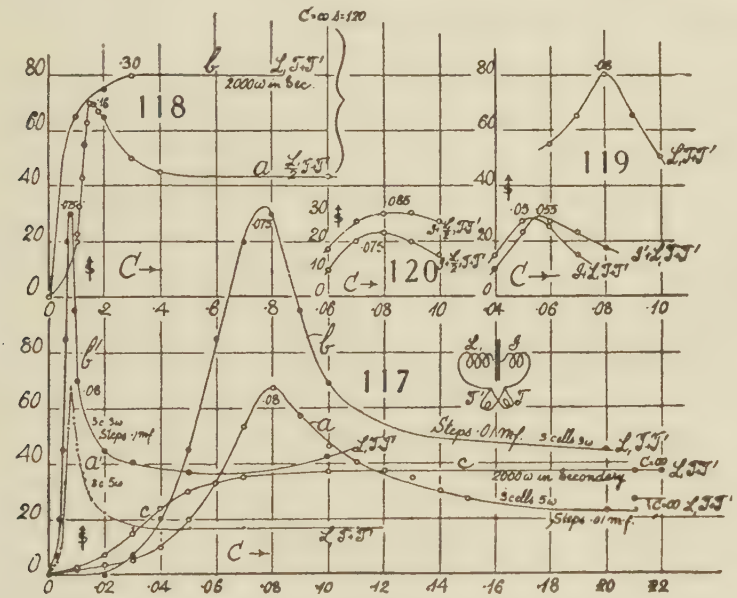

A spring interrupter of the usual hammer type with platinum contacts was next tried. Its note was audible and placed by the ear at a frequency of about $n = 100$ per second. The results are given in figure 118a, where it was necessary because of the large n and therefore intense secondary currents, to withdraw about half the core out of the inductor L_1. The curve here is quite different from figure 117. The crest is not symmetrical and the flat but relatively high minimum finally ascends to an enormously high asymptote, $s = 120$, for $C = \infty$ (short circuit). Estimating the crest as placed at $C = 0.16$ microfarad,

$$L = 1/(4 \times 9.63 \times 0.16) = 0.162 \text{ henry}$$

(if the note is $\flat b''$), which is somewhat less than half the value for the preceding full circuit, as it should be. Such an apparatus is extremely convenient, if the nonsymmetrical graph (possibly associated with the brush on sparking)

can be modified. Using the full core and 2,000 ohms in the secondary, the curve *b* without a definite crest and corresponding to the curve *C* in figure 117 was obtained. If the crest is placed at $C=0.3$ microfarad, the maximum elevation, $L=0.35$ henry, which is again a correct order of value.

A number of incidental experiments were made with the inductors I, I' (now used as test objects), while L_1 supplies the induced current. Figure 119 is a summary of results with the lighter mercury-break, the coil combinations being indicated on the curve. The maxima selected are also shown. If $\omega^2=4\times9.63\times10^6$ (bb''), the results are

L_1, $T+T'$	$C=0.08$ mf.	$L_1=0.33$ hen.
L_1+I, $T+T'$	0.05	$I=0.19$
L_1+I', $T+T'$	0.055	$I'=0.15$

smaller steps in C would have been desirable.

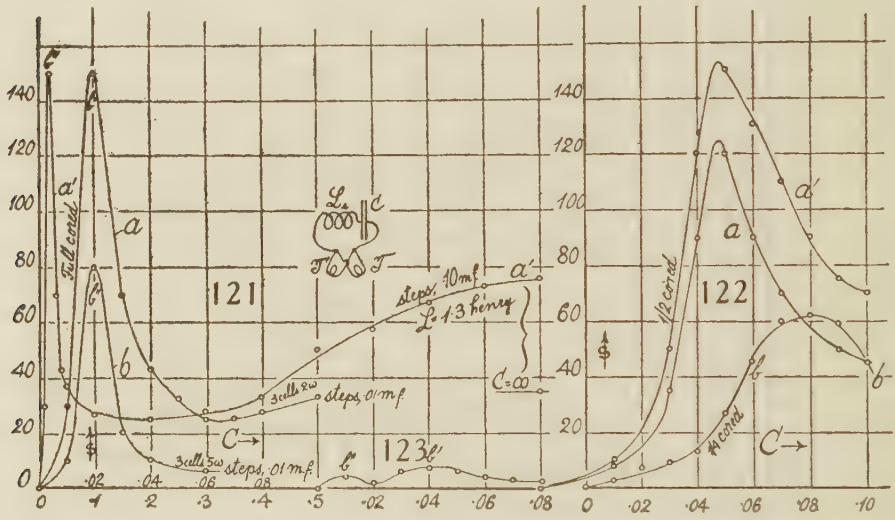

The same experiment performed with the platinum spring-interrupter and the approximately half-coil xL_1 (coil half withdrawn), figure 120, gave in the same way

xL_1, $T+T'$	$C=0.18$ mf.	$xL_1=0.14$
xL_1+I, $T+T'$	0.075	$I=0.20$
xL_1+I', $T+T'$	0.085	$I'=0.16$

The crests in both groups of experiments are unfortunately very flat.

44. Increased currents—The surprisingly good performance of the platinum spring-interrupter induced me to test it further by increasing the current; for it is clear that the sharpness of the crest must increase, as the currents are continually larger. The limits to this method are given by the insulation of the condenser, which would eventually be sparked through and should therefore be specially constructed. Nevertheless, the graphs of figure 121, obtained with the inductance $L_3=1.4$ (roughly), indicate the availability

of the method. The curve *b* for weak currents is at once improved in the curves *a* or *a'* for stronger currents, in relation to sharpness of peaks. It is also obvious that continuous change of *C* between the steps would ultimately be necessary. The usual disk type is not satisfactory for this purpose, as sparks soon break across the air-gaps.

With the crests at $C=0.02$ microfarad, $L=1/9.63\times0.02=1.3$ henries, the only demand being smaller stops near the crest. Withdrawing the core partially reduced *L* to 0.15 henry. The note was *b''*.

The graphs figure 122, *a*, *a'*, show the results when the core is drawn out about one-half and *b* when drawn out about three-quarters. With the crests placed at $C=0.047$ and 0.08 microfarad, the values are $L=0.55$ and 0.32 henry respectively, the note being again *b''*. The necessarily flat crest of the graph *b* could have been sharpened by increasing the current in the primary.

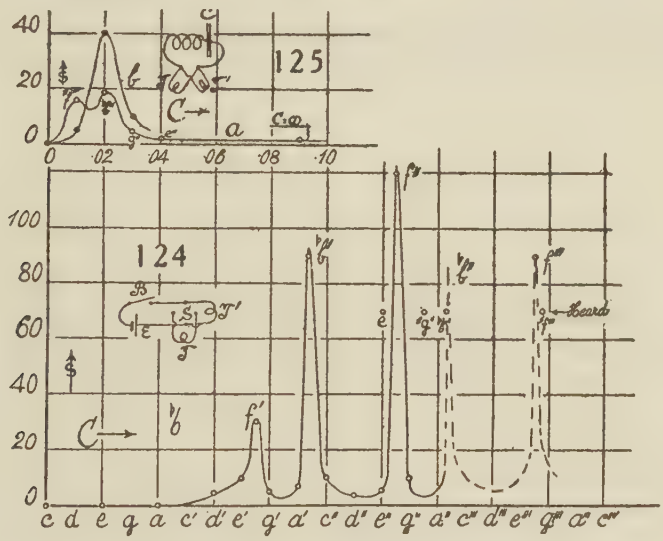

Attempts made very cautiously (fig. 123) with a larger coil, and very weak currents gave a sprawling graph with crests at $C=0.01$ and 0.04. These are probably the notes *b'* and *b''* and give $L=2.6$ and 2.7 henries, respectively.

45. Longer and wider organ-pipe—This was provided with the object of getting a lower fundamental, the pipe being of inch brass tubing and 24.1 cm. long between telephones. A survey of the harmonics made with the motor-break (3 cells, 100 to 200 ohms, telephones in parallel, and without other induction coils) is reproduced in the graphs, figure 124, with extremely sharp crests, so that only approximate pitch location was possible; *i. e.*, intervals within a fraction of a semitone produced enormous fringe displacement differences. Probably, from the width of the tube, there was no reaction below *f'* (traced to *c*). The multiresonance of thinner tubes in this region is thus absent. At *b'* and *b''* occur sharp cusps, with the fringes projected out

of the field of view. If these are (phase adjustment) the first and second overtones of the pipe for a fundamental at $\flat b$, it is as usual difficult to account for the f' (which is quite strong) unless it also evokes f''. The electric oscillation (see below) contributed a marked f''', which could not be reached by the motor-break.

In the sequence survey, only a faint d'' ($s = 20$) could be detected.

The new pipe, producing almost the same notes as the thin, narrow pipe, is disappointing. The oscillation phenomenon, from the larger body of air to be kept in motion by the telephones, was bound to be weaker. Little was, therefore, done with the tube in this place, beyond the tests shown in the graphs, figure 125, with the circuit as shown in the insert and a platinum break in the primary (3 cells, 5 ohms). The small induction coil furnished its own appurtenances, the core being quite in.

In one respect the data of curve *a* are novel, for the harmonics marked on the graph could be distinctly heard in the telephone. If one computes the frequencies n which for $L_3 = 1.4$ should belong to the chosen capacities, the series is

$C = 0.01$	0.02	0.03	0.04	0.05 mf.
$n = 1{,}350$	955	780	670	600
f'''	$\flat b''$–b''	g''	e''–f''	$\# d''$
Heard, $\# f'''$	$\flat b''$	g''	e''	(d'')

which is an attempt at coincidence and might be improved with a larger L value. It seems clear that the frequencies of electric and acoustic oscillations near f''' were close enough to excite the high harmonic, and this accounts for the distorted curve *a* in figure 125. The $\flat b''$, moreover, is the octave above the survey cusp in figure 124. None of the other crests were sufficiently approached by the C values to be stimulated.

Repeating this experiment with a modified break, only the $\flat b''$ harmonic could be heard and the graph took the normal form of curve *b* in figure 125. These experiments indicate the difficulties encountered with the platinum spring-break, inasmuch as it is liable to change its pitch capriciously, accentuate successive harmonics of the organ-pipe, and lead to distorted graphs. The curve *a*, for instance, should probably be indented in the way suggested in figure 125. The motor-break is relatively free from such annoyances.

46. Long, thin pipe—Relatively large currents are needed to energize the preceding wide pipe, and this sometimes makes the spring-break rattle and function irregularly. The long, thin pipe (23.7 cm. long, scant 1 cm. in diameter) is not only much more sensitive in relation to the pin-holes, but responds to a nearly quiet spring-break and the fringe displacements are usually remarkably constant. The results are summarized (fig. 126) in the curves *a* and *b*. The curve *c* is a later repetition at the curious bump between $C = 0.3$ and 0.5 microfarad, showing it to be real. After passing $C = 0.3$ microfarad, the break in the primary begins to be more and more noisy. This indicates, I think,

that the primary crest is actually being approached, as $C = \infty$ shows less fringe displacement. If the effective frequency were still a'' and the crest were to be located at 1 microfarad, $L = 0.03$ microfarad would be the coefficient of the primary. The crest is certainly higher and the coefficient smaller.

To interpret figure 126, it is necessary to make the survey in pitch given in figure 127, the circuit being without inductances other than those in the telephones. The tube harmonics are thus a' and a'' (in the phase adjustment; the sequence note should thus be at a). The lower a of the graph probably evokes one of these upper notes. One would expect an intermediate e'', but the pipe gives f'' and below (between a and a') is a d' not easily accounted for, although quite strong. If a'' is effective, $\omega = 10^3 \times 5.53$ and $\omega^2 = 10^7 \times 3.06$,

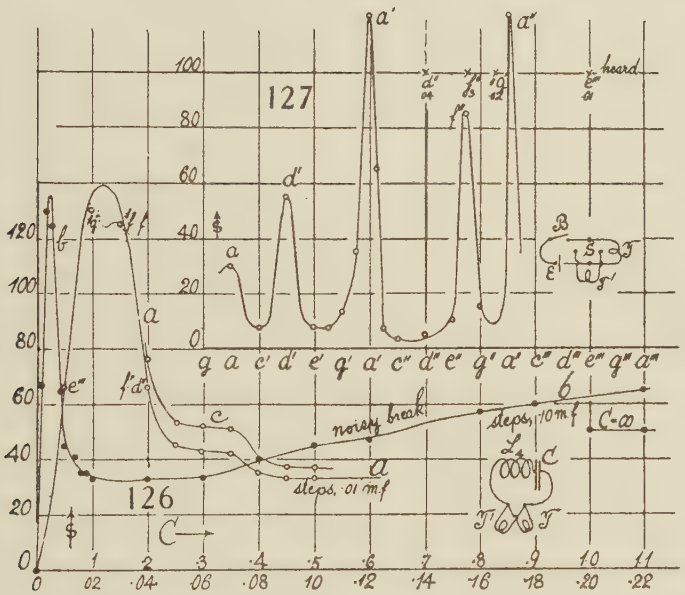

the datum already used. Placing the crest in figure 126, curve a at $C = 0.025$, the inductance would be $L_3 = 1/30.6 \times 0.025 = 1.31$ in as good agreement with the earlier results as may be expected. The notes heard in the telephone are marked on curve a, figure 126, and also inserted in figure 127. They vary somewhat with the adjustment of the break; but the high notes e''' and g'' are pretty clear and fixed. It is interesting to find the frequency at the bump of curves a and c, postulating $C = 0.06$ here. It is d'', and for this there is no warrant in figure 127. Some other reason must therefore be sought for it. So also the notes heard in the telephone, as indicated in figure 127, have no definite relation (excepting the f'') to the pipe harmonics. Possibly d', d'', f'', $\#g''$, e''' may be plate harmonics. Alternatively, one may suspect the occurrence of forced vibrations, with the spring-break dominant. The impotence of the long, wide pipe in § 45, for instance, is evidence in point.

47. Short, thin pipe—With the present pipe (cut down to length 10 cm., diameter 1 cm.) no greater sensitiveness need be expected; but the obtrusive harmonics would be diminished, it was thought. This is hardly the case in the survey in pitch, summarized in the lower curve *a* of figure 128. Crests occur at about half a semitone below d', g', d'', g'', and an intense one (found by the electric oscillation) at d'''. The crest at g'' is for some reason (break irregularity) very small, though none the less definite. One may as usual suppose that pipe and plate harmonics are superposed. No crests were found below d'.

If we consider g the fundamental, the odd and the even harmonics would all be present (except the first) in the phase adjustment. This is quite unex-

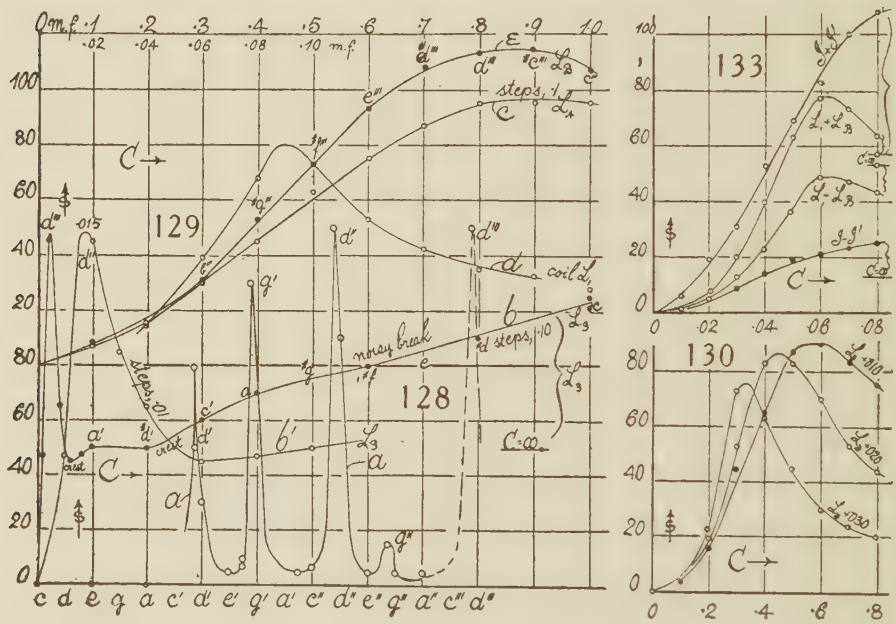

pected, unless there is secondary stimulation. The telephone resistance was 600 ohms.

When tested by the small inductor L_3 with platinum break (3 cells with resistance in the primary; about 1,000 ohms in the secondary), the graphs *b* (steps 0.1 microfarad) and *b'* (steps 0.01 microfarad) were obtained. The crest may be located at $C = 0.015$ microfarad. Putting $\omega = 10^3 \times 3.54$ for the slightly flatted d'', since $\omega^2 = 10^7 \times 1.256$, $L_3 = 5.29$ henries. This is about four times too large, so that if $\omega^2 = 10^7 \times 5.02$, $L_3 = 1.32$ henries, the correct order of value. Hence the dominant note must have been d''' as indicated by the cusps in figure 128, curve *a*. In curve *b*, beyond the minimum, the spring-break begins to rattle sonorously. The curve then rises, finally to fall again into $s = 50$ for $C = \infty$. It seems probable that the spring-break and the electric oscillation are approaching resonance.

The primary of L_3 was now provided with a new weak secondary L_A of

about 150 turns of wire. On being tested, it gave the results reproduced in curve *c*, figure 129. The crest here is apparently near $C=0.9$ microfarad, but may be beyond the figure. If the note is d''', $L=0.022$ microfarad, or somewhat smaller.

To this secondary L_A the coil L_1, with the core removed, was now added. The effect is shown in figure 129, curve *d*. With the crest placed at $C=0.45$ microfarad and the same note d''', the new coefficient would be $L_A + L_1=0.044$ henry, giving 0.022 henry for the coil L_1 alone. On thrusting the core into L_1, the current was almost entirely cut off; but a crest at $C=0.06$ to 0.07 could just be detected. If the note is again d''', this makes $L_1=0.3$ about, which is correct in order of value.

It would not have been difficult to increase the currents in the secondary by the corresponding increase in the primary; but because of the danger of sparking through the condenser, this was not attempted.

As the crest of the core L_A is not quite within reach, another similar coil, L_B, was wound with somewhat thinner wire. The graph is given in figure 129*e*, where the crest is definitely between $C=0.8$ and 0.9 mf. If $C=0.85$ is taken, $L=0.0234$ henry. In their initial progress the curves *c*, *d*, *e* run very closely together.

In case of the graphs, figure 130, $L=0.010$, 0.020, 0.030 henry, respectively, were added to the secondary circuit, L_B. Taking $C=0.57$, 0.45, 0.35 for the crests, since $\omega^2=10^7\times 5.02$, $L=0.011$, 0.021, 0.033 henry if $L_B=0.023$ henry, which is good corroboration for all the inferences involved.

48. Long and short pipes compared. Combined primaries—The frequent occurrence of crests which have no equivalent in the electric oscillations, silent crests as it were, induced me to prepare a very long (length 30 cm., diameter scant 1 cm.) thin pipe, which would naturally be expected to harbor many nodes of high pitch. The acoustic survey of this pipe so far as attained is shown in figure 131, which was difficult to construct by ear methods, because of the sharpness and proximity of the cusps. The maxima e', g', a', e'', g'' stand forth very well; but below c' there is liable to be too much intricacy to be fully made out. Between e'' and g'' one is often at a loss, and it was impracticable to go higher.

In figure 132*a*, the case of L_B, alone, is worked out, capacities (see insert) varying in steps of 0.1 microfarad. There is no real crest, but rather a flat plateau to the curve, after $C=0.8$ microfarad is passed; but the low $C=\infty$ proves that a marked crest must occur. If we take $C=0.8$ microfarad as the maximum, the note for $L_B=0.023$ will again have to be d''', as in figure 128. This is out of immediate correspondence with figure 131, except in relation to g' and g''; but it is otherwise not unexpected in relation to g', since the pipe is just three times as long as the short pipe. As usual, the notes vary slowly in pitch on the plateau, but relatively fast nearer the anterior parts of the graph. The probability of e''', g''', a''' cusps is without evidence in figure 132*a*, and there is no indication that a continuous C change would have

introduced other cusps. The distribution of notes in the earlier curve may therefore be reproduced here.

Owing to the remoteness of the crests in curve *a* (L_B, telephones only), the additional inductance of coefficient L_1 (0.32 henry) was inserted. The latter was provided with a primary (without break) joined in series with the primary of L_B (see insert). The resistances being low, the simple platinum break-hammer of L_B functioned satisfactorily. For convenience, the secondaries were also joined in series, making a total coefficient $L=0.32+0.02=0.34$ henry.

The graph 132*b* was obtained with the long pipe (length 30 cm., diameter 1 cm.) in this way. The curve is interesting, as it actually exhibits two crests. If the first is located at $C=0.15$ microfarad and the note is below $e''(\omega^2=4\times4.46\times10^6)$, $L=0.37$ henry, in excess of the actual value stated.

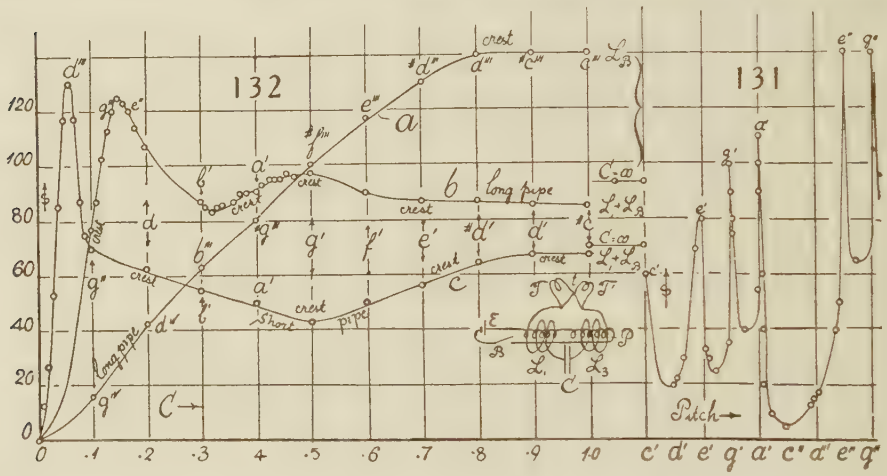

If the crest is located at $C=0.14$ microfarad and the note is $g''(\omega^2=4\times5.91\times10^6)$, $L=0.30$ henry below the actual value. The crest found in the graph, $C=0.15$, may therefore, in correspondence with the e'', g'' vagueness of figure 131, be regarded as a superposition of the two. Again, if the second crest is placed at $C=0.5$ microfarad and the note is $g'(\omega^2=10^6\times5.91)$, $L=0.34$ at once in fair agreement with the actual value, even if the crest is flatter. On the other hand, e', a', a'', gave no interpretable electric equivalent, the pitch *a* being left out entirely in figure 132*b*, as the annotations "crest" indicate. Again one suspects the dominance of the spring-break.

The same adjustment was now made for the short pipe (length 10 cm., diameter 1 cm.) with results recorded by the figure 132, graph *c*. There is here but one crest, near $C=0.06$ microfarad. If the note (according to fig. 128*a*) is near $d'''(\omega^2=10^6\times50.2)$, $L=0.33$ henry, a little short of the actual value, showing that the rounded $C=0.06$ microfarad is not the peak of the crest.

From the total coefficient $L=(0.32+0.02)=0.34$ henry, I now computed

the frequencies corresponding to each of the steps $C=0.1$, in the curves b and c. For $C=0.1$, 0.2, etc., the nearest note has been inscribed in the curves. Particularly in case of graph c, it is noteworthy that the crests found in the graph figure 128a, with the possible exception of d', make no impression on the former, as the attached legends, "crests," indicate. Thus, for instance, the g' crest in figure 128a actually coincides with the minimum at $C=0.5$ in figure 132c, where the note is g'. The same has been indicated in figure 129c, in figure 132c, and elsewhere. Curiously enough, in curves b, c of figure 132, the acoustic g' crest lies respectively at a crest and at a trough. Hence also the reasonable surmise that the troughs of the acoustic graphs (pitch) ought to coincide with the troughs of the electric graphs, receives no warrant from the experiments. It has been suggested that if the passage in C from step to step were made continuously, the missing crests might appear; but in a number of cases in which this was tried, the crests in question remained absent, unless they were foreshadowed by the steps and merely intensified by continuous changes of C. Hence, since the survey is made by a direct current interrupted by the periodic break without appreciable electric oscillation (*i. e.*, no condenser, see fig. 124), whereas in case of the platinum spring-break of fixed pitch, the presence of a condenser determines the oscillation (both acoustic and electrical), the missing crests must be in some way associated with this difference of excitation. The direct current, periodically interrupted, is under better conditions to force a vibration than is the self-starting electric oscillation. Practically this is an advantage, since an abundance of harmonics would be bewildering. If C_0 is the step unit, so that $C=n_cC_0$, and if N is the frequency of the nth harmonic found, $N=n_kN_0$ (even harmonics in the phase adjustment, N_0 being the fundamental frequency)

$$n_k^2n_c=1/(16\pi^2N_0^2LC_0) \text{ constant},$$

so that a series $n_k^2n_c=n'^2_2n'_c$, etc., is implied, each pair $n_k^2n_c$ corresponding to a crest. But as a rule only one pair is found.

In other respects, the remarks already made relative to high and low C values apply. The purpose of using the electric oscillations to interpret the amazing presence of very low notes associated with very short, slender pipes has thus in a measure succeeded.

49. Opposed mutual inductions and similar comparisons—In figure 133 I have recorded another set of experiments, in which two coils in series L_1 and L_B in the secondary, or I and I', were actuated by their primaries, also in series, in the same or in opposed directions. Hence the sum or the difference of induced electromotive forces is active in the secondary and the currents, s, are correspondingly high or low. The crests, however, remain appreciably unchanged in their C position; *i. e.*, the coefficients of inductance remain the same. I and I' are nearly equal, L_1 and L_B quite different, as heretofore stated. In the former case (I, I'), the crest is an extended plateau.

If we regard s as equivalent to current, the two cases may be described as

$$\frac{s}{s'}=\frac{M_1+M_B}{M_1-M_B} \quad \text{or} \quad \frac{s+s'}{s-s'}=\frac{M_1}{M_B}$$

so that the ratio of coefficients of mutual induction should appear, if s had been standardized in terms of electrical current.

Figure 134 makes a comparison of the currents in the same secondary (the half-coil of L_1), if in one case the current is cut down by a high resistance (here 1,500 ohms), curve b, and in the other left without resistance, apart from

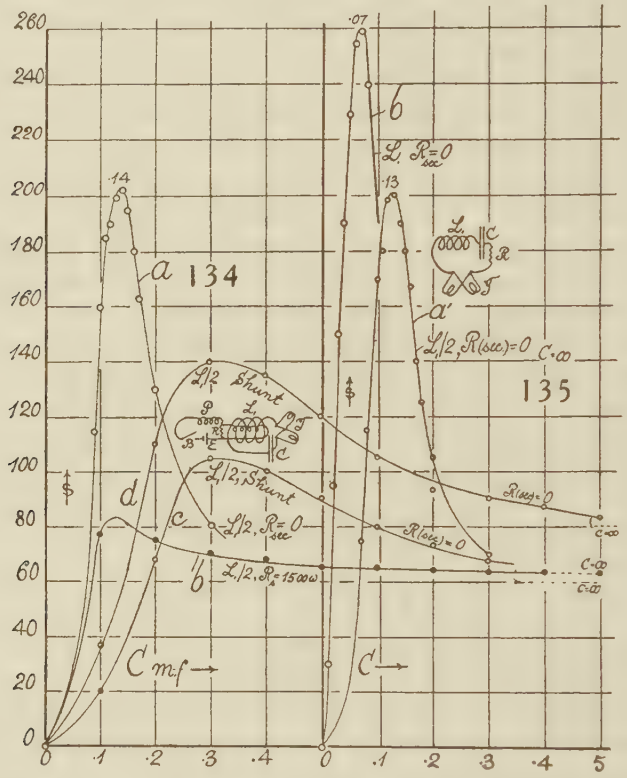

that of the coils themselves. In the latter case the fringe displacement is quite out of the field of view (limit about $s=140$) and the slide micrometer must be used to restore the fringes. This involves no difficulty, since a single new fiducial position of fringes is adequate and the displacement in question is read off on the micrometer. The distortion of curve produced by the resistance is striking, so that the crest is only recognizable with difficulty in curve b.

In figure 135 the other half-coil of L_1 is treated, curve a, in comparison (curve b) with the whole coil L_1, in both cases without additional resistance. Naturally, s is not directly proportional to the currents. The sharpness of both crests is again striking, relatively speaking. In curves a, figures 134 and 135, the crests are at $C=0.14$ and $C=0.13$ microfarad, respectively, so

far as determinable. Since the pipe-note is d''', $\omega^2 = 10^7 \times 50.2$, the coefficients for the half-coils are $L_1/2 = 0.143$ and 0.154 henry, respectively. The crest of the full coil, L_1, is at $C = 0.07$ microfarad, so that $L_1 = 0.286$ henry. The difference $(0.143 + 0.154 - 0.286)$ is 0.011 henry, which may be ascribed to the accessories used twice in the former case.

50. Primaries in parallel—Instead of cutting down the secondary current by inserting resistances, R, until the fringes remain in the field of view, as in figure 134, curve b, better relations are to be anticipated from a shunt in the primary, P. The method is shown in the insert, figure 134, where R is the shunt. Both primaries are actuated by the same spring-break, B, the primary of $L_1/2$ being in parallel with P.

Results obtained in this way are given by the graphs c and d in figure 134, for two different values of R. They are in fact less distorted than curve b of the same figure. A surprise was encountered in computing the coefficient L for different frequencies, viz,

d'''	$\omega^2 = 50 \times 10^6$	$L_1/2 = 0.067$ henry
g''	22×10^6	0.15
d''	12×10^6	0.268

if $C = 0.3$ at the crests as the graphs c and d imply. Turning to figure 128, it follows that the poorly developed crest g'' of that figure must have been selected, for the $L_1/2$ value is then of the right order.

These results make it desirable to ascertain the principle underlying the selection of harmonics in question. Accordingly, in figure 136, using the same method with primaries in parallel (see insert), the solution is attempted by varying the resistance of the shunt from $R = \infty$ to $R = 1$ ohm. When $R = \infty$ and the whole current is therefore sent through P_2 as well as P_1 (which merely actuated the break here), the crest $C = 0.15$ (nearly) does indeed require the d''' harmonic in the pipe. This is still more the case when the $L_1/2$ coil (0.16 henry) is loaded with the additional small inductance of coefficient $L_B = 0.02$. But when the resistance R is successively decreased ($R = 100$, 30, 10, 5 ohms), the crest is at $C = 0.3$, implying the harmonic g'' in the pipe as just computed. When decreased still further ($R = 2$, 1 ohm), the crest moves apparently to higher C values of at least 4 microfarads. The crest, moreover, now becomes a plateau and a peak can not be identified. If d'' were in question, the C should be about 0.5 microfarad, which the graphs do not fully admit. It is possible that a mixture of notes, sometimes d'' and sometimes g'', may supervene.

However, it seems clear that the pitch of the crest depends on the intensity of current in the primary, P_2, and increases with this intensity. It requires vigorous vibration of the telephone-plate, in other words, to shake out the d'''. Otherwise, with dwindling intensity, g'', etc., will appear in succession. This was curiously substantiated in a later repetition of the measurement for $R = \infty$, also given in figure 136. In place of the former d''' and steep crest, a g'' note with rounded crest and slowly falling curve now appears, showing

that very slight modification of the vibration conditions may totally change the choice of the pitch of the vibration, for both the d''' and g'', when once selected, are quite persistent throughout the remaining test on a given day.

To return to the difference in the form of the two curves for $R = \infty$ in figure 136, the rapid fall from d''' in one case and the very deliberate descent from g'' in the other, are referable to the rapid change of pitch in the former case, compared with the slow change in the latter. This is indicated by the resonance note corresponding to $C = 0.1$, 0.2, etc., recorded at the bottom of the figure and holding for all curves except $L_1/2 + L_B$. It thus follows that the cusps in the acoustic survey of the pitch of the pipe (like fig. 128) are virtually much sharper in their C values for the case of d''' than for lower pitch, so that g'' can be stimulated by a wider range of near notes, or at least of C values, than can d'''.

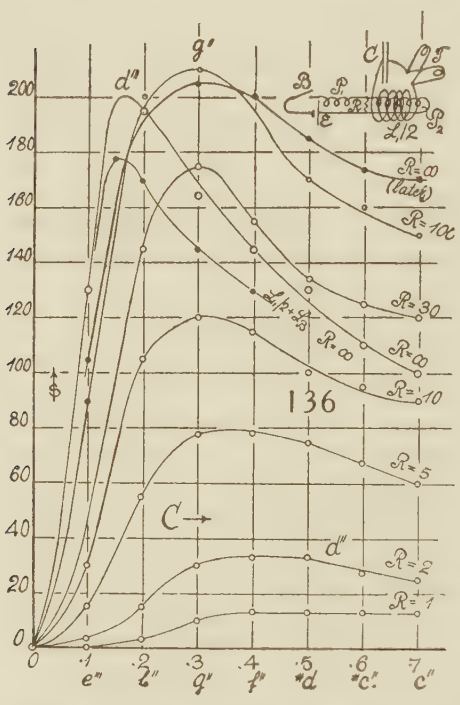

There are, however, other facts left unexplained, as, for instance, the difference in form of the curves $R = \infty$ in figure 136 compared with the corresponding curves without a shunt, figures 134*a* and 135*a*, for practically the same conditions. The latter are almost symmetrical and slender as compared with the former. Quite persistent when first obtained, they could not be reproduced. The cause lies probably in the spring platinum-break, which incidentally changes its relatively low pitch somewhat, and thereby evokes different groups of high overtones in the telephone-plate. In proportion as one or more of these correspond to the pitch and overtones of the pipe, the graphs obtained are more salient. Additional light will be thrown on the subject by the following chapter.

CHAPTER III

MUTUAL RELATIONS OF PIN-HOLE PROBES. QUILL-TUBES

51. Outer pin-hole of the pipe enlarged—If the outer pin-hole of the pipe *tt* (insert, fig. 138) connecting the telephones is removed and replaced by an $\frac{1}{8}$-inch stopcock *K*, the inner pin-hole *r* leading to the U-gage, *U*, being left in place, the results obtained in the application of the preceding method of *C* variation are peculiar. As shown by the adjoining graph, when the cock is

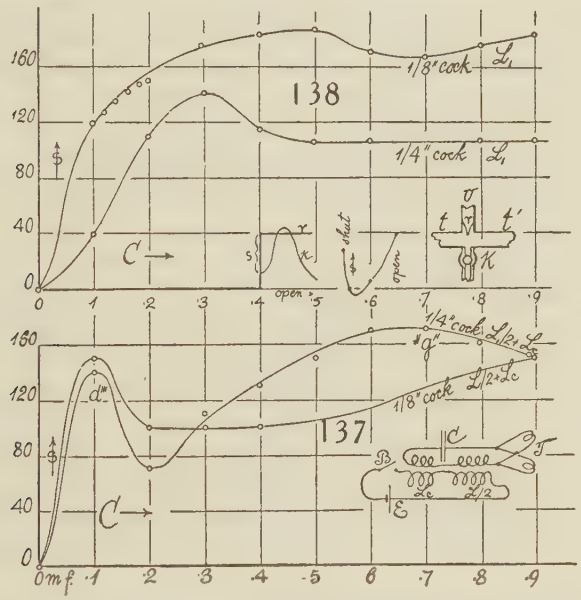

all but closed, the fringe displacement *s* for an appropriate *C* value is quite marked, but rarely more than about one-fifth of what the pin-hole removed would have given. If the stopcock is now gradually opened, the fringe displacement drops to zero and may even become negative. On opening the cock farther from this minimum degree, the *s* values rapidly increase to a value even above the original (crevice) datum. Thus it appears as if the effect of the crevice were at first like that of pin-hole *r*, but negative, the two coöperating with *r* in excess. As the crevice enlarges slightly its reciprocal potency diminishes more and more, passing through zero and therafter counteracting *r* or even exceeding it (negative displacement *s*). After this, with further widening of the crevice, the *K* effect rapidly vanishes and *r* only is active. The two graphs *r* and *K* are shown in the insert, where $s = r\text{-}K$, illustrate this point of view. The behavior of the crevice is naturally very variable. Sometimes $s = 0$ is not reached and *s* is always a positive minimum.

For each set of the stopcock, moreover, the s values pass through definite maxima or minima with C. Negative minima were usually found for C varying in 0.01 microfarad from zero, whereas the positive maxima occurred with C varying in 0.1 microfarad from zero. The phenomenon is suggestive and will presently be specially treated.

Here, figures 137 and 138, I wish to record the results when the cock K is wide open (one-eighth inch bore) and when it is quite removed (one-quarter inch bore). Figure 137 shows the fringe displacements with the coils $L_1/2$ and L_C in circuit, the primaries and secondaries in series, the primary of the latter actuating the spring-break. The s values are quite marked, but three or four times weaker than the crest found with the absent pin-hole inserted. Both curves, though different in form, have the same initial crest at about $C=0.1$ microfarad. This is a d''' if $L_1/2 + L_C = 0.2$ henry, as estimated. The graph for one-eighth inch bore shows no salient features thereafter; but the other graph (one-quarter inch bore), which now exceeds it, passes a second definite crest at $C=0.7$ microfarad, about, which should be near $\#g'$. Naturally, the pipe with these two different holes in the middle has different pitches for the two cases, the remarkable feature being that with these large apertures there should be any middle node at all.

In figure 138, the same kind of experiments are carried out with the two halves of the coil L_1, only, in the secondary. The graphs are now totally different in shape from the preceding. Although the inductance is greater, there is no initial crest, the two found being at $C=0.3$ and $C=0.5$ microfarad, and here the curve with the one-eighth inch bore or opening is the stronger. The pitch should be near $\#c''$ and $\#g''$ respectively. In the latter case, the remote crests for the wide tube happen to coincide.

Hence, the endeavor to reduce excessive fringe displacement s by enlarging the outer pin-hole did not succeed, the graphs being exceedingly complicated. The phenomena introduced in this way, however, deserve further attention.

52. Reversal of outer pin-hole probe—In figure 139*b*, where tt' is the pipe connecting the telephones at T and T', the pin-holes r and s are set to coöperate with each other. The stream-lines run from the apex to the base of each cone, so that beyond r at the U-gage, there is evidence of pressure. The mean density of the node between r and s is an excess. Only the points of the pin-hole cones are effective. They may be pricked in thin metal foil, and will, as a rule, act positively or negatively, according as the puncture is carefully made from within or from without. Size of hole and slope of walls may be important, but the volume of the region in which the action is completed is astonishingly small. Roughly, one may surmise that within the apex of the hollow cone there is marked vorticity. (cf. § 88.)

In figure 139*c*, the adjustment for electric oscillations are diagrammatically given (e electromotive force, 3 cells with resistance, B platinum spring-break of low frequency, P primaries in series, L actuating the spring-break, L_1 is the secondary, with capacity C and telephones T, T', connected by the pipe tt').

Figure 140 shows the fringe displacement s for the summational adjustment of pin-holes, when the capacity in the secondary is varied in steps of 0.1 microfarad. There is a maximum at $C=0.3$ microfarad about, corresponding to the oscillation pitch near d'', and a minimum at $C=0.8$ microfarad corresponding to f', at which the pipe makes its nearest approach to silence, though there is abundance of multiresonance left here. Nevertheless, the

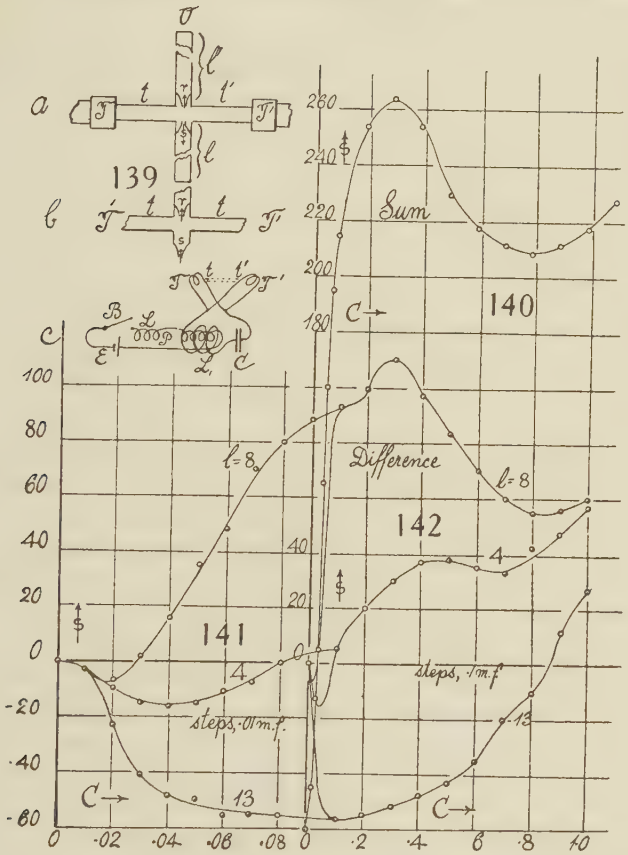

crest for $C=0.3$ and the trough for $C=0.8$ must dominate the whole of the subsequent experiments.

The lengths of the pin-hole pipes (l, l') in the summational case will be treated later.

It follows that if the pin-hole probes, r, s, are adjusted as in figure 139a (T, T' telephones in phase, tt' acoustic pipe, interferometer U-gage beyond U) they will counteract each other. The effect at U will be differential, either a pressure or a dilatation, according to the relative efficiency of the pin-hole probes.

The inner of these, r, is left constant in quill-tube length, l', and its effect will be persistently positive. The outer pin-hole, s (fig. 139a), carries a

quill-tube extention l, of variable length. Such a quill-tube (l) as heretofore shown, is a musical instrument with a pin-hole embouchure; but the effects obtained in the present paper are enormous as compared with the older evidence.* It is presumable that the effectiveness of s and also of r will depend on the frequency of the note of the pipe tt' primarily (remembering that a telephone-plate overtone may be in question) and on the natural frequency of the pin-hole quill-tube secondarily.

The experiments with counteracting pin-hole probes were made, as summarized in figures 141 and 142, by successively increasing the length of the outer pin-hole tube from $l=4$ to $l=13$ cm.; for each value of l, the capacity C was changed in steps of 0.01 microfarad from 0 to 0.1 microfarad (fig. 141), and in steps of 0.1 microfarad, from 0 to 1 microfarad (fig. 142), to bring out the nature of the phenomenon. The curves show that an even wider range of C would have been desirable, for all curves seem to point to a further crest beyond the diagram. The length of the quill-tube prolonging the inner pin-hole r was kept constant throughout, at somewhat above $l'=10$ cm.

In figure 141 for $l=4$ cm. (length of quill pin-hole tube) the outer pin-hole s dominates, the curve being in the negative or dilatational field up to $C=0.8$ microfarad. There is a well-developed negative crest at $C=0.04$, probably near g'''.

When l is increased to 8 cm., the negative crest wanes, falling to somewhere between $C=0.01$ and $C=0.02$ microfarad; but the curve soon becomes strikingly positive, so that the inner pin-hole r prevails.

The further increase of l to 13 cm. of length shifts the curve back to the negative region. There is now no discernible crest, but all negative fringe displacements are very large. It is thus probable that between $l=8$ and $l=13$ there is an instability, at which the curve drops almost suddenly from positive to negative (curve $l=13$ is not liable to be the lowest) regions. Clearly much smaller steps in length must be interpolated if the nature of the phenomena is to be disclosed. The crests of figure 141 are not discernible in the summational curve, figure 140, possibly owing to the extremely rapid changes of frequency.

Figure 142 is a later continuation of the work for the larger ranges of decreasing frequency, already specified. Comparing it with figure 140, we notice a distinct tendency to reproduce its crest and trough. This is obvious in case of $l=8$ cm.; it is more obscure for $l=4$ cm. and nearly absent at $l=13$ cm. The secondary phenomena may thus be of prime importance. As a rule the s values vary more markedly in the lower frequency ranges ($C=0.1$ to 1 microfarad) than in the higher ($C=0.01$ to 0.1 microfarad); *i.e.*, the pin-hole probe seems here to be more responsive.

53. The same. Cases of smaller length increments—Data obtained in the same manner as in the preceding are given in figures 143 to 146, the steps being 0.01 and 0.1 microfarad respectively. Figure 143 shows that whereas the graphs $l=2$, 3, 5, 7, though different in character, follow each other in

*Carnegie Inst. Wash. Pub. No. 310, 1921, § 25; No. 310, Part II, 1923, § 5

regular succession for values of C below 0.06 microfarad; but between $l=7$ and $l=9$ cm. there is instability, so that the former graph drops over a relatively large range in s, from positive to negative values. There is a definite crest for $l=7$. The other curves run into a plateau, which in figure 144 appears merely as double inflection. Consequently, in the latter case, the interval 0.1 to 0.2 microfarad was also worked out in steps of 0.01, but no ignored crests were detected. In figure 145 the steps of l are taken larger to show that oscillation of graphs has not ceased.

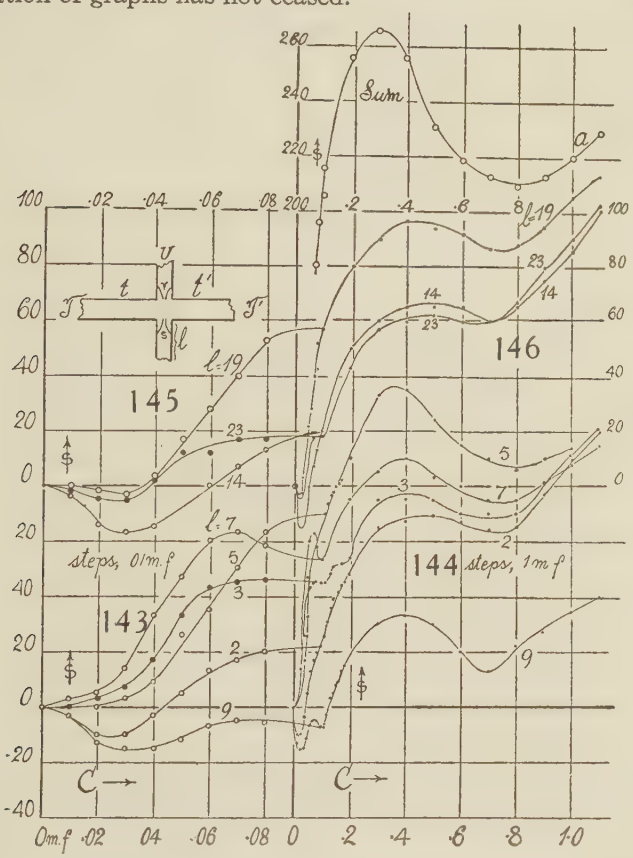

Figures 144 and 146 clearly indicate that all the graphs are dominated by the summational curve a (pin-holes in series), at least in so far as the position of minima is concerned. The maxima, however, are shifted to the right, *i. e.*, to lower frequency, as if the pipe-note had flattened from d'' to b' or more.

In figures 141 to 146 the inner pin-hole prevails, at least in the region from $C=0.1$ to $C=1.0$ microfarad, the curves tend to be strongly positive throughout. Search was therefore made for an outer pin-hole which would have the same negative excess qualities if placed in the outer position, s in the inserts. After many trials one only (No. II) was found. The fringe displacement with this probe was much more sluggish than in the preceding experiments, indicat-

ing a pin-hole of much finer bore. For this reason, perhaps, the results obtained (figs. 147 to 150) are less incisive, as it was necessary to wait some time before the full fringe displacement was assured.

In figure 147, for steps of 0.01 microfarad, the curves $l=2$, 4, 6 cm. are a progression, with the crests moving to the right. After this there is an instability with a drop in s values from $l=6$ to 8 and 10, the crests tending to the left. In the former cases, the inner pin-hole is still dominant, but ceases to be so in the latter ($l=8$, 10 cm.). One may notice, in general, that positive tendencies in s here replace negative tendencies in figures 143 and 145.

In figure 148 for $C=0.1$ to 1.1 microfarad, the resemblance to the summational curve (supplied in figure 150*a*) is practically eliminated. The strong summational crest at $C=0.3$ microfarad is obscurely replaced by troughs, if at

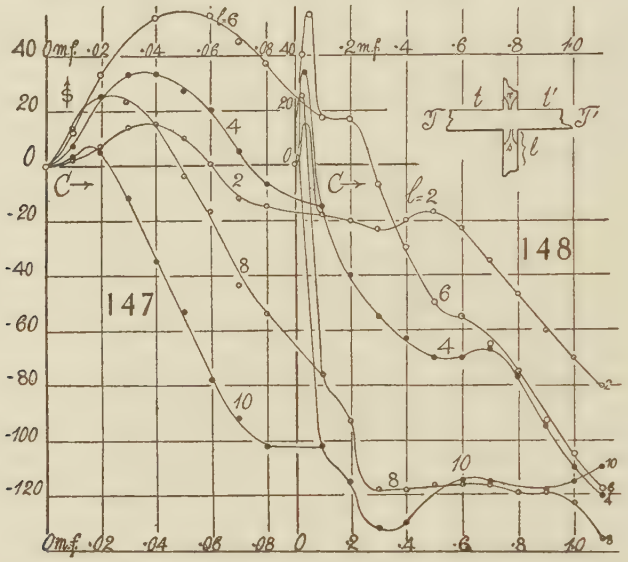

all. The trough at $C=0.8$ has often no correspondence, but there is in this region a shift of maxima. The intense negative characteristics of this pin-hole for $l=8$, 10 cm., are remarkable. They are borne out in figure 150 for $l=11$ cm.

Remarks of the same nature may be made with reference to figures 149 and 150 for a larger range of l values and with unbroken quill-tubes. The s drop from $l=6$ cm. to 11 cm., is of the same nature and the curves closely resemble the preceding series, though the experiments were made later with a different adjustment. The summational crest suggests a differential trough (in $l=6$ obscured by rapid descent), the summational trough a differential crest, though much shifted. The drop from $l=6$ to 11 cm. is reconciled only after $C=0.8$ microfarad is passed.

Unfortunately, in endeavoring to improve this pin-hole, No. II, by washing it, the negative character completely vanished. It must have been due, therefore, to something like atmospheric accretions accumulated in years, by which the pin-hole was incidentally constricted in such a way to give it its

negative quality. The attempts to reproduce it failed throughout. Other pin-holes examined, *A*, *B*, *C*, *G*, etc., all showed the customary positive character. *D* was a wider quill-tube (diameter 5.5 mm.) than the others (diameter 3.5 mm.), and with this its isolated behavior may be associated. The search for the lost negative quality in short pin-holes like No. II will be undertaken elsewhere (cf. § 88).

A more systematic and extended survey with the modified pin-hole II is given in figures 151 to 153, on the same plan as heretofore. In case of the lengths of pin-hole tube, $l=2$, 4, 6, 8, (10) cm., the capacity C, was varied in

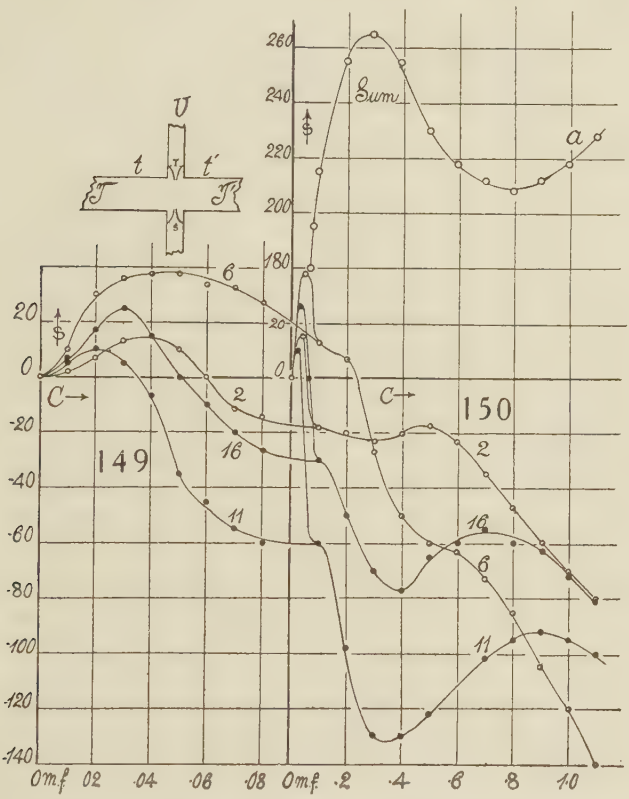

steps of 0.1 microfarad only, to prevent confusion of curves. The graphs rise from $l=2$ to $l=6$, the latter showing exceptionally high s values. From $l=6$ to $l=8$ cm. there is a vibrational instability in the quill-tube and a consequent drop of curve, which continues to $l=(10)$ cm.

The sectioned tube was replaced next day by a single tube, and this is recorded in an even lower curve at $l=10$. Curves (10) and 10, however, are of the same character, and the difference in location is more probably due to favorable change in the pitch of the spring-break, or to a small difference of length. The series $l=10$ to $l=20$ cm. is given both for $\Delta C=0.01$ microfarad below $C=0.1$ microfarad, and for $\Delta C=0.1$ microfarad above $C=0.1$ microfarad. In figure 151 the progressive march of curves upward over the enor-

mous s interval is quite remarkable; but after $l=20$, the curve suddenly drops again to the marked negative s values of $l=22$ cm. A second vibrational instability has thus been encountered. The same routine with more complicated graphs is seen in figure 153, $l=10$ to 20 to 22 cm.

The experiments were then pushed farther for $l=22$, 24, 26, 29 cm.; but to retain the clearness of the diagram, only the latter is given. The graphs again march regularly upward, even 29 being, as yet, far from the goal reached by $l=6$ cm.

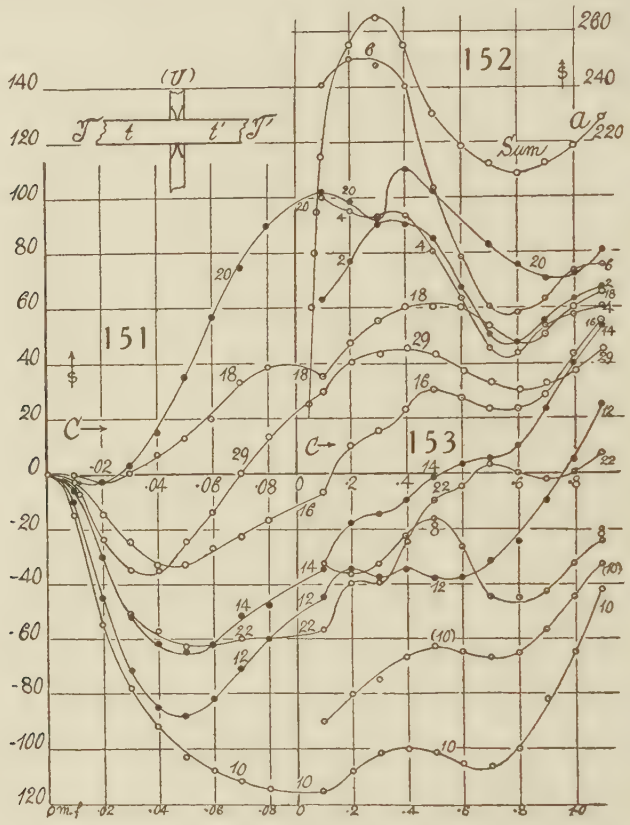

Figure 152 is the summational curve for pin-holes in series. It rises to $s=265$, about, which is but little larger than the combined s difference between $l=6$ and $l=10$, about $\Delta s=150-(-100)=250$ at the same C.

54. Summary—It is difficult to specify any characteristic of these curves, in view of their sinuosities. As a whole the fringe displacement for $C=0.1$ microfarad is such that it will answer the purposes of discrimination, at least at the outset. These data may be tabulated as follows:

$C=0.1$ microfarad												
$l=$	2	4	6	8	10	12	14	16	18	20	22	29 cm.
$s=$	63	100	140	−33	$\begin{Bmatrix}-90\\-115\end{Bmatrix}$	−45	−35	−7	35	105	−57	30

They are constructed in figure 154, which may be regarded as summary of figures 151 to 153. The detailed account which the pin-hole probe gives of the nature of the vibration in quill-tubes is thus amazing. Figure 154 admits of a straightforward interpretation. When the quill-tube of the outer pin-hole is elongated, the vibration for a given harmonic within ceases more and more, to eventual silence. Hence the inner or positive pin-hole is continually more effective to a positive maximum. After this the outer pin-hole vibration drops to the next harmonic of lower frequency. Corresponding to the longer tube, the outer vibration is then suddenly intensified and is in excess of the inner pin-hole vibration. Negative values of s, therefore, supervene, to be gradually diminished, in turn, on further elongation of the outer tube. The positive increments of the graph, figure 154, are thus continuous and the changes gradual, the negative increments sudden, and the action impulsive. This figure and others of a similar nature shows that to pass from cusp to cusp and elongation of quill-tube of about 14 cm. is needed. An efficient probe has a node at the reëntrant apex of the pin-hole.

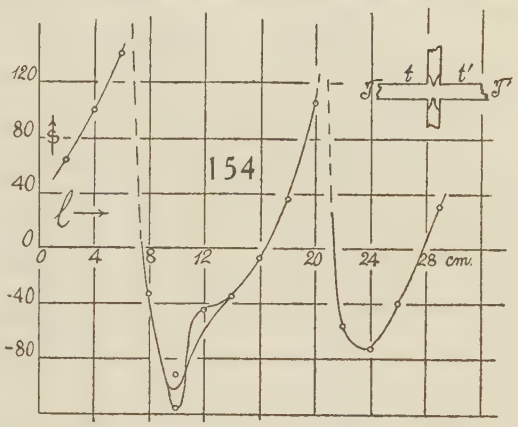

The above work, which encounters the superposition, more or less, of four harmonic graphs, those of the electric oscillation and the pipe acoustic oscillation and those of the two pin-hole tubes individually, is naturally destined to run into complications. It was therefore thought best to avoid theoretical speculation. The abscissas, $C = l/L(2\pi n)^2 = \lambda^2/L(2\pi v)^2$, increase with the squares of period or wavelength. Increasing l of the outer pin-hole increases λ. If a C is found to fit it, it does not generally fit the fixed l' of the inner pin-hole nor the pipe tt'. There is a further outstanding factor in the fit of the bore, etc., of the pin-hole to the note. Finally, overtones in the telephone-plate will be changed, with small changes in the pitch of the electric spring-break.

If we turn back to figure 128, giving the survey in pitch of the tube tt', we are struck by the extremely sharp cusps at the harmonics, alternating with intervals of complete silence. This implies the use of a motor periodic break of variable frequency. In contrast with this succession of cusps, such a curve as figure 140, obtained with the spring-break of constant low pitch, is illuminating. The tube tt' is never silent. It follows that high harmonics fitting the pipe tt' must be shaken out of the telephone-plates throughout and in succession, each in turn accentuated by the pipe. The drop of curves observed in figures 143 and 147, however, is probably incident in the quill-tube itself, additionally; but the absence of silence in all of them is to be referred to the pipe tt'.

It follows that if sharp cusps and precise values of L or C are to be obtained, the motor periodic break will have to be used in connection with tt'.

55. Pin-holes in series. Change of length and electric capacity—It has been shown in the preceding paragraph that the efficiency of a pin-hole probe (caet. par.) depends essentially on the quill-tube length and that the response is a maximum when this length favors the occurrence of a note at the reëntrant apex of the cone. It is desirable to test this inference with the pin-holes in series, as shown in the insert of figure 155, *i. e.*, to prolong both l and l' in definite steps. Figures 155 and 156, made with pin-holes No. II and No. III, respectively (the latter poor in response), have a preliminary bearing on this inquiry. In figure 155, the original length is $l=2$ cm. and the corresponding

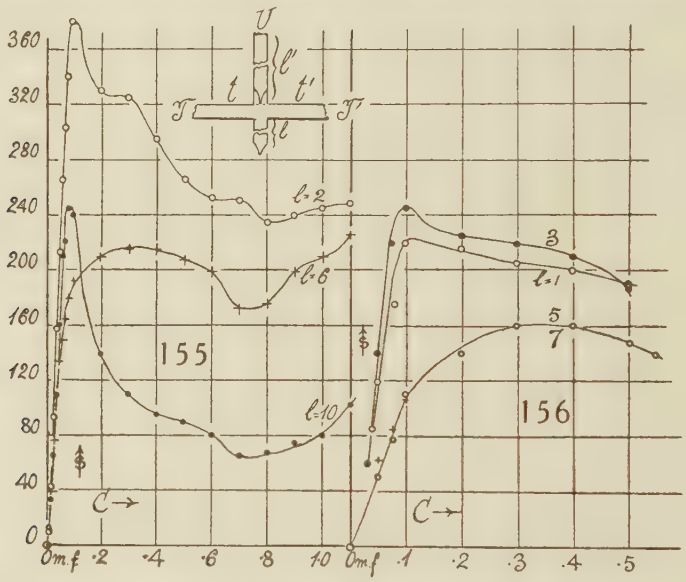

harmonic is strong ($C=0.1$ microfarad) and of high frequency near d'''. Prolonging the quill-tube to $l=6$ cm., the initial harmonic vanishes and is replaced by one with a flat crest at $C=0.35$ microfarad near g''. If the tube is further prolonged to $l=10$ cm., the high frequency crest near d''' again appears. All the graphs give evidence of the minimum between $C=0.6$ and 0.8 microfarad, to be associated with the pipe tt'.

In figure 156, the pin-hole tube was only $l=1$ cm. long; but for $l=1$ and 3 cm., the maximum near d''' is again apparent. Prolonging the tube to 5 cm. or to 7 cm. deletes the crest at $C=0.1$ and replaces it by a flat crest near g'' ($C=0.35$) as before.

The curves for increasing length l in general show reduced s-values in succession, so far as observed.

The elongation of the quill-tube l is an enlargement of the volume of the pipe tt' and must eventually interfere with its period. This is a complication

which makes it difficult to disentangle the curves, and the graphs of the systematic work are therefore omitted. They convey no information beyond the content of figures 156 and 157. A 2-cm. addition had almost no effect. Naturally the larger pipe, *tt'*, dominates the small cavity of *l*.

The tube *l* was thereafter elongated, on the salient side of the probe, keeping the distance of the pin-hole from *tt'* constant. These additions were also ineffective (to 5 cm.) unless they were very long (10 cm.), thin quill-tubes. The insensitiveness of the pin-hole probe on its salient side to these alterations was to be expected.

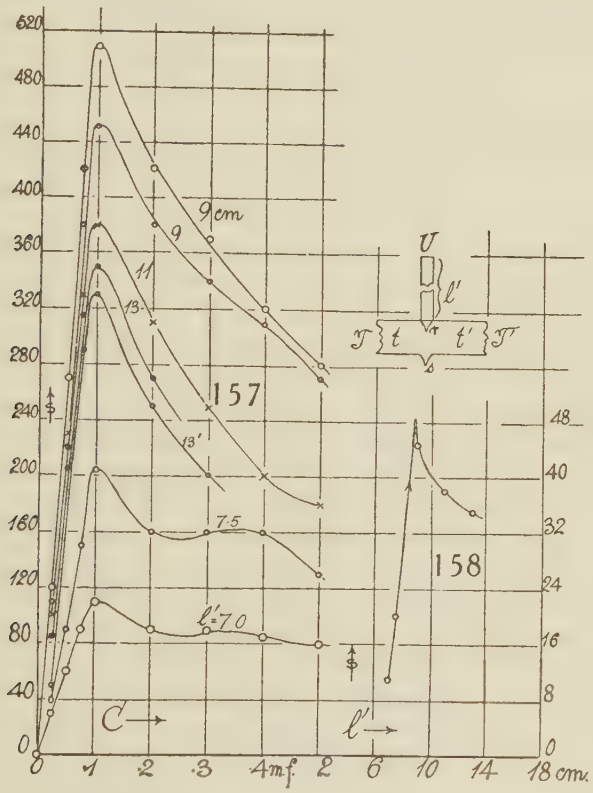

Figures 157, 158 give the results obtained on elongating the inner probe (*l'* in the insert), leaving the pin-hole *r* in place. This does not interfere with the volume of the pipe *tt'*. The tube *l'* terminates at *U*, the large cistern of the mercury U-tube, and *l'* can not therefore be decreased much below 7 cm. The graphs correspond very closely to an inversion of figures 151 to 154; *i. e.*, there is a very rapid rise from $l'=7$ to $l'=90$ cm., indicating instability, this time of a positive character (see fig. 158), because *r* is the positive pin-hole. From $l'=9$ to $l'=13$ cm. the curves descend gradually, as the *r* effect is diminished by the absence of a strong node at the pin-hole until the next rise appears with the succeeding harmonic. The crest remains at $C=0.1$ through-

out and increases enormously in sharpness when the quill-tube length favorable to the particular harmonic in question is attained.

These graphs are therefore interesting, as they suggest a reason for flatness of graphs and obscure crests. Thus the graph for $l'=7$ cm. is nearly without marked salience.

The endeavor to continue this work for greater lengths, l' (figs. 159 and 160), ran counter to an incidental break of pitch from about d''' to d'', so that a continuous curve could not be constructed. Such unfortunate changes are not rare and seem to result from changes of temperature modifying the stresses in the telephone-plates. The new results for the crests at $C=0.25$ microfarad are, however, consistent, and their relation to l' is a continued decrease of s as the quill-pipe joining r to the U-gage reservoir grows longer. One may therefore conclude that the d''' curve of figure 158, if it could have been prolonged, would continually descend from a general maximum of about $l'=9$ cm. This is therefore here the best length for the junction.

56. Effect of the number of pin-holes—Notwithstanding a number of investigations with the same bearing made in the earlier work,* the precise cause of the positive or negative quality of the pin-hole remains obscure. Inverting the pin-hole probe usually changes this quality, though it does not always pass from positive (fringe displacement, $+s$) to negative ($-s$). I have supposed that the slope of the pin-hole walls might here be discriminating, the stream-lines passing from the apex to the base of the hollow cone. This suggests itself for a pin-hole made of a constricted glass quill-tube. But as the pin-hole may be made quite as efficiently by merely puncturing a piece of metal foil (cemented to the end of the tube), either from within or from without, by a fine needle, the explanation given seems to be inadequate. One might therefore suppose that the inside of the probe, when it holds a node, is necessarily at higher pressure than exists on the salient side or in the free air, for reasons similar to those suggested by Bernoulli's principle. A vibrating column necessarily holds an excess of energy per cubic centimeter compared with the still air outside. In such a case the inversion of the pin-hole tube should change the sign of its quality; but this also is not always the case. Nodes, moreover, may be present on both sides.

As the question is thus open, I have thought it desirable to begin a systematic investigation by the present methods, and figures 163 and 164 show the effect of increasing the number of pin-holes of about the same size, etc., punctured from without (see insert, fig. 163, showing pin-holes in the plate p on the quill-tube q). The results are again in marked degree periodic. With one and two pin-holes the d'' crest is prominent, but after this the d''' crest prevails. The sensitiveness or acoustic pressure s is decreasing in cases corresponding to from one to three pin-holes (fig. 164), then rapidly increasing from three to seven pin-holes, decreasing again from seven to eight pin-holes, and thereafter increasing to nine pin-holes or over. The plate was then

*Carnegie Inst. Wash. Pub. No. 310, 1921, § 1, 18

removed and the clear quill-tube (q) used above. The acoustic pressure, s, is now a maximum and exceptionally high. Finally, the quill-tube itself was removed, leaving a round one-quarter inch opening in the pipe tt', opposite the inner probe r. The acoustic pressure, s, at once drops enormously. In a measure, this would be expected from the weakened node in tt', even though the pitch drops also. Notwithstanding the complicated relations, the curves are consistent.

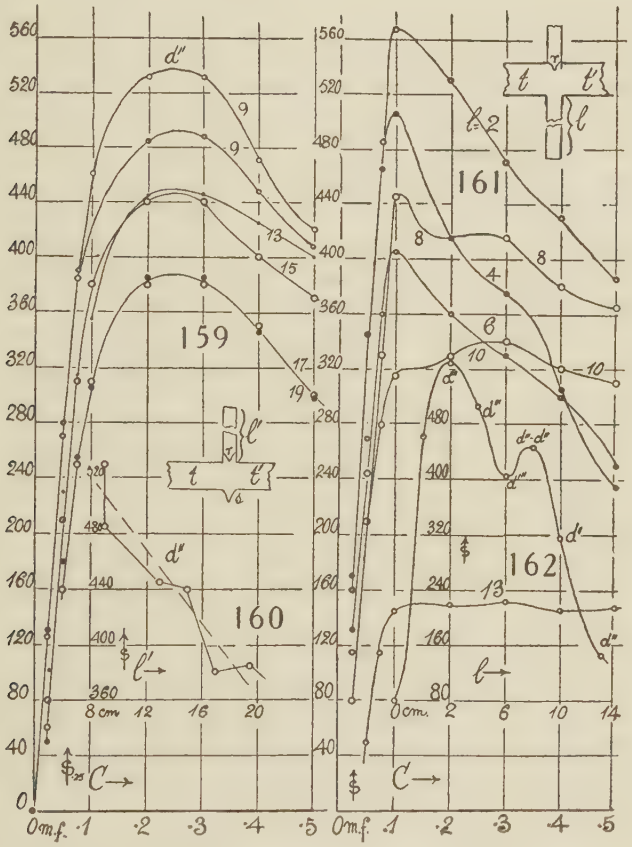

These results are throughout surprising. The probe r being left unchanged, a positive contribution in s must be supplied by the plate p. It is probable that this is done by tuning tt', until the node within r is most intense. This occurs ultimately when p is quite removed.

A variety of experiments was made with extremely fine pin-holes. Such observations have to contend with the difficulty that the fringe displacements are very sluggish. It is necessary to wait some time before the full displacement is approached, and one is never sure that it has been. In fine single pin-holes the maximum s is usually reached by a rapid upward trend at $C = 0.1$, and thereafter the curve meanders. Naturally, the quills should be

of constant length, preferably $l = 2$ cm. It is with these fine pin-holes that negative displacement is most frequently in evidence when the quill is reversed, so that the puncture is inward, as at p', in comparison with p, figure 165.

Figure 165 is a record of three identical probes, identically punctured so far as possible. In case of No. 1, both displacements s are positive; but curiously enough, the reëntrant adjustment (p') is ahead of the salient adjustment

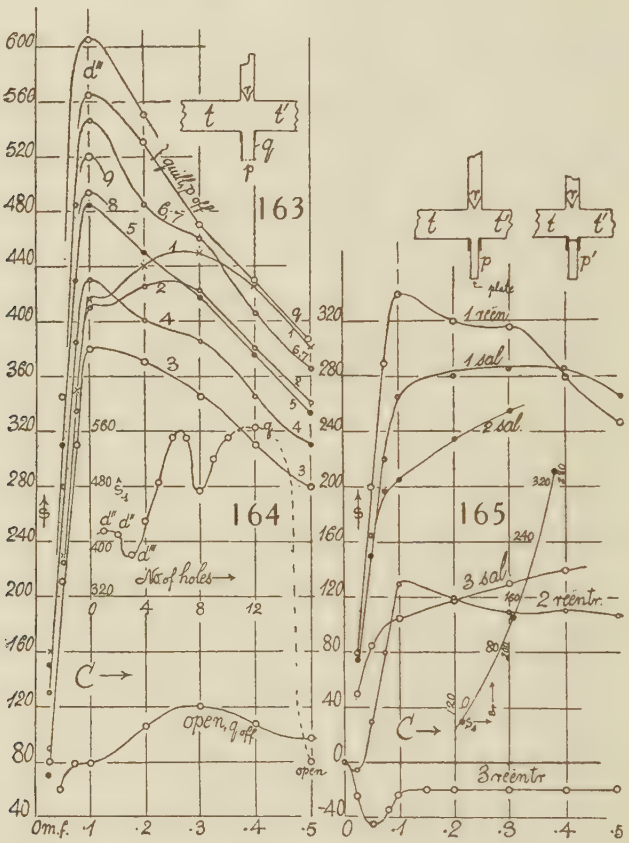

(p). This shows that the mere reversal of the tube does not suffice to reverse the sign of s, but that some additional quality of the pin-hole itself is in question. In No. 2, the salient s values are far in excess of the reëntrant values. The latter are in general positive, though they begin with a negative hook. In No. 3, the salient s values are positive but weak; the reëntrant values are now persistently negative, the curve after $C = 0.1$ microfarad, terminating in a plateau. The shoulder of this curve is near d''' in pitch, like the more pronounced cases Nos. 1 and 2. In contrast with this, the crests of the curves for salient cases are in relatively low pitch, if crests are present at all.

The three probes, though nominally identical, differ in behavior for reasons which one can not even conjecture. It is probable that No. 3 (negative case) is the finest hole. It is noticeable that the reëntrant cases fall from positive toward negative much more rapidly than the salient cases, which accounts for the reversal in case No. 1. A comparison of salient (s_s) and reëntrant (s_r) s value at $C=0.1$ microfarad is given (scale reduced one-half in the auxiliary curve of figure 165. The data are clearly related; a pin-hole which has the negative quality shows it in both the salient and reëntrant adjustments.

Unless the foils p are punctured alike and with the same needle, the relation of s_s and s_r exhibited in figure 165 ceases to hold. In an extended series of measurements (Cs graphs from $C=0$ to 0.5 microfarad, which must be omitted here), 14 pin-hole probes, all 2 cm. long, were selected at random. Nos. 1 to 10 were quill-tubes carrying punctured plates; B, a thin brass tube; I, II, III, the conical glass pin-hole probes already used above. The graphs obtained all shouldered at $C=0.1$ microfarad and then reached a flat maximum at $C=0.3$ to $C=0.4$ microfarad. The relations of s_r and s_s for $C=0.1$ are summarized in figure 166. One notes that for Nos. 1, 5, 7, 8, and 9, $s_r/s_s=1.1$; for Nos. B, 3, 6, $s_r/s_s=0.9$; for Nos. 2, 4, I, $s_r/s_s=0.7$, and here the first glass cone is included; for Nos. 10, II, III, $s_r/s_s=0.4$, the last results being straggling, and the brass probe No. 10 is classified with the glass cones II and III. It is impossible to suggest any reason for the occurrence of these groups from an inspection of the pin-holes. The arrangement would not have been very different at other C values. Thus at the crest $C=0.3$ to 0.4 microfarad, the data found are recorded in figure 167. We have the same groups with No. 7 more nearly in place, granting that the groups are probably quite incidental. In case of Nos. I, II, III, and 10, the Cs graphs were definite and similar; but this does not prevent I from falling into the higher group. Many of the punctures were very fine and displacements sluggish (particularly 6, 8, 9; 1, 2, 3). In § 90 this complicated subject is taken up again from a different line of approach and with better success.

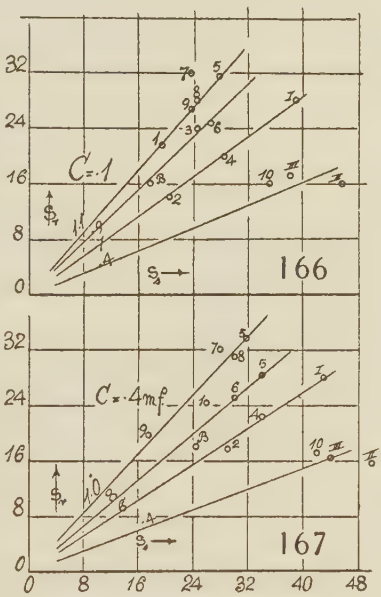

57. Outer quill-tubes of varying lengths, all open—The astonishing effect produced (fig. 163) by an open quill-tube, 1 to 2 cm. long, induced me to develop this result further, as shown in figures 161 and 162. It seemed probable that a node in the middle of the quill l might cause this pipe to act as if it were constricted there. One observes that lengths from $l=2$ to 6 cm.

maintain the crest at d'''. At $l=8$ cm. it is developing at d'', which seems to be retained thereafter, though at $l=13$ cm. the crest has merged into a practically even plateau. With the exception of the kink at $l=8$ cm. the effect of the tube-length l is a rapid decrease of acoustic pressure or fringe displacement s, quite contrary to what one would have expected. It seems as if the node within r were promoted by high pitch and therefore a short pipe l. The long quill-tube l thus acts similarly to a few holes in the plate p, figures 163 and 164, *i. e.*, figure 162, if reversed, would qualitatively reproduce the initial part of figure 164. In figure 161 the straight fall of curve from the crest at $l=2$ and 6 are noteworthy.

Figure 161, moreover, suggests reasons for the frequent occurrence of plateau-like maxima. It is probably associated with friction in the long quill-tube. The tube responds weakly with either d'' or d''', no matter what the excitation pitch. Excited with d'' it may sound d'''.

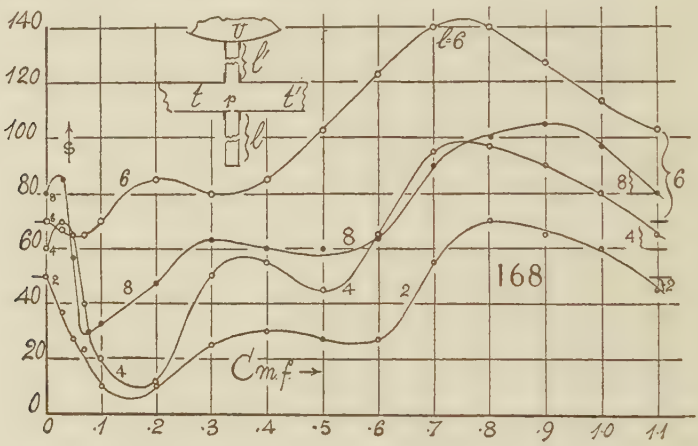

Some time after the initial datum for a quill-tube $l=1$ cm. in figure 162 was supplied and reduced to the same scale. This indicates the occurrence of a crest at $l=2$ cm., unless the short tube-length (1 cm.) weakens the node in tt' disproportionately. Finally, for $l=0$ cm. (quill adjutage q off) the datum of figure 164 may be taken; so that figure 162 exhibits the quill-tube effect fully. Such adjutages are effective for a mean range of length, say between 1 cm. and 10 cm. On either side of this the acoustic pressure (s) rapidly falls off to low values. (Cf. § 60.)

58. Data for identical reëntrant plate pin-hole probes of different lengths—Plate (punctured copper foil) pin-holes are not usually as sensitive as the glass cones carefully adjusted; but the acoustic pressures appear none the less clearly. In figures 168, 169, and 170 I have recorded the results of an incidental series of experiments which came out very satisfactorily and gives new information. The adjustment is shown in the insert figures 168 or 170, where p is the plate.

In the present experiments, l' was left constant and about 6 to 7 cm. long, while the length of l was successively varied from $l=2$ to $l=24$ cm. On varying C (for each length) from $C=0.02$ to $C=1.1$ microfarads, the graphs of figures 168 and 169 were obtained. These are so full of detail that to obviate a bewildering diagram of interlacing curves the two zero-lines of the graphs have been successively raised, $s=10$ or 20 scale-parts. Since all curves begin with $s=0$ and the zero-line is further shown at the end, this vertical displacement of graphs need not be confusing.

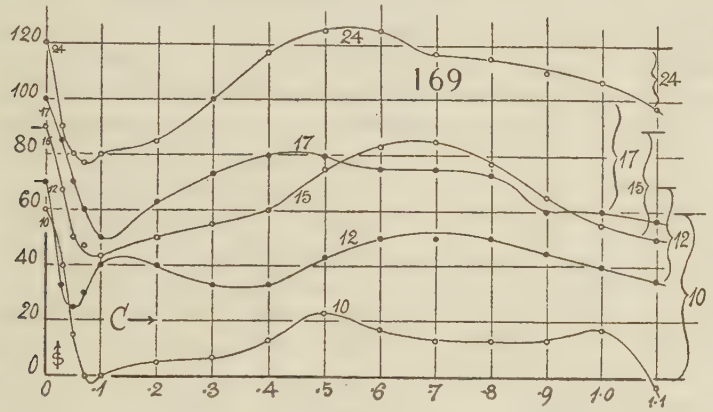

A great variety of primary and secondary troughs and crests occur in which some of the ornamentation may be due to failures of the telephone-plate to deliver the overtone needed. At the higher pitches ($C<0.5$ microfarad) the acoustic pressures s of the graphs are prevailingly negative, at lower pitches ($C>0.5$ microfarad) prevailingly positive; but when l exceeds 10 cm., graphs in the negative region (dilatations) are the rule.

So far as the crests can be specified, they are given in the following table. When l exceeds 12 cm. the curves are liable to meander.

$l=$	2		4		6		8		10		12		15		17		24	
	C	s	C	s	C	s	C	s	C	s	C	s	C	s	C	s	C	s
First crest	....	....	0.05	+10	....	....	0.02	+ 5	....	....	....	....	....	....	....	....	....	....
First trough	0.15	−45	.07	−52	0.06	− 5	0.07	−50	0.08	−62	0.05	−45	0.10	−47	0.11	−51	0.07	−43
Second crest	0.40	−20	0.35	− 4	0.20	+15	0.30	−16	0.50	−37	0.15	−27	....	....	0.45	−20	....	....
Second trough	0.55	−35	0.50	−15	0.30	+10	0.5?	−20	0.8?	−47	0.35	−38	....	....	0.6?	−26	....	....
Third crest	0.80	+20	0.75	+40	0.75	+72	0.90	+25	1.00	−43	0.70	−19	0.65	− 4	0.7?	−25	0.55	+ 7

The second row of troughs and the last row of crests are the most outstanding, and they have been reconstructed in figure 170, showing the acoustic pressures s for the successive lengths of quill-tube l. The troughs, curve t, are throughout negative (dilatation), the crests, curve c, at first strongly positive (pressures), but thereafter also negative. The little hooked crests, curve a, at the beginning ($C<0.05$ microfarad), are found in $l=4$, 6, and 8 cm. only. This little graph, a, may be regarded as an inversion of graphs c

and t. The pitch of the crests lies between $C=0.7$ and 0.9 microfarad, shifting from f' to e' roughly. The pitch of the troughs shifts relatively much more, say from $C=0.05$ to 0.15 microfarad, almost from f''' to f''.

Notwithstanding this vagueness in pitch, the interpretation of the phenomena given by figure 170 is very clear, the graph for troughs corroborating the graph for crests, acoustic pressures are a maximum when roughly $l=7$, 14, probably 21 cm. and minima for $l=9$, 18, etc., *i. e.*, for mid-values of l between the maxima. It is particularly remarkable that the troughs are least dilatational at the l values of the maxima of the crest graph.

Furthermore, since the inner quill-tube length is $l'=6$ to 7 cm., one may infer that the maxima of figure 170 occur when (see insert, fig. 170) $l=l'$, $l=2l'$, etc. Hence the pipe tt' is here most efficient in producing acoustic pressure (caet. par.) when the quill-tubes l and l' are equal in length. This high acoustic pressure, s, occurring in cases of geometric similarity of the pipes, is probably an important result, remembering that l carries the reentrant pin-hole and is a closed organ-pipe, while l' is an open organ-pipe. The nodes, which are to be located in the middle of l' and at the p end of l, should in cases of maximum acoustic pressure have the highest excess density over atmospheric density, or again, the least density deficiency.

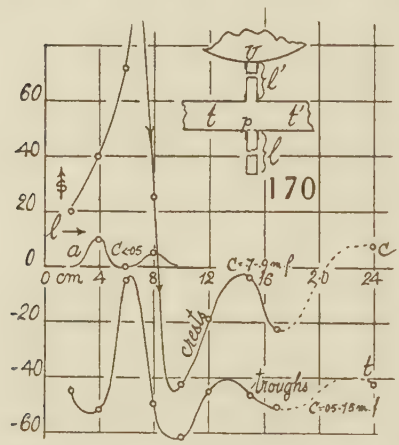

If we regard l' as an open pipe and l as a closed organ-pipe (in virtue of the plate pin-hole) then a wave-length which fits the former tube-length will not as a rule fit the latter, for the closed pipe should be half as long as the open, for the same fundamental pitch. Hence at $l=6$ cm., if the inner quill-tube is most active, the outer should be least so. Acoustic pressure should therefore result, if we postulate (§ 60) that the stream-lines pass from tt' to U in this case. If the pin-hole p is most active, they pass from U to tt' into the atmosphere (dilatation).

Inasmuch as the overtones of the quill-tubes must also be similarly treated, a diagram, like figure 171, will assist in locating the positions of crests and troughs in such graphs as figures 168 to 170. In figure 171 the lengths of quill-tubes l, l' are laid off horizontally, the corresponding wave-lengths λ, λ', resonantly sustained by the tubes, vertically. In the experiments, $l'=6$ nearly, is kept constant. Hence the wave-lengths in question are suggested by the horizontals marked $\lambda'=12$, 6, 4, etc. On the other hand, l is varied, the oblique lines marked $\lambda=4l$, $4l/3$, etc., suggest the resonant wave-lengths possible in the pin-hole tube. Now, as l was increased in steps of 2 cm. ($l=2$, 4, 6 cm., etc.), the verticals at these points, at their intersection with the horizontal and oblique lines, will point out the resonant wave-lengths to be

expected. These intersections have been accentuated in figure 171 by open circles for crests and closed circles for troughs.

Suppose, now, we let the impressed wave-length λ_c, due to the electric oscillation, diminish from a high value (C large) to zero, at $l=6$ cm., for instance. We should first encounter a trough above the diagram at the intersection-point of $\lambda=4l$. This trough is also implied in the graph $l=6$ of figure 168, beyond the diagram on the right. Next we encounter the fundamental crest at a, figure 171, strongly marked in figure 168. We then reach, in succession, trough b, crest c, trough d, crest e, etc., alternations quite like the graph 6 in figure 168, when c decreases. Below e the overtones will

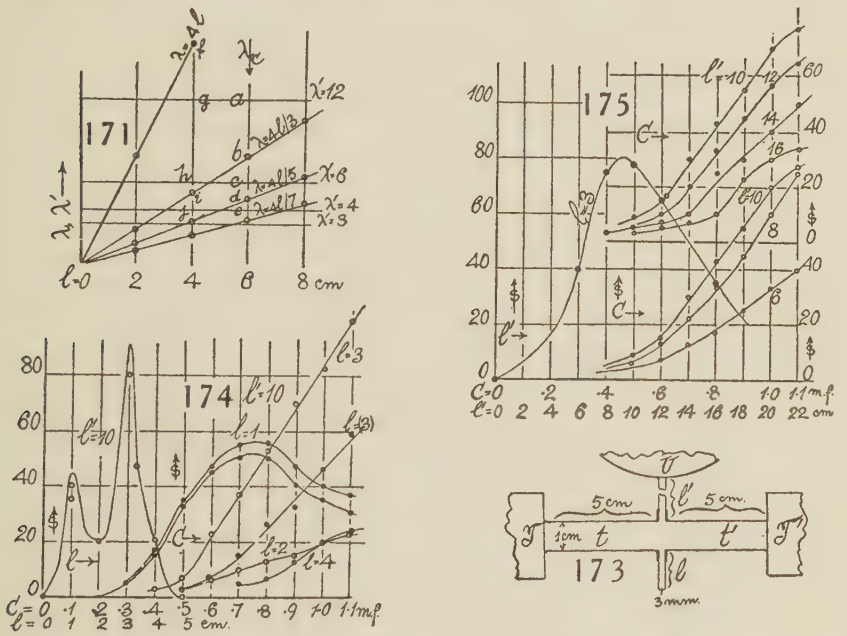

naturally be more and more vague or nonexistent. This also is borne out by figure 168.

Finally, it is not necessary that trough and crest should alternate. For instance, if $l=4$ in figure 171, the trough f is followed by crest g and crest h before the next trough, i, appears, followed by the crest j. Below this there is further interference. This lack of rhythm is also a marked feature in the graphs, figure 168, et seq.

To work out a scheme of this kind quantitatively would be difficult, because the overtones of the telephone-plate are a further powerful interference, the importance of which would first have to be estimated. For the present it is more urgent to see in how far similar acoustic pressures may be produced quite without pin-holes. This is done in paragraph 60, where the fringes are to be enlarged in the interest of greater s values for the smaller pressures anticipated.

59. Inner quill and outer conical glass pin-hole—To estimate the relative intensity of the present acoustic pressures, the experiments of figure 172, were added. Here the outer tube (see inserts) is the glass pin-hole probe, IV, (heretofore used within) and the inner tube is a clear quill, 6 to 7 cm. long. These experiments are thus an inversion of the set given in figures 161 and 162, in which the pin-hole is located within, with an outer quill. In figure 172, when the outer pin-hole is salient, the acoustic pressures are positive with crests at $C=0.3$ and 0.93 microfarad and a trough at 0.47. They are much in excess of the reëntrant case, in which the pressures are negative (dilatations) with (negative) crests at $C=0.1$, 0.47, and 1.1 microfarad, and troughs at $C=0.2$ (?) and 0.7 microfarad. Since the reëntrant curve is inverted, troughs

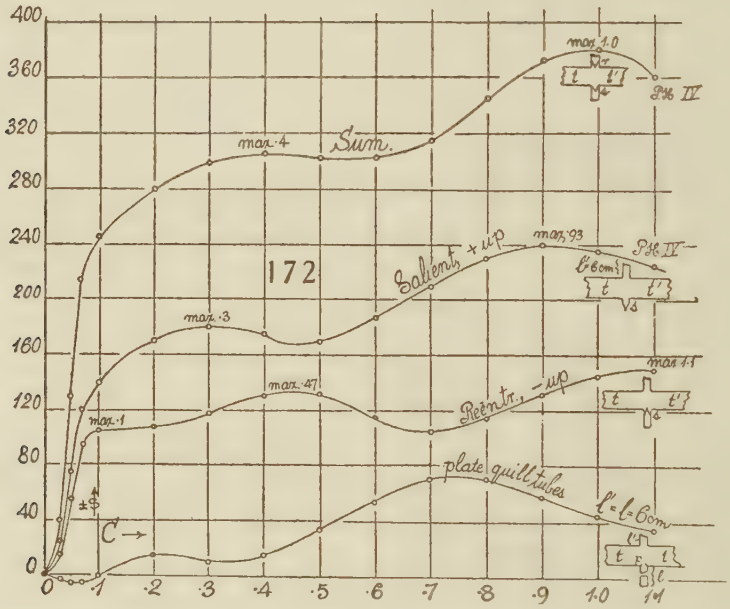

correspond to crests and vice versa in the two curves in question. Hence at $C=0.47$, the two troughs (salient and reëntrant) coincide in their C position; but the crests in the reëntrant curve are shifted from $C=0.3$ to 0.1 and from $C=0.93$ to 0.7 microfarad. Beyond $C=1.1$ microfarads there is probably further coincidence of troughs, and one is inclined to associate them with the tt' pipe. The two graphs thus depart from each other in the location of crests different from the set in figure 161, except in the location of the $C=0.3$ crest. They are, moreover, far below the latter in range of pressures, though here a variation of the l' values should first be tested for favorable pairs of l and l' lengths. The extent to which the glass pin-hole curves exceed the plate pin-hole graphs is shown by the highest graph for the latter ($l=l'=6$ cm.) at the bottom of figure 172.

If the two pin-holes were to coöperate, *i. e.*, be used in series, the upper

graph of figure 172 would be expected. This is again quite different from the preceding, with crests at $C=0.4$ and 1.0 microfarad.

The dissimilarity of curves in figures 161 and 172 is astonishing, even if different telephonic overtones should have been incidentally awakened. It seems, therefore, as if the quill-tube l', which terminates in the capacious but closed U-tube reservoir (10 cm. diameter, 1 cm. deep) is not to the same extent free as the quill-tube l, which terminates in the atmosphere.

60. Coöperating quill-tubes without pin-holes—In the preceding paragraphs counteracting pin-hole probes of successively different lengths, as well as pin-hole probes of different lengths, in series, were tried out, with the results that the acoustic pressure varied with length periodically, in the manner stated.

The outer (salient) pin-hole was then removed and replaced by a succession of clear-bore quill-tubes. Periodic results of the same nature, varying with the length of the other quill-tube, were again obtained, and under favorable length adjustments the highest acoustic pressures hitherto detected (same scale for s throughout) were recorded.

It is natural, therefore, to remove both pin-holes, to replace them by clear quill-tubes of lengths l and l', as in figure 173, l' communicating with the capacious reservoir, U, of the interferometer U-gage. The acoustic pipe tt' is actuated by telephone-plates near its ends, to which the telephones are sealed. Hence tt' may be regarded as communicating freely with air, at the farther ends of l and l'; for though U is closed, it is about 10 cm. in diameter and 1 cm. deep.

Owing to the small acoustic pressures to be expected, the fringes of the interferometer were enlarged more than twofold. Hence the s values of the graphs are correspondingly magnified.

In the experiments given in figure 174, the inner quill was left constant at $l'=10$ cm. while the outer was varied from $l=0$ to $l=7$ cm. No fringe displacements, s, were obtained at $l=0$ (one-quarter inch tubulure in tt') nor above $l=5$ cm. of quill-tube length, l.

The curve ($l'=10$) on the left records two sharp cusps at $l=1$ and 3 cm., a curious result to be interpreted by the aid of the curves on the right, in which C is varied from 0.4 to 1.1 microfarads for each value of l.

The C graphs for $l=1$ cm. are different in type from the others ($l=2$, 3, 4 cm.), showing a well-developed crest at $C=0.75$ microfarad. They change in value with slight differences of adjustment of the short quill-tube, $l=1$ cm., so that two graphs are given as examples. On the other hand, from $l=2$ cm., which is again low in s, the graphs rise with great rapidity to the graph for $l=3$ cm. Again, two curves, $l=3$ and $l=(3)$, are given, the change being due to slight alterations in the insertion of the 3-cm. quill-tube. From the high values of acoustic pressure, s, for $l=3$, the graphs fall again to the low values for $l=4$ cm. and to zero at $l=5$ cm. This curious kind of variation, as exhibited in the graph $l'=10$ cm., may be referable to two independent crests superposed.

The acoustic pressures, s, are always positive, showing that the l' quill is dominant; but for $l=0$ and l above 5 cm. all acoustic pressure vanishes. The very steep cusps of the l' l graph indicate the great delicacy of vibrational equilibrium. It is difficult to reinsert the outer quill so as to quite reproduce an original graph.

In figure 175 the conditions are reversed; the outer quill is kept constant at $l=3$ cm. (favorable length in fig. 174), while the inner quill is extended from $l=0$ to $l=16$, in steps of 2 cm. In the C graphs on the right of figure 175 there is an accelerated rise of acoustic pressure, s, between $l'=0$ and $l'=6$ cm. A maximum of s values is reached at about $l'=10$ cm. Thereafter the s values gradually fall again with changes in the form of the C graphs. The variations as a whole are exhibited in the sl' graph $l=3$ on the left side of figure 175. The present phenomena are therefore more uniform in character than those of the preceding figure 174. For $l=0$, and later for $l=5$, 7, to 20 cm., no acoustic pressures ($s=0$) were obtainable. On either side of $l=3$ cm. the

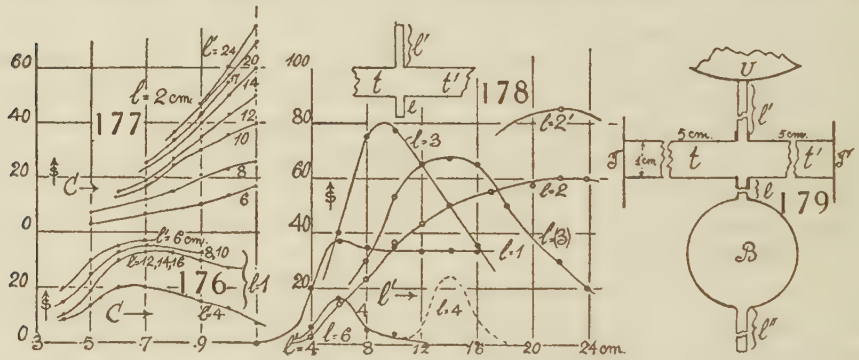

graphs therefore fall off abruptly, as heretofore. However for $l<3$ cm. the graphs were found still to rise, showing that $l=3$ is not as favorable an adjustment for maximum s, as it was in figure 174.

Briefly, therefore, the acoustic pressures must be regarded as produced by the nodes of the inner quill l'; but this is ineffective, except in the presence of short critical lengths of the outer quill, l. Since both quill-tubes are clear, such a difference of behavior may be associated with the fact that l' terminates in the closed though capacious U-tube reservoir, whereas l, open to the atmosphere, acts by virtue of its node like a valve.

A systematic repetition of the work, given in part in figures 176 and 177 and the summary (fig. 178), added nothing essentially new. The curves of figure 176 ($l=1$ cm.) all exhibit crests at an intermediate pitch $C=0.7$ mf. This tendency is quite lost in figure 177, for $l=2$, where the curves are accelerated and possibly even intersect on the left. By merely changing the insertion of the outer quill, $l=2$ cm., it was possible to obtain an upper curve as high as $s=85$ at $C=1.0$; on the other hand, by adding an extension of but 5 mm., the Cs curve dropped almost to zero throughout—all of which shows

the capriciousness of the present group of experiments with clear quill-tubes. At $l=4$ cm., the curves were much like figure 177, but lower. Here at $l'=14$ an isolated high *Cs* graph was obtained in the first experiments, which could not be reproduced in many subsequent trials. This suggests that with extreme delicacy of length (l) adjustment, other isolated maxima might be brought out. At $l=6$ cm. or larger, the *Cs* graphs were at $s=0$ throughout.

Figure 178 gives the acoustic pressures corresponding to the different outer quill-tube lengths, $l=1, 2, 3, 4, 6$ cm., in their dependence on the inner quill-tube lengths, l'. It is a curious collection of apparently unrelated graphs. Figure 177 shows, however, that at a lower pitch (the equivalents of $C>1.1$ microfarads), longer outer quills than $l=4$ would be available; for below $C=0.5$ microfarad almost no acoustic pressure is ever appreciable, whereas above $C=1.0$ microfarad all the graphs (even when $l=6$ cm.) show a tendency to rise. The chief crests fall in their l' position as l increases from $l=2$ cm. Thus $l+l'=2+22$, $3+14$, $(3)+10$, $4+6$, $6+0$ at the crests.

The puzzling feature of figure 178 is thus the short range of lengths ($l=1 \ldots 4$ cm.) which is admissible in the outer quill-tubes, if acoustic pressures s are to be obtainable. Meanwhile, the inner quill l' admits of relatively very large elongation. Except perhaps for $l=1$ cm., high C values, or low pitch is favorable to acoustic pressure. Hence all details relative to the insertion, etc., of the l quills become of *critical* importance and the observed variations of s are liable to be capricious over wide ranges of s. With long, wide tubes attached at l no acoustic pressures were obtainable.

Negative s to the extent of a few fringes was occasionally recorded. In one instance a short end of thin rubber tubing (2.7 cm. long, 5 mm. in bore) inserted at l gave $s=10$ of negative acoustic pressure consistently. Such a result is hard to explain. On constricting the outer end of the rubber pipe enormous positive pin-hole effects were of course obtained. Thus there may have been a slight constriction of the inner end of the rubber tube, producing the reëntrant effect; but this is not probable.

61. Reversal of the preceding adjustment—After finishing the work of the last paragraph, a large number of isolated experiments were made with a further bearing on the phenomena. Taking the favorable length $l'=20$ cm. and slightly varying the $l=2$ cm. (very nearly), it was found that acoustic pressure could be increased to even $s=120$ in the given scale with a quill-tube 3 mm. in bore. On replacing the outer quill to $l=1.8$ cm., the pressure fell to $s=60$, showing that the adjustment at l must be accurate to fractions of a millimeter. Furthermore, on increasing the bore d of the tube $l=2$ cm. to $d=5$ mm., acoustic pressure practically vanished. Reducing the bore to 1 mm. (retaining $l=2$ cm.), $s=20$ was observed; while for a length of $l=1$ cm. of this 1-mm. tube, $s=45$ resulted. Hence the bore is equally important, as if a critical frictional resistance were in question.

The inner quill-tube, l', is less exacting. Replacing it by ends of rubber hose, 4 to 5 mm. in bore, I obtained ($l = 2$ cm., bore 3 mm.)

$l' =$	16	18	22	25 cm.
$s =$	80	90	110	100

the favorable case just cited.

The desirability of inverting the character of the preceding experiments, by using the shortest possible l' pipe (junction of the tt' pipe with the U-gage reservoir) and elongating the l quills, presented itself. Would the results in s be symmetrical and acoustic dilatations result from such a reversal? This was pronouncedly not the case. In fact, the apparatus now was relatively inert.

Tests made for $l' = 3$ cm., bore 3 mm. (smallest available), and l increasing from 1 to 50 cm., as a rule, gave no response in s, except at certain definite

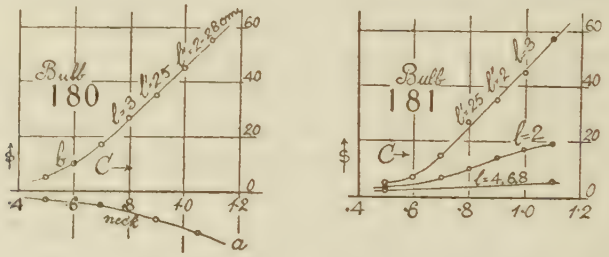

lengths, when the long quill sounded a high overtone of the deep telephone-note. Thus I recorded ($C = 1.0$ mf.)

$l' =$	3 cm.			
$l =$	20	40	50	60
$s =$	5	15(a''?)	17(f''?)	5

A number of trials produced nothing better. The evidence, therefore, is definitely always a pressure; but when l is prolonged for a small l', the maximum s is not more than 20 per cent of the s value produced with long l' by the short l pipe in the preceding paragraph. There the l pipe node, under conditions of resonant vibration, acted like a valve to increase the acoustic pressure in tt', which in turn was further amplified by the l' pipe nodes.

The most hopeful way of furthering the present inquiry seemed to consist in balancing the U-reservoir on one side of tt' by a bulb B (fig. 179) about 6 cm. in diameter, with two necks l, l''. The quill-tube, $l = 3$ cm. long, was used as a junction. Here the bulb alone with the neck at l'' about 5 mm. in diameter, 1 cm. long, gave the small but definite negative reaction shown in figure 180a. Inserting the quill-tubes at l'', the curves b were obtained, practically coincident for all lengths, $l'' = 2$ to 28 cm. The graph represents only about half of the acoustic pressure obtainable from $l = 2$ cm., alone.

The effect of the l'' length is thus nearly negligible. Not so, however, the l length at the junction. Figure 181 shows that for $l = 3$ cm. there is a

distinct maximum rise of the *Cs* graph; for $l=2$ it is much lower and for $l=4$, 6, 8 cm., etc., lower still and just noticeable. Here again, therefore, the critical tuning conditions are associated with l and the bulb has merely changed the favorable length from $l=2$ to $l=3$ cm. Compared even with figure 177 the pressures are low.

62. Quill-tubes of constant external diameter, reduced in length and bore conjointly—We finally come to a probable solution of the preceding intricacies. Quill-tubes, inserted coaxially with short pieces of rubber tubing, are necessarily shouldered at one end (insert *a*, fig. 182). The quill-tube *q* thus effects a reduction of the diameter of the anterior tubulure *p* and may therefore in a measure take the place of a pin-hole. To test this surmise, tubes of the same diameter, but of small bore, the length of which is successively diminished, may be taken. The adjustment is shown in figure 182*b*, where l is the length of small-bore tube inserted in the wider quill *q*. As before, tt' is the telephone-pipe with the quill-tube l' (here 27 cm. long for convenience), joining tt' with the U-gage. The *Cs* graph for the former quill-tube ($l=2$ cm., diameter, $d=0.3$ cm.) is repeated from the preceding experiments for comparison.

The other graphs of figure 182 refer to the small-bore tubes $d=0.2$ cm. in diameter and respectively $l=2$, 1, 0.5 cm. in length, in question. In the former case they are inserted saliently; in the latter ($l=0.5$ cm.) the insertion may easily be made at the rear (reëntrant) or at the front end (salient) of a short piece of slender rubber tubing (2 cm. long, 0.5 cm. diameter), acting as a quill-stem.

When $l=2$ cm. the graph is slightly negative. When $l=1$ cm. the saliency of the insertion is manifested, as *s* is positive within the limits of *C*. By a different insertion of l, this graph could have been made negative. When $l=0.5$ cm. we have an approach to a coarse pin-hole. Placed in the outer end of the rubber junction with tt, the corresponding graph is strongly positive. Placed at the inner end of the junction with tt', the graph soon becomes strongly negative, though it is a complicated graph with double inflections. There is in such a case both an anterior and a posterior wider quill-end, perhaps, and a better mode of insertion must be devised. At all events, the short capillary tube with rubber prolongation now acts like a pin-hole probe with a node on the inside of the rubber quill, at the constricting hole, and in a position where a maximum of vorticity may be expected. The *Cs* graphs change sign on reversal.

In figure 183 (in which the results as a whole are more negative than figure 182), the experiments were repeated with the attached bulb *B* (see inserts). The graph, $l=2$, $d=0.3$ cm., is supplied for reference. The case $l=2$, $d=0.2$, is much like the preceding, without the bulb. So is graph for $l=1$, $d=0.2$ cm., though here there is a remarkable shoulder to the graph at $C=0.9$ microfarad, after which there is an almost sheer descent toward negative values. The case $l=0.5$, $d=0.2$ cm. has again been worked out both for salient and reëntrant adjustments, as shown by the inserts. The same con-

clusions may be drawn as before. The bulb effect is a depression into negative values.

The hump of the curve $l=1$, $d=0.2$ cm. deserves further mention. Since the constriction l is in the main reëntrant in relation to the bulb B, it is probable that as pitch descends (C increasing), the resonance note of B is being approached. When it is reached beyond the limits of the figure, the curve should pass through a negative trough at the resonance pitch of B. Similarly the reëntrant graph $l=0.5$, $d=0.2$ shows accelerated fall after $C=0.9$ microfarad. All the curves instance the desirability of higher C values (lower pitch).

It is now clear that if the work of figures 182 and 183 were continued, by further reducing both l and d conjointly, the relatively enormous full pin-hole effect in s would ultimately be reached, without any need of slope in the walls

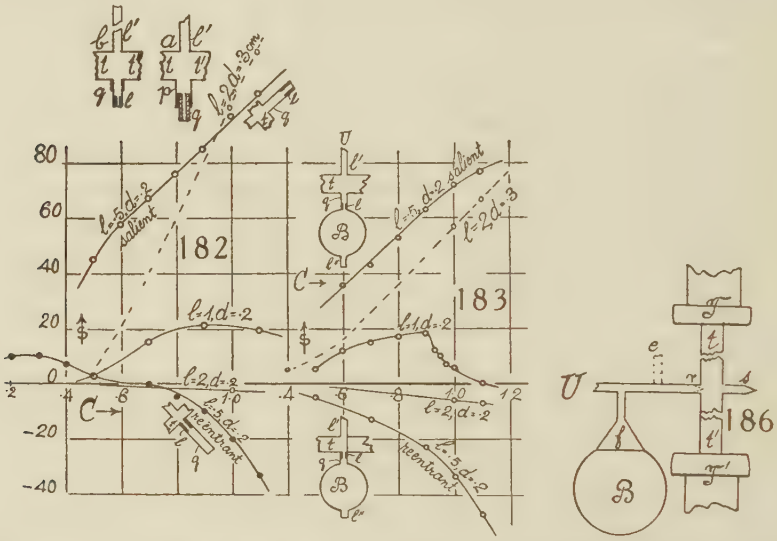

of the pin-hole. Whether this is conical or not seems thus to be without consequence. A node at the pin-hole inside the quill-tube, the latter functioning like a closed organ-pipe, is accountable for the acoustic pressure s; and s increases with the intensity of the node, *i. e.*, with the increased perfection in the tuning of the probe relatively to the acoustic pipes, like tt'. The node carries the excess mean pressure over atmospheric pressure. The streamlines run from the pin-hole into the quill-tube of the probe, regarded as a closed organ-pipe. Hence, if the pin-hole node is within the acoustically vibrating region tt' (organ-pipe with salient pin-hole probe) there is acoustic pressure; if the pin-hole node is outside of the region tt' (reëntrant pin-hole probe) there is mean dilation in tt'. A single pin-hole may be reënforced by a second one in series with it, between tt' and the U-gage.*

The reversed experiment was equally decisive. Some results are given in

* A supplementary series of experiments will be discussed in § 84 et seq., particularly in § 90.

figures 184 and 185, the insert in the latter giving the adjustment. The inner quill l' was kept 15 cm. in length, and this carries the cylindrical constriction l'' (0.5 cm. long, bore $d=2$ mm.), immediately adjoining tt'. The outer quill was elongated from $l=2$ cm. to $l=16$ cm. and one notes a marked change in the form of the Cs graphs, even in passing from $l=2$ to $l=4$ cm. Some of this is referable to the capricious behavior of the telephone-plate in its supply of overtones, perhaps.

As it takes some time to trace any one of the Cs graphs, the ls graph given in figure 185 was worked out directly for $C=1.0$ microfarad and $l'=15$ cm. The strong cusplike maximum for $l=2$ cm. is here again encountered (as in fig. 178, for instance), and its sharpness shows the accuracy of tuning the l

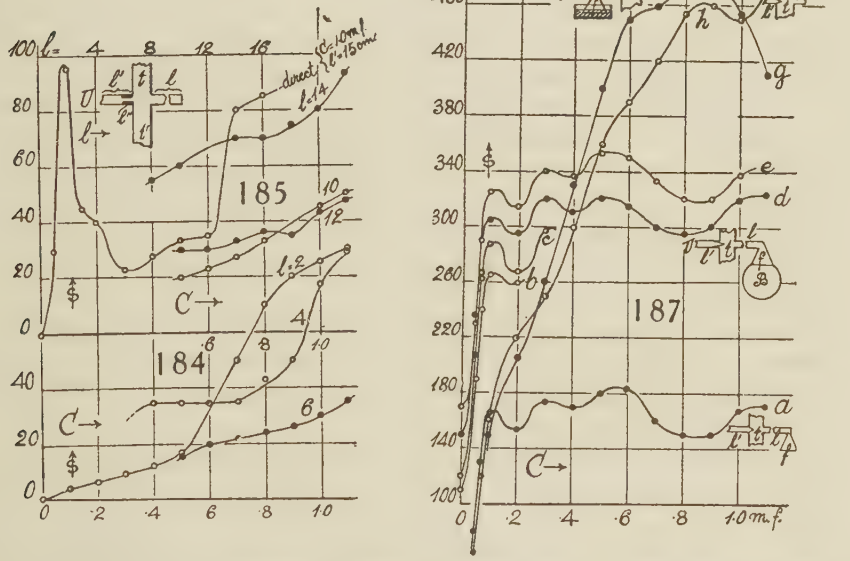

length, required. Beyond the diagram (above $l=16$ cm.) there is to be another but flat crest. The fall to and rise from the long meandering trough from $l=4$ to $l=12$ cm. is noteworthy.

Thus we have here again the pin-hole effect on a small scale, which could be increased by simultaneously decreasing length l'' and diameter d of the cylindrical constriction simulating the pin-hole to a critical value.

The consistent results thus obtained prove that a strictly cylindrical aperture at the constriction of the quill-tube suffices to produce the pin-hole phenomena, at least on a smaller scale; and that conical walls are not necessary. One suspects that the abundant production of vortices on the inside of the probe at the shoulder (node) of the constriction is the ultimate cause of the pin-hole phenomena. Such ring vortices, whose line of symmetry coincides with the axis of the pin-hole, would produce a smaller outflow from the pin-hole probe, as compared with the inflow into it at the node. In other

words, the flow excess through the pin-hole is into the region of excess vorticity.

At the same time, this argument loses some of its cogency when it is recalled that the node in the pipe *tt'* (fig. 182), which reciprocates with the node in the probe, *ql*, has been ignored. Hence in paragraph 90, identical quill-tubes, on opposed sides of a pin-hole pricked in a sliver of mica, will be examined. It will be found that even such an ideally thin pin-hole has opposed properties on its two sides, changing $+s$ into $-s$ on reversal of the mica plate.

63. Acoustic pressures in case of a soap-bubble—The acoustic pressures encountered in the above experiments are often many times larger than the pressures within a moderately sized soap-bubble. One might infer, therefore, that such a bubble could actually be blown with the telephonic apparatus and pin-hole probe described. It seemed worth while to try this with an apparatus sketched in figure 186, where *TT* are the two telephones vibrating in series and *tt'* the acoustic pipe joining them. At *s* is the salient pin-hole. The quill-tube *rU* connects with the U-gage for registering the acoustic pressure. A T-branch at *f* carries a small funnel, from which the bubble *B* may be blown and a second T-branch at *e*, with a stopcock, may be used for blowing the bubble; but it is usually more convenient first to blow the bubble from *f* and then insert it. If desirable, a second pin-hole may be used at *r*, in series with *s*.

If the bulb *B* is rigid, even a flask of one-half liter capacity, the acoustic pressure at *U* appears at once, and in these experiments was about $s=250$. With an appreciable leak in the flask it fell immediately to zero. Hence the apparatus itself was in good condition.

Soap-bubbles of various sizes were now blown and attached as shown. In every case the pressure fell to the value corresponding to the radius of the bubble. With large bubbles, $s=60$, with smaller ones $s=120$, with flattish films $s=50$, for instance, were recorded, all much within the acoustic pressure inside a rigid system. This pressure decreased about 10 per cent when the telephones were silenced and increased again when they sounded—a result to be expected, since the air of the bubble escapes slowly at the pin-hole *s*, in the absence of acoustic vibration. For the same reason, *s* slowly increases as the bubble contracts. While the telephones are sounding, however, there is no escape of air from the pin-hole and the pressure *s* remains constant till the bubble bursts, some time afterward.

Thus, to develop the acoustic pressure in full requires rigid walls throughout. One might have supposed that in the endeavor to reach the limit of this pressure there would be ingoing current at *s*, figure 186, *i. e.*, continual inflow of air in the direction *sr*, in which case the bubble would be inflated with continually decreasing interval pressure; but this is not the case, and the acoustic pressure can not rise above the resistance corresponding to the

elastic walls of soap-film. Current at *s* inward is impossible, though any outward flow is checked when acoustic vibration occurs.

The inversion of this experiment is of particular interest. The adjustment is sketched in the insert (fig. 187, curve *d*). The bubble *B* with its funnel *f* here replaces the outer quill-tube *l*, and thus the bubble contributes an increment to the atmospheric pressure in *t*, the pipe joining the telephones. The pin-hole probe *l* communicates with the U-gage, as usual, with a quill 17 cm. long.

In the absence of the bubble, the low graph 187*a* was obtained. The small acoustic pressures here are the result of the necessarily long quill-tube connector *l* (12 cm. long) in this experiment; for with the 2-cm. quill the graph takes the high excursion shown at *h* in figure 187. It does not differ much from the graph *g*, obtained in the former experiment, when the funnel *f*, depending from *l'*, is closed by a plug of liquid.

Bubbles were now blown of different sizes and attached at *l*. Examples of the results are recorded by the graphs *b*, *c*, *d*, *e*, in the first two of which the bubble burst early. Curves *d* and *e*, however, were carried through without mishap. It will be seen that these graphs are exactly like graph *a* in shape, throughout; but they are all raised to different high *s* values, owing to the surface tension of the bubble *B* (see insert) attached to the funnel *f*.

Thus the pin-hole probe *l* builds up the acoustic pressure in the gage *U*, from whatever pressure it finds in the sounding-pipe *t*, provided the *Ul* system is rigid. If it is not, the limiting pressure of the elastic walls can not be exceeded. The graph *h* rises so rapidly that the crests in *a b* . . . . . *e* are present, if at all, as mere sinuosities; but four of these may be recognized, all displaced toward lower pitch (larger *C* values) as compared with the *a* . . . . *e* graphs.

CHAPTER IV

PIPES WITH RELATIVELY MASSIVE AIR-COLUMNS. ORGAN-PIPES. HORNS

64. Pin-hole record for variable organ-pipe. Apparatus—The closed organ-pipe, *p*, of one-inch brass tubing, shown in figure 188, is provided with a well-fitting greased plug, *a*, so that the depth *d* may be varied at pleasure. The pipe is blown by the jet-pipe *j*, the front of which has been compressed wedge-shaped to a narrow cracklike crevice, through which a thin sheet of air is forced. This air lamella is cut parallel to its surface by the thin blade *f*, sharpened where it meets the air-current. Moreover, *f* is adjustable on side-slides, so that the width of embouchure, *e*, may be varied to get the clearest tone in any case. Finally the long, slender probe *bc* (45 cm. to U-tube) is inserted out of the way of the air-jet from *j*, so that the pin-hole at *c* may be near the bottom of the organ-pipe. The advantage of the pipe is its loud tone and the fact that air is not blown into the pipe at the embouchure. If *d* denotes the depth of the plug below the outlet, clear notes were obtained from the pipe as follows:

d=...	15	14.5	13.5	12.5	11.5	10.5	9.5	8.5	7.5	6.5	5.5	4.5	3.5	2.5	1.5	1.0	0.5 cm.
Note.	c''	$\#c''$	d''	$\flat e''$	e''	f''	g''	a''	$\flat b''$	c'''	d'''	e'''	g'''	c'^{v}	e'^{v}	g'^{v}	c^{v}

only the last being conjectural. As it was found that a steady fringe displacement, *s*, could be obtained, the pipe in the first experiments was blown by the mouth of the observer.

65. Results—Experiments with air-blown pipes are not easily put under control, and the individual observations are liable to be straggling. Thus, the intensity of the note depends markedly on a proper spacing of the embouchure *e*, among other things. In figure 189, in which this intensity or acoustic pressure *s* is expressed in terms of the depth *d*, of the plug *a*, below the mouth of the pipe, *ef* was set for the strongest note. Circles open or closed denote different series of observations, *bc* remaining constant (45 cm.) in length and the pin-hole *c* at the bottom near *a*.

On starting, there is a low-pressure hiss before the pipe-note breaks forth. The pressures here are invariably negative (as would be supposed) and of the value given by the graph marked *wheeze*. The negative pressures may, of course, be much enhanced if for any reason the pipe does not sound while the jet velocity is increased. This was also often the case when the very high, shrill harmonics are evoked from the pipe. In general, at the beginning, the pressure throughout the pipe is markedly below that of the atmosphere. As soon as the pipe strikes its note, however, there is a definite pressure, *s*,

usually in marked degree, positive as instanced by the graph figure 189. Though drawn through straggling data, its implications are clear enough. If the pipe is shallow ($e'''-c'''$), acoustic pressure s is here negative, as one should expect from the proximity of the plug a to the embouchure, among other things. Between c''' and e'', however, acoustic pressures, built up from the initial negative pressure-level, are positive, passing through a maximum at about g'', $d=10$ cm. For the deep pipe, between e'' and c'', the pressures are negative again, and there is a pronounced trough at about d''. This would not have been expected. The wheeze graph seems to show a similar tendency here and the high negative values are further enhanced by it.

Since the endeavor was made to keep the embouchure e at the distance of maximum efficiency, the crests and troughs can hardly be ascribed to it. Nor would this account for sinuosities if e were constant. There would be a mere passage of s through a maximum.

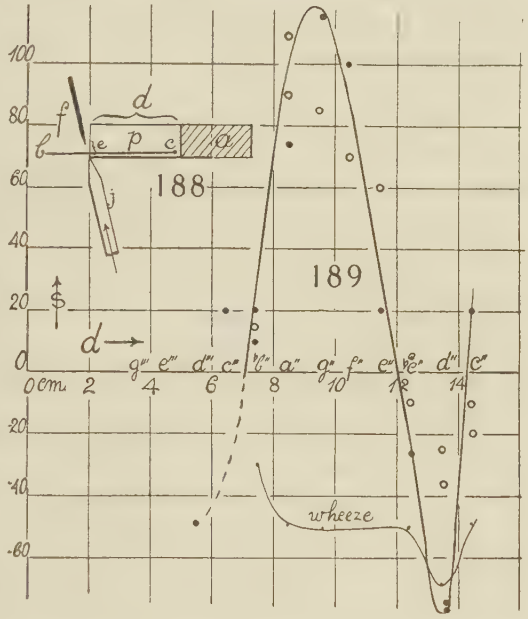

It seems, therefore, that the undulatory results obtained must be associated with the length of quill-tube (45 cm.) carrying the pin-hole. This is in accord with the indications of the preceding paragraphs. To test this surmise, the quill-tube was elongated 10 cm. ($x=55$ cm. in length). It was now found that at $d=7.5$ cm., the small s deflections of figure 189 could easily be built up to $s=100$ or even 120, whereas with $x=45$ cm. they were liable to be small or negative.

Though this result seems to verify this surmise here, the experiments of the next paragraphs, with stronger and continued air-currents, are quite out of keeping with it; for connectors between pin-hole probe and U-tube of any length (even 10 feet) made very little difference in the results. It is not, therefore, opportune to conjecture further explanations of these very complicated phenomena until additional experiments with organ-pipes blown by more steady and persistent air-pressures are at hand.

66. Further experiments—For the new experiments, a large Fletcher bellows actuated by an electric motor was installed. The pin-hole of the preceding experiments (punctured in thin metal plate) was replaced by a glass cone pin-hole. The latter (shown at g in figure 190, where p is the

organ-pipe blown by the jet *j*, and adjustable blade *f*) was now mounted in the plug *a*, the pin-hole being flush with the bottom of *p* and displaced with it. A wide stem, *bc*, 0.6 cm. in diameter and 16 cm. long, was needed to receive the glass quill-tube *g*, properly sealed in. The end *b* was then joined to the U-tube by rubber tubing, the length of which was here of little consequence. A long connector was therefore preferred, as it kept the vibrations of the acoustic installment from shaking the interferometer U-tube. With an air-pressure as furnished by the bellows (not quite steady), the fringes oscillated between limits reaching their largest displacement when the air-current was smallest. The overblown pipe, therefore, loses acoustic efficiency for the given embouchure. The Fletcher bellows was chosen here because its mean pressure is constant, and it has the great advantage of starting the pipe-note with an initial puff, as it were, more easily than a steady blast.

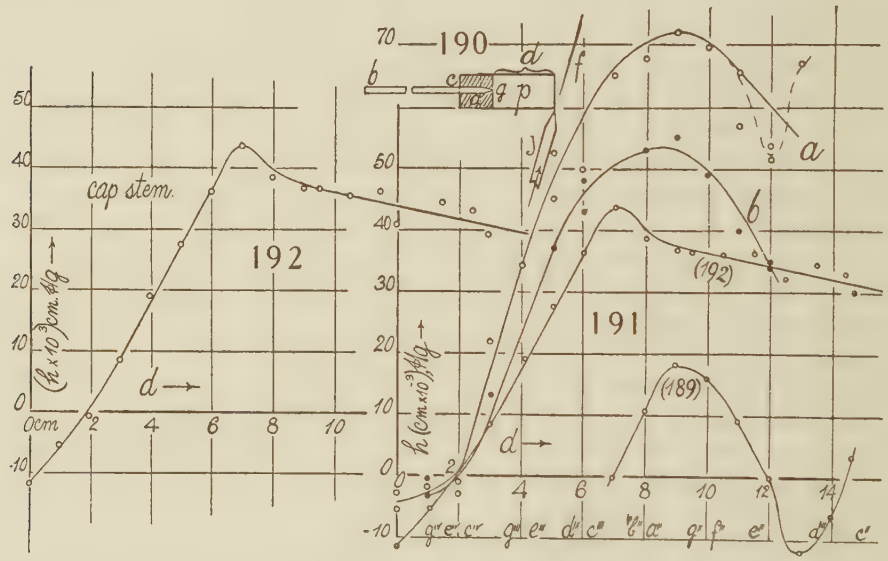

Figure 191 (curves *a* and *b*) gives the results of the acoustic pressure *h* in centimeters of mercury, observed at the bottom of the pipe *p*, when the depth *d* varies. The jet pressure in curve *a* was somewhat above that in curve *b*, the embouchures being adjusted accordingly. These two graphs differ not only in appearance from the preceding graph, figure 189, but the acoustic pressures represented are much larger. For if Δr be the micrometer displacement corresponding to Δh (mercury head), $\Delta h = 0.71\Delta r$ at an incidence of 45°, while a direct standardization of the ocular scale-parts *s*, showed

$$100\Delta s = 10.8\Delta r$$

in scale-parts, each of the latter being 10^{-3} cm. Thus, for the same Δr,

$$\Delta h/\Delta s = 0.71/0.108 = 6.6$$

Hence the unit of the scale of figure 191 is 6.6 times that of figure 189. More-

over, the ocular scale-part s corresponds to $0.108 \times 10^{-3} \times 0.71 = 76.7 \times 10^{-6}$ cm. Hg. or about the millionth of an atmosphere; that is, roughly, dynes/cm^2.

For convenience, the graph, figure 189, reduced to the same scale as figure 191, has also been inscribed in that figure.

If we compare figure 189 for relatively low jet-pressure, with figure 191, curve a, for high jet-pressure, we notice that the crests or optima of the graphs fall somewhere between the depths $d = 8$ and $d = 10$ cm., in both cases. The pipe responds best for notes between g'' and b'', though the crest of the curve b for somewhat lower jet-pressures is smaller in depth, d. The difference between the curves is the much greater breadth in pitch of the graph, figure 191, for positive h. In the latter curves negative acoustic pressures do not appear, so far as tests of the crest is reached, and below the crest, not until the pitch is below c^{iv}, or $d < 2$ cm. in pipe-depth. Remembering that irregularities due to the set of the embouchure are inevitable, the relation is almost as if the curve a were dropped in a vertical direction, until the crests coincide, except that the development of negative pressures (s) for such a case does not appear. It is particularly noticeable that the trough above $d = 12$ cm. (near d'') is suggested in all cases.

The reason for an optimum of the pipe for pitches between a'' and g'' is not easily conjectured, because outside influence due to pin-hole and its connection with the U-tube enter into the consideration; but it seems to me probable that the optimum is a property of the organ-pipe itself and referable to the embouchure device. One notices, for instance, that at any fixed pitch (or depth d of pipe), the maximum fringe displacement is gradually reached within the lapse of seconds. Energy is thus being continually supplied to the acoustic vibrations, with the effect of gradually increasing its amplitude to a limit. This energy can only be withdrawn from the wheeze or siffle at the thin edge f of the embouchure; and one concludes that a mean pitch of wheeze notes is most efficiently present, in correspondence with the optimum or crest-pitch of the organ-pipe itself.

Another conjectural reason for the graph, figure 191, may be sought in the possible loss of the efficiency of the pin-hole at different pitches. Frequencies larger than c^{iv} may very well need a different size of pin-hole to give positive displacements s than smaller frequencies and a particular optimum frequency corresponding to size of hole would be expected. Similarly, the pin-hole in copper foil (fig. 189) may behave differently from the pin-hole in glass at the same pitch, in relation to positive and negative acoustic pressures. It was found, however, that the pin-hole responds to shrill overtones with undiminished strength, so that the behavior of the pin-hole is probably not in question here.

67. Reduced diameter of pin-hole probe connector—It has been stated that the length of the tube cb between pin-hole g (fig. 190) and U-gage seemed to make little difference here. The question thus arises whether a reduced caliber of the stem bc would have any marked effect, such as one

should expect if the pin-hole probe, in accordance with the above investigations, behaves like a slender organ-pipe with a pin-hole embouchure. Accordingly the stem *bc* was variously constricted with capillary tubes, cotton inclosures, etc., such as might be supposed to dampen vibration and render the pin-hole probe ineffective. To my surprise, these insertions had but a relatively small, if any, effect in the large number of special tests at a given pitch, made in succession. If the bore is too small, the fringes eventually drift, owing to the viscosity of the air passing the capillary tube. These questions will be resumed in paragraph 69.

In figure 192 (also inserted in fig. 191 for comparison), I have given a complete set of data made with the same glass pin-hole when the capillary stem (*bc*, fig. 190) 13 cm. long was but 0.08 cm. in inside diameter. The optimum depth is here at $d=7$ cm. (somewhat smaller than in fig. 191) and the reduction of intensity compared with curve *a* about 20 per cent; but this is to be ascribed to decreased jet-pressure or velocity. The intersection of the graph with the axis ($\Delta h=0$) is the same as before. The graph from here rises almost linearly to the crest and thereafter wavers, falling slowly. The trough above $d=12$, however, fails to appear. Cutting down the bore of capillary tube further by inserting a wire slightly less in diameter (0.06 cm.), but admitting of a definite fringe displacement, the results were about the same. It seems impossible, therefore, that in so fine a bore anything like acoustic vibration should be possible. There is a mere conduction of static pressure to the U-gage.

The data of figure 191 are more fully recorded in the following table:

Clear, one-quarter inch connector														
$d=$	2	3	4	5	6	7	8	9	10	11	12	13	cm.
$\Delta h\times 10^3$..	−2.1 −0.7	21.7	34.1	52.5	49.7	65.0	67.7	72.1	69.6	56.8 65.5	51.5 53.7	67.0	cm. Hg.
Same. Smaller pressures														
$d=$.....	2	3	4	5	6	7	8	9	10	11	12	13	cm.
$\Delta h\times 10^3$..	−0.6 −3.5	13.2	18.7	37 45	43 48	62	53	55	49	34 40	34 35	..	cm. Hg.
Capillary connector, bore 0.08 cm., length 13 cm.														
$d=$.....	1	2	3	4	5	6	7	8	9	cm.				
$\Delta h\times 10^3$..	−1.9 −5.5	−.6	8.5	19.1	27.6	36.2	43.6	38.5	36.6	cm. Hg.				
$d=$.....	..	..	..	..	..	..	9.5	10.5	11.5	12.5	13.5	14.5	15 cm.	
$\Delta h\times 10^3$..	..	..	..	..	..	..	37.2 35.6 36.6	35.6 35.9	36.8 36.4	32.2 31.5	34.6	33.8 33.3	29.5 cm. Hg.	

68. Steady blast—In relation to figure 193, the pipe was blown by a steady current of air furnished by a rotary blower controlled by a motor. The graphs *a*, *b*, *c* were obtained with the glass pin-hole, the jet-pressure being least in curve *a*, and largest in curve *c*, with *b* intermediate, so far as could be controlled. The ordinates are screw-micrometer displacements Δr, at the depth *d* below the pipe-mouth, and we have, as before, $\Delta h = 0.71\ \Delta r$ cm. of mercury. Again, the data are not smooth, owing to the difficulty in obtaining the best set for the blade *f* at the embouchure *e*, and the graphs *a*, *b* have been drawn through the highest points, as there is no consistent sinuosity. In curve *c*, however, where a larger number of trial settings of the blade were made for each depth, *d*, to obtain the best, the sinuous character of the

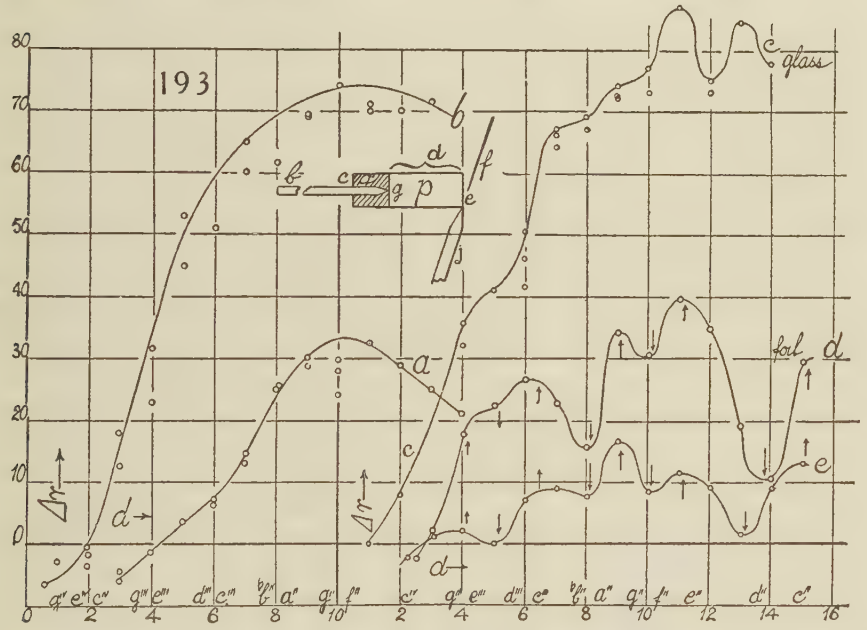

graph could not be eliminated. The optimum in cases *a* and *b* seems to be at $d = 10$ cm., but in case *c* it would be somewhat higher. The curves, moreover, cross the axis ($\Delta r = 0$) at $d = 1$, 2, 4 cm., as the jet-pressure or velocity diminishes. At low pressures the high notes often fail to respond; but this result may be secured by placing the hand or any reflecting object at the proper distance from the pipe-mouth. The note is then stimulated by its echo. In fact, the fringe displacement (*s*) will rise and fall as the reflecting object is moved nearer or farther from the mouth. Another interesting feature is the growth of the *s* value, here again appreciably within a minute or more. Energy is very gradually being absorbed by the vibration. Care must of course be taken to keep the jet-slit clean.

The graphs *d* and *e*, figure 193, were obtained with the pin-hole in copper foil, less sensitive than the glass pin-hole. The jet-velocity in case *d* is the

higher, *e* being very low. I expected in this case to reproduce the negative pressures ($-\Delta r$) of figure 189, but these were not obtainable. The curves *d* and *e* are particularly interesting, because the sinuosities seem evidently to correspond almost throughout. This is the first case of a consistent result of this kind; but it follows, nevertheless, that the sinuosities may be more than an incidental part of the phenomena and not merely due, for instance, to some maladjustment in the set of the embouchure blade. In fact, the deep trough between $d = 12$ and 14 cm. is also present in figure 189. The question thus arises, to what are they to be referred. It is again suggested that the troughs may represent harmonics unfavorable to the quill-tube of the pin-hole probe; for without being the cause of the main phenomenon of acoustic pressure, the pin-hole quill-tube may nevertheless modify it by periodic increments, if the tube (as was the case in fig. 193, *d*, *e*) is clear.

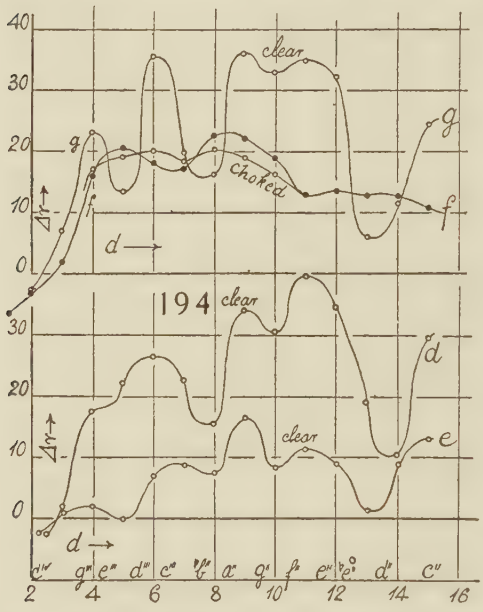

The slow growth of the full amplitude was again very marked in cases *d* and *e*. The high-frequency intensity is weak, because this would need an accentuated jet-velocity as the pitch increases. Thus, if the jet is stopped, the opening puff is intense.

From the graphs *d* and *e* an approximate location of the maxima would place them as follows:

Maxima.....	*c'''*	*e''*	♯*g''*	♯*c''*	*f'''*
d = ...	15	11	9	6	4 cm.

so that the depths are nearly as 5, 4, 3, 2, 1. The minima lie at

Minima.....	♯*d'''*	♭*b''*	♯*f''*	*d''*
d = ...	5	7·5	10	13

these being the organ-pipe notes to which the quill-tube does not easily respond. They lie in their *d* values, almost exactly between the maxima.

These interesting relations suggest a final experiment of direct comparison of the empty and nearly choked quill-tube (45 cm. long) as to acoustic pressure, Δr, generated under otherwise like conditions. The inside diameter of the quill-tube was 0.230 cm. It was closed at the pipe-end with a pin-hole foil. To nearly choke it, a cotton-covered straight copper wire 0.19 cm. in diameter was inserted, running from end to end. This leaves a free shell space of but 0.02 cm. thick between wire and glass, and the air resistance introduced was such that at least 1 minute was needed to obtain the maximum

fringe displacement, at any pitch. It seems impossible that acoustic vibration could occur within the long, rough shell in question. The Fletcher bellows was used to actuate the jet of the organ-pipe, because of the fixed mean pressure to be obtained at a relatively high value.

The results are given in figure 194, curve *g*. They are a pronounced corroboration of the curves *d*, *e*, and prove that the decadence of the latter graph in high pitch is the result of falling jet-pressure. There are the same crests and troughs in all curves; in curve *g*, however, the chief maxima are nearly of the same height.

The corresponding results, when the same quill-tube probe was all but closed from end to end by the copper wire in question, are given in the graphs *f*, there being two different series along the main branch. This curve is quite different from curve *g*. The marked oscillation of the latter has largely been eliminated and *f* is more like the preceding graphs with glass pin-holes and wide connector-tubes. In other words, the tendency of *f* is to run along the troughs of *g*, as if the oscillation effect of the clear quill-tube were superimposed on the acoustic pressure independent of it.

We may, therefore, come to the conclusion that the acoustic pressure at the base of the closed organ-pipe may be conveyed as static pressure to the U-gage. This pressure may be periodically (with pitch) enhanced if there is oscillation in the quill-tube as well. In the case of wide connector-tubes (one-quarter inch) the pin-hole embouchure is probably unable to stimulate appreciable vibration in the connector and the acoustic pressures obtained are without the systematic undulatory character. Hence such tubes, whether clear or partially choked from end to end, register about the same pressure.

69. Miscellaneous tests—If the high-pitch note is produced not as a fundamental, but as an overtone with very high jet-velocity, the intensity is indefinitely high. In fact, the conditions of the graphs, figure 193, may be reversed. Thus for a mean pipe-depth and fast jet, the high fifth overtone was of intensity $\Delta h = 116 \times 0.71 \times 10^{-3} = 10^{-3} \times 82$ cm. of Hg. (narrow spacing of blade), while for a wider spacing the fundamental began with an intensity of but $\Delta h = 7 \times 10^{-3}$ and regularly increased, for a gradually decreasing jet-velocity, ultimately to $\Delta h = 56 \times 10^{-3}$ cm. Hg. Here, therefore, graphs descending from left to right would have been obtained, had it been possible to maintain the high jet-velocity.

With the connector-pipe *bc*, figure 193 (inset), nearly choked with cotton, but still admitting of a slow current of air through it, conditions under which acoustic vibration would hardly seem possible, the following intensities Δr were successively found with a gradually decreasing jet-velocity, unfortunately:

Cotton in.....	$10^3 \Delta r$....	93	..	75 cm.
Clear tube, *bc*:	$10^3 \Delta r$..90	..	78	.. cm.

Thus the connector-pipe *bc*, all but choked with cotton, is just as efficient as the clear pipe, so that conveyance of pressure to the U-gage seems alone

to be in question. A similar experiment in which a capillary tube 0.08 cm. in bore was inserted into *bc* gave alternately:

Cap. tube in: $10^3\Delta r$.....	104	 59	.....cm.
Cap. tube out: $10^3\Delta r$.....	80....	..	42 cm.

showing that fall of jet-pressure is alone in question. Finally, a thermometer capillary with a bore of but 0.03 cm. and length 16 cm., and requiring several minutes to reach the maximum at the U-gage gave:

Cap. in: $10^3\Delta r$.....37 cm. Cap. out: $10^3 \times \Delta r = 17$ cm.

the fall of jet-velocity in the long interval of waiting being here again in evidence. Thus a connector-tube of any length, or even a capillary tube of bore sufficient to admit of a reasonable flow of air through it, functions equally well to connect the pin-hole probe with the U-gage.

70. Mean total pressure in organ-pipe. Soap film—From what has preceded it is obvious that when the above pipe (*p*, fig. 195) is not sounding,

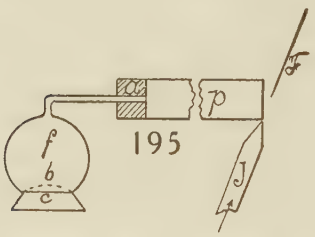

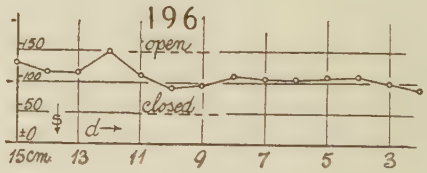

the pressure within must be negative. The graphs for $d = 0$ cm. give a value not larger than $10^3\Delta r = 10$ cm., or $\Delta h = 7 \times 10^{-3}$ cm. of mercury, *i. e.*, 9×10^{-5} atm. below the pressure of the atmosphere. The usual jet-velocity used is here understood.

It remains to determine whether the mean pressure at the node varies from this negative datum (caet. par.) when the pipe is sounding. In other words, does the excess pressure within the rigid boundary of pin-hole probe and U-tube also occur at the organ-pipe node on the outside of the pin-hole; or, has the whole vibrating air-column within the above pipe the same mean negative pressure?

To answer this expeditiously, I adjusted a soap-film *c*, figure 195, in the thistle-tube *f* communicating with the organ-pipe *p* through the perforated cork *a* at the bottom. The film dipped at the flare of the thistle-tube retreats to the position *c*, where it is in stable equilibrium at a diameter of 2.3 cm. On sounding the pipe the effect is always to bulge the film upward as at *b*, showing that *f* is below atmospheric pressure. If the note is too intense, or if the blade *f* at the embouchure is withdrawn, the film may break loose from its position *c* and move upward into *f* against the resistance arising from its surface-tension, *T*. But for the usual strength of notes used, the bulge *b* was about 0.5 cm. high. This implies a soap-bubble $R = 1.2$ cm. in radius.

The excess pressure within such a bubble would be $p=2\ T/R$ dynes/cm^2. If $T=50$ dynes/cm. for the soap-film, $p=100/1.2$ dynes/cm.^{2}, or 8.5×10^{-5} atm., or 6.5×10^{-3} cm. of mercury. This, therefore, is the pressure deficiency at the node within the organ-pipe resulting from the jet velocity at the embouchure; and it is the same order of value obtained with the pin-hole probe and U-tube above.

Thus it follows that the mean pressure within the organ-pipe is the same throughout and may be either incremented or decremented, depending on the way in which the pipe is blown (jet *j*). The positive pressure excess registered by the pin-hole probe at a node and which may mount even to 1 mm. of mercury for intense notes exists only within the pin-hole probe and its rigid accessories, the connector pipe and U-tube. If the walls are not effectively rigid (if for instance, part of the region is closed by a soap-film) the pressure within the probe also can not exceed that of the film.

The importance of these results in their bearing on an explanation of the probe is obvious.

71. The same. Direct U-gage measurement—As the bearing of this experiment on an explanation of the pin-hole probe is important, it was corroborated by direct tests. For this purpose the funnel *f* (fig. 195) was removed and replaced by a quill-tube connected at the far end with the U-gage. The results are given in figure 196, being fringe displacements *s* (negative upward) for successive pipe-depths *d*. These data are necessarily very fluctuating, depending on the position of the plate *F* (fig. 195). When this closed the pipe, the displacement *s* was least; when *F* was removed (open, silent pipe), *s* was usually greatest. Some of the notes (for instance, at $d=12$ cm.) did not readily strike and high negative pressure is recorded. The mean pressure may be taken as $-s=100$; or, if a scale-part is estimated at 10^{-6} atm., $-p=100\times10^{-6}\times76=0.0076$ cm. Hg, with a range from 0.003 to 0.011 about. All of this corroborates the above estimates and suggests a further reason for *s*-differences when the position of the plate *F* is changed.

72. Apparatus. Broad horn (190)—Hitherto in my work short and slender pipes (5 to 10 cm. long, 1 cm. in diameter) were used in connection with the telephones. These, as it were, are at the mercy of the telephones. The present investigation of broad and long pipes contrasts with this and leads to a number of interesting results bearing on the acoustic pressure (*s*) indicated by the pin-hole probe. As first found, the phenomena with the conical horn were so much simpler than the complicated graphs for the cylindrical pipe that the use of the former in connection with measurements of alternating currents seemed promising. Later work did not bear this out. The horn (figs. 197 and 198, inserts) used had the conical shape, being 30 cm. deep, 13 cm. in diameter at the mouth, and 3 cm. at the base (apex angle 19°). It was attached to a telephone (see fig. 197, *T* and *H*), as this seemed to be the only way of activating the horn when air-currents must be excluded.

The attachment was secured through a perforated cork and thin brass tube, 2 cm. long and 1 cm. in diameter, flanged and cemented to the telephone-cap. Thus the telephone-plate was about 2 cm. behind the flat bottom of the horn. The absence of all constriction might have been desirable, but the data do not show it.

Two methods were used for sounding the horn at all pitches. In the first a secondary of a transformer (fig. 197) with known capacity c and inductance L, the capacity (as usual) being variable at pleasure, operated the telephone T and the pitches available lay between a and a''. Higher frequencies were tested later. This method is necessarily discontinuous from capacity to capacity. The break B in the primary was the common spring-contact and

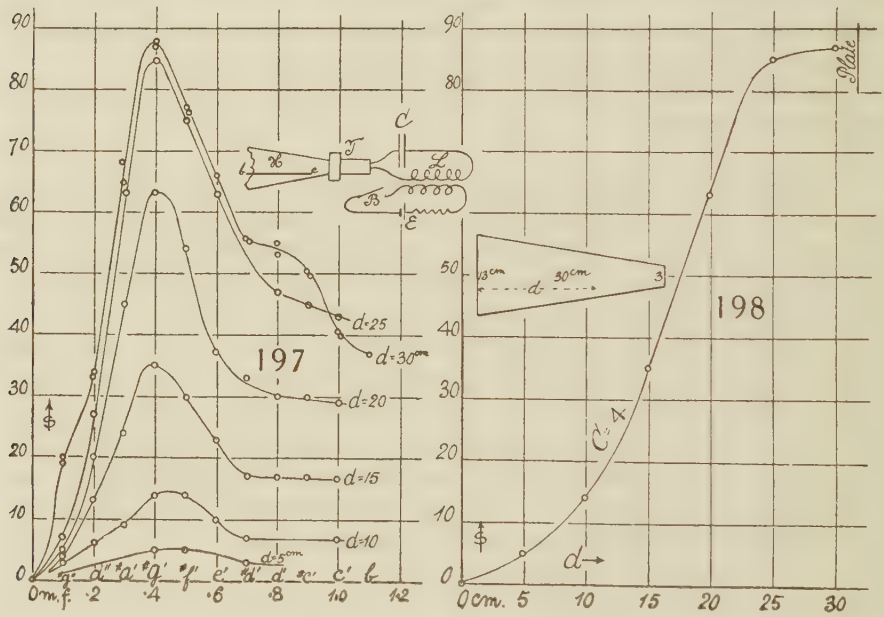

it seemed to suffice, care being taken not to change the tension of the spring and modify the frequency factor. The horn sounds with the usual loud blare, characteristic of the pitch of the spring-break and the pitch to be measured is not heard by the ear without special devices. This is also for other reasons a serious drawback.

In the second method (fig. 199, insert), a simple circuit from two storage cells, ε, with resistance R, was periodically broken by the commutator-motor device B, the speed of the motor being controlled by a resistance (electric siren). Both methods have been described above. Contact difficulties at the commutator are here not infrequent. The pitch in this case must be determined by the ear if the method is to be adequately expeditious, but it has the advantage of a continuous method. Frequencies g' to a'' were first available. The lower frequencies g to a' were added later.

The pin-hole probe on a long quill-tube, connecting it with the U-gage, was inserted into the horn at the place to be tested.

73. Results for horn—These are given in the graphs, figure 197, as obtained with the transformer method, the abscissas showing the capacities in microfarads with a fixed L (about 0.38 henry) in the secondary. The ordinates are the acoustic pressures s, measured by the pin-hole probe when sunk to a depth d below the mouth of the horn (s is roughly in 10^{-6} atm.).

What strikes the eye at once is the relative simplicity of this group of curves when compared with similar graphs for cylindrical and other pipes. For all depths, d, below the mouth of the horn, there is a dominant crest at about $C=0.4$ microfarad, though near the mouth ($d=5$, 10 cm.) it seems to shift slightly into larger C values (flattens). Only in case of $d=30$ cm. at high pitch or very low pitch is there a bulge suggesting a crest about $C=0.1$ microfarad and above $C=0.8$ microfarad, but they vanish even at $D=25$ cm. Nevertheless the crest is wide and the horn suspiciously sonorous at all pitches, g'' to c'.

If from these graphs we plot s against d for $C=0.4$ (near the crest), the curve, figure 198, of very definite character results. It indicates the increase in the intensity (s) of vibration from the mouth to the base of the horn. The rise is at first accelerated and finally rapidly retarded toward the telephone plate. Throughout much of its extent it is nearly straight. The chief feature of the graphs obtained with electric oscillation is the continuity of sound at all pitches. This continuity, s, in general increasing as pitch falls, will in case of cylindrical pipes occur even without a crest.

If we put $C=0.4$ microfarad and $L=0.32+0.06$ henry and compute the frequency as $1/n=2\pi\sqrt{LC}$ the result is $\#g'$, $n=408$. If $C=0.35$ at the crest, $n=435$ or a' is the pitch. Hence the pitch of the horn, so far as it can be found, lies between $\#g'$ and a'. If it were a little shortened, the latter would be acceptable.

The results obtained with the electric siren, where the pitch is directly and continuously given by the ear, are summarized in figures 199 and 200. Here the currents are more intense and the a' crest for the pipe-depths $d=28$ and 25 cm. runs out of the field. Otherwise its location is in correspondence with its former C value and at $d=10$, 5, and 2 cm. it again shifts, but now to higher frequency.

In figures 199, 200, however, there is a new crest near f'' which does not appear in the preceding graphs. It is, moreover, highly variable with the depth d below the mouth of the horn, and is strong only near the telephone-plate. The feature of these siren graphs (differing from the oscillation graphs) is the occurrence of sharp maxima of sound between long intervals of silence.

In figure 201, the intensity s is plotted against the pipe-depth d, for the a' crest, the f'' crest, and the b' shift alluded to. The a' curve in the present cramped scale is much the same as in figure 198, and is the horn fundamental regarded as a closed pipe. The f'' vibrates as if it were the first overtone with

two nodal crests, but enormously dislocated in pitch. With the transformer method it should appear at $C=0.14$ microfarad, and hence if sharp might be overlooked between 0.1 and 0.2 microfarad in this very crowded region. In fact, the bulge at $d=28$ cm., $C=0.1$ microfarad in figure 197 is thus explained.

In figure 202, I have given the siren-graphs for the 2 and 4 feet octaves of the broad horn, made at a somewhat later date. This work is difficult, because the motor-break does not run smoothly. The graphs are a reduced repetition of those for the 1 and 2 feet octaves. As obtained from a 1-foot horn, figure 202 is probably a response to the overtones of the telephone-plate evoked by the lower register. Again, f' drops off so quickly with the pipe-depth d that one suspects it may be an incidental note of the telephone.

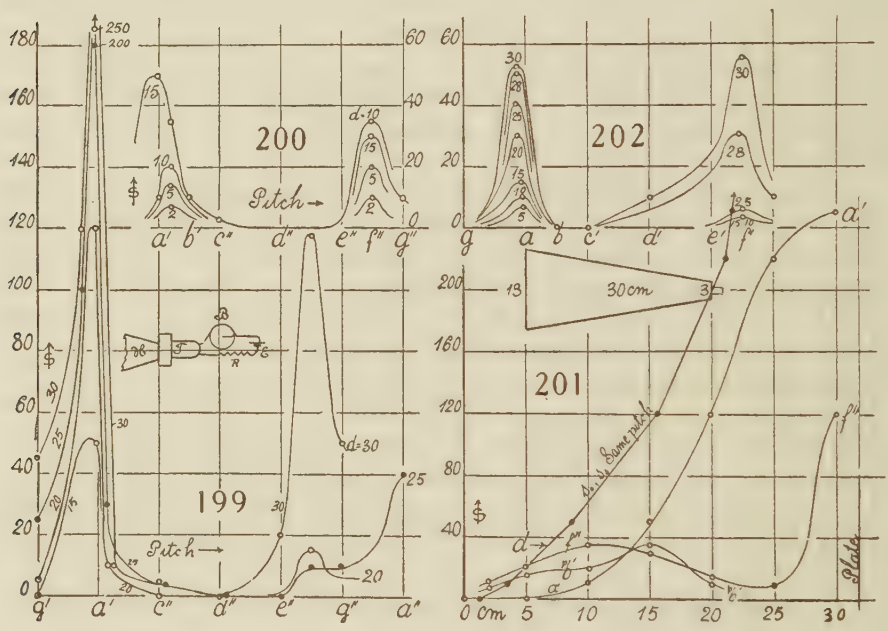

Turning to the transformer graphs 197, there is nothing in the f' region to suggest a crest, but a mere decay of the sound intensity s. The a region could not be reached. Again, the continuity of noise evoked by electric oscillation contrasts with the characteristic sharp crests and flat troughs of the electric siren.

The oscillation graphs for intervals of 0.01 microfarad between 0 and 0.1 microfarad consisted merely of a group of divergent lines with a rapid fall between $d=30$ and $d=25$ cm. They need not therefore be reproduced here.

The divergent results obtained from the electric-oscillation method and the siren pointed to the spring-break as the probable cause. The pitch of this in the most favorable position happened to be a, so that an overtone a' would be usually present in the spring itself or in the telephone-plate. In fact, by changing the tension and therefore the pitch of the spring, the crests

(some examples $d=25$ cm., const., are given in fig. 203) could be shifted from about $C=0.35$ to even $C=0.55$, a low C value for the crest usually accompanying a high intensity (s) value and vice versa. In fact, on further change of the spring it was even possible to obtain graphs (for $d=25$) like figure 204, with three well-defined crests near $\#g''$, $\#f'$ and between d' and $\#d'$. The graphs thus depend essentially on the pitch of the spring, and the simple cases of figure 197 are the result of resonance between the spring-break and the electric oscillation which it unlooses. The shift of crests and the continued noise of the horn are to be ascribed to beats between the two vibrating systems in relation to the fixed pitch of the horn. As this is near a', the highest intensities, s, will be obtained when this is the common (or octave) pitch throughout the three oscillations.

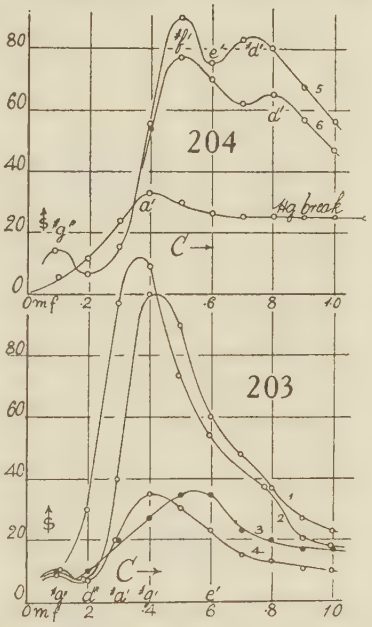

To return to figure 197, of the three coupled vibrating systems, two, viz, the spring-break and the horn, are in the same key (frequency taken as a and a'); the third, the electric oscillation, is varied nominally over a wide range of frequencies (c''' to c'). It seems probable that the massive air-column of the horn, reacting on the telephone-plate, forces the electric oscillation to remain at the horn frequency a', with different amplitudes passing a maximum when the electric oscillation is also at a', *i. e.*, in resonance. Hence the difference in figures 197 and 199, since in the latter no reacting mechanism is available. The continuous noise in figure 197 throughout all frequencies must thus be regarded as a case of forced vibration of the L circuit with synchronism at a'. At the same pitch the nodal intensity of the free system (siren, s_s) increases much faster than the nodal intensity of the forced system (electric oscillation, s_o), as shown by the graph in figure 201, where the horizontal scale s_o is increased four times.

Finally, the decreasing nodal intensity s toward the mouth of the horn is enhanced by its increasing sectional area. This somewhat obscures the linear relation of the fringe displacement s to the corresponding nodal pressure, as I shall indicate in the subsequent section, in which large cylindrical pipes are tested.

74. Slender horn—The attempt was now made to get correlative evidence from a horn of smaller angle (figs. 205 to 210). The horn in question (fig. 207) was 41 cm. long and tapered from a diameter of 6.5 cm. at the mouth to 1.5 cm. at the apex end (angle 7°), fitting at once into the telephone with

the plate at 44 cm. from the mouth of the horn. Being longer than the broad horn, it is thrown off the a' key. Its thinness should make it rich in overtones.

The graphs, figures 205 and 206, in which the intensities s are plotted against the capacity of the secondary of the activating transformer for a fixed pipe-depth d, show that overtones are present in variety and for $d > 20$ cm., pronounced in character, as fully revealed by the curves. Crests are marked near $C = 0.1$, 0.2, 0.3, 0.4, 0.9, and figure 207, therefore, gives the intensity at different depths, d, for the constant pitch of the crests in question, respectively $\#g''$, d'', $\#a'$, $\#g'$, $\#c'$. A full treatment of these graphs, though interesting, would require too much space. We note that in figure 207, crests are universal at pipe-depth $d = 10$ cm., and that this feature soon vanishes for the broad horn of the preceding section. Similarly all graphs pass through crests at $d = 35$ cm., except the low-pitch curves $C = 0.8$ or 0.9 microfarad. In this case the horn vibrates as a closed organ-pipe, whereas in the others, with

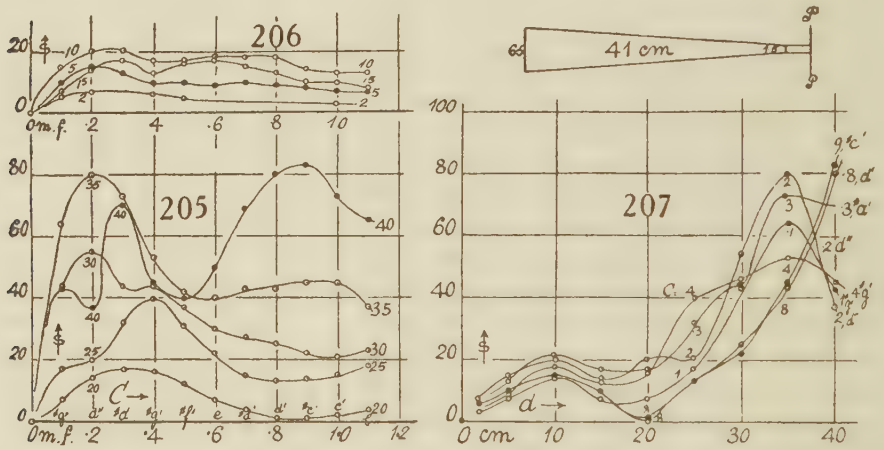

troughs at the apex, as an open organ-pipe. Between $d = 10$ cm. and $d = 35$ cm. the detailed progress between the main crests is complicated, but fully shown.

Figure 208 gives the survey in pitch made with the electric siren and ear. In the corresponding groups, 205 and 208, the maxima near $\#g''$, d'', g' may be taken as equivalent. The $\#a'$ crest at $C = 0.3$ in figure 205 for $d = 40$ cm. does not appear, and may, therefore, be taken as due to the spring-break. The graphs g' and g'', figure 210, are essentially similar and are open-pipe curves with troughs near the apex. The fifth d'' is a closed organ-pipe curve with a crest at the apex. All the graphs would have passed through crests at $d = 10$ cm.

Figure 210 (siren) is essentially simpler than 207 (electric oscillation), which means that the ear can not compete with pitch determination in terms of capacity C, where detail is sought for; but the ear has nevertheless the advantages already stated, as there is continuity without crowding in high pitch, and there is no disturbing third vibratory system (spring-break).

Hence the discrepancy in the d'' graphs at pipe-depth $d=40$ cm., where the ear requires a crest and the capacity work a trough, is interesting. Both may occur in this region of intense vibration, lying close together. The g' and g'' curves of figure 210 correspond to the general run of curves in figure 207, if we disregard the exceptional cases $C=0.8$ or 0.9 microfarad. These are much like d'' in figure 210.

75. Cylindrical pipe—This was 28 cm. long and 2.8 cm. in diameter (fig. 213, insert), with the plate of the telephone 34 cm. below the mouth of the pipe. The transformer graphs s, C are given in figures 211 and 212, with detail measurements between $C=0$ and 0.1 microfarad in figures 213 and

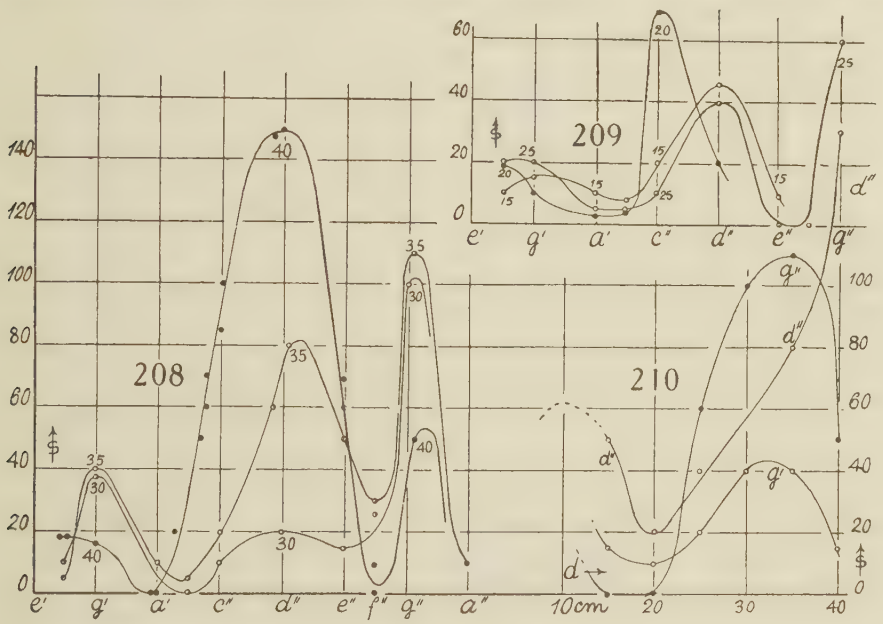

214, for all pipe depths, $d=0$ to 28 cm. The curves of the broad horn are reduced to the same scale in the first figure, for comparison. When blown, the pipe responded to d', which implies overtones at a'' and above.

Owing to the high intensities, small crests are possibly drawn out and less apparent; but the general detail is much greater than in the preceding work with horns. There is a continued increase of intensity, s, when the pitch is being continually lowered, and in this respect these graphs again differ radically from the tests with the electric siren presently to be given. Nowhere is there an approach to silence. As a whole, the graphs suggest that a smoothed common crest of spring-break and pipe oscillation is absent and therefore the electric oscillation finds no steady oscillation with which to resonate.

Owing to the excessive ornamentation of the graphs, I have made sections

(in s and d for constant C) only at $C = 0.1$, 0.3, and 1.0 microfarad, and these graphs are given in figure 215, corresponding to the notes $\#g''$, $\#a'$, and c'. The low note c' falls rapidly as the mouth of one pipe is approached, from its high initial intensity. The three curves and others which might be added are all different from each other, and hard to construe. It looks as if beating wave-trains had been encountered.

A much more serviceable general result is obtained with the electric siren, and these graphs for intensity s and pitch are given in figures 216 and 217. Crests at a', e'', and a'' are prominent, though there are some humps and minor crests. The intensity of these crests is sustained very nearly to the mouth of the cylindrical tube, at least as far as $d = 5$ cm. The records

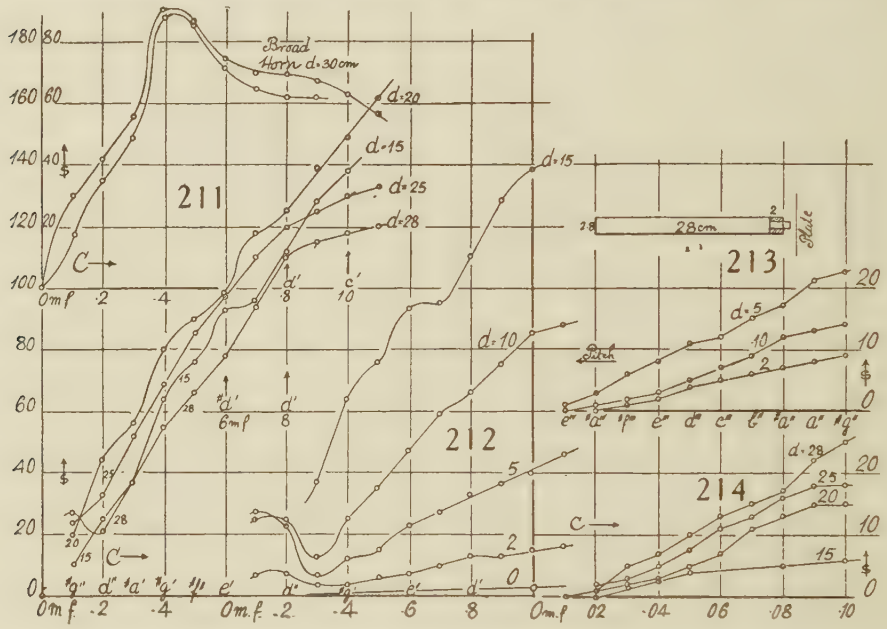

for a d' pipe are puzzling; but a'', the first overtone of d', is probably awakened both by the a' and the g'' of the siren, while the e'' will presently appear as an open organ-pipe harmonic.

The corresponding s and d graphs are found in figure 218 and can not be correlated with the transformer set (215), where they would, moreover, be in the crowded region. The new graphs for a' and a'' are of the same nature (having the same crest and trough), except near the bottom, $d = 28$ cm., where the conditions are no doubt complicated by the nearness of the telephone-plate. The e'' graph differs from them radically and is probably an open organ-pipe graph. This loses its intensity rapidly from the middle toward the mouth ($d < 15$ cm.), whereas the a' and a'' graphs carry their high s to within $d = 5$ cm. Finally, a'' has been recognized as the first overtone of the d' pipe-note and the a' partakes of the same form, as already instanced.

One might suppose that by decreasing the steps in C to 0.01 microfarad, salient high-pitch maxima would appear in the transformer graphs. Figures 213 and 214 show that this is not the case. The period of coherence of the transformer oscillations is either too short or the successive impulses are out of step with each other and interfere in their integration by the pipe. If T is the period of the oscillation, xT the period of coherence, and T' the period of the break circuit, then $T'-xT$ is the interval without stimulation. The binominal increases for a given x, as T is smaller, and one may therefore look for increased intensity s as T is larger. This is in conformity with all the transformer graphs, even for the cylindrical pipe.

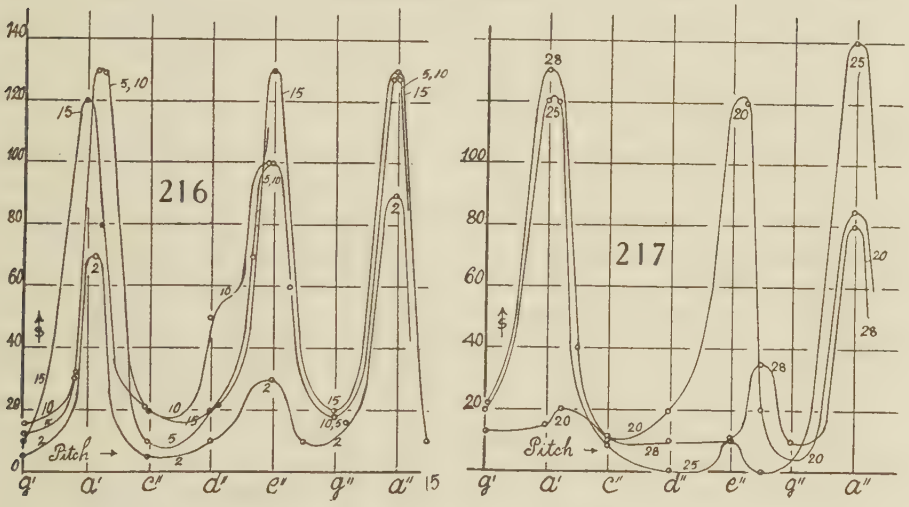

Experiments were made with the much slower (frequency) mercury break, but the s values were too small. An example is given in figure 204. The crest at $C=0.4$ microfarad is too flat and beyond $C=0.6$ microfarad s is practically constant. Four storage cells were used in the primary.

76. Extensible pipe—Since there are three vibrating systems in the transformer method, two of them should be made adjustable if the third is given to obtain the largest acoustic pressure values (s). An extension was therefore added to the pipe so that its length could be increased continuously, from $d=28$ (note d') to 35 cm. (note b). By setting this for a maximum s at any C, the remainder of the curve was then worked out. A remarkable result presented itself, with an important bearing on the pin-hole probe, inasmuch as the graphs now consisted of right-line elements between breaks.

In figure 219 the largest s was first established by tuning for the pipe-depth, $d=30$ cm. (the probe being at the bottom of the tube, as usual). The graph obtained for varying C (0 to 1.1 microfarads) starts with a linear sweep as far as $C=0.3$ microfarad (a'), then bends abruptly to a second linear sweep

as far as $C=0.9$ microfarad, after which the course is curved to the crest beyond the figure.

It seems obvious that each of these lines corresponds to a given kind of vibration, *i. e.*, to a given overtone which breaks abruptly into the next available overtone.

The behavior of the untuned pipe ($d=28$ cm.) for the given spring-tension is shown in the lower curve. There is a break at $C=0.2$ (d'') and at $C=1.0$ (c') microfarad. In the repetition (black circles) the break at $C=0.7$ ($\#d'$) is probably an accidental small change in the tension of the electrical spring-break. Between these points the graph is strikingly linear.

After the tube was further elongated to the pipe-depth 35 cm. (now nearly in resonance with the spring-break), where a second and much stronger maxi-

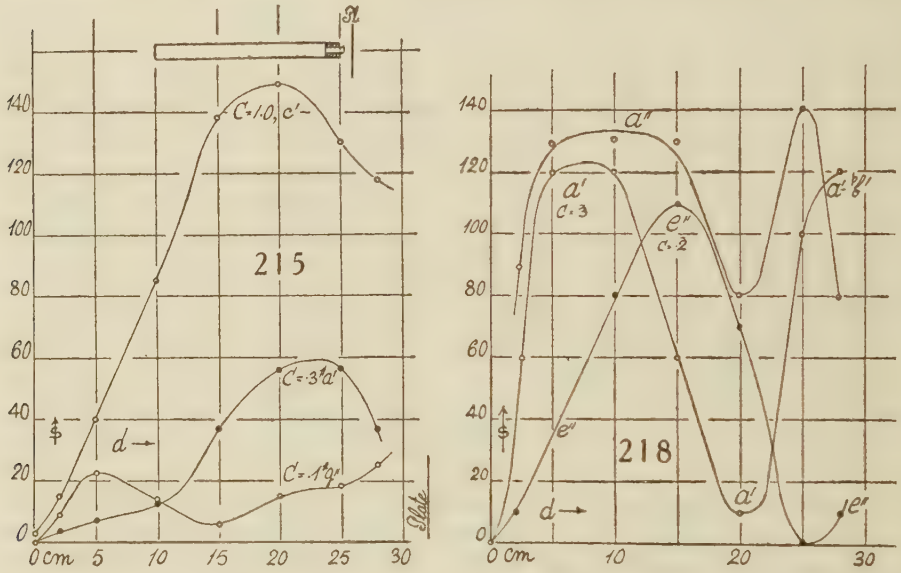

mum (fig. 220) appeared. The rectilinear progress between $C=0.1$ to 0.3, 0.4 to 0.6, 0.6 to 0.9, 0.8 to 1.2, 1.3 to 1.5, 1.6 to 2.0 microfarads is throughout marked. Even near the crest $C=1.2$ the tendency is still observable. This relatively enormous crest ($s=475$) is in keeping with the near resonance of spring-break, organ-pipe, and electric oscillation.

It seemed worth while to test the case further with untuned lengths between $d=28$ cm. and $d=34$ cm., and throughout large C ranges (0 to 2 microfarads). The graphs are given in figures 221 and 222 for an altered transformer-spring tension. The case for $d=28$ now turns out quite differently from figure 219, but this is the necessary result for modified spring-tension or pitch. Broken rectilinear paths are the rule for $d=28$, 29, 31, 33. The two latter, with their roof-like crests, are astonishing. The graph for $d=34$ (very near the maximum $d=35$) points at highly unstable conditions of vibration. Split crests like this one between $C=0.4$ and 0.8 are rare.

Finally, in figure 223, for the optimum $d=35$, the successively tuned pipe is compared with the untuned pipe. Below $C=0.5$ the divergence is not large, both starting under tuned conditions. Thereafter the divergence rapidly increases, the tuned pipe naturally being in excess. From $C=0.8$ on, passage of the untuned (n) condition to the tuned condition (t) is indicated by arrows. To get the maximum s values it is thus necessary to retune the pipe at all pitches. Linear progression is a characteristic chiefly of the untuned pipe. One may note that successive tuning (resonance throughout) has raised the crest to nearly $s=550$ (over 0.4 mm. of mercury).

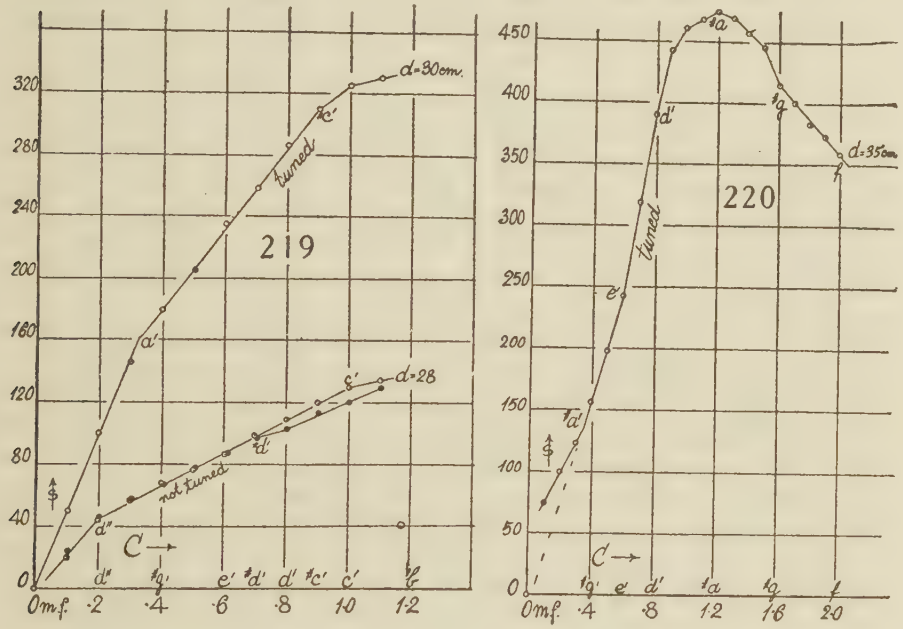

The same figure shows the corresponding behavior at the smaller maximum at $d=31$. Linear progress is interrupted by the tuning indicated by the arrows.

77. Closed organ-pipe—The open-mouthed organ-pipe is very noisy, so that in this respect the doubly closed organ-pipe shown in the insert, figure 224, is preferable. Here p is the pipe 27 cm. long in the clear, T the attached activating telephone, and bc the pin-hole probe. The point c may either be thrust to the rear, near the telephone, or (as in figure) the pin-hole c may be near the front of the tube. This should make no difference in the acoustic pressure s, other things being equal. The telephone T was activated by the transformer method, as the specific results of this method are particularly in question.

The graphs 1 and 3 (the former raised for clearness), for the same tense spring-break adjustment left unchanged, but with the pin-hole respectively

in the rear (bottom) and in the front of the doubly closed tube, are practically identical. They again consist of linear parts (as above), with abrupt breaks. Each exhibits two crests, respectively above a' and near $\#d'$.

The graph 2 with a loose spring-break differs from 1, and graph 4 differs both in intensity and character from all the graphs. But this is due to the fact that the spring-break has to be reset (frequency change) and not to the fore-and-aft positions of the pin-hole. While in graph 4 the $\#d'$ crest is marked, it is quite absent in graph 2. In both the $\#a'$ crest is abortive, particularly in 4.

The endeavor to tune the pipe by adding an extension (fig. 225, inset) was not very successful, probably because the slide-joint at the draw-tube

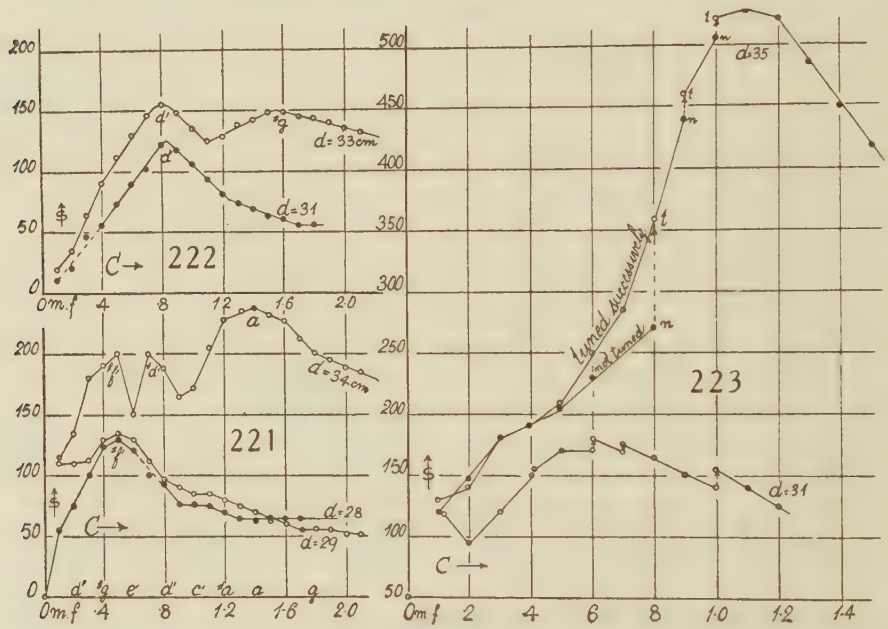

can not conveniently be made tight. The greatest intensities were obtained for pipe-depth $d=29$ cm. and the figure in the upper graphs shows two independent results. The crests at $\#a'$ and d' are accentuated, all being harmonics of the spring-break pitch. The elongated tube $d=35$ cm. (lower curve gives an example) merely adduces a case of weak repetition. After tuning the spring-break by reducing its tension, the intermediate graphs (fig. 225, $d=35$ cm.) were obtained in successive experiments. The crest has fallen in pitch ($\#g'$) and the harmonic near d' is practically absent. It is generally preferable, therefore, to select a suitable fixed length of pipe p and to tune the spring-break in conformity if high s values are sought.

78. Alternating current—The attempt to energize the primary of the induction coil by an alternating current proved unsatisfactory for the reason

that while the induction is relatively feeble as compared with the break-circuit methods used heretofore, the heating effect of these continuous currents is out of all proportion. The current for the primary was obtained by stopping down the 110-volt lighting circuit with a resistance of about 20 ohms, not including the impedance of the primary. The frequency of the secondary was modified as before by changing the capacity C from 0 to 1.1 microfarads. The results so obtained are summarized in figures 226 and 227. The curves are interesting as a whole, as they consist conspicuously of right-line elements, with breaks between $C=0.6$ and 0.7 and others near $C=3$ microfarads.

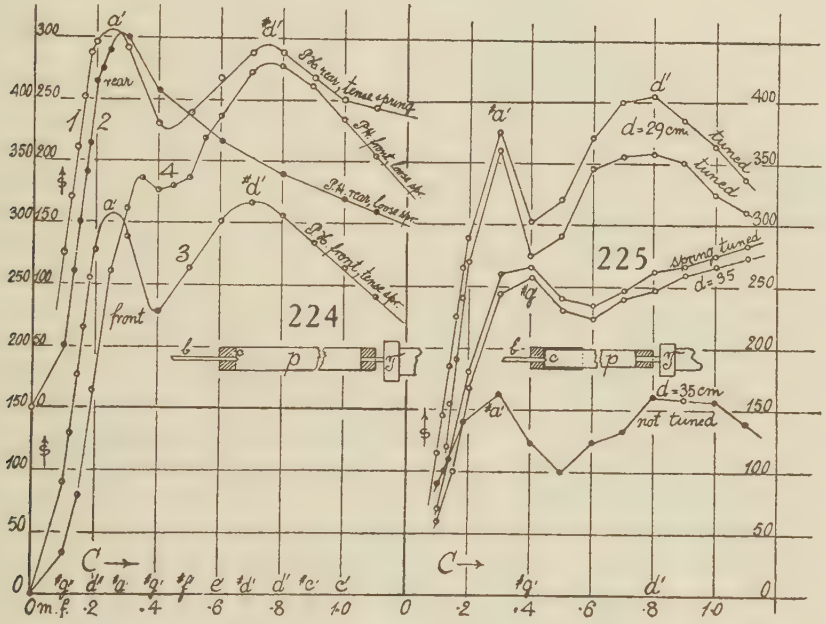

In case *a* (pipe and alternating current in the same key) the observations were begun at $C=1.0$ microfarad and finished as expeditiously as possible to keep the wires cool. After completing the series, the drop of s at $C=1.0$ (see figure) was about one-seventh of the full deflection, $s=70$. In case *b* the progress of observation was in the reverse direction of increasing C. The graph, partly for this reason and partly because of less perfect tuning, is much lower, though the two independent series made are practically coincident and show the same peculiar break between $C=0.6$ and 0.7 microfarad. In case *C* the tuning is still less perfect and the break at $C=0.6$ is just perceptible.

The tuning of the pipe must be done with nicety and requires an adjustment of pipe-length to within a millimeter. As the alternating current makes 60 cycles per second, the harmonics of the key of B^{-1} are in question. The curve *d* (raised $s=20$) was obtained from a pipe specially adapted for tuning,

with wires cooled after long waiting; in case of *e* the wires had been used and were warmer. There is here an additional break at $C=1.0$. At $C=0.1$ there is scarcely any perceptible deflection, so that the graphs start their upward sweep abruptly about at this point. The curves are chiefly interesting because of the sharp breaks between linear elements, and an investigation of the relations of successive values of ds/dC with their relation to frequency is again suggested.

79. Remarks—In my work heretofore I have associated the fringe displacement *s*, *i. e.*, the nodal intensity or acoustic pressure, with the usual

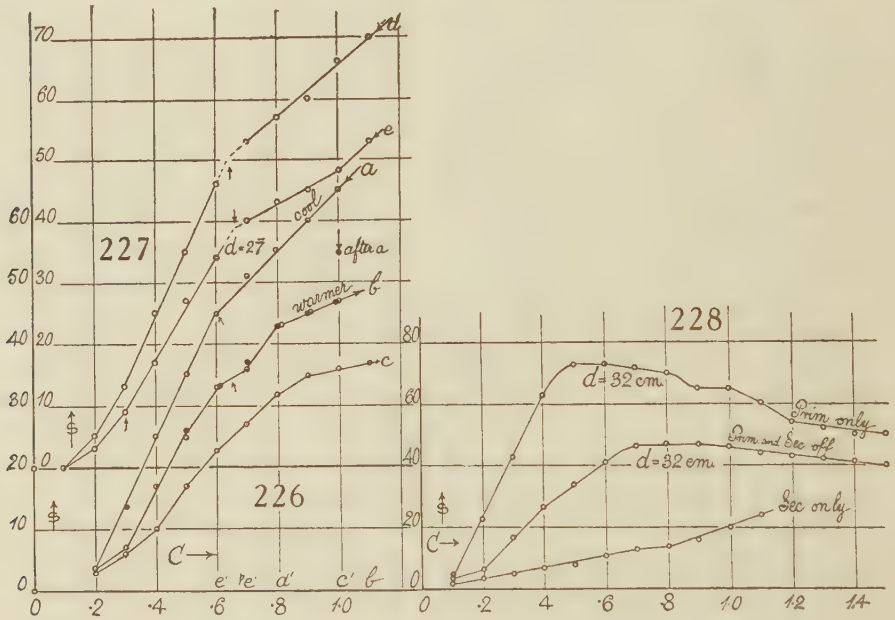

energy (E per unit of volume) equation. If n is the frequency and a the amplitude of the sound-wave, we may therefore write

$$E=p+\rho v^2/2=ks+(\rho/2)a^2 4\pi^2 n^2$$

At the mouth of the tube s is zero and a the maximum; at the bottom or node, a is zero and s a maximum. The expectation that a similar equation could also be used to interpret the fringe displacement at a given point for different frequencies is not warranted. For if we put $4\pi^2 n^2=1/LC$, $p=ks$, and assume E to be constant along the linear elements of the graphs, the result is $(s-s')=(\rho/2KL)\ (a^2/C-a'^2/C')$, whereas the graphs suggest $\Delta s \propto \Delta C$ simply, along each element.

The view that the oscillation frequency (n) of the organ-pipe is impressed on the oscillation frequency (n') of the secondary actuating the telephone-

plate is also unsatisfactory. For if Y is the amplitude of the electric circuit under a harmonic electromotive force $E \cos \omega t$,

$$Y = E/\sqrt{(\omega'^2 - \omega^2)^2 + k^2\omega^2}$$

where $\omega = 2\pi n$ and $\omega' = 2\pi n'$ are the angular frequencies of the free and frictionless acoustic and electrical circuits, respectively, and K is the coefficient of friction. This may, as usual, be reduced to proportionalities in the form $Y = 1/\sqrt{(1-x^2)^2 + \alpha^2 x^2}$ where $\alpha = K/\omega'$, $y = Y/(E/\omega'^2)$, $x = \omega/\omega'$. This y has a crest for $x^2 = 1 - \alpha^2/2$.

If $\omega' = 1/LC$ and K is relatively very small, the equation reduces to

$$Y = \frac{ELC}{1-\omega^2 LC}\left(1 - \left(\frac{K\omega LC}{1-\omega^2 LC}\right)^2/2\right)$$

approximately, where ω, K, L are constant and C variable. Hence, even if we neglect the term in K and associate Y with the fringe displacement s, an equation in this form is not serviceable in identifying $\Delta s \propto \Delta C$ along linear elements, unless $\omega^2 LC$ is small compared with 1. This would not be the case with the fundamental or any harmonics of the cylindrical pipe. Even if ω refers to the frequency of the spring-break taken at pitch a, the equation remains inapplicable.

This suggests a simpler approach through the capacity equation $Q = CV$, whence $\Delta s \propto \Delta i = (dV/dt)\Delta C$; or the slopes of the linear elements of the graphs are to be associated with the effective time-rate at which the potential of the condenser changes. The value of dV/dt depends on the form of residual wave on which the new impulse is superimposed. Moreover, a reason for the broken linear relations of s and C is now apparent, for the fringe displacement s measures the difference of level of the surfaces of mercury in the U-gage. It, therefore, also measures the potential energy localized in the stationary wave at the point of the pin-hole probe, though it does this with a coefficient which may be either positive or negative. The stream-lines run from the outside to the inside of the pin-hole embouchure.

80. Charging circuit—Following the suggestion at the end of the last section, a change of circuit was chosen in which the condenser C (fig. 230, insert) is charged directly an open circuit. Here B is the spring-break (conveniently kept in resonance with the lighting circuit in the key of B), E and R electromotive force (2 cells) and resistance, T, p, telephone and organ-pipe, I, II, primary and secondary of the transformer. When B is open, C is charged by E and discharged on closing. The coils I and II were eventually to be removed.

Figure 230 shows the sC graphs for the intervals 0 to 1.1 microfarads. These are successive measurements, each graph (1, 2, 3, 4) being in turn moved 0.1 microfarad to the right for clearness. The pipe was carefully tuned for the largest s available, in all cases. The results are a set of data strikingly linear and parallel in their main features, except for the occurrence,

almost capriciously, of the breaks indicated by the arrows. As the spring interrupter was kept in tune (beats), the breaks in question are results of an accidental intonation of another harmonic, as soon as the conditions for it are at hand, or the instability of the original harmonic is excessive. This happens for capacities below 0.5 microfarad, while 0.4 microfarad usually suffices for the breakdown.

It seemed desirable to determine how far this behavior would be prolonged, and in figure 229, the graphs 5, 6, and 7 are worked out between $C = 0.9$ and 2.2 microfarads, and in No. 8 between 0 and 2.2 microfarads. The tendency to linear and parallel variation persists; but the breaks occur far more capriciously, as one would expect for these regions of low pitch. No. 7 after

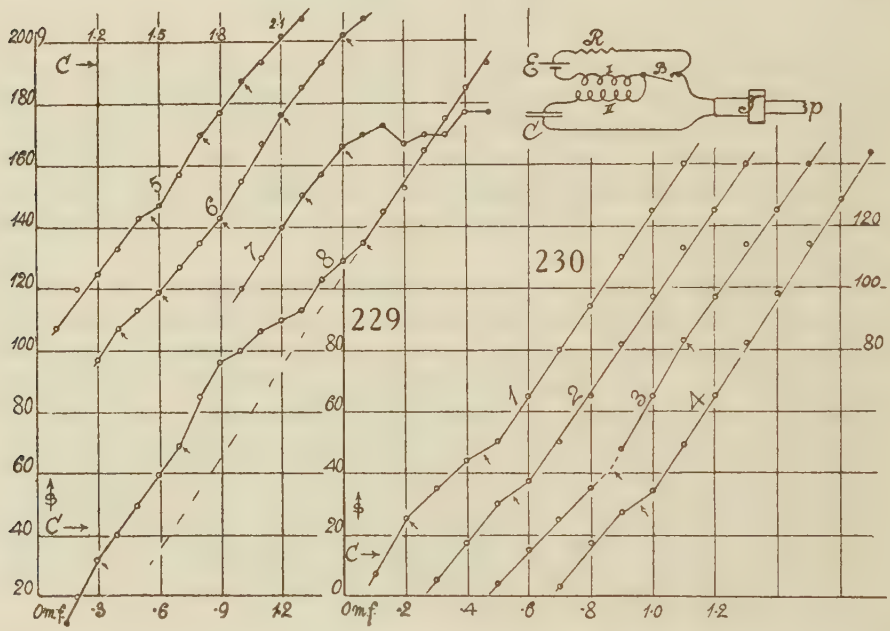

$C = 1.5$ microfarads breaks almost to the horizontal. No. 8, where the whole interval is tried out, is interesting, as the slope of the line at the lower and at the top end are about the same (see dotted line). One also notes that after these breaks the curve does not recover, but the s remains continuously below the prolongation of the lower part of the curve. This would also be expected, since the fringe displacement s measures the difference of level of the mercury surfaces of the U-gage and hence the wave-energy potentialized at the pin-hole. Each new increment is added to the stored energy or may also be withdrawn from it, as in figures 221, 222, and 223 for instance, following the crest.

In figure 228, the results are given for cases in which the primary (insert, fig. 230) or secondary, or both primary and secondary, are removed, the pipe being tuned for each case, separately. With the primary only in circuit

(secondary removed) a distinctly higher pitch was heard, though the pipe-depth is about the same. In this case and when both *I* and *II* are cut out, the graphs have definite crests, and these graphs are as a whole more curvilinear than the preceding. With *II* only in place, the largest fringe displacements, *s*, obtainable are too small to be of much service. In fact, taken together, these graphs are throughout small in their *s* values, as compared with figures 229 and 230, with both *I* and *II* in place; and the latter, in turn, 4 to 5 times less in sensitiveness than the above graphs for a completely separated primary and secondary. The marked tendency to preserve linear progress in the present cases has, however, been put in evidence.

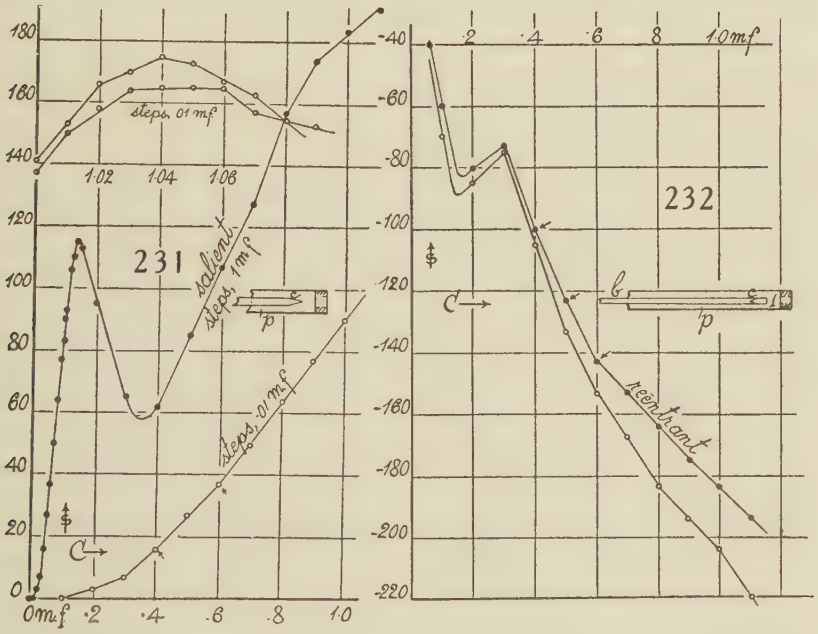

81. Reëntrant pin-hole probe—At the present stage of research, a determination of the correlative behavior of the reëntrant pin-hole probe is pertinent. Accordingly the cylindrical pipe of length 29.3 cm. and diameter 2.8 cm. activated by the telephone (as above) was chosen; but the pin-hole probe *bc* (fig. 232, insert) now carried a reversed pin-hole at *c*. As this was a sensitive glass cone, it ended in a quill-tube at its farther end, the whole being about 2 cm. long from the pin-hole. The quill-tube mouth was in all cases placed about 1 cm. from the bottom of the pipe *p*.

The *sC* curves were first worked out for the salient adjustment of pin-hole and the results are given in figure 231. There is a very definite crest at $C = 1.4$ microfarads, about, as shown by the smaller curves, giving the details between 0 and 0.1 microfarad and 0.1 and 0.2 microfarad. The trough is equally definite at about $C = 3.5$ microfarads.

The pin-hole end was now reversed and the results of figure 232 (two runs) were obtained. Thus the reëntrant pin-hole probe is astonishingly sensitive, the s values being even larger than in the preceding salient case. The negative crest at $C=1.4$ and negative trough at $C=3.4$ also appear clearly; but they are not nearly so salient as in figure 231 and there is less tendency toward a limit of s beyond $C=1.1$ microfarad.

Thus one is urged to ascertain how this strong response will vary, if the quill-tube shaft of the pin-hole is gradually lengthened, as in the insert, figure 235 or 238, where p is the organ-pipe with the mouth of the quill-tube (as before) 1 cm. from the bottom of the pipe p (U-gage being beyond b), but with the reversed pin-hole at a distance x from the bottom. This x is successively enlarged, till it reaches beyond the length of the pipe p.

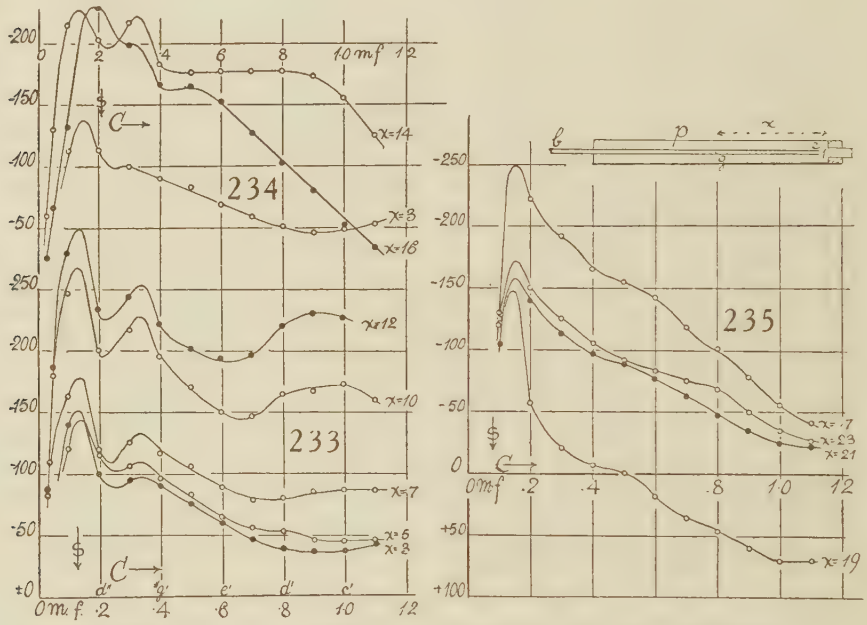

The graphs for each x are worked out (s plotted positively downward) and given in figures 233, 234, 235, and 236. Far from losing in value, the sensitivity (s) increases with x periodically and to such an extent that an enlarged scale had to be adopted in the figures. The graphs, figures 233 and 234, moreover, show two initial negative crests (owing probably to incidental change of the pitch of the spring-break as compared with the case of figures 231 and 232), at $C=1.4$ and 3.5 microfarads, about, beyond which they tend to decrease, as a rule, but at $C=0.9$ (roughly) the suggestion of a trough at $x=3.5$ cm. passes into a crest at $x=10$, 12, 14 cm. At $x=16$, the initial trough at $C=1.5$ microfarads only tends to survive and the others to vanish. This behavior is kept up in figure 235 for $x=16.5$, 19, 21, 23. With $x=25.5$ 27.5, 29.5, however, the crest at $C=0.9$ microfarad is again introduced, so

that it appears and disappears, periodically. In figure 236 the crest at $C=1.5$ microfarads is very distinct, as it has been throughout, while for $x=29.5$ and perhaps $x=25.5$ there is a strong suggestion of the reappearance of the crest at $C=3.5$ microfarads. A certain capriciousness in the intonation is of course to be expected.

82. The same; *s* and *x* graphs—The relation of nodal intensity s to the distance x of the pin-hole from the bottom of the pipe (p) is an interesting interpretative relation. It is given, so far as possible, in figure 237. Unfortunately, measurements at the first crest at $C=1.5$ microfarads were not included. I shall, therefore, have to consider the relations for $C=0.1$ and $C=0.2$, though these leave much to be desired, even if they include the crest

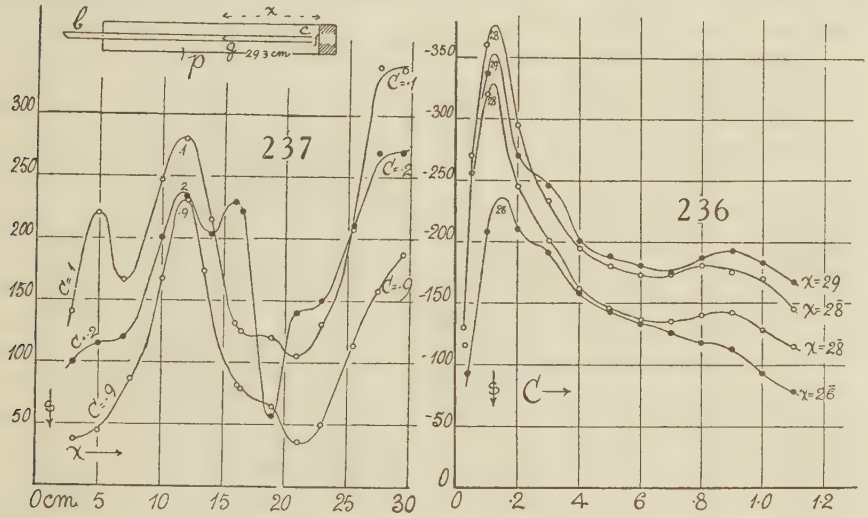

between them. The two graphs suggest a crest at about $x=12$ cm. and at the end of the pipe $x=29.5$ cm. and a trough at about $x=20$ cm. Since the quill-tube attached to the pin-hole extends to 1 cm. of the bottom of the pipe p, this makes the quill-tube length δ trailing the pin-hole, $\delta=x-1$, so that one may suspect that crests alternating with troughs lie at one-third, two-thirds, and three-thirds of the length of the quill-tube.

There is, however, an additional crest in the Cs graphs, *i. e.*, the fluctuating and flat crest at about $C=0.9$ microfarad. The relations of this in its sx graphs are also given in figure 237, and fully corroborate the inferences drawn, except in so far as the first crest at $x=11$ cm. is higher than the second at $x=30$, about. The graph, however, considering the difficulties encountered, is remarkably definite as a whole. The trough is again at $x=21$ cm.

Whether the crest at $\delta=10$ cm. stimulates the crest above $\delta=28.5$ cm. or the reverse, or whether both are directly evoked, will have to be specially examined; but the extremely curious fact is brought out by these graphs

(fig. 237) that the narrow quill-tube of diameter 0.35 cm. vibrates like a closed organ-pipe with a pin-hole embouchure and exactly like the surrounding wide brass closed organ-pipe 2.8 cm. in diameter, even when the lengths of both are nearly 30 cm. Furthermore, the node at the bottom of the brass pipe p (fig. 237, insert) corresponds to the ventral segment at the mouth c of the quill-tube pipe, bc, and the node of the latter at g to the ventral segment of the brass pipe, particularly when g lies at the mouth of p. Pipe node thus becomes a quill-tube ventral segment; *i. e.*, the pressure increasing from the mouth of the bottom of p and surrounding the quill-tube (therefore not affecting the slender air-column within), finds a sudden release at the mouth if the quill-tube c, and a wave opposite in phase passes up the quill-tube, so that the inside of the pin-hole and the bottom of the brass pipe are the seats of corresponding nodes. Together they constitute a doubly closed pipe, telescoped to one-half its normal length.

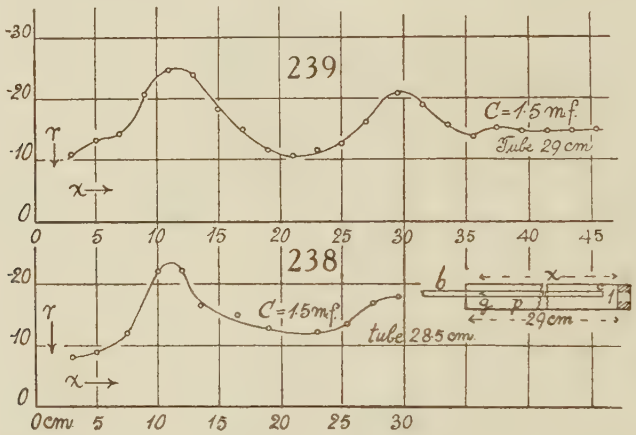

83. The same. Direct tests—To test the question further, I made direct measurements (keeping $C = 1.5$ microfarads the position of the initial crest) with the same apparatus, but using the slide micrometer instead of the ocular micrometer (s) and the graph of r (in 10^{-3} cm.) and x is given in figure 238. Here we have a distinctly marked crest at $\delta = x - 1 = 10$ cm., and a trough at $\delta = 20$ cm. The second crest beyond $x = 28.5$ cm. is again less intense than the nearer one.

The question now occurs as to how far this interesting periodic relation may be expected to go; whether it will still be marked after the quill-tube length gc exceeds the length of the pipe p. Accordingly, the apparatus was overhauled, freshly tuned, and better facilities for measuring the lengths x from pin-hole to the bottom of p, were provided. As before, the mouth of bc at c is kept 1 cm. from the bottom of p, so that quill-tube length is $\delta = x - 1$ cm. Figure 239 shows the data (r, x) as given by the slide micrometer. The striking result is obtained that the periodicity practically vanishes soon after (at $x = 37$ cm.) the pin-hole lies outside of the surrounding brass tube

of length 29 cm., for between $x=37$ and 45 cm. the r is constant. Hence, a trailing quill-tube or rubber hose of this length should be used if the pin-hole probe is to serve for pitch determination apart from its own pitch preferences. Moreover, if the evanescent trough and crest at $x=35$ and 37 cm. respectively, may be included, the distance between trough and crest (semi wave-length) diminishes rapidly as well as the amplitude, r. Crests project farther above the final mean altitude r than the troughs fall below it. The values for crests and troughs, so far as these can be made out, are again $\delta=10, 20, 29$ cm.

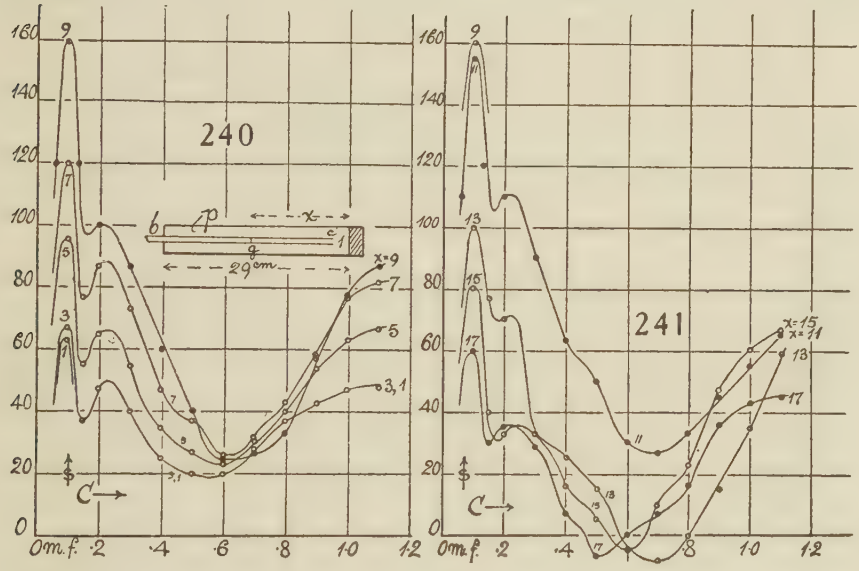

84. Plate pin-hole with anterior and posterior quill-tubes—The very definite contrast obtained in the results of the salient and reëntrant position of the glass (conical) pin-hole probe suggested similar experiments with a pin-hole pierced in a soft, thin metal plate (copper or aluminum), with the two sides as nearly identical as possible. As shown in figure 240, this plate g is cemented between two lengths of quill-tube b g and g c, c being open and kept at 1 cm., from the bottom of the pipe p, actuated by the telephone. The fixed quill-tube b g was 30 cm. long and joined at b with thin rubber pipe of about the same diameter, and over 50 cm. long, connecting b with U-gage beyond. The length g c (open at c) was variable and increased in steps of 2 cm. from 0 to 28 cm., the pipe p being 29 cm. long. Quill-tube lengths were thus $\delta=x-1$. My expectation was that the initial positive nodal pressure would eventually be quite wiped out and become negative, since the probe g c (counteracting b g salient) is reëntrant. It was, therefore, astonishing to find the original positive pressure not only remaining positive, but increasing (periodically) as the length of the reëntrant probe g c increased. This shows

that the occurrence of a node in the pin-hole probe near the pin-hole is not necessarily coincident with the occurrence of excess pressure on the same side, as I have usually supposed. In fact, it will now appear that the two sides of any pin-hole are specifically different, so that, for instance, an air-current passing through in one direction might do so without break in the continuity of the jet, whereas, if passing through in the other direction, the jet might break up into turbulent motion. These initial differences would then be enhanced by favorable acoustic conditions of length, etc., or the reverse.

The s C graphs for a pin-hole about 0.035 cm. in diameter pricked in thin copper foil from the outside are given in figures 240, 241, and 242, for values of $x-1=\delta$ from 0 to 28 cm. The added quill-tubes were 0.35 cm. in diameter.

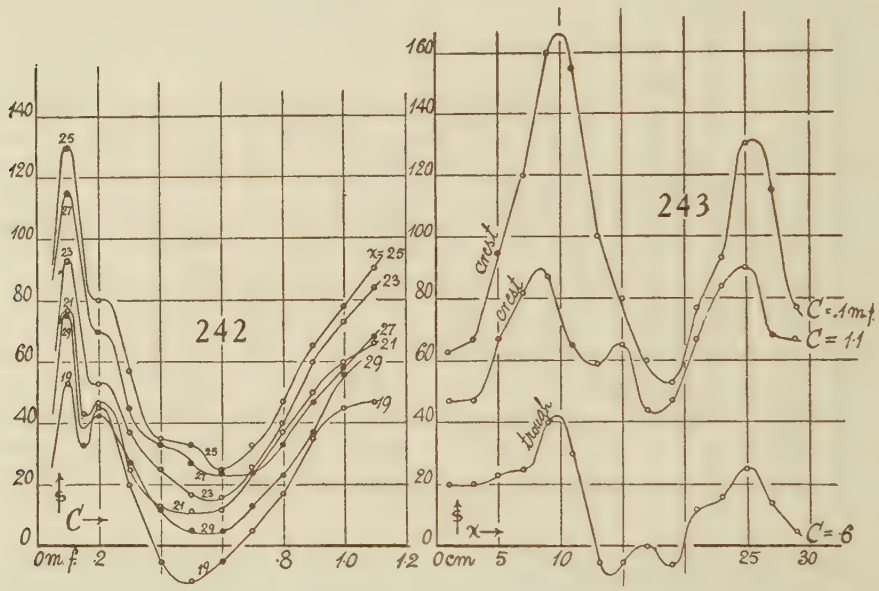

The graphs for $\delta=0, 2, 4, 6$ cm., figure 240, are similar in character, but with $\delta=8$ cm. a change enters, so that intersections occur. The dominating crest is near $C=0.1$ microfarad, a weaker one at about $C=2.5$ microfarads, and a final one beyond $C=1.1$ microfarads. The trough is near $C=0.6$ microfarad, but shifts continually and periodically.

In figure 241, the graphs for $x-1=\delta=8, 10, 12, 14, 16$ are exhibited, $\delta=8$ and 10 being nearly the same. The change here occurs at $\delta=12$ and 14, so that graphs again intersect. The second crest is often uncertain and the trough shifts as before, particularly at $\delta=12, 14, 16$ cm. The first crest ($C=0.1$) dominates again and is steady.

Finally, figure 242, for $\delta=18, 20, 22, 24, 26, 28$ cm., the graphs are more nearly of the same kind, except that for $\delta=26, 28$, changes of form with the resulting intersections occur. In other respects the remarks already made apply.

The xs-graphs are given in figure 243, and they are taken from the preceding figure for constant $C=0.1$ (crest); $C=0.6$ (trough); and $C=1.1$ (crest nearly). The first of these is definite and we observe $(x=\delta+1)$.

$\delta=0$	9	18	25	29 cm.
trough	crest	trough	crest	trough

The distance apart of crest and trough diminishes as do their respective amplitudes when δ increases.

The other two graphs ($C=0.6$ and 1.1 microfarads) suffer from lack of definiteness, though they in general corroborate the preceding. The humps between $x=12$ and 13 cm. are unexpected, but they need not be errors of adjustment.

It is seen that the troughs in this essentially salient plate pin-hole are usually positive, though negative s occurs for $\delta=12$, 14, 16, 18 cm. The crests are strongly positive. Hence, the excess pressures occur on the side of the plate pin-hole (burr side) in the direction in which the puncturing needle advanced, even though the endeavor was made to ream these holes cylindric. The residual burr side is here positive, nevertheless.

85. The same. Plate pin-hole reversed—To test this it was, however, necessary to reverse the pin-hole plate. This was done by cutting the quill-tube at 2 cm. from the plate, reversing the short (pin-hole) end and resoldering it to its quill-tube. The puncture was now burred toward the outside, so that the U-gage should register pressure deficiency.

The sC-graphs for the reversed-plate pin-hole are given in figure 244. There is an obvious tendency of these to be mirror images of the preceding set (figs. 240, etc.) in the initial parts of the graphs, when the negative crest at $C=0.1$ microfarad is intense (as, for instance, when $x=7$, 9, 11, 13 cm.); but with $x=15$ a new departure is made, with the chief crest at $C=0.2$. So also the final tendency of these graphs to become positive is not in symmetry with the preceding set (fig. 240). The periodicity in figure 244 is as a rule much more crowded.

Because of this, the sx-graphs, figure 245, were taken at $C=0.1$ microfarad and 1.0 microfarad only. The negative troughs at $x=9$ ($\delta=8$ cm.) are both marked; the negative crests at $x=5$ ($\delta=4$) and $x=16$ ($\delta=15$) are suggested. The phenomena as a whole are too complicated for discussion apart from the graphs.

86. The same. Further experiments—As the quill-tubes, anterior and posterior, were slightly different in diameter (0.3 cm. and 0.35 cm., respectively) in the last case, a test with tubes of identical bore (0.35 cm.) was repeated. The pin-hole plate was of thin aluminum foil in this case and 0.035 in diameter. It is called salient if pierced from the outside, so that any burr would fall within the quill-tube probe. The connection with the U-gage was at least 75 cm. long, with a glass quill 30 cm.

The results for the salient case are given in figures 246 and 247. The

pin-hole is less sensitive and the graphs simpler; but as a whole they conform to the corresponding behavior of the copper-plate pin-hole. They need not, therefore, be referred to in detail.

In figure 248, I have constructed the *sx*-graph for the main crest $C=0.1$ microfarad and for the far crest near $C=1.0$ microfarad. The sinuous fluctuations are peculiar, but there is no reason for dismissing them. The case of $C=1.0$ is particularly anomalous. When, $C=0.1$, the troughs and crests occur in succession at $\delta=0$, 9, 18, 28 cm., with a low value at $\delta=32$ cm. While the crests graphs are nearly all positive, the troughs graphs (*sx*), also given by the figure, are prevailingly negative, with a succession of the promi-

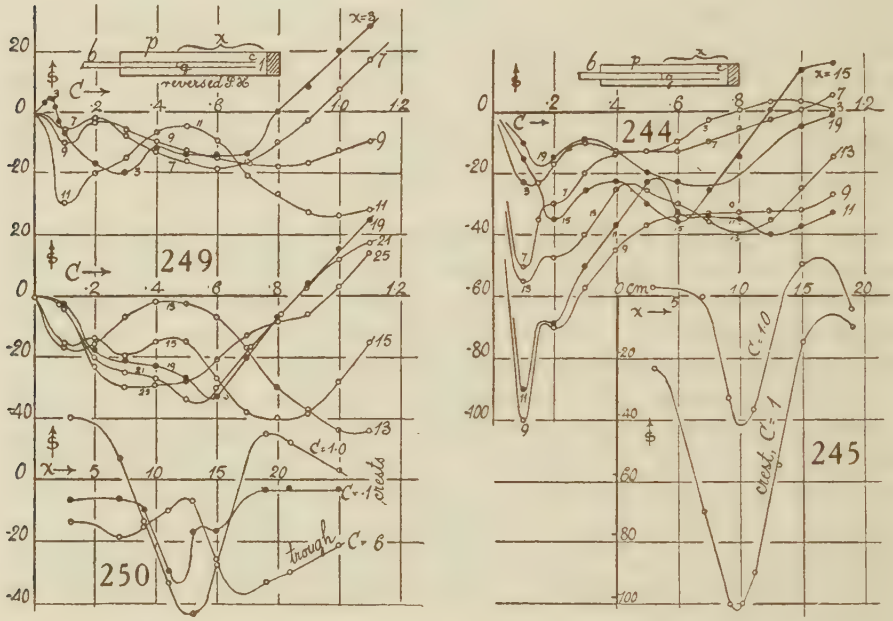

nent negative crests and troughs at $\delta=5$, 12.5, 22 cm. approximately, the tendency being to fall between the troughs in their x position; yet a curious resemblance between the cases $C=0.7$ and 1.0 microfarad is noticeable.

Finally, figure 249 gives a summary of the *sC*-graphs for the reversed position of the aluminum-plate pin-hole. The curves are very complicated, but in the main resemble the results for the reversed copper-plate pin-hole. Crests of the salient cases are changed to troughs for the reëntrant case, but with a marked tendency of all crests and troughs to shift in their C position periodically. The strong $C=0.1$ trough, for instance, for $x=3$ is now given by a crest at $C=0.05$ and a trough at 0.3 microfarad.

The *sx*-graphs, figure 250, in this case are taken for $C=0.1$ and 1.0 (crests) and for $C=0.6$ (troughs). The result at $C=1.0$, with a crest at $\delta=2$ and 18 cm. and a trough at $\delta=12$ cm., is the more definite. The graph for troughs

tends to reverse the case for crests. The hump in the $C=0.1$ graph is unexpected.

If, now, we compare the plate pin-hole with the much more sensitive conical glass pin-hole probe, we reach the anomalous result that the burr side of the former (the side opposite to the one first pierced by the needle) and the reëntrant side of the cone correspond. If the U-gage is on this side it will register pressure. If the pin-holes are reversed, the registry is negative, or pressure deficiency. Modification of the steadiness of the jet through the pin-hole by its edges in some way seems alone left to account for this.

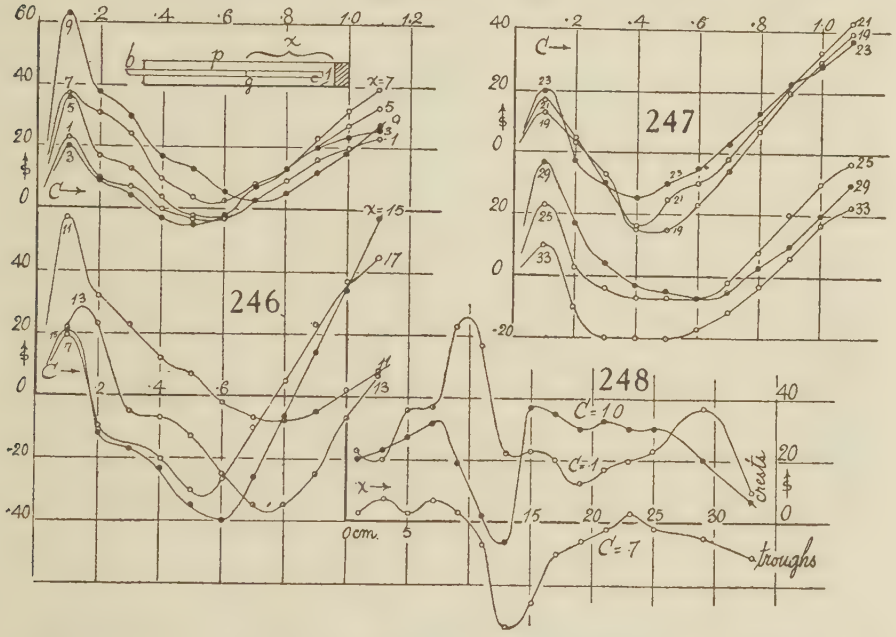

87. Salient glass pin-hole with anterior quills—The sensitive glass pin-hole g in the insert of figure 251 is to be provided with the anterior quill-tube gc, of length $\delta=x-1$, the mouth being 1 cm. from the bottom of the pipe p. The rear tube bg is wide and long (75 cm.) connecting at the far end with the U-gage. The experiments are thus an inversion of the set in figures 233 and 237. Since bg is salient and gc reëntrant, one would expect a diminished effect in s, as compared with bg alone under like circumstances. The reverse is emphatically the case, as the nodal intensity of the highest crest is over eight times that of the lowest trough, both obtained by anterior quill-tube additions. The pipe p was 29 cm. long and all vibrations in tune, as heretofore.

The Cs-graphs in figures 251 to 253 show a chief crest at about $C=0.12$ microfarad. There is a subsidiary one near $C=0.25$ microfarad (not examined in detail) and a final one beyond $C=1.0$ microfarad. For short-tube additions ($\delta=2$ to 6 cm.) there is very little difference. Hence, though the pin-hole

cone was surrounded by a small perforated cylinder of cork to obtain a plane bottom for *cg*, this seemed to be a useless improvement. Beyond $x=9$ cm., however, the graphs rise and then fall with great rapidity, and this is also true again beyond $x=25$ cm.

The *sx*-graphs are given in figure 254, taken at $C=0.1$ and $C=1.0$ (crests) and at $C=0.6$ microfarad (troughs), remembering that the troughs fluctuate in their C positions. The graph for $C=0.1$ microfarad is very definite and the maxima almost cusplike. The graphs for the $C=1.0$ crest and the trough graph happen to be nearly coincident, and they corroborate the high graph

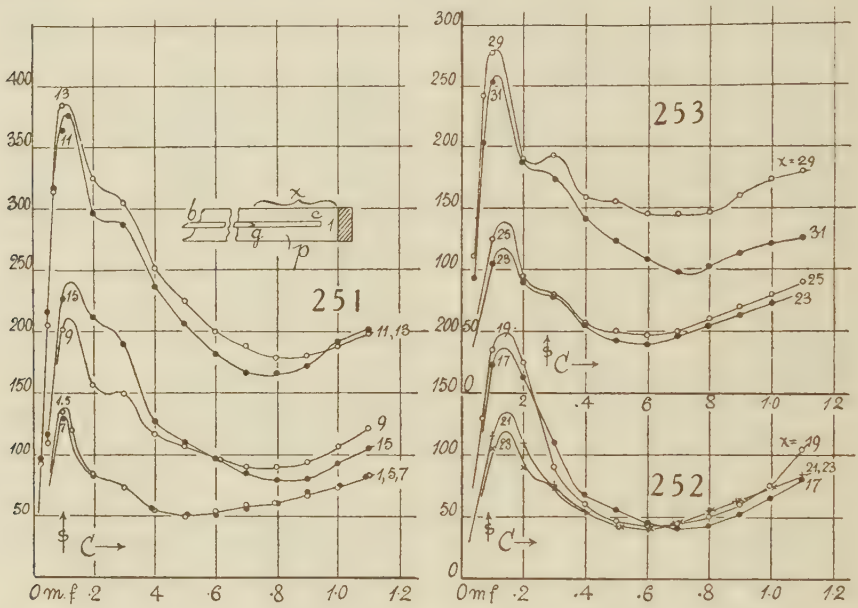

in a general way. The distribution of maxima in minima is as follows ($\delta = x-1$ being the quill-tube length added):

Crest.....$\delta=11$ —— 28 cm.
Trough..... —— $\delta=22$ ——

the maxima decreasing rapidly in intensity and becoming more crowded as δ increases. The relation of the data for δ is again, as 1, 2, and a very scant 3, attributable to viscosity.

The position of the main cusp and trough in these experiments is higher than heretofore, when they were found below $x=10$ and 20, respectively. This may result from unavoidable progressive differences in tuning, but it is to be noticed.

Comparing figures 254 and 237, we see that the enhancement due to anterior quills is of the same order and sign as the pin-hole effect ($\pm s$), whether the pin-hole is salient or reëntrant.

To corroborate the *xs* results of figure 254, direct experiments to trace the

graphs at the crest value $C = 0.12$ microfarad, were made. Two examples of these are given in figures 255 and 256, curve a in terms of the quill-tube length $\delta = x - 1$ added. As the excursions are too large for the ocular micrometer, the slide micrometer was used, wherefore $(r) = 10\ (s)$ about, is the expanded scale-unit of the ordinates. The two graphs are identical in their features. They differ somewhat from each other in corresponding ordinates (nodal pressures), owing to the unavoidable changes of pitch during the long intervals of observation. The chief maximum at a mean length of $\delta = 12$ cm. is now, curiously enough, edentate. It is again to be ascribed to slight differences in pitch, or inadequate tuning of the organ-pipe with reference to the spring-

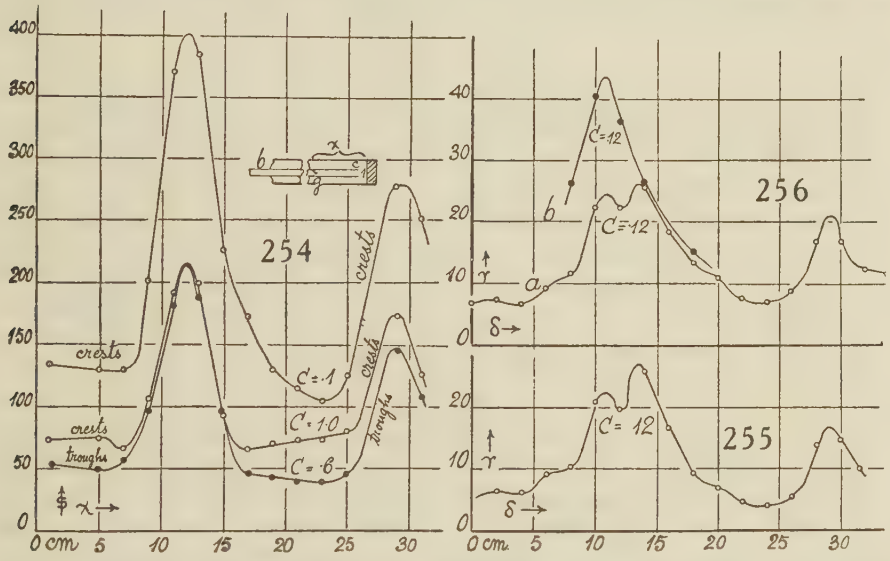

break, to which the sharp cusp in figure 254 is very sensitive. Apart from this the chief crests and troughs in figures 255 and 256 may be placed at

Crest δ.....	12	——	29 cm.
Trough δ.....	——	24	——

somewhat higher even than figure 254. The edentate feature has frequently occurred in the graphs obtained heretofore.

Subsequently, by a side adjustment shown in the next paragraph, this work was partially repeated, with results summarized in figure 256, curve b. The organ-pipe here was scrupulously tuned. As a consequence, the graph is again cusplike (as in fig. 254) and its amplitude ($s = 10r$) fully equal to that in the earlier figure. Hence, the edentures obtained are actually introduced by an inadequate pitch adjustment. The chief maximum is now at $\delta = 11$ cm., as in figure 254.

88. Rear quill-tubes variable—In the preceding series of experiments the quill-tube connection between pin-hole probe and U-gage was very long

(75 cm. and over) and left constant in length, while the anterior quills between the pin-hole and the open end in the pipe p were varied in length. In the present series the case is to be reversed. To make this possible, the apparatus was modified as shown in the insert, figure 257, where the quill-tube connectors bc with the pin-hole probe at g enter the sides of p at about 1 cm. from the bottom. The closed shank of the U-gage is at the mouth of b. One is thus enabled to reduce the length $bg = \delta'$ to about 5 cm. with a little uncertainty, owing to the conical form of g. The length $gc = \delta$ may of course also be varied. The slide micrometer ($1or = s$) was used, as before.

In all these experiments there are necessarily two pin-hole probes, bg and gc, counteracting each other. The efficiency of one will thus be a maxi-

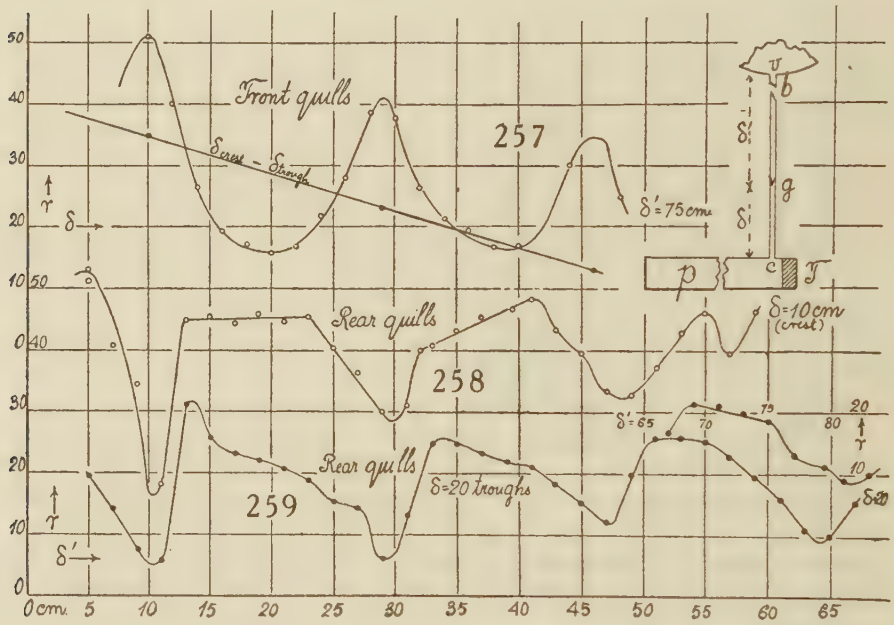

mum when the other is at a minimum. It was, therefore, first necessary to make the survey (r, δ) of the effect of varying δ when δ' is constant and very long (75 cm.). These results are given in figure 257 as obtained with a carefully tuned pipe p. The graph is remarkably regular, with the cardinal points.

Crests: δ.....	10	——	29	——	46	cm.
Troughs: δ.....	——	20	——	39	——	cm.
Double amplitude ..	$2a = 51 - 16 = 35$		$40 - 17 = 23$		$31 - 18 = 13$	

so far as they can be located. The amplitude falls off slowly with δ, as usual, and the wave-length decreases. Troughs lie between the crests and vice versa, very nearly. It is particularly noticeable that crests fall more than troughs rise, these being nearly stationary.

If the successive double amplitudes ($r_{crest} - r_{trough} = 2a$) be coördinated with the crests δ, the graph, figure 257, is nearly linear and $2a = 0$ should occur

at $\delta = 68$ cm., but the effect is more liable to be asymptotic. The relation is nearly $2a = 41 - 0.6\delta$. The subject will be resumed below (fig. 260).

The quill-tube *gc* was now kept at the length $\delta = 10$ cm., corresponding to the maximum in figure 257, while *bg* was varied in length from $\delta' = 5$ cm. to 59 cm. The results of the survey, given in figure 258, are quite peculiar and decisive. In the first place, the crests in δ' (fig. 258) coincide in quill-tube length with troughs in δ (fig. 257). This ceases to be fully the case when δ exceeds about 45 cm., but one can hardly expect that the joining together of these long lengths of quill-tube can be made without some shift. Moreover, there is the cone at *g* which introduces uncertainty at the abutting δ, δ' lengths.

In the second place, the first trough in figure 258 is very sharp and the final crest apparently edentate. This indicates a shift of pitch, probably, so that the pipe *p* was no longer adequately tuned. The second and third crests, as suggested in figure 258, are astonishingly truncated over a wide δ' interval. The fringe position in these experiments, moreover, is not quite steady, but fluctuating over a small interval, to be associated with variation in the action of the spring-break. Granting this, the crests and troughs may be thus placed:

Troughs: δ'	11	——	30	——	48 cm.		
Crests: δ'	——	17	——	37	——	57 cm.	

where the appearance is of troughs falling midway between crests. The close resemblance of this arrangement with the preceding (δ) is striking; but now the crests are nearly stationary, with the troughs rising rapidly.

The high acoustic pressures registered here are to be noticed. The first crest gives $r = 0.053$ cm., which corresponds to more than a third of a millimeter of mercury. That such pressures are producible by vibration in long quill-tubes is quite unexpected.

If, instead of placing the δ quill at a crest-length ($\delta = 10$ cm.), it had been placed at a trough-length ($\delta = 20$ cm.), this should merely drop the graph toward the abscissa; and the troughs might even become negative if δ' were not the dominating pin-hole probe. The results actually obtained (fig. 259) show more than this, for the curve has appreciably changed form. The troughs are still sharp, but the truncated crests are less interpretable than in figure 258, although the preceding distribution of crests and troughs may be accepted. The tendency at the beginning toward a sawtooth graph is unmistakable. Crests fall; troughs rise. Clearly the pin-hole probe δ' dominates, so that the graph is never in negative regions. One may regard δ' as measuring the node at the pin-hole in δ and that the mean value of this never quite vanishes. The pin-hole acts as an embouchure to the quill *bg* while vibration in *gc* is actuated by the pipe *p*. The excess pressure is on the side of the shaft of the musical instrument actuated by the pin-hole.

Later the graph, figure 259, was prolonged as far as $\delta' = 86$ cm., a part of

which is raised in the diagram. The data to be obtained from these experiments are summarized in the following table:

δ	Sharp crests δ'	Displ. r	Sharp troughs δ'	Displ. r	Double amplitude $2a = \Delta r$	Mean δ'
20 (trough)	13	31	11	6	25	12
	33	25	29	6	19	31
	51	26	47	12	14	49
	70	21	64	10	11	67
	—	—	81	9	—	—

The sharp-edged crests and troughs of the saw-tooth waves are meant. Their average distance apart is about 18 cm. and there is no marked diminution of wave-length with increasing tube-length δ' here. The double amplitudes decrease as shown in figure 262, slowly and retardedly (the first three, however, linearly) so as to reach an asymptote somewhat below $\Delta r = 2a = 10$. This should be a steady fluctuation, as the saw-tooth shape becomes less abrupt, more smoothly sinuous, beyond 1 meter of quill-tube length, probably. There is here no evidence that the sinuous curve will eventually straighten out. It is again astonishing that these thin tubes (diameter 0.35 cm.) can sustain such prolonged waves for so great a distance, in spite of the viscosity of air. The $2a$ values, denoting pressures, are proportional to energy values per cubic centimeter.

We may now summarize the results of the last paragraphs, as obtained with two identical collinear counteracting quill-pipes (diameter 0.35 cm.), one of which may eventually be nearly a meter long, separated by a pin-hole somewhere between the ends (see fig. 257, etc.). We note that coördinated acoustic oscillation occurs in both pipes throughout the long distances.

If the pin-hole were in a plate and the edges identical on *both* sides, and if, furthermore, the pipes, δ' and δ, were equally long, it is difficult to believe that any differentiation of the two sides could occur. If the lengths δ' and δ are unequal, that corresponding to the length of any harmonic might be supposed to concentrate the stronger node at the pin-hole and that the pressure excess would be on that side toward which the stronger node pushes, postulating compression to be more effective in the transfer of air through the pin-hole than the following dilatation at the node. The case is conceived to approximate to the pull of a vibrating string on its abutments, without any corresponding push. The abutments are drawn toward each other twice in a period. This case was examined for pin-holes, in § 51 et seq.; but it suggests no reason for the reversal of pressure difference when the identically sided pin-hole is reversed and is thus inadmissible.

89. Further experiments, $\delta = 10$ cm., δ' variable—It seemed worth while to repeat the interesting series (fig. 258), where δ is at a crest-length, in such a way as to prolong the curve further. This has been done in figure 261, where δ' eventually reaches 93 cm. The last part of the graph has been

dropped 10 scale-parts in r, as it goes beyond the figure. There is no essential difference between figure 261 and figure 258, apart from the capriciousness of intonation. The crests are again almost stationary in their r values, while the troughs rise rapidly with δ' to a limit. Their position is

$$\delta' = 11 \quad 30 \quad 47 \quad 65 \quad 85 \text{ cm.}$$

so that the wave-length here can not be said to decrease; rather the reverse. The truncated crests which eventually tend to become sinuous can not be similarly defined as to their δ' position. We may, however, construct the

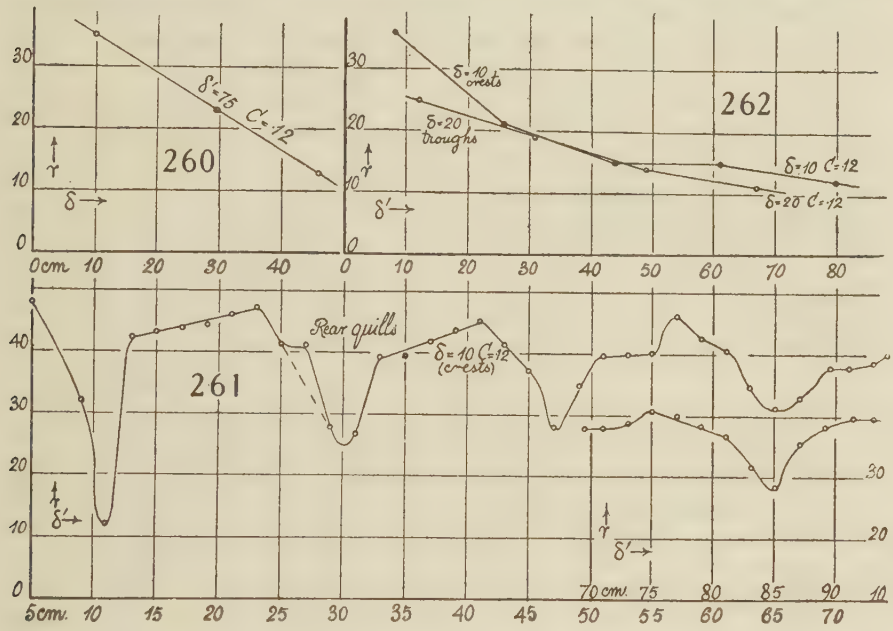

r difference of crest and the ensuing trough and assume this to hold for their mean δ' position. Thus the amplitudes $2a = r_{crest} - r_{trough}$ are obtained.

(Mean) $\delta' =$	8	26	44	61	80 cm.
$2a =$	36	21	15	15	12

These values are also given in figure 262. At the outset the $2a$ for the crest-graph is much in excess of the $2a$ for the trough-graph, as one might expect; but after a quill-pipe length of $\delta' = 30$ cm., the tendency of both is not so very different, and they indicate an eventual oscillation of r over an amplitude of about $2a = r_{crest} - r_{trough} = 10$. It is probable that figure 260 would take the same course if prolonged.

90. Pin-holes varied—By far the most efficient probe thus far has been the quill-tube cone, yielding as much as $s = 600$ acoustic pressure with the given telephone-exciter or sound intensity, or over four times as much as the above plate pin-holes (caet. par.). The glass probe is essentially

a hollow truncated cone, so that the oscillating air-current strikes a sharp circular edge. Pressure is observed in the interior of the cone, and dilation (relatively) on the outside. If we imagined an air-current toward the inside were converted into pressure, whereas an outward jetlike current were not, at least in the same degree, we should simulate the action of the probe. Being an embouchure, the need of an optimum diameter of pin-hole is implied, but it will presently appear that the need of a sharp edge is even more imperative, and it seems natural that there should be more vorticity in one side of the pin-hole than on the other.

In many respects, however, the plate embouchure is more interesting, for here one can modify the bore and edge character of the pin-hole, which

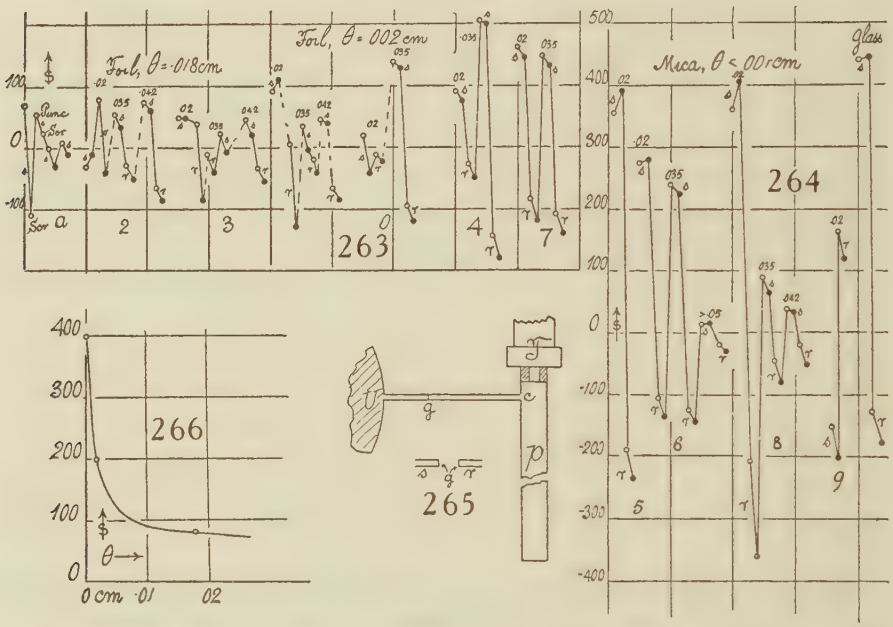

in case of the glass quill-tube cone has to be ground sharp to size. It has, therefore, been necessary to give further attention to the simple plate device (see *g*, fig. 265) and the more important results are recorded in figures 263 and 264, the abscissas merely indicating the consecutive experiments. It was further found that the direction of the initial current in the telephone made considerable difference. Hence, the latter is provided with a switch and its first position (I) is indicated by open circles, the opposite position (II) by black circles. It was thought that the difference was merely an expression of less efficiency of the telephone in the former case; but this is not true, as so many of the black circles are negative in *s*. In each case, the plate pin-hole probe (plate on a quill-tube 2 cm. long, 0.35 cm. in diameter) was tested both in the salient (*s*) and the reëntrant (*r*) position in relation to the **U**-gage (see insert, fig. 265). Diameters of the pin-holes pricked by a fine cambric needle

are also given. The very fine pin-holes (diameter 0.02 cm.) are unfortunately too slow for convenient use. Finally, the thickness θ of the foil (plate) in which the pin-hole is pricked from the outside of the tube is entered, making the record complete. The insert, figure 265, gives the adjustment of quill-tube *bc* with pin-hole at *g* to the pipe *p* actuated by the telephone at *T*, and the interferometer **U**-gage. Pipe spring-break of the circuit and electric oscillation are in tune with the relation of *Ug* (6.5 cm.) to *gc* (10 cm.) corresponding to a maximum fringe displacement *s*. At the beginning of the record (fig. 263*a*) is the above aluminum pin-hole. After being scratched on the inside of the tube to close the burr, it becomes strongly negative, though salient. Punctured a second time, it is again positive, and thereafter soon loses its efficiency. Nos. 2 and 3 are similar pin-holes of varying size. The diameter effect within its range is not definite, showing that some other factor determines its behavior. Salient in position I, it is as a rule strongly positive and reëntrant in position II more strongly negative; but there are many exceptions.

Nos. 1, 0, 4, 7 were punctured in much thinner aluminum foil, and the favorable effect of this is at once apparent in the improved efficiency (larger *s*) of the probes. In other respects the remarks already made apply. Nos. 4 and 7 were constructed with greater skill.

These experiments at once indicate the nature of the missing factor, for, heretofore, the thickness of the foil has been ignored. It is clearly of as great importance as the diameter of pin-hole.

Following this suggestion, I next pricked pin-holes in mica plate, split as thin as admissible and much below 0.01 mm. The results in figure 264 show the enormously increased efficiency obtained, ordinates being even five times as large as those in the original thick foil. No. 5 was only examined for diameter 0.02 cm. In No. 6 there is but little difference between the first two diameters. In puncturing the third, the hole was accidentally frayed to about twice the area wanted and beyond the admissible range. Hence, the low efficiency, *s*.

There is, however, always difficulty in successfully enlarging the pin-hole. For instance, in No. 8 the original efficiency (diameter 0.02) is very large, particularly in the negative, but the fringe displacement is annoyingly slow. On enlarging the bore to 0.035 and 0.042 cm., its efficiency is lost. No. 9 is another peculiar case in which the fine pin-hole is negative in the salient and positive in the reëntrant position, a rare inversion of the usual occurrence.

The final graph shows the corresponding behavior of an efficient glass pin-hole, one of the best. The fine-hole mica probe is thus of the same order of excellence.

If we take the highest of the *s* values, corresponding to any thickness of foil θ, and plot *s* against θ, we get a graph (fig. 266) of hyperbolic contour, giving a mean estimate of the results obtained. The smallest manageable thickness of plate is thus of cardinal importance; in other words, the pin-hole should be a sharp circle, and anything of the nature of a capillary

tube, however short, is detrimental. The viscosity of air is here liable to ruin the experiment.

And yet the two sides of the pin-hole behave quite differently to the current of air propelled through it by the alternating nodal pressure. Hence, the production of vortices at the pin-hole by the acoustic pressures seems alone to be in keeping with the observed results. The oscillating air-columns in contact at the pin-hole are successively shooting vortices into each other and the pressure difference results because, owing to the structure of the pin-hole in question, one of the air-columns does this more efficiently than the other. One should expect the pressure to be largest on the side of less vorticity; for it is here that the energy of the discharge current across the pin-hole has been in greater measure converted into vortex motion within the pin-hole probe.

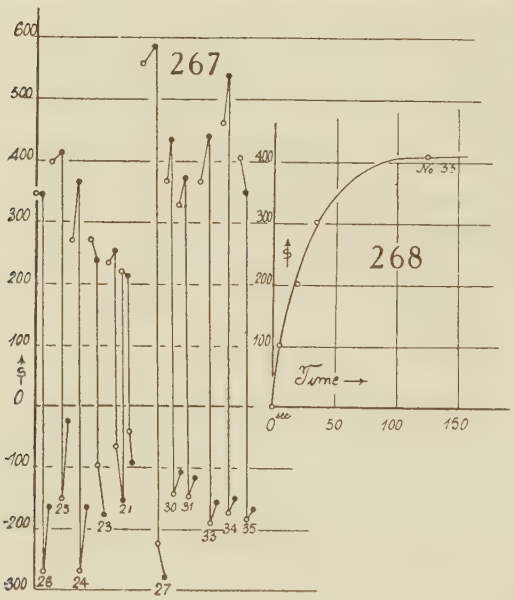

Though a large number of further experiments were made, the results at first showed no improvement, and the success obtained was always a matter of chance. Typical examples are given in figure 267 in case of probes Nos. 21 to 26, all with holes 0.02 cm. in diameter. In the former (21), paired holes were also tested, insuring a shorter interval of displacement; but as a rule the second hole is liable to decrease the sensitivity, as only in rare cases will two equally good holes be pierced. A distinct advance of technique, however, is attested by the probes Nos. 27 to 35, in which the piercing needle passed through the mica into a small stick of wood placed immediately behind the mica and receiving the full stress of the puncture. The grain should be parallel to the needle. The *perfection* of contact of wood support and mica plate insures the best results (No. 27).

The salient position of probe punctured from the outside is always positive (pressure in gage) and the reëntrant position negative; moreover, the effect of positions I and II of the telephone-switch is generally, though not uniformly, consistent. Nevertheless, an initial thrust of telephone-impulse in the salient position and a pull in the reëntrant position are seen, as a rule, to be equivalent in effectiveness. If the thrust produces the greater positive value, the pull will follow with the greater negative value. Dependence of sensitivity on size of hole in relation to pitch could not be found. In figure 268, the time

needed to obtain the full displacement in case of holes 0.02 cm. in diameter is graphically given by noting the seconds elapsed during successive displacements of $\Delta s = 100$. After the first minute, at least 10 per cent is added to the displacement and not more than 70 per cent of its full value is observed during the first half minute. In this respect the glass pin-hole cone, which admits of a larger aperture and is practically instantaneous in its response, is preferable, even if the mica-plate pin-hole often shows the superior sensitivity of No. 27, for instance. Finally, mica punched from without is almost invariably positive and corresponds, therefore, to the salient cone.

CHAPTER V

MISCELLANEOUS EXPERIMENTS WITH THE INTERFEROMETER U-GAGE

Pressure Phenomena of the Electric Wind

91. Apparatus—The spectacular group of experiments, which we use to perform once a year, seem but rarely to have come to any useful maturity. I can recall only the electronic measurements of Professor Chattock. Having the apparatus at hand, it seemed interesting to look at them in detail, and in the attached figures I will summarize the main results.

The simple apparatus as originally used (fig. 269, insert) consisted of

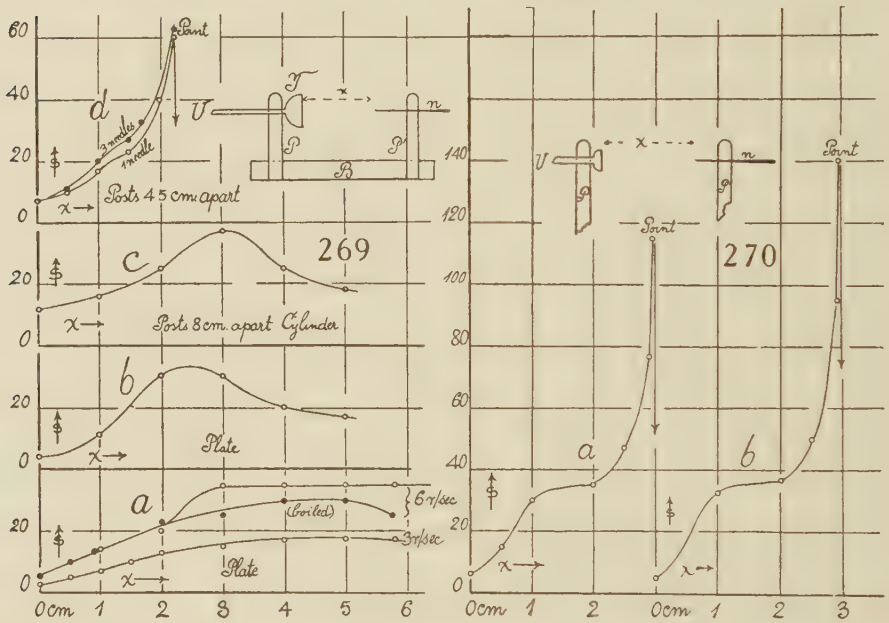

the two brass posts, P, P', usually 8 cm. apart and fixed in the hard (or soft) rubber base B. T supported by P is a small thimble of brass perforated by the slender tube U, which leads to the interferometer **U**-gage. The post P' carries the darning-needle n coaxially with U, and both n and U fit snugly, so that they may be slid to different distances, x, apart. P and P' are in contact with the poles of a small Wimshurst machine, capable of delivering half-inch sparks. The latter was usually turned by hand near a clock beating quarter seconds, and the speed of rotation of six turns (sometimes three turns) per second for each plate was easily maintained.

92. Needle electrode—The group of curves, a, refers to a hard-rubber base with posts, P, P', 8 cm. apart. Irregularities are referable to freakish

action of the machine, quite apart from rotation; but it is noticeable that the pressures (s, approximately in 10^{-6} atmosphere) are roughly double for 6 rot./sec. as compared with 3 rot./sec. I was disappointed at the relatively low pressures here in evidence, and therefore scraped and boiled the hard-rubber base in dilute acid for greater insulation. The resulting graph actually shows reduced sensitivity and now suggests a maximum. In curve b a soft-rubber base was tested. The graph is smoother, with a very definite crest, but no better in s, and finally, the graph c on a cylindrical hard-rubber base is no advance on the others.

Improved conditions appear with graph d, referring to posts P, P' but 4.5 cm. apart. Whether one or three sharp needles are used is relatively

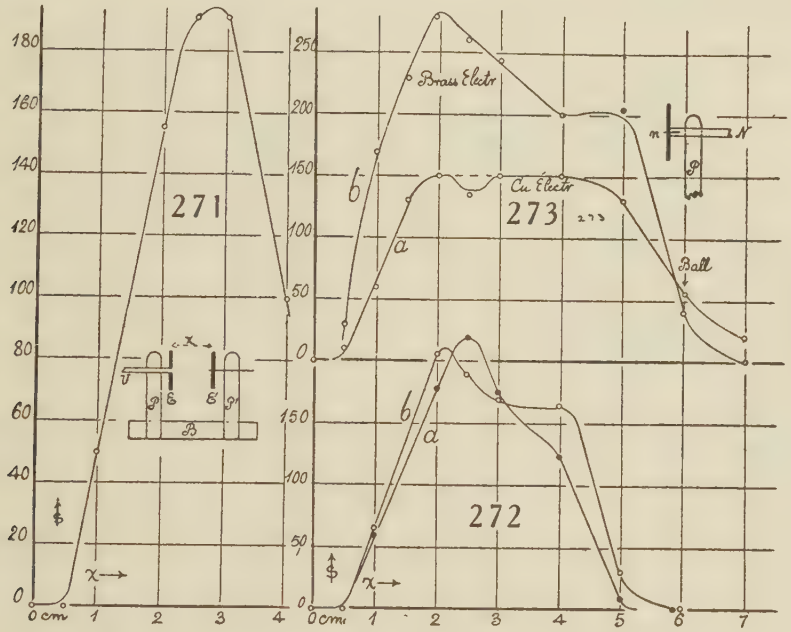

immaterial; but this graph is rapidly accelerated upward. Close inspection of the data convinced me that the graph essentially consists of two constituents, one of which tends to a low crest as heretofore, while the other begins at the maximum and runs with great rapidity to high s, while the needle projects but a few millimeters beyond the post P'. When the needle-point retreats just within the post, the curve drops instantly to zero. Sparks, or sputtering, is equivalent to $s=0$.

To accentuate this result, the thimble was cut down (the form is practically immaterial) as in the insert, figure 270, admitting of larger x between the same posts. The graphs a and b (for a somewhat wider x space) fully bear out the surmise, and the cusp of b has risen to nearly four times the height of the crests in a, b, c, figure 269. What the larger x insures is probably greater axial momentum of the ionized wind, which in its complete form

must be a ring-vortex symmetrical to the needle. A point immediately in front of a surface of high potential gives the latter a longer range of action. Eventually, the life of the ions and their space density would be in question.

The position of charged masses (like the poles of the electric machine) must materially affect the form of the graphs by deflecting the air-currents. Such objectionable features are to be scrupulously removed in the next section. No pressures (s) are observed until the charge of the machine exceeds a certain specific threshold or ionizing potential, after which the appropriate pressure (s) appears at once. In the reverse case, pressure (s) vanishes before the machine is discharged. The greatest difficulty thus far has been the fluctuating potential of the machine, due, so far as I can see, to casual partial self-discharge within.

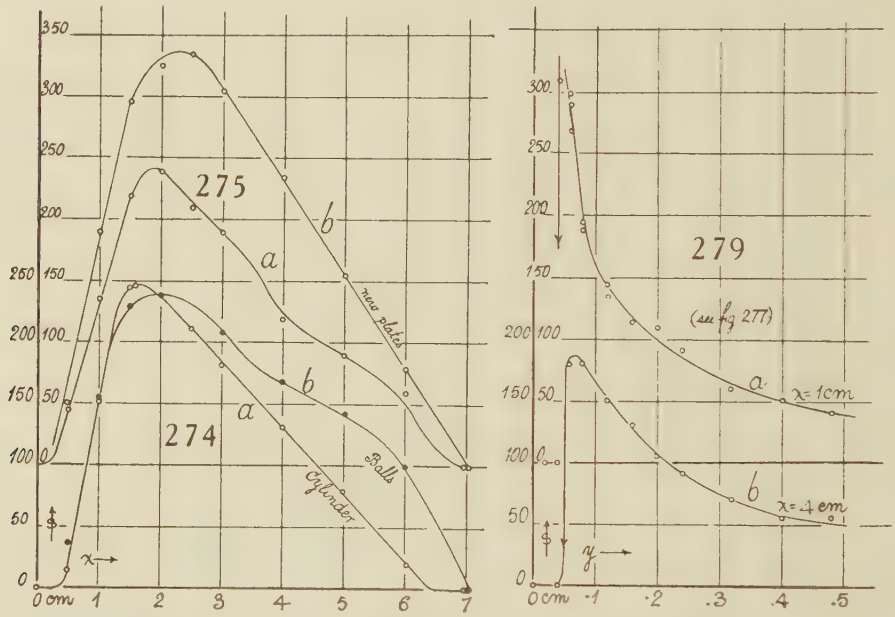

93. Mucronate electrode—Borrowing a term from the botanists: What is needed, therefore, is a slightly convex electrode E', with a sharp fixed needle-point projecting less than a millimeter from its center (see insert, fig. 271) and (convexities toward each other) facing a similar but unarmed electrode E. P, P' as before are 4.5 cm. apart.

The results obtained with this mucronate electrode (fig. 271) are astonishing, for the curve sweeps aloft in some cases to over five times the heights of the original crests. Thus far these graphs have not started until $x = 0.5$ cm. is passed. They are peaked at the upper end, and soon thereafter drop from the sharp crest to $s = 0$. They imply a degree of sensitivity that makes interferometer observation difficult, every little irregularity of the Wimshurst being magnified.

To increase the range of the experiments, it was necessary to place the posts P, P' further apart. This was done on the same base by a metallic extension carrying P' from about 4 to 8 cm. Results so obtained are given in figure 272, the graph b having an improved E electrode. The presence of the massive extension, however, probably deflected the air-current; hence, the graphs fall off rapidly in this region.

The hard-rubber base with posts 10 cm. apart was therefore substituted

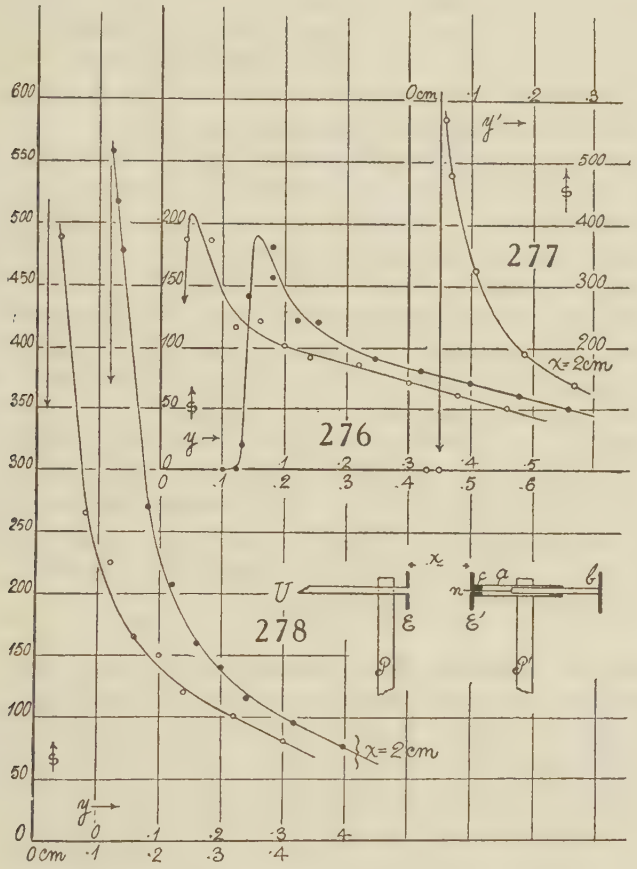

and the results given in figure 273 worked out. These fall off at $x=6$ cm., which is the position of one of the poles of the electric machine. In case of graph b the mucronate electrode was improved, as shown in the insert. A brass rod N (5 mm. in diameter) carries the sharp needle-end n all but embedded in its end with the point just projecting. A remarkable increase of sensitivity is thus obtained, owing in part to the more careful polish of the slightly convex electrodes. The crest almost reaches $s=300$, but the descent is still irregular.

It was therefore necessary in the next experiments to place the poles

of the electric machine quite beyond the posts P, P'; for it is only when the poles lie outside of the space between the planes of the electrodes that significant values of s are observed. Figure 274*a*, obtained with cylindrical pole pieces, is a summary of the first group of results and, as it happens, the smoothest thus far completed. Both branches separated by the crest are nearly linear. Figure 274*b* was obtained with ball poles. The anterior branch is still linear, but the rear branch has an unexpected bulge upward at $x=5$. Figure 275*a* is a careful repetition of this group of measurements. The double inflection between $x=4$ and 5 cm. is not removed and the last s values relatively low. As the fringe displacement s is not steady, but fluctuating, for reasons referable only to the generator, it seemed useless to endeavor to go further without overhauling the machine.

Some of the tin plates of the Wimshurst having become damaged in use, these were replaced and a few other alterations made. Figure 275*b* summarized the new result. The crest is over 30 per cent higher than in the earlier cases, evidencing the marked improvement in the efficiency of the machine and the graph is again regular, with two approximately linear branches on each side of the crest; the latter has shifted somewhat to the right. Nevertheless, the fluctuation of s values, apparently due to casual partial internal discharges of the machine, was not improved and remains outstanding.

As a crest invariably appears in all the curves, it seems obvious to refer it to the limiting potential of the machine. After the maximum sparking distance x is passed, the strength of the field (kilovolts/cm.) between electrodes rapidly diminishes until it reaches a threshold field-strength ineffective in s. Furthermore, s is an expression for the convection current if the same electrode is used. Hence, the sx-graphs give indications of both potential and current values, but not simply.

94. Mucronate electrode with micrometer—The adjustment is shown in the insert, figure 278, where the electrode E' is attached to the one-quarter inch brass tube a, partially stopped at c by a perforated cylinder. The tube a contains the micrometer screw b, the end of which is tipped by the needle n. Hence, by turning b, the point n may be moved from within $E'c$ and made to project by any small amount beyond it. The zero of this apparatus is arbitrarily found at the position of the micrometer-screw (reading y), at which pressure s suddenly begins to appear at E. Before this sparks or sparklets continually jump across from E' to E and $s=0$. The first s for $y=0$ is casual, the fringe displacement s appearing and vanishing alternately with much interferometer turmoil. Immediately thereafter (fig. 276), y increasing, s is definite and near the maximum, which here seems to occur for a projection of $\Delta y=0.06-0.03=0.03$ cm., since at $y=0.03$ cm., $s=0$. Figure 276 gives two examples of the cuspidal graphs. Almost half the efficiency is lost after this projection $y=2$ mm., but this is a moderate result as compared with the following.

The relatively low s values in figure 276 indicated some maladjustment.

The electrodes E and E' were therefore freshly turned, polished, and adjusted more fully in parallel. The effect of this is astonishing, as shown in the graphs, figure 278. Both graphs drop from an actual cusp; for the initial data were

$y=$	0.02	0.025	0.03	0.04 cm.	etc.
$s=$	0	560	520	480	

At $y=0.025$ the sparking is intermittent, so that it is difficult to catch the fringes between sparks. At $y=0.02$, $s=0$, and therefore the point of the needle is just within the effective limit of the disk electrode. Hence, the cusp appears within a tenth of a millimeter from the critical boundary of the disk and is 70 per cent higher in s than the crest of figure 275. Had it been possible to approach the surface closer, there is no doubt that a higher order of s values would have been obtained. The field for $x=2$ cm. may be estimated as 10 kv./cm., insuring the stream of ions just before sputtering.

The corresponding phenomena for other spark-gap (x) values are now to be treated. In figure 279, curve a, $x=1$ cm., while y increases from 0 to 0.32 cm. At this small distance sparks readily jump across, even when $y=0.05$ cm., and they pass between parts of the electrodes rather than from the appreciably salient needle-point. At times, sparking may suddenly cease, whereupon high pressure (s) takes its place. This was the case with the first points ($y=0.06$ or less) in figure 277. Thus there is no doubt that this graph is cuspidal, though it can not be tested. The s-drop with increasing y is naturally fast, and $s=0$ would soon occur, since $x-y$ is small.

The case for $x=4$ cm. (fig. 279, curve b) differs from curve a, as in the former the cusp seems to be actually rounded. The height s of the crest, moreover, is less than was expected (cf. fig. 275 a, b), which leads me to suspect that the adjustment was somehow less accurate. The fall is relatively slow.

95. Contributory results—Some relevant measurement of the potential variation of the machine is desirable to account for the preceding results. These data were obtained with a simple electrometer in which the indications were given by the deflections of a light horizontal flexure needle of aluminum. It was not thought necessary to standardize the apparatus, as the deflections suffice the present purposes. One pole of the Wimshurst machine was put to earth and the other joined to the electrometer. An example of the results is given in figure 280, in which the potential is rated in arbitrary scale-parts for different widths, x, of mucronate spark-gap. The graph V shows the free potential with the machine making 6 rotations per second. V_r is the residual potential retained after the machine comes to rest ($r/t=0$) without being discharged. This is the threshold potential and the electric wind of the preceding paragraphs does not blow ($s=0$) until this potential is exceeded. One may note in particular that V is constant after $x=1.5$ cm. for the mucronate electrode used. For $x<1.5$ cm. the V and V_r values are coincident and fall off very rapidly.

If we write $F = V/x$, treating the axial field F as uniform, the graphs F and F_r are obtained. Both curves have their crests at $x = 1$ cm., which should therefore be the strongest field used. The preceding experiments (figs. 274, 275, etc.) reach their crests at $x = 2$ to 2.5 cm., therefore, in a materially weaker field F. It is to be observed, however (see fig. 271), that for $x = 1$, the electrodes are already so close together that the electric wind must in large measure be not axial but radially outward. Hence, only a component pressure acts at the electrode E. Not until the value of x has become larger ($x > 2$ cm.) will the wind in the main be axial. This at least seems to be the most plausible method of accounting for the sx crests in question (cf. fig. 282), the electric wind being a vortex-ring whose plane is parallel to the electrodes and whose axis of symmetry is the needle.

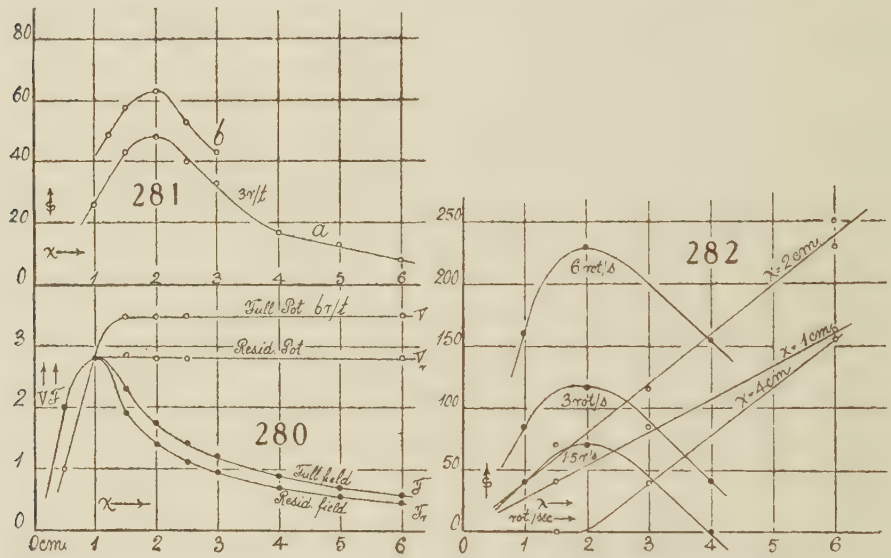

It is somewhat surprising that the limiting potential is practically independent of the speed of the machine. Thus far, spark-gaps $x = 1.5$, 2.0, and 4.0 cm., each at rotations 1.5, 3, and 6 rot./sec., the same limiting potential, $V = 3$, was built up, more gradually of course for the slower motions. For $x = 1$ cm., the limit was $V = 1.2$ independent of the speed of rotation. For $x = 0.5$ cm., $V = 0$. Thus the excess potential is removed by the leakage of the spark-gaps like the mucronate electrode, or at other incidental saliences of the machine. The electric wind appears in the nature of a current running through the machine. One can hardly expect $s \propto 1/x$, however, and the graphs for $x > 2$ conform more nearly to $s_0 - s \propto x$.

The size of the hole in the electrode E (fig. 270) is of little consequence. Closed with a flat, smooth-headed brass nail, loosely, the same s values were obtained.

Using a still smaller Wimshurst machine, the character of graphs remained

the same, but the s values were much reduced. Examples are given in figure 281, in which the curve a has a longer pointed mucronate electrode than b. The crests are again at $x=2$ cm. Judging from sparks, the potentials furnished by the machines were larger for the small machine. But the plates of the smaller machine were less than 0.8 of the diameter of larger and the former could be rotated at only 3 *r/sec.* The available electric currents, and hence the corresponding s, differ largely. Hence, s may again be regarded as responding to the current flowing in and out of the machine after the residual potential is exceeded.

Using the aluminum electrometer, the potentials came out as about 4.0 for the smaller to 3.0 for the larger; but the currents s run as $s=250$ to 600 for the larger, compared with $s=60$ for the smaller in the above graphs.

The endeavor to use the mucronate electrode in case of an induction-coil just below sparking, in a given gap, did not succeed. Values of s between $s=7$ and 15 (in later experiments $s=30$) only, could be obtained for $x=3.5$ cm.; and there was even then incipient sputtering, which is fatal to large s.

It remains to determine the effect of the speed of rotation (*r/sec.*) of the given electric machine on the s values. This is a complicated question, for the answer depends on the incidental charge of the machine, as well as on *r/sec.* I endeavored to overcome the uncertainty by rotating for some time in each case, hoping that in this way (beginning with the charge zero) the normal condition would be established. The results are given in figure 282, which contains both s, *rot./sec.*, and sx-graphs.

When x is constant, s increases, nearly proportionally to the angular velocity of the plates, 1.5, 3, and 6 rotations of each plate per second being instanced. The lines pass through zero as x increases from 0 to 1 to 2 cm., the optimum spark-gap. The rates at which s increases with *r/sec.* thus steadily increase. After this ($x=2$ to 4 cm.) the line merely drops, the rate of s increases, with *r/sec.* remaining about the same. Thus, for instance, if $x=4$ cm., 1.5 rotations per second leave s unchanged at zero.

The effect of this on the sx graphs is apparent. Figure 282 shows that the crests persist at $x=2$ cm., but that the graphs drop as a whole when r/s diminishes from 6 to 3 to 1.5.

96. Velocity of the winds—An estimate may perhaps be obtained if we use Bernoulli's equation and put $v=\sqrt{2p/\rho}$. In the graphs, figures 269 to 276, the s values at crests are very commonly $s=300$, and they mount to even $s=550$. Since the unit of s is about 10^{-6} atm., these data may at once be taken as pressures in dynes/cm^2. Thus the velocities in the two cases are roughly $v=770$ cm./sec. frequently and $v=1{,}000$ cm./sec. in very favorable cases. These are astonishingly large values. In the small time of x/v, where $x=6$ cm., there is very little time for the decay of ions. The change of s with x is thus to be associated with a ring-shaped vortex of air, whose axis is the needle prolonged. Hence the currents near the electrode E, when x is small, must be largely radial and outward, as already instanced.

When the needle retreats into the effective confines of the E' electrode, the latter begins to sputter. At small distances sparks may pass across. The pressure s drops to zero very nearly. This sputtering immediately following high s values when y is small is very interesting, since it recalls the behavior of the sensitive flame in acoustics. Here also a uniform linear column breaks down into an oscillating column. Hence, one is tempted to conclude that in sputtering the ionized winds may be treated as alternately positive and negative and hence produce no pressure at E. The phenomenon is not an electric oscillation, of course, as its frequency must conform to the motion of air-currents.

If we take $v = 1{,}000$ cm./sec., the maximum estimated above, the limiting frequency would be $n = v/2x$ and hence, if the spark-gap is $x = 2$ cm., $n = 250$ or about c' of the 2-foot octave. This is naturally much too high, say ten times; but, on the other hand, an immediate reversal of alternating air-currents is improbable, so that the relations are not out of the question. It is curious that sputtering frequently occurs for a slow-moving machine and will cease when the machine moves faster.

Alternatively one may simply assert that the field insulation breaks down when the electrical pressure or field potential energy, $F^2/8\pi$, has reached a certain value. The energy which drives the air-current is then converted into the heat of the minute sparks and the electric wind ceases. With regard to the electrical circuit, we may thus conclude that in the absence of sputtering, the ions are taken from E' to E by air convection; hence the pressure, s. On the other hand, when sputtering occurs and $s = 0$, the electric current phenomenon, is akin to the conduction of electricity in electrolytes, though with far more tempestuous collision of ions, as these are shot at each other with a velocity (according to the above estimates) somewhat short of 1,000 cm./sec. There is no electric wind ($s = 0$), in spite of the appearance in the dark of a current of sparklets from E' to E.

A series of experiments in which the actual saliency, y', of the needle from the plane of the electrode E' was measured (in the above graphs, figure 279, the $y = 0$ refers to the first occurrence of sputtering) gave the following data:

$x = 2$; $y' =$	0.03	0.05	0.06	0.07	0.11	0.19	0.27 cm.
$s =$	0	0	570	478	324	188	138

also summarized in figure 277, on a reduced scale. Thus sputtering begins when the needle protrudes half a millimeter from the electrode. Endeavors made to sharpen the rather fine needle brought no consistent results.

A needle placed in the U-tube electrode produced only a just perceptible negative pressure.

97. A method for measuring the energy of X-rays. Introductory apparatus—This important problem has recently been attacked with surprising success by Mr. H. M. Terrill, who gives references to the earlier work. He uses a bolometric method, and constructs an apparatus which should be

generally available in the laboratory, provided the extremely delicate conditions of constant environmental temperature can be met. I had been working on an air-thermometer method when Mr. Terrill's results appeared; but I have not thus far obtained anything separable from temperature effects, at least from the rather primitive X-ray generator which I used. Moreover, it is not probable that any results worth recording will be obtainable in a steam-heated room. In the summer time, however, I think the method should be feasible in a basement room, so that a brief account of the method may be given here.*

In figure 283, U, U' is the interferometer **U**-tube, the closed shanks of which are provided with the tubulures t t', each carrying a lateral branch with a stopcock, c, c'. The tubes t and t' communicate with the boxes A and B of thin waxed wood or aluminum, about 10.6×6.2×7.8 cm., or 517 cm³. in volume. To this must be added the volume, v, above the mercury surface, 69 cm³., making a total of 586 cm³. as the effective volume in each of the closed regions.

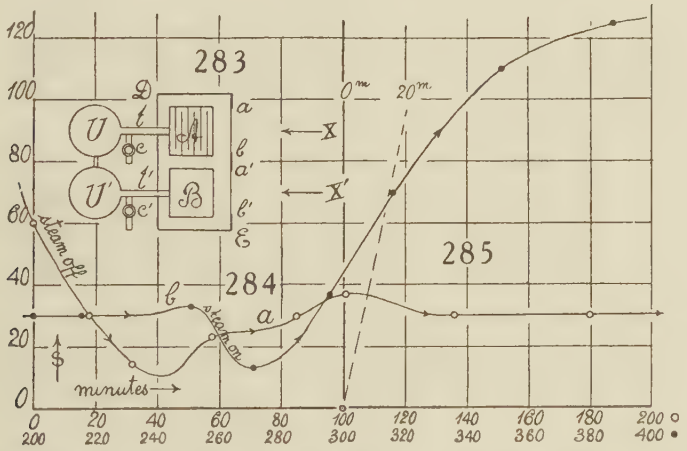

Whereas the box B is empty, the box A is provided with a succession of metallic curtains, alternating and extending not quite across the box, preferably of lead. But as the lead foil available was not thin enough, 12 sheets of copper foil, each 0.004 cm., thick were used instead. The boxes AB were surrounded by a heavy metallic case, DE, the inside of which was filled with cotton batting, on which the boxes reposed. On the side to be illuminated by the X-rays, X X', however, there was a clear space, ab, $a'b'$, for the introduction of the radiation, paper screens being provided to obviate air-currents.

Thus it was supposable that whereas both chambers A and B would absorb heat radiation under like conditions, the A chamber only (supposing the metal sheets sufficiently thick in the aggregate) would absorb the X-radiation. The heat produced in this way would correspondingly increase the pressure on that side. One may, therefore, when A receives radiation

*H. M. Terrill, *Phys. Rev.*, vol. 28, p. 438, 1926

(X), close the cock c and open c', and when B receives radiation (X') close c' and open c; or, preferably, close both stopcocks c and c' and let the radiation X be received symmetrically by A and B. In the latter case the thermal effects balance each other, whereas the X-ray effects heat A only. The total mass of the copper sheets was 28.7 g. There were 12 sheets about 6 by 10 cm². in area. As each sheet is 0.004 cm. thick, this makes a total thickness of half a millimeter of copper only, which is inadequate for complete absorption, but may be used for orientation. Lead, in addition to its density, would have the further advantage of low specific heat.

98. Computation—It will first be necessary to ascertain what temperature increment in A corresponds to the passage of one fringe. In order to obtain an estimate, we may regard the whole region A to be at the same temperature, as the volume in the gage is but 12 per cent of the whole. If v is this volume, V being the volume of the box A, p, m, τ, the pressure mass and absolute temperature of the air, initially

$$p(v + V) = R\, m\, \tau \tag{1}$$

As the change of temperature is very small, we may neglect squares of small quantities and differentiate logarithmically, whence

$$\frac{\Delta p}{p} + \frac{\Delta v}{v + V} = \frac{\Delta \tau}{\tau} \tag{2}$$

Here, $\Delta p/p = \Delta h/h$, the ratio of mercury heads, h being the barometric height. Δv is equal to $\pi r^2 \Delta h/2$ if r is the radius of U, since but half the mercury depression is on the pressure side. Finally, $v = \pi r^2 t$, if t is the thickness of the air-space in U. Hence:

$$\Delta \tau = \tau \Delta h \left(\frac{1}{h} + \frac{1}{2(t + V/\pi r^2)} \right) \tag{3}$$

But Δh per fringe is $\lambda/2 \cos \varphi$, where $\varphi = 45°$ is the angle of incidence of rays. This is equivalent to about $\Delta h = 42 \times 10^{-6}$ cm. of mercury, or 5.5×10^{-7} atm. per fringe. Thus, if $h = 76$ cm., $\tau = 300°$, $t = 1$ cm., $V = 517$ cm³., $r = 4.7$ cm., $\lambda = 6 \times 10^{-5}$ cm.

$$\Delta \tau = 8.6 \times 10^{-4} \text{ °C. per fringe} \tag{4}$$

Since the thermal discrepancies are supposed to balance in A and B, the X-radiation absorbed in A may be computed as $\Delta H = (m\sigma + m's')\Delta \tau$ where m is the mass and σ the specific heat of the metallic curtains. To this the mass, m', and specific heat σ', of the air within A is to be treated as a correction. Putting $m = 28.7$ g., $\sigma = 0.091$, $m' = 0.62$ g., $\sigma' = 0.24$, $\Delta H = (2.61 + 0.15)\, \Delta \tau$ per fringe, or with the given value of $\Delta \tau$ in (4)

$$\Delta H = 2.4 \times 10^{-3} \text{ ca./fr.} = 10^6 \text{ ergs per fringe.}$$

If we take the mean datum for the X-ray energy, trapped by Mr. Terrill, $H = 3.9 \times 10^6$ ergs in 5 min., or 7.8×10^5 ergs/min., one ought to expect $H/\Delta H = 7.8$ fringes per minute, or about 78 fringes in a run of 10-minute periods.

As the X-rays here in question are intense, it is thus only under conditions of exceptionally constant temperatures in the environment that trustworthy data can be looked for, even if a somewhat larger solid angle is in question in the above apparatus.

99. Data—A large number of experiments were made, both with and without X-radiation, in the endeavor to minimize the temperature discrepancy. These, however, led to no trustworthy results, and it seems impossible, in the winter time and in a heated room, to control the temperature effect. I shall merely, in figure 284, give an example of a typical run without X-rays. Here s, or 1.4 times the number of fringes, is the ordinate. The weather being

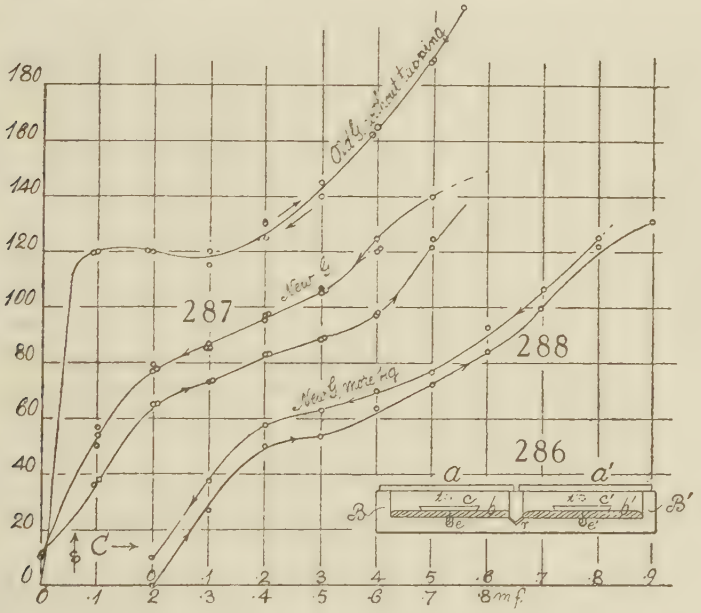

warm, the room was heated in the morning only and again in the late afternoon. After the steam was turned off, the apparatus (including the U-gages, covered on all sides with metal box and wadding) settled into a steady state between (a) and (b). Thereafter, with the inflow of steam heat at (b), the thermal variation recommences.

In the same diagram I have inserted (fig. 285) the above rise of temperature reduced to s ($s=4.6$ per minute), to be anticipated from strong X-rays. It appears that in the summer time, in a good basement room, the experiment should be feasible, and it was therefore postponed for the present.

100. Apparatus. Results. Modified U-gage—This modification consists, as shown in figure 286 (where BB' is the cast-iron body of the shallow U-gage, bb' the mercury content, the pools being connected by the narrow channel r, and aa' the cover-glasses of the reservoirs, 10 cm. in diameter and

about 1 cm. deep), in floating the two plate-glass disks c, c' only about 5 cm. in diameter on the respective and much wider mercury surfaces. The disks are kept in place by platinum stems cemented to the middle of the lower sides of c and c' and projecting downward into the depressions e, e' drilled into the body B, B', at the centers of the pools. Short tubulures t, t' communicate with the atmosphere.

In a gage so constructed it was thought that the surfaces c and c' would remain more rigorously in parallel for relatively large displacements. The tests showed that the general manipulations were not much more difficult than with the older gage with large plates $c\ c'$. In other words, there was no unreasonable quiver of fringes, unless an excess of mercury charge, bb', had been introduced.

Two fatal discrepancies, however, soon showed themselves. In the first place, the floating glass plates $c\ c'$ would have to be rigorously plane parallel; otherwise any rotation of c relative to c' around a vertical axis would be apt to change the fringes, both as to size and inclination, enormously. Rotations of this kind, moreover, would be almost inevitably incident to the usual run of experiments.

The other is the hysteresis-like error reproduced in figure 287. When the fringe displacement s increases, the s values are too small, and when it decreases s values are too large, and this in spite of the vigorous tapping under which each of the observations were made. Without tapping the results would have been chaotic, whereas in the old gage tapping is rarely necessary. Supposing that the change of mercury was insufficient (*i. e.*, the pools too shallow), an excess charge was introduced. Observation was now inconvenienced by the tendency of fringes to quiver; but the graph, figure 288, was obtained in this way. Hysteresis has in fact diminished, but it is still prohibitive and the annoyance of tapping the gage interferes with its use when continuous phenomena are to be observed.

If we inquire into the reason for the behavior in question, it seems obviously referable to friction. Probably a film of air collects around the stem and walls of the cavities e, e'. When the stem approaches the walls, therefore, it would be held against them by mercury pressure in virtue of the usual capillary phenomena. Steps were therefore taken to remove all air-films by charging the mercury in vacuo. Unfortunately, the plate a', owing probably to some molecular strain, failed to sustain the air-pressure long enough for a full test and the gage was completely wrecked by the explosion. A new gage with new plates was then constructed and carefully exhausted many times. The new results, however, were in no wise superior to the summary in figures 287 and 288. If anything, they were worse. Tapping was absolutely essential. The stem method of anchoring the floating plates is thus impractical, even if the extra quiver of the mercury with small plates is admitted.

UNIVERSITY OF MAINE
3 7550 01353520 9